Characterization of Novel Cellulase and Glucose Isomerase-producing Bacteria and Optimization of the Enzyme Production Conditions and Their Potential Applications in Environment and Industry

A thesis presented to

The Faculty of Graduate Studies

Of

Lakehead University

By

MOKALE KOGNOU ARISTIDE LAUREL

In partial fulfilment of the requirements for the degree of

Doctor of Philosophy in Biotechnology

Abstract

Cellulases and glucose isomerases are vital enzymes in converting cellulose into fructose. Cellulases catalyze cellulose conversion to glucose, while glucose isomerase catalyzes the reversible isomerization of glucose to fructose. There is a growing interest lately in producing bio-based chemicals and materials from fructose. Soil bacteria produce these enzymes. The characterization of bacteria for enzyme saccharification of biomass is essential for fructose production and reducing the time and cost of current bioconversion processes. From this perspective, we characterized novel cellulase and glucose isomerase-producing bacteria from soil samples and optimize their enzyme production. Coculturing and whole-cell immobilization for glucose isomerase and bacterial resistance to environmental factors were also investigated.

Six bacterial strains, *Paenarthrobacter* sp. MKAL1, *Hymenobacter* sp. MKAL2, *Mycobacterium* sp. MKAL3, *Stenotrophomonas* sp. MKAL4, *Chryseobacterium* sp. MKAL5 and *Bacillus* sp. MKAL6 were isolated from mixture soil samples collected at Kingfisher Lake and the University of Manitoba campus and identified using 16S rRNA gene sequence analysis. Using plate assay techniques, these strains were selected for cellulase and glucose isomerase production based on the clearance zone appearance. These strains displayed various morphological and biochemical characteristics.

Enzyme production was quantified using the 3,5-dinitrosalicylic acid (DNS) method. The efficient cellulase production in these strains occurred at the culture conditions of 35-40°C, pH 5-6, 1-2% CMC and 96 h of incubation. The presence of yeast extract, casein hydrolysate, Tryptone, sucrose, potassium chloride, cobalt chloride and magnesium chloride in the culture medium enhanced their cellulase production at their respective optimal pH and temperature. Tween 20 improved enzyme production only in strains MKAL2 (27.87-31.72 U/mL), MKAL4 (28.93-32.00

U/mL) and MKAL6 (33.99-35.91 U/mL) compared to control (23.23-28.71 U/mL). However, strains exhibited the highest cellulase activity (78.87-190.30 U/mL) when sucrose was used as a carbon compared to carboxymethyl cellulose (9.66- 18.06 U/mL). The response surface quadratic model was reliable in predicting cellulase production during the fermentation process with strains MKAL1, MKAL2, MKAL4 and MKAL5. The molecular weight of the cellulases is about 25 kDa.

Similarly, strains preferred the temperature of 40°C, pH 6-8 and 4 days of incubation for maximum glucose isomerase production. Xylose (8.35-11.92 U/mL) induced higher enzyme production production compared to CMC (3.28-5.82 U/mL) and glucose (1.88-3.82 U/mL). However, 1% xylose boosted maximum enzyme activity in all strains. The same trend was observed in the culture medium containing a mixture of peptone/yeast extract or tryptone/peptone (12.65-22.78 U/mL) or 2-2.5% wheat straw (9.81-13.90 U/mL). The response surface quadratic model was reliable in predicting glucose isomerase production during fermentation with strains MKAL1, MKAL3, MKAL5 and MKAL6.

Five cocultures (A, B, C, G and J) constructed from these strains exhibited synergism in cell growth and glucose isomerase production. The highest level of synergism (15.17 U/mL) was found in coculture J composed of *Mycobacterium* sp. MKAL3 (4.06 U/mL) and *Stenotrophomonas* sp. MKAL4 (3.37 U/mL) with a synergism degree of 2.04. The synergism was unique to growth on wheat straw as it was completely absent in xylose-grown cocultures. The wheat straw degradation synergism could rely on specific compounds released by strain MKAL3 that promote the strain MKAL4 activity and vice versa. However, immobilized strains MKAL1 (10.92 U/mL), MKAL2 (9.45 U/mL), MKAL3 (12.01 U/mL), MKAL4 (8.50 U/mL) and MKAL5 (9.69 U/mL) improved glucose isomerase production in the wheat straw fermentation process compared to the control (8.01-9.96 U/mL) at different sodium alginate concentrations.

All strains were capable of aggregating, forming biofilm and adhering to solvents. They accumulated chromium, lead, zinc, nickel and manganese and were resistant to lincomycin. Ciprofloxacin displayed the highest inhibitory activity and reduced viable cell numbers over 24 h. The ciprofloxacin also inhibited biofilm formation significantly by strains and increased crystal violet uptake in strains resulting in a change in permeability and structure of the bacterial cell wall layer.

This study revealed novel findings that bacterial strains *Paenarthrobacter* sp. MKAL1, *Hymenobacter* sp. MKAL2, *Mycobacterium* sp. MKAL3, *Stenotrophomonas* sp. MKAL4, *Chryseobacterium* sp. MKAL5 and *Bacillus* sp. MKAL6 can use low-cost agricultural residues for glucose isomerase production and enhance their enzyme activities through cocultures and whole-cell immobilization, minimizing down-streaming costs.

Acknowledgements

This present work was carried out to study the enzyme potential of isolated soil bacteria. We benefited from the collaboration of people to whom we would like to express our gratitude:

To my supervisors, Dr. Wensheng Qin (Lakehead University), Dr. Zi-Hua Jiang (Lakehead University) and Dr. Chunbao (Charles) Xu (Western University), for agreeing to supervise this work, for the rigorous follow-up and for the well-done job taste that you taught me, for the advice and encouragement, you have given me.

To my supervisory committee members, Dr. Zacharias Suntres, Dr. Jinqiang Hou and external examiner Dr. Guoxing Quan (Natural Resources Canada) for sharing their knowledge and support for my thesis despite their many occupations.

To the Natural Science and Engineering Research Council of Canada (NSERC) for the funding necessary to carry out this work through the Discovery Grant (RGPIN-2017-05366) to Dr. Wensheng Qin.

To Kristi Dysievick, Christina Richard, Michael Moore, Dr. Susanne Walford and Dr. Brenda Magajna for advice and follow-up during teaching sessions as a graduate assistant.

To my labmates, Chonlong Chio, Janak Raj Khatiwada, Sarita Shrestha and Xuantong Chen, for their excellent laboratory atmosphere, understanding and constant support during this work. The road was long but not interminable; good luck to you.

To my wife Motseu Josiane Laure, my parents, Kognou Mathieu and Djouadji, and brothers and sisters, Adjuikem Kognou, Lyne Carole, Saah Kognou Christian Landry, Kekounou Djuine Kognou Dallya and Kognou Tchinda Kevin Aubin for their multifaceted support and encouragement during my thesis.

Table of Contents

List of tables

CHAPTER 2

CHAPTER 3

CHAPTER 4

CHAPTER 5

List of figures

CHAPTER 1

CHAPTER 2

CHAPTER 3

CHAPTER 4

CHAPTER 5

Appendix

Introduction

The development acceleration of human societies and, consequently, demands for raw materials, products, and consumer goods have accentuated this requirement exerted on researchers to innovate new production processes and improve existing processes. Biotechnology has brought to this problem development tools that are essential today for industry and fundamental research where chemical methods alone struggle to meet environmental requirements and ensure process profitability.

According to the Food and Agricultural Organization of the United Nations (FAO, 2019), the consumption of caloric sweeteners, including fructose, is projected to rise from 33 million tonnes in 2017 to 213 million tonnes in 2027 due to the increase in world population, particularly in Asia and Africa. However, The United States and Canada are the two principal countries to use fructose, possibly due to the abundance of corn, agribusiness influence, politics, and economics.

To support this world demand, the agricultural crop residues can be a potential feedstock for fructose production because of their availability, low value, and rich lignocellulosic composition. The potential of agricultural crop residues is estimated at 55 million tonnes in Canada (Bentsen et al., 2016). Cellulose is the dominant waste material from agriculture. It occurs in different forms (amorphous and crystalline) in combination with other materials, such as lignin and hemicelluloses (Paudel and Qin, 2015). Due to the recalcitrant structure of lignin, the lignocellulosic biomass requires pretreatment. This pretreatment helps in the separation of its main biomass components. This process also decreases the cellulose crystallinity and solubilizes hemicellulose. It increases the surface area for enzyme binding and microbial attack.

The commercial production of fructose relies on the multienzyme hydrolysis of cellulose into two steps based on two major enzymes: cellulases and glucose isomerase (Souzanchi et al.,

2019). These enzymes are secreted by microorganisms including pure or mixed cultures of aerobic and anaerobic bacteria, yeasts, fungi and algae (Ginesy et al., 2017). Soil is a vast cellulolytic bacteria untapped reservoir. Many investigators have reported that some soil bacteria are good cellulose degraders because they grow fast at low temperatures and possess a high synergy between cellulases (Saxena et al., 1993; Schwarz, 2001; Ekperigin, 2007; Abghari and Chen, 2017).

However, strategies such as coculturing and whole-cell immobilization can be used to improve wild bacterial strains for enhanced enzyme production. Due to their morphological or physiological properties, Bacteria can form consortia and degrade lignocellulose synergistically.

The growing worldwide interest in fructose is because it is a highly attractive substrate in the cellulosic biomass conversion into bioproducts, biofuels and chemicals (Sun et al., 2018) and, therefore, a topical frontier to explore. The glucose isomerase world market is approximately one billion US dollars (Singh et al., 2020), while cellulases will reach 2300 million USD by the end of 2025 (Global cellulase market report, 2021). Hence, the need to search for bacteria with high-level production of these enzymes, efficient utilization of resulting sugars and appropriate fructose production performances.

This work aimed to find novel, efficient cellulase and glucose isomerase-producing bacteria from soil samples. To accomplish this goal, we have specifically proposed,

(1) To characterize cellulose-degrading bacteria and improve their cellulase production,

(2) To characterize glucose isomerase-producing bacteria and enhance their glucose isomerase production,

(3) To evaluate the effect of coculturing and whole-cell immobilization on glucose isomerase production in wheat straw fermentation and study the potential mechanism of cooperation in bacterial cocultures for a synergistic degradation,

(4) Investigate potential virulence, antibiotics and heavy metals resistance, solvent adhesion, and biofilm-forming capabilities of these cellulolytic bacteria.

This study hypothesized that:

(1) Soil is a potential reservoir for important bacteria with highly cellulolytic performances,

(2) Soil bacteria in coculture and immobilization forms secrete hydrolytic enzymes that act synergistically and, therefore can reduce the time and cost of current bioconversion processes,

(3) Soil bacteria can be pathogens.

References

Abghari A, Chen S (2017). Engineering *Yarrowia lipolytica* for enhanced production of lipid and citric Acid. *Fermentation*, 3, 34-49.

Bentsen NS, Lamers P, Lalonde C, Wellisch M, Bonner J (2016). Mobilization of agricultural residues for bioenergy and higher value bio-products: Resources, barriers and sustainability. IEA Bioenergy.

Ekperigin MM (2007). Preliminary studies of cellulase production by *Acinetobacter anitratus* and *Branhamella* sp. *Afr J Biotechnol*, 6, 28-33.

FAO (2019). OECD-FAO agricultural outlook 2018-2027, https://www.oecd-ilibrary.org/agriculture-and-food/data/oecd-agriculture-statistics_agr-data-en pp.

Ginesy M, Rusanova-Naydenova D, Rova U (2017). Tuning of the carbon-to-nitrogen ratio for the production of L-arginine by *Escherichia coli*. *Fermentation*, 3, 60-69.

Global Cellulase (CAS 9012-54-8) Market Growth 2021-2026 (2021). Available from: https://www.360researchreports.com/global-cellulase-cas-9012-54-8-sales-market-16610450. Accessed October 30, 2020.

Paudel PY, Qin W (2015). Characterization of novel cellulase-producing bacteria isolated from rotting wood samples. *Appl Biochem Biotechnol*, 177, 1186-1198.

Saxena S, Bahadur J, Varma A (1993). Cellulose and hemicellulose degrading bacteria from termite gut and mould soils of India. *Indian J Microbiol*, 33, 55-60.

Schwarz WH (2001). The cellulosome and cellulose degradation by anaerobic bacteria. Applied Microbiology and Biotechnology, 56: 634-649.

Singh TA, Jajoo A, Bhasin S (2020). Production and application of glucose isomerase from

Streptomyces enissocaesilis and amylase from *Streptomyces* sp. for the synthesis of high fructose corn syrup. *SN Appl Sci*, 2, 1968.

Souzanchi S, Nazari L, Rao, Yuan Z, Tan Z, Xu C (2019). Catalytic isomerization of glucose to fructose using heterogeneous solid base catalysts in a continuous-flow tubular reactor: Catalyst screening study. *Catal Today*, 319, 76-83.

Sun J, Li H, Huang H, Wang B, Xiag LP, Song G (2018). Integration of enzymatic and heterogeneous catalysis for one-pot production of fructose from glucose. *ChemSusChem*, 11, 1157-1162.

CHAPTER 1

Literature Review

1. Lignocellulosic biomass

Essentially of plant origin, lignocellulosic biomass represents billions of tons of residues from the agricultural and food industries and municipal waste produced annually, which requires treatment and management. These residues include straws, trunks, stems, branches, leaves, pulps and others. Historically, the plant cell walls of these residues contain lignocellulosic biomass. The latter consists mainly of three biopolymers: cellulose, hemicelluloses and lignin, and other low-content components such as pectin (a heteropolysaccharide), structural proteins or nitrogen compounds, minerals and water. The content of these three main constituents, cellulose, hemicelluloses and lignin, varies according to the material's type and source: hardwood, softwood or grasses. Generally, 35 to 50% of the dry weight of this biomass is made up of cellulose, and the latter is the component that determines the dense structure of this wall, while 20 to 35% of the dry weight is made up of hemicelluloses and 5 to 30% lignin (Wu et al., 2020). Hemicelluloses are three-dimensional hetero-polymers with few crystalline regions, which contain different C5 (xylose and arabinose) and C6 (mannose, galactose, rhamnose and glucose) sugar monomers. They have an amorphous structure and a degree of polymerization of around 200. B-1,4-glycosidic bonds link their units at the main chain level, and β-1,2-, β-1,3- bonds and β-1,6-glycosidic in the side chains. Lignin is a non-linear, heterogeneous, three-dimensional complex polymer consisting of phenylpropane (Guaiacylpropane (G), syringylpropane (S), p-hydroxyphenylpropane (H)) aromatic and hydrophobic units, formed by the polymerization of their precursors, cinnamic alcohols (Wang et al., 2017). These units are linked together by covalent bonds, either C-O-C ether bonds or C-C bonds. Lignin acts as a cement providing hardness to the cell wall and resistance

against biological attacks by microorganisms or insects. Cellulose, hemicellulose and lignin are linked together by chemical bonds, of which the hydrogen bond is the central intermolecular bond. Glycosidic and hydrogen bonds link cellulose and hemicellulose, while hemicellulose is closely linked to lignin by covalent bonds, making total separation difficult. However, the interactions between cellulose and lignin are hydrogen bonds (Cai et al., 2017).

Previously, lignocellulosic biomass was used as a direct energy source, usually by direct combustion, and after it was transformed into charcoal by carbonization. However, recently, the direct conversion of lignocellulosic biomass into valuable bioproducts is gaining momentum since it is a raw material with high potential, which can be converted directly into biofuels and bioproducts due to its high carbohydrate content which essentially comes down to the presence of the cellulosic fraction (Sindhu et al., 2016).

2. Cellulose

Cellulose is the most abundant natural polysaccharide. Thus, cellulose is a sustainable resource with valued applications from agro-industrial and agricultural wastes. It is a linear polysaccharide composed of glucose units connected by β-1,4-glycosidic bonds, and the smallest repetitive unit is cellobiose. Its structure is partially crystalline and insoluble at room temperature in organic solvents, diluted acids and alkalis (Toushik et al., 2017; Zhong et al., 2019). Its structure is also interspersed with disordered or disorganized domains (amorphous cellulose), constituting 5–20 % of the microfibril. These amorphous regions are linked by suboptimal hydrogen bonding interactions, making them accessible to water molecules and enzymatic attacks. The complete cellulose enzyme degradation to glucose is achieved by the synergistic action of three enzymes:

endoglucanases, exoglucanases and β-glucosidases (Lenting and Warmoeskerken, 2001; Ioelovich, 2008).

3. Cellulases

3.1. Classification of cellulases and their functional properties

Cellulases are hydrolytic enzymes that break down β-1,4-glycosidic bonds between glucose units of cellulose. The cellulose conversion into glucose can be performed by chemical or enzymatic hydrolysis. Under extreme conditions, chemical hydrolysis uses inorganic acids, leading to lower molecular weight sugars and other degradation products. Cellulases are a complex enzyme system belonging to glycosyl hydrolase families and composed of three enzymes: endoglucanase, exoglucanase and β-glucosidase, which act synergistically for the complete cellulose hydrolysis (Figure 1). Thus, endoglucanase and endoglucanase synergistically transform cellulose into small oligosaccharides, and then β-glucosidase hydrolyzes oligosaccharides into glucose (Sindhu et al., 2016). Specifically, endoglucanase randomly attacks internal sites of the amorphous regions and generates new chain ends and oligosaccharides with varied lengths. It is inactive on crystalline cellulose but active on soluble cellulose forms like carboxymethyl cellulose and amorphous. Exoglucanase or cellobiohydrolase acts on reducing (cellobiohydrolase type I) and non-reducing (cellobiohydrolase type II) ends of the cellulose chain, releasing glucose and cellobioses. It is active on crystalline substrates like avicel, cellooligosaccharides, etc. β-glucosidase acts on non-reducing ends and hydrolyzes cellooligosacharides and cellobiose to glucose. It is inactive on both amorphous and crystalline cellulose (Sharma et al., 2016). The

enzyme hydrolysis of cellulose into glucose units depends on crystallinity, polymerization degree, particle size and pore volume and availability of surface area (Sher et al., 2021).

Three properties govern the cascading depolymerization activity of cellulase, namely (1) synergism, (2) processivity, and (3) substrate-channeling ability of the enzyme. The catalytic mechanism (Figure 2) is the classical acid-catalyst hydrolysis model (Obeng et al., 2017). This model relies on two critical amino acid residues (a proton donor and a nucleophile) that facilitate the enzyme cleavage of glycosidic bonds by stereochemical modification (i.e., retention or inversion) of the anomeric carbon configuration (Garvey et al., 2013).

3.2. Main sources of cellulases

Cellulases are produced by several microorganisms such as anaerobic bacteria in the ruminant digestive tract (*Clostridium* spp., *Ruminococcus* spp., *Caldicoprobacter* spp.), aerobic bacteria (*Bacillus* spp., *Cellulomonas* spp.), filamentous fungi (*Aspergillus nidulans*, *A. niger*, *A. oryzae*, *Fusarium* spp., *Trichoderma viride*, *T. reesei*), and actinomycetes (*Microbispora* spp., *Thermomonospora* spp., *Streptomyces* spp.) (Shida et al., 2016; Singhania et al., 2017; Soni et al., 2018; Kumar et al., 2019; Sampathkumar et al., 2019; Verma et al., 2021). Fungi are the most cellulase producers, and *Trichoderma reesei* is widely used for cellulase production. Other fungi such as *Humicola* spp., *Penicillium* spp., *Gloeophyllum* spp., *Melanocarpus* spp. and *Aspergillus* spp. exhibit high enzyme production (Kumar et al., 2019; Ramesh et al., 2020). Cellulase is constitutive of bacteria, whereas fungi produce cellulose only in the presence of cellulose. Extremophile bacteria are also widely used to produce high stability cellulases because they can survive in harsh conditions (Kumar et al., 2019). Bacteria from the genus Bacillus (*B. amyloliquefaciens*, *B. licheniformis*, *B. circulans*, *B. subtilis*, *B. agaradhaerans*, *B. pumilus* and *B.*

thuringiensis) and genus Clostridium (*C. acetobutylicum*, *C. cellulovorans*, *C. cellulolyticum*, *C. cellulovorans* and *C. thermocellum*) are the main cellulase producing bacteria (Soni et al., 2018). Mesophilic bacteria (*Cytophaga hutchinsonii*, *Cellvibrio fulvus*, *Cellvibrio gilvus*, *Erwinia carotovora* and *Paenibacillus* spp.), archaebacteria (*Pyrococcus horikoshii* and *Thermotoga neapolitana*) and various organisms (protists, molluscs, insects, nematodes, crustaceans and annelids) have been also well documented for their cellulase activities (Ando et al., 2002; Varghese et al., 2017).

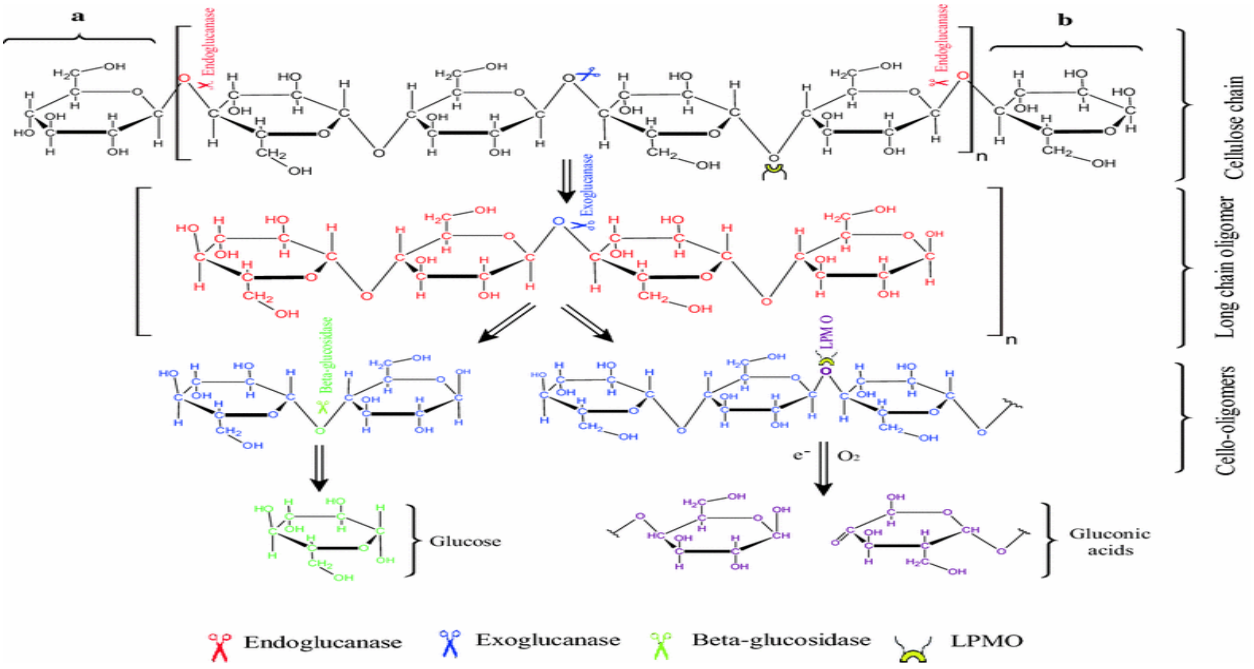

Figure 1. Different steps of cellulose hydrolysis: (a) the non-reducing end, (b) the reducing end. Endoglucanase cleaves amorphous cellulose sites to yield long-chain oligomers; exoglucanase processively attacks crystalline areas to produce cello-oligomers, and β-glucosidase hydrolyzes cellobiose to fermentable sugars. Lytic polysaccharide mono-oxygenase (LPMO) oxidizes glycosidic linkages along the cellulose chain to yield gluconic acids (Adopted from Obeng et al., 2017).

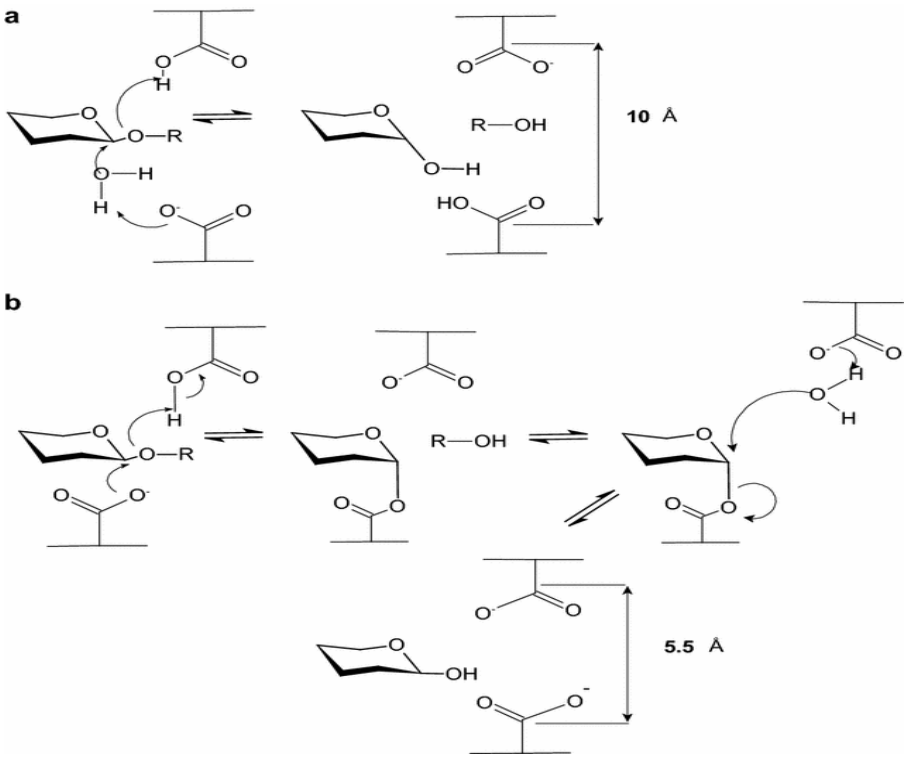

Figure 2. Molecular mechanism of cellulase: inversion (a) and retention (b) mechanisms leading to effective cellulosic substrates hydrolysis (Adopted from Obeng et al., 2017).

3.3. Parameters affecting cellulase production

Enzyme production is the most critical stage in enzyme technology because this step determines the overall process cost. The method used by microbes to convert polymers into monomers via enzyme production is fermentation. Each microorganism has specific requirements for optimum enzyme production. Enzyme activity optimization is generally performed using either a one-variable-at-a-time or statistical approach. Consequently, enzyme production is widely affected by various growth parameters such as fermentation method, pH, incubation temperature, incubation period, nitrogen and carbon sources (Ohara et al., 2018).

Two fermentation method types are used for enzyme production: submerged (SmF) and solid-state fermentation (SSF). In SmF, all essential nutrients are dissolved in liquid media to be utilised by microbes. The extracellular enzyme is produced in the medium and separated by centrifugation. This method allows easy sterilization, parameter monitoring and a quick down streaming process. However, little moisture is used in SSF. Nitrogen sources induce protein synthesis that is essential for extracellular enzyme production (Soccol et al., 2017).

Most cellulase-producing microorganisms prefer temperature ranges of 25-35°C (Maryana et al., 2015; Zhao et al., 2018; Ezeilo et al., 2019, Verma et al., 2021). Some cellulases from recombinant microbes (*Geobacillus* sp. HTA426, *Geobacillus* sp. 70PC53, *Bacillus* sp SR22, *Talaromyces emersonii*, *Thermoascus aurantiacus*, etc.) exhibited the best cellulase production performance at elevated temperatures of 60 to 100°C (Hong et al., 2007; Ng et al., 2009; Voutilainen et al., 2010; Potprommanee et al., 2017; Dos Santos et al., 2018; Patel et al., 2019; Ajeje et al., 2021).

Most microorganisms produced cellulase in pH 5-7 (Liming and Xueliang, 2004; Lah et al., 2016; Dey et al., 2018; Sirohi et al., 2019, Ariff et al., 2019). Only a few microorganisms as *Aspergillus terreus* AV49 (pH 4.0), *Bacillus velezensis* (pH 4.72), *Trichoderma asperellum* UPM-1, *Trichoderma* sp .414 and *Penicillium decumbans* (pH 4.5) required pH lesser than 5 for better cellulase production. However, *Micromonospora* sp., *Halomonas* sp. PS47, *Bacillus halodurance* IND18, *Trichoderma viridae* and *Bacillus subtilis* IND19 were most efective at pH 7.2, 7.5, 8 and 8.41 respectively (Nair et al., 2018; Ariff et al., 2019; Verma et al., 2021).

Various substrates have been used for fermentation cellulase production. Insoluble carbon sources (cotton, avicel, etc.) promoted higher cellulase than soluble carbon sources (lactose, sucrose, cellobiose, carboxymethyl cellulose, etc.) at the same concentration. Pure cellulose is too

expensive to produce on a large enzyme scale. However, agricultural, industrial and municipal lignocellulosic wastes are particularly attractive in bioconversion because they are cheaper carbon sources for enzyme production (Paniagua et al., 2016). The recalcitrant structure of lignin limits cellulosic biomass biodegradation. Thus, biomass pretreatment before enzyme hydrolysis is required. The pretreatment causes a disturbance in the biomass structure by increasing cellulose accessibility, reducing cellulose cross-linking with hemicelluloses and lignin, modifying biomass morphology, reducing cellulose crystallinity and increasing biomass porosity. Several lignocellulosic wastes such as wheat straw (Eitner et al., 2016; Ursachi and Gutt, 2020; Sharma et al., 2021), wheat bran (Biswas et al., 2019, Verma and Kumar, 2020; Vu et al., 2022), Sugarcane bagasse (Pramanik et al., 2020; Tiwari et al., 2022), Rice husk (Cacua et al., 2018; Nugraha et al., 2021), rice bran (Li et al., 2022), orange peel (Padmanabhan et al., 2022), pulp (Kosan et al., 2020), corn stover (Lu et al., 2020), corn cob (Winarsih and Siskawardani, 2020; Elegbede et al., 2021), corn fiber (Beri et al., 2020; Beri et al., 2021), cotton fiber (Banerjee et al., 2020), saw dust (Zapata et al., 2018; Banerjee et al., 2020), tobacco waste (Dai et al., 2020), soya bean hull (Bittencourt et al., 2022), castor bean meal (Herculano et al., 2011), oil palm trunk (Ezeilo et al., 2020), *Arachis hypogaea* shells (Sulyman et al., 2020) were used for cellulase production.

3.4. Recent approaches and future strategies

The obstacles to industrial enzyme applications are production costs and low enzyme yields. Although many investigations have been reported for enzyme production, there is a lot of need to improve the efficiency of biomass waste exploitation technologies at different levels (biomass composition, media compound optimization, operational parameters and microbial strains) to decrease enzyme production costs.

3.4.1. Biomass composition

Lignin monomer composition (syringyl/guaiacyl unit ratio) and cross-linking (ether and ester linkages) between lignins and branched side chain polysaccharides such as hemicelluloses and pectins impact polymerization and further the saccharification process. Alkaline pretreatments efficiently cleave ester linkages. The manipulation of transcriptional control of lignification enzymes of the phenylpropanoid biosynthetic pathways has recently been used to improve biomass feedstocks (Xie et al., 2018; Yadav et al., 2020). O-diphenolic precursor introduction has newly enhanced lignin removal after pretreatment. Furthermore, overexpression of a modified methyl transferase and bacterial lyase could reduce lignin polymerization degree (Yuan et al., 2021; Yao et al., 2022).

3.4.2. Media compounds and operational parameters

Modification of nutritional and physicochemical parameters (media, temperature, pH, agitation, incubation period, inoculum size, moisture level, inducers, minerals, additives, nitrogen and carbon sources) could increase the fermentation yield and reduce production costs. Siani et al. (2015) reported that media engineering enhanced cellulase production in *Penicillium oxalicum* by 1.7-fold.

Due to the inherent complexity and heterogeneity of lignocellulosic biomass, efficient biodegradation requires the efficiency of different hydrolytic cellulases, which can tolerate stress from solvents (ionic liquids, organic solvents, concentrated seawater) and simplify the scale-up of industrial processes in non-conventional media (Kazlauskas, 2018). Also, ionic liquids are highly attractive for dissolution, fractionation, and biomass enzyme depolymerization (Socha et al., 2014). However, the deactivation/destabilization of cellulases in non-conventional media is a

major challenge for their application in the biocatalytic conversion of biomass (Guerriero et al., 2016). Therefore, cellulase destabilization in non-conventional media requires engineering strategies for their application in biomass degradation (Kazlauskas, 2018; Contreras et al., 2020). Succinylation of the cellulase cocktail from *Trichoderma reesei* boosted nearly 2-fold cellulose conversion by 15% (v/v) 1-butyl-3-methylimidazolium chloride (Nordwald et al., 2014). The enhancement in activity upon succinylation was due to the apparent preferential exclusion of the Cl- anion in fluorescence quenching assays. These experiments induced charge modification without substitution in cellulase. However, the actual charge substitution charge remains unknown. Wolski et al. (2016) revealed cellulase (Cel7A) from *Talaromyces emersonii* was more active and stable than wild-type *Talaromyces emersonii* cellulase or *Trichoderma reesei* cellulase in ionic liquid co-solvents. Pottkämper et al. (2009) isolated cellulases active in ionic liquid from metagenomic library. Chen et al. (2013) enhanced the activity of a thermophilic cellulase Cel5A using ionic liquid pretreated switchgrass. Siva et al. (2022) reported enhanced cellulase production by *Aspergillus niger* using culture medium containing iron oxide magnetic nanocomposites.

Statistical optimization methods have overcome classical empirical method limitations in fermentation processes. The response surface methodology (RSM) has effectively standardized fermentation parameters such as pH, temperature, agitation, substrate concentration, nitrogen, and carbon source type. Plackett–Burman, Box-Behnken, and central composite designs alone or in combination are the most used statistical tools for independent variable screening and fermentation condition optimization, significantly influencing enzyme production. Cellulase productions by *Bacillus amyloliquefaciens* MBAA3 (Thakkar and Saraf, 2014), *Actinomyces* sp. (Liu et al., 2020) and *Pseudomonas aeruginosa* (Ibrahim et al.,2021) were enhanced using Plackett–Burman design. Using a combination of Plackett–Burman and central composite designs maximize *Trichoderma*

reesei RUT C30 cellulase production (Singhania et al., 2007). Box-Behnken design also enhanced cellulase production in *Saccharomyces cerevisiae* SCPW 17 (Amadi et al., 2020), *Aspergillus heteromorphus* (Bajar et al., 2020), *Aspergillus niger* ITV 02 (Infanzón-Rodríguez et al., 2020), *Botrytis ricini* URM 5627 (Silva et al., 2021) and *Mucor circinelloides* and *M. hiemalis* (Al Moussa et al., 2022).

3.4.3. Microbial strain

3.4.3.1. Mixed cultures strategy

The hydrolysis of cellulose to glucose relies on the synergistic action of endo-β-1,4-glucanases, cellobiohydrolases, and β-glucosidases (Malgas et al., 2017). However, some factors influence cellulase synergy, such as ratio and cellulase concentration in the reaction mixture. For instance, low endoglucanase ratios lead to the most potent synergistic action in the endoglucanase-exoglucanase mix (Boisset et al., 2001). Also, the access of a cellulase mixture to binding sites where endo-β-1,4-glucanases facilitate the cellobiohydrolase release limits the synergistic activity (Jalak et al., 2012). Physical and chemical substrate heterogeneity also influences the synergy degree between cellulases. Therefore, the molecular mechanism of understanding cellulose hydrolysis by cellulase mixtures is crucial and remains to be elucidated (Contreras et al., 2020). However, Chownk et al. (2019) showed a synergistic action of *Bacillus* sp. and *Microbacterium* sp. for improved cellulase production on rice straw pretreated with dilute acid. Associated with a microalgae *Chlorococcum* sp., cellulase activity of *Bacillus licheniformis* KY962963 was enhanced using a one variable at a time approach and Box–Behnken design (Shah and Mishra, 2020). Coculture of *Bacillus licheniformis* and *B. paralicheniformis* enhanced cellulase production

on microcrystalline cellulose and chicken manure-supplemented rice bran media (Kazeem et al., 2021).

3.4.3.2. Mutagenesis and protoplast fusion

Microbial strain improvement has been performed by mutation, selection or genetic recombination resulting in isolating mutants with high productivity. Mutations are primarily harmful but can occasionally improve biocatalytic performance. The mutation relies on a vital property conferred by DNA and thus, creating new variations in the gene pool using UV radiation and chemicals (Ethidium bromide, N-methyl-N'-nitro-N-nitrosoguanidine, Ethyl Methanesulfonate, etc.) (Adsul et al., 2007). Recently developed by Tsinghua University, atmosphere plasma mutation is a remarkable mutagenesis strategy leading to rapid mutation, highly diverse mutants and simple and safe application. It is a whole-cell mutagenesis tool based on a radio-frequency atmospheric-pressure glow discharge plasma. It exhibits higher mutation rates than UV radiation or chemical mutagens while maintaining low treatment temperatures for phenotypic enhancement in many microbial strains (Ottenheim et al., 2018). Mutants of *Talaromyces pinophilus* OPC4-1 developed by consecutive UV radiation, N-methyl-N`-nitro-N-nitrosoguanidine and ethyl methane sulfonate treatment improved cellulase production (Liu et al., 2020). Ega et al. (2020) improve the cellulase activity of *Bacillus subtilis* VS15 by creating mutants using ethyl methyl sulfonate, N-Methyl-N′ nitro-N-nitrosoguanidine, and ultraviolet light followed by recursive protoplast fusion. Silva et al. (2020) revealed a novel *Trichoderma reesei* mutant RP698 with enhanced cellulase production obtained by exposure to ultraviolet light. Peng et al. (2021) reported an enhanced cellulase activity in a mutant of *Trichoderma afroharzianum* obtained by random mutagenesis (N-methyl-N'-nitro-N-nitrosoguanidine, ethyl

methanesulfonate, atmospheric and room temperature plasma) with adaptive laboratory evolution strategy (high sugar stress). Papzan et al. (2021) enhanced cellulase activity of *Trichoderma* sp. through two-step protoplast fusion.

3.4.3.3. Gene modification, metabolic pathway and genetic engineering application

Genetic engineering plays a vital role in desired product improvement by altering the genetic makeup of the wild-type strains, modifying the genes involved in carbohydrate biosynthesis, and facilitating increased sugar yield to enhance the production of the required component or product. Cloning cellulases encoding genes from microbes and their expression analysis can result in a significant upsurge in using viable natural resources for developing low-cost industrial applications. Efficient molecular and genetic engineering methods can generate desired and required modifications in robust genetic circuits and deliver dominant gears for engineering acquired organisms to produce cellulase. The aspiring aim and current task are to present the existing scenario and prospective enigma of genetic manipulations of different biological systems and further investigate the intricacy of gene architecture for ample cellulase production shortly (Misra et al., 2019). Many genetic approaches (forward and reverse genetics) improved the inhibitor tolerance capability of microbial strains. Forward genetics approaches use ALE (Adaptive Laboratory Evolution is a practical approach for studying the genetic and biochemical basis for microbial adaptation under a selection pressure) or mutagenesis approaches to develop mutants with desired phenotypes. In contrast, reverse genetics is an omics-based system, metabolic engineering methods to associate genetic contenders with desired phenotypes and further transfer the genetic contenders into the host strains for sturdiness improvement. Afterwards, genetic information can be read by technologies such as next-generation sequencing

(NGS) and mass spectrometry (Phaneuf et al., 2020). Synthetic biology is a technique to construct a novel biological system to produce fuels and chemicals from renewable sources cost-effectively. The engineered biological systems created by synthetic biology include enzymes with new functions, genetic circuits, and engineered cells with unique and desired specifications. In many cases, the ultimate objective is to rationally manipulate organisms to facilitate novel functions which do not usually exist in nature. It is a sustainable approach to enhancing the production of cellulase enzymes. Using recombinant expression technology, highly active and stable cellulases at a low cost can be produced (Srivastava et al., 2019).

The genetic algorithm (GA) application has been used in modelling and optimising cellulase production. Process parameters were optimised using mathematical (MO) and genetic optimizers to obtain a combination of variables for the highest possible enzyme activity. This investigation highlights that GA could be a potential optimizer for waste utilisation processes. Sirohi et al. (2018) used a genetic algorithm for enhanced cellulase production by *Trichoderma reesei*. Li et al. (2022) enhanced cellulase production in *Penicillium oxalicum* R4 using Box–Behnken design and an artificial neural network–genetic algorithm.

Epigenetics (an emerging area that alters a gene's expression rate) increased cellulase production by modulating various genetic factors like the promoter, transcription factors, repressors, and accessory proteins. Cai et al. (2022) showed that the knockout of DNA methylation modulator gene dmm2 significantly increased cellulase production in *Trichoderma reesei*. Sun et al. (2022) revealed that selected regulatory or functional genes within an arbitrarily defined stage could be pooled to enhance cellulase production in *Trichoderma reesei*.

Cellulase genes isolation from various thermophilic bacteria improved cellulase activity through recombinant technology (classical approach, whole-genome isolation, whole metagenome

isolation and bioinformatics) relying on manipulating the regulation of cellulase expression by upregulating activators and/or downregulating repressors of cellulase genes (Sahoo et al., 2018).

Glycosylation of cellulases is an effective enzyme engineering way for better applications. Most fungal cellulases are both N- and O-glycosylated in their native form. Glycosylation confers many beneficial properties to cellulases, including enhanced activity, thermal and proteolytic stability and structural stabilization. Manipulating glycan structures use the genetic tuning of glycan-active enzymes expressed from homogeneous and heterologous fungal hosts (Chung et al., 2019). Pena et al. (2020) reported that targeting Cel7A linker flexibility by point mutations, including modification of glycosylation sites, is a promising design strategy to improve cellulase activity in *Trichoderma reesei*.

3.4.4. Industrial applications of cellulases

Cellulases are used in various industries such as agriculture, food, wine, Fermentation, biofuel, biorefinery, detergents, textiles, pulp and paper (Sharma et al., 2016; Ejaz et al., 2021).

3.4.4.1. Textile industry

The textile industry has been confronted with rising environmental problems, so enzyme treatment has emerged as an environmentally friendly solution and relies on biostonewashing (or biostoning), biopolishing, bioscouring, lyocell defibrillation, biocarbonization and wool scouring processes. In the biostoning process of denim garments, cellulases promote dye removal from the fibril surface without affecting fiber strength and creating the shaded look of the fabric. They can also be combined with other enzymes such as proteases, lipases and xylanases to achieve a particular end. Bioscouring consists of removing non-cellulosic material from the surface of the

cotton fabric. The combination of pectinases and cellulases allows cellulases penetration in the cuticle and hydrolyzes the primary cellulosic wall, ultimately destructing the cuticle resulting in enhanced scouring efficiency. Pectinases play a crucial role in enzyme scouring by digesting the pectin, thereby removing the connection between the cuticle and the cotton fiber's main body. This treatment helped in retaining fiber strength with increased fabric softness. Biocarbonization and wool scouring is a biological fabric cleaning method from the cellulosic and vegetable matter impurities using cellulases or a combination with pectinases promoting fiber weight and strength maintenance. Acidic cellulases eliminate fibrils from pure lyocell, whereas mixed lyocell fabrics have been successfully treated with cellulases active at neutral pH. These treatments increased softness and appearance, prevented fuzz and pill, and improved appearance even after repeated washings (Juturu and Wu, 2014; Ahmed and Bibi, 2018).

3.4.4.2. Pulp and paper industry

Through deinking and pulping treatments, cellulases have successfully removed pollutant particles without affecting paper brightness and strength. Refining wood material generates small particles that cause a reduction in the pulp's drainage rate during papermaking. Combined with hemicellulases, cellulases improved pulp beating degree and handsheet tensile index. Biodeinking prevented fiber yellowing using cellulases and hemicellulases, which release ink from the fiber surface and enhance the fibres' brightness, cleanliness and strength (Kuhad et al., 2011).

3.4.4.3. Laundry and detergent industries

Cellulases are commonly used in detergents for cleaning textiles. They promote softness and color brightness fabric enhancement and remove dirt particles entangled in the garments. They can be associated with proteases and lipases for the same purpose (Sharma et al., 2016).

3.4.4.4. Animal feed industry

Cellulases are used in milk yield production, feed digestibility and nutritional availability in ruminants. Cellulases degrade partially lignocellulose materials leading to better emulsification that improves digestibility and nutrition availability to the animals. Combined with xylanases, they significantly reduce a high fiber diet viscosity in poultry and pig feed. By consuming a pretreated meal with cellulases, ruminants produce more milk (Asmare, 2014).

3.4.4.5. Food Processing industry

Cellulases are used in food biotechnology in various processes such as juice clarification, purees concentration, fruit sensory property alteration, nectar viscosity reduction, olive oil extraction, bakery product quality enhancement, carotenoid extraction for food color production, citrus fruit bitterness control, antioxidant release from fruit and vegetable pomace, and barley malting improvement in beer manufacturing (Raveendran et al., 2018).

4. High-fructose corn syrup production and its new applications for 5-hydroxymethylfurfural and value-added furan derivatives: Promises and challenges

Adapted from: Aristide Laurel Mokale Kognou[1], Sarita Shrestha[1], Zi-Hua Jiang[2], Chunbao (Charles) Xu[3], Fubao Sun[4], Wensheng Qin[1]*

Journal of Bioresources and Bioproducts, 2022

[1]Department of Biology, Lakehead University, Thunder Bay, Ontario, Canada

[2]Department of Chemistry, Lakehead University, Thunder Bay, Ontario, Canada

[3]Department of Chemical and Biochemical Engineering, Western University, London, Ontario, Canada

[4]School of Biotechnology, Jiangnan University, China

*Corresponding author: Wensheng Qin

Abstract

High fructose corn syrup has been industrially produced by converting glucose to fructose by glucose isomerases, tetrameric metalloenzymes widely used in industrial biocatalysis. Advances in enzyme engineering and commercial production of glucose isomerase have paved the way to explore more efficient variants of these enzymes. 5-hydroxymethylfurfural can be produced from high fructose corn syrup catalytic dehydration. 5-hydroxymethylfurfural as a promising platform chemical can be further converted into various furanic compounds chemically or biologically for various industrial applications. Although the chemical conversion of 5-hydroxymethylfurfural into furanic compounds has been extensively investigated in recent years, bioconversion has shown promise for its mild conditions due to the harsh chemical reaction conditions. This review

discusses protein engineering potential for improving glucose isomerase production and recent advancements in bioconversion of 5-hydroxymethylfurfural into value-added furanic derivatives. It suggests biological strategies for the industrial transformation of 5-hydroxymethylfurfural.

Keywords: High fructose corn syrup, glucose isomerase, rational enzyme engineering, directed evolution, furanic derivatives, biocatalysts

4.1. Introduction

High-fructose corn syrup (HFCS) is derived from cornstarch via two steps: (a) enzymatic hydrolysis of starch to glucose followed by isomerization of glucose into fructose and (b) fractionation process (Souzanchi et al., 2019). HFCS is rich in fructose than pure glucose in corn syrup (100% glucose). Various HFCS formulations are available, such as HFCS 90 (90% fructose and 10% glucose), HFCS 55 (55% fructose and 45% glucose), and HFCS 42 (42% fructose and 58 % glucose), which are named according to the % amount of fructose (and glucose) present (Fernandes, 2018; Neifar et al., 2019). The enzymatic isomerization of glucose into fructose by glucose isomerase (or xylose isomerase) is crucial. This step most often comes up against glucose isomerase inactivation at high temperatures and acidic pH. The higher affinity of glucose isomerase for glucose than xylose, cation-dependence and optimal fructose concentrations also affect this step (Nam, 2022). High temperature and high glucose content shorten the isomerization time. An increased risk of microbial infection can occur at low reaction temperatures. Thus, using an enzyme at high temperatures and acidic pH could improve the process efficiency and reduce the formation of by-products (Pederson, 1993). To overcome these problems, improved processes were developed by screening new overproducer strains, optimization of growth conditions,

mutation induction, protoplast fusion, enzyme engineering, immobilization and co-immobilization (Neifar et al., 2020). Several immobilizing agents maintained the involved enzymes in the HFCS production and their reuse during several operating cycles (Shokri et al., 2021). The combination of the different steps into a one-step process by enzyme co-immobilization increased the fructose yield (Basso and Serban, 2019). Enzyme engineering obtained enzymes that meet high thermostability, acid tolerance and resistance to substrate/product inhibition (Wiltschi et al., 2020). There is scope for further improvement in enzyme engineering to expand an economically feasible commercial process. However, many investigators have reported an increased risk for diseases (heart disease, diabetes, liver disease, cardiovascular disorders and metabolic syndromes) over recent years due to HFCS consumption (Olsen and Heitmann, 2009; Bocarsly et al., 2010; Mock et al., 2017; Ibrahim et al., 2018; Ozkan and Yakan, 2019; Sadowska et Rygielska, 2019). They also showed that 5-hydroxymethylfurfural (HMF), formed on long storage of HFCS, negatively affects human health (carcinogenic agent), causing controversy on HFCS food additive (Shapla et al., 2018; Gregorc et al., 2020). However, HMF is a precursor of valuable bio-based chemicals and materials synthesis. Thus, HFCS can be used for other purposes. Challenges in molecular enzyme engineering and new applications of HFCS are discussed in this paper. First, challenges in enzyme engineering for the HFCS production are described, then a review on value-added HMF derivatives and recent advancements in HMF conversion through biocatalysts. Finally, this paper expands on challenges in HMF bioconversion and perspectives to produce HMF derivatives on a large scale.

4.2. Challenges of HFCS Production

Several methods including chemical modification of glucose isomerase, X-ray crystallography and isotope exchange helped in elucidating the action mechanism of glucose isomerase for the conversion of glucose to fructose. This mechanism involves acid/base catalysis and is governed by three steps: (1) substrate ring opening , (2) isomerization through a hydride shift from C-2 to C-1 and (3) product ring closure (Figure 3) (Desai et al., 2017). Understanding the mechanism of action of GI has led to the development of molecular engineering models (rationale enzyme engineering and directed evolution of enzyme) to enhance the GI activity in the production of HFCS.

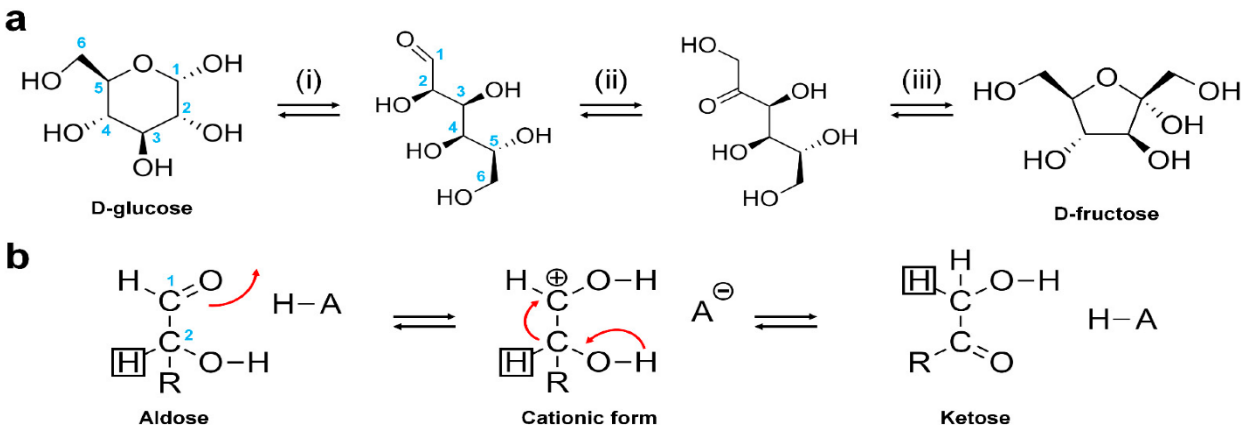

Figure 3. Action mechanism of glucose isomerase in the conversion of glucose to fructose , (a) Three major steps involved, (b) Hydride shift model (Adopted from Nam, 2022).

4.2.1. Rational enzyme engineering

Molecular enzyme engineering is focused on homologous enzymes and the study of enzyme-substrate interactions (enzyme active site) and reaction mechanisms based on

biochemical, sequence and structural information for the mutant design. Limited knowledge of the protein dynamics role and the quantitative input of specific interactions and catalysis are challenges in rational enzyme engineering. The study of enzyme-substrate interactions can lead to beneficial mutations and enzyme activity loss. However, data on protein sequence and rapidly developing computational tools keep increasing and making enzyme engineering more valuable by improving enzyme properties (catalytic rate, substrate scope, stability to solvent and high temperatures).

Glucose isomerase rational engineering was conducted for more cost-efficient HFCS production. The fructose yield, increasing with increasing temperature, and investigations on glucose isomerase thermoresistant variants were efficient in glucose isomerization. It was also possible to increase the thermoresistance of a highly active enzyme (Jin et al., 2017; Dai et al., 2020). Activity improvement at lower pH is another engineering target in HFCS production because this prevents the browning effect and impurities development (Neifar et al., 2020). The substrate specificity of GI was also changed, creating more space in the active site and providing additional hydrogen bonds. Therefore, xylose preference was switched to glucose which is advantageous for HFCS production. Besides these applications, enzyme mechanisms and specific residues' roles (metal-binding groups) were elucidated through enzyme rational engineering. Mutagenesis studies on several microbes (*Escherichia coli*, *Streptomyces rubiginosus*, *Streptomyces olivochromogenes*, *Streptomyces* sp., *Bacillus* sp., *Pichia pastoris*) revealed essential roles of active sites residues of GI for pyranose or furanose ring-opening and metal-mediated hydride transfer (Liu et al., 2015). A double glucose isomerase mutation from *Streptomyces* sp. at the histidine level (His 54 and His 220) increased its stability to calcium inhibition following the narrowing of the catalytic ion binding site. This mutation increased its thermostability due to the

helixα1 stabilization by new hydrophobic interactions (Hajer et al., 2014). Park et al. (2018) characterized a mutant glucose isomerase tolerant to calcium and zinc from *Anoxybacillus kamchatkensis* G10. It has also been shown that a double mutation in the amino acids Gly219 and Phe53 improves the activity and thermostability of this enzyme (Hlima et al., 2013). Other amino acids such as Ala103, Gly and Phe94 are involved in glucose isomerase thermostability and acid tolerance. Driven by ribosomal RNA promoters, an antibiotic resistance marker-free system increased glucose isomerase expression in *Streptomyces rubiginosus* (Wang et al., 2019). Ribosomal RNA would be influential promoters used in protein and metabolic engineering.

For better performance in cell-free biocatalytic procedures, improving an *in vivo* application of enzyme engineering is more complicated than engineering enzyme variants. GI is well-expressed in some cell hosts allowing to estimate expected *in vivo* enzyme activity from cellular expression and *in vitro* kinetic parameters. However, this activity affects the xylose/glucose supported the growth of host cells, especially under anoxic conditions. Thus, due to the complexity of the cytoplasmic matrix, it is difficult to predict and measure real *in vivo* activity. Also, having two metal-binding sites, GI can link *in vivo* any metal with harmful effects on activity, making required kinetic and biochemical properties difficultly definable for host cell growth rates. *In vivo* performance tests could be an excellent way to improve GI activity. The design and use of targeted mutants' libraries would be beneficial because positive effects and better prediction would be high. This would limit investigations to discover improved enzymes. However, the active site of GI is highly conserved. Thus, the prediction of mutations is unlikely because most conserved residues surrounding the active site are involved in metal and substrate binding. It is, therefore, challenging to introduce mutations at this level. The pH of cell host cytoplasm is generally slightly acidic so that lower pH could improve *in vivo* performances (Lee

et al., 2017; Silva et al., 2021). Other approaches such as metal specificity change or substrate binding affinity enhancing could positively impact *in vivo* performance of GI. Currently, enzyme properties linked to the performances *in vivo* are not elucidated. Therefore, the rational engineering of GI is complicated because of the two metals requirement, metal-enzyme interactions and variable *in vivo* metal availability. Given these challenges, the applicability of mutant based on *in vivo* strategies will be crucial for glucose isomerase engineering in HFCS production.

4.2.2. Directed evolution of enzyme

Glucose isomerase activity through microbial glucose metabolism can be enhanced by directed evolution or by introducing a better performing enzyme. Directed evolution of an enzyme is a natural selection-like strategy (Figure 4). It screens enzyme variants with improved properties through host cells expressing a library of randomly mutated enzyme-encoding genes. It requires no structural information and screening methodologies can lead to variants discovery working better under specific conditions (including in vivo activity). Random mutants from a parental enzyme are created by error-prone mutagenesis, DNA shuffling, site-saturation mutagenesis, chemical mutagenesis, using different mutator strains or retrotransposon Ty1 replication system (Rigoldi et al., 2018). These random mutagenesis methods need balancing a high mutation frequency (increasing library genetic diversity) and restricted mutation load (avoiding library-quality loss by lethal mutation introduction). The quality of mutant libraries was improved by computational methods that remove potential lethal mutations. Screening of libraries can be carried out *in vitro* and *in vivo*. *Escherichia coli* and *Saccharomyces cerevisiae* are the most frequently used host microbes used for the directed evolution of enzymes because of the availability of their tools for recombinant protein expression and molecular genetics (Qi et al., 2015; Hou et al., 2017;

Liu et al., 2018; Jeong et al., 2020). However, directed evolution and improvement *in vivo* performance tests can be performed on either two different organisms or the same organism. In the latter case, directed evolution avoids complications related to possible mutation divergent effects in various host organisms. It has been used for GI expression in *S. cerevisiae* and *E. coli* to enhance the glucose/xylose fermentation process. Most enzyme libraries were screened *in vivo* using *S. cerevisiae*. However, *S. cerevisiae* growth rate on glucose/xylose is limited by the activity of GI. So, the selection of improved GI variants was made through differences in growth properties (Seike et al., 2019). Directed evolution is beneficial, but variants' biochemical properties of GI governing glucose/xylose conversion rates observed in many investigations are still poorly elucidated (Lee et al., 2017). Also, due to incomplete metal loading of heterologously expressed glucose isomerase and misloading problematic, metals incorporation and availability on the activity of GI are largely unexplored problems (Lee et al., 2020). Exploring enzyme properties and mutations around metal-binding sites can influence glucose/xylose metabolism by microorganisms. Directed evolution will allow reshaping basic features of glucose isomerase to improve its catalytic characteristics (kinetic parameters optimization), thermal and pH stability, or fructose yield with applicability in industrial HFCS production.

Due to the health concerns over sugar for the potential causes of many diseases such as diabetes and obesity, the demand for sugars in the beverage and food market could decline. On the contrary, there has been a growing interest lately in the production of bio-based chemicals and materials from bioresources including cellulose, glucose, fructose and HFCS. The main difficulty in producing high yields of bio-based chemicals from cellulose is the complex chemical composition of cellulosic biomass. The high carbohydrate content of cellulosic biomass (~75%) is converted to sugar by thermo-chemical pretreatment and hydrolysis (saccharification). These

treatments represent 20% of the capital and operating costs. Therefore, low-cost sugar production from biomass is the primary driver for biomass feedstocks to produce biobased chemicals (Mthembu et al., 2021).

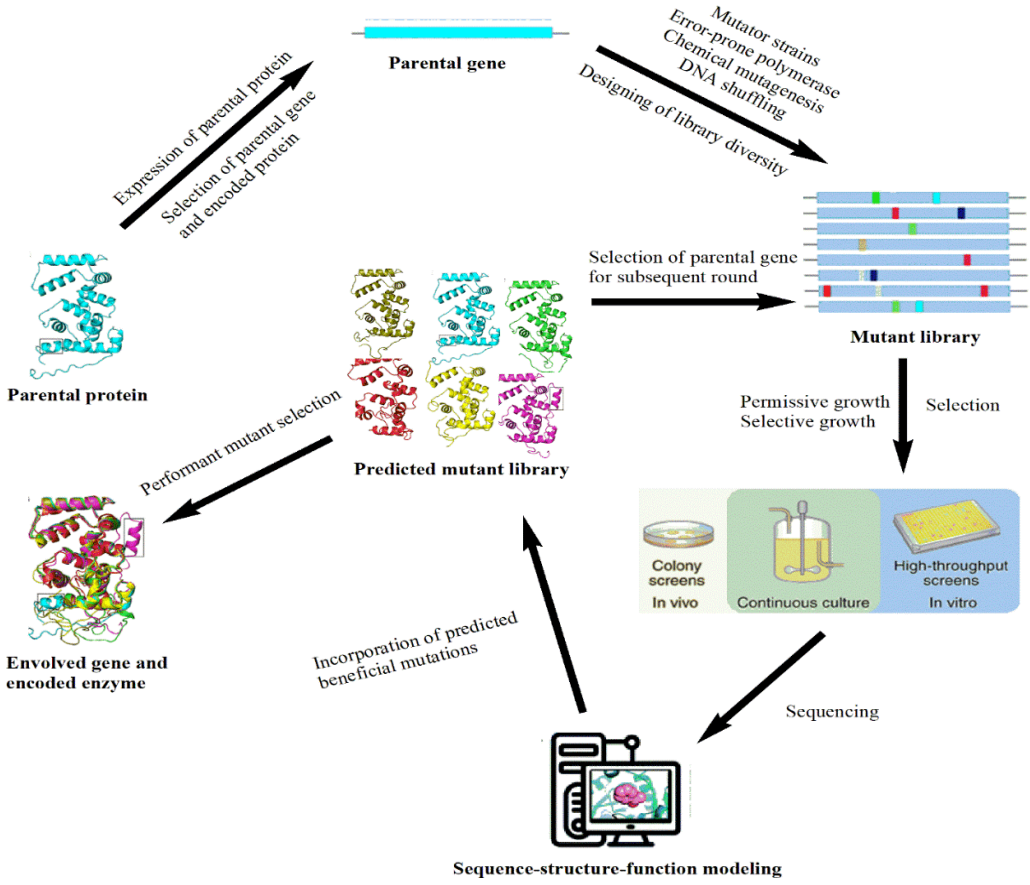

Figure 4. Different steps of directed evolution methodology.

4.3. HMF – a New Application of HFCS

One of the essential derivatives of renewable biomass is 5-hydroxymethylfurfural (HMF), an alternative to producing petroleum-based chemicals, pharmaceuticals (anti-carcinogenic, antioxidant, anti-proliferative, anti-inflammatory, and anti-apoptotic agent), resins, solvents and fungicides. HMF is present in several food products (Crops, cereals, fruits, vegetables, HFCS and

other sweetening agents) and biomass that are the precursors of its production. The global HMF market is expected to reach around 61 million USD in 2024 compared to 56 million USD in 2019 (Market study report, 2019). The current price of HMF is estimated between 500 and 1,500 USD/kg, which is three times higher than the price of its chemical analogues of fossil origin currently in use (Mika et al., 2018). However, the polarity and instability of HMF which forces precise reaction conditions control (temperature and reaction time) are major barriers to its synthesis. Due to the lower cost of glucose relative to fructose, investigators have studied the isomerization reaction of glucose to fructose. Various strategies were developed to reduce the HMF yield loss by hydrolysis, based on aprotic solvents (dimethyl sulfoxide) or two-phase systems with a water-immiscible extractive solvent (methyl isobutyl ketone, toluene) to isolate HMF from its formation. Other strategies use an ionic liquid solvent, a solvent or in mixtures of water/organic acids (acetic, formic, lactic, maleic, oxalic), inorganic (sulfuric, hydrochloric), salts ($MgCl_2$), $LaCl_3$ catalysts, solid acids (cation exchange resins, vanadyl phosphates, H-zeolites, niobic acid, etc.). However, these chemical processes require harsh operating conditions (high temperature, high pressure, etc.). They also lead to the production of hazardous by-products in high yield (Hu et al., 2018). Therefore, the bioconversion of HMF gained great interest in recent years. Many investigations have reported the HMF biotransformation using whole-cell and enzymes. Still, the low end-products rate and lower economic and industrial applicability were the major limitations of these studies (Saikia et al., 2021).

By triple dehydration, glucose and fructose are converted into HMF under hot acid catalysis (Figure 5). Their catalytic conversion into HMF is generally conducted using homogeneous and heterogeneous catalysts. HMF yields are higher when the substrate is fructose because it already has a five-membered ring structure (furanose), the same as HMF. On the other

hand, glucose has a very stable six-membered ring structure (pyranose), which is difficult to enolize and dehydrate. Its conversion to HMF is therefore limited by the enolization step, which has a strong energy barrier, limiting direct glucose dehydration to HMF and, therefore, affects HMF selectivity and yield. Thus, selectivity of both the isomerization and dehydration steps is essential in glucose conversion to fructose (Tongtummachat et al., 2020). Due to the instability and high price of HMF, catalytic conversion of these carbohydrates into HMF valuable derivatives is a promising approach and can reduce process energy consumption and cost.

4.3.1. HMF Derivatives as Monomers for Polymeric Materials

Many techniques were used to synthesize useful target molecules from HMF derivatives including reduction, oxidation, esterification, enzymatic polymerization, ring-opening polymerization and free-radical polymerization or other reactions (Figure 6).

4.3.1.1. Symmetrically functional derivatives of HMF

The preparation of symmetrically functional monomers has been possible due to the functional groups' presence on opposite sides of the HMF heterocyclic ring.

4.3.1.1.1. HMF to Furandicarboxylic Acid (FDCA)

FDCA is synthesized from hydroxyl and formyl groups oxidation of HMF. It is an essential precursor for the synthesis of green degradable and nontoxic plasticizers in the polymer industry. The conversion was performed by aerobic using various catalysts. These are Pt catalysts supported TiO_2 and ZrO_2, RuO_2 catalysts with Mg-based supports, γAl_2O_3 catalyst with Au nanoparticles, magnetic Pd catalysts, Ru/C catalysts and Au catalysts with various supports (Sajid et al., 2018;

Megias-Sayago et al., 2020; Weerathunga et al., 2021). Enzyme-catalyzed oxidation was performed with HMF oxidoreductase (HMFO), 2,2,6,6-tetramethylpiperidine-1-oxyl/Candida antarctica lipase B (TEMPO/CaLB), aryl-alcohol oxidase (AAO), galactose oxidase (GO), horseradish peroxidase (HRP), methanol oxidase, laccase, decarboxylase, periplasmic aldehyde oxidase (PaoABC), unidentified peroxidase (UPO), and novozym 435. Whole-cell biotransformation of HMF (*Pseudomonas putida* S12, *Burkholderia cepacian* H-2, *Chaetomorpha linum*, *Raoultella ornithinolytica* BF60, *Acinetobacter oleivorans* S27, *Acinetobacter calcoaceticus* NL14, *Synechococcus elongatus*, *Pseudomonas putida*, *Aspergillus flavus* APLS-1, and *Comamonas testosterone* SC1588) were also used to produce FDCA (Cajnko et al., 2020; Sheng et al., 2020; Saikia et al., 2021). Polyamides, polyurethanes, (co)polyesters and other interesting polymers (thermotropic and photograded polyesters) were synthesized from FDCA and its derivatives due to the presence of two carboxylic acid groups. (Co)polyesters are of growing interest, and several researchers have investigated their synthesis, physical properties, structural analysis and sorption behavior toward carbon dioxide, oxygen and water (Figure 7). Because of their similarity with polyethylene terephthalate (PET) and polybutylene terephthalate (PBT), poly (ethylene-2,5-furandicarboxylate) (PEF) and poly (butylene-2,5-furandicarboxylate) (PBF) are among FDCA based polyesters the most studied. Poly (propylene-2,5-furandicarboxylate) (PPF) was used as the replacement of poly(propylene-2,5-terephthalate) (PPT), and studies have reported its thermal behavior, solid-state structure, and barrier properties. (Co)polyesters were also prepared from varieties of other monomers (longer aliphatic linear diols, aromatic diols and renewable aliphatic acids) (Rajesh et al., 2020).

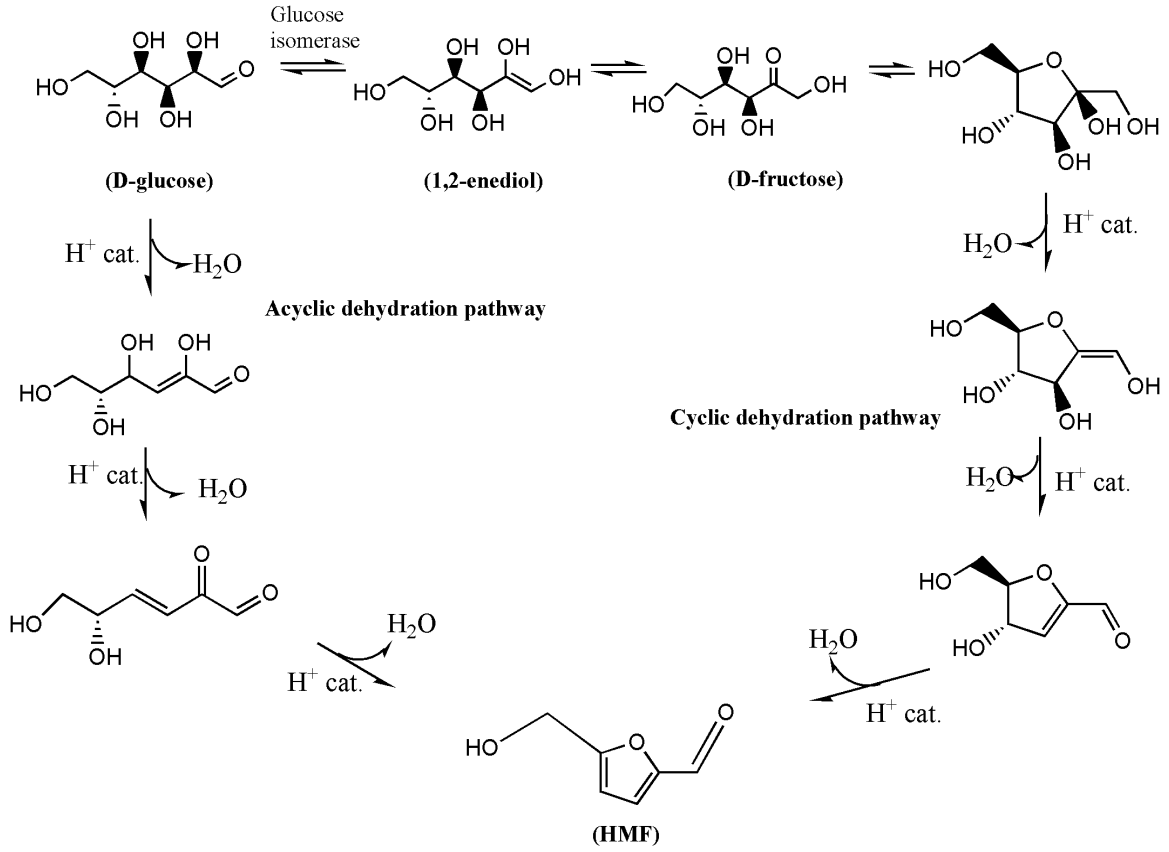

Figure 5. Mechanism of 5-hydroxymethylfurfural (HMF) synthesis from glucose and fructose. The cat. represents catalysis.

4.3.1.1.2. HMF to 2,5-Dihydroxymethylfuran (DHMF)

DHMF is another valuable building block chemical obtained by the reduction of HMF (Figure 8). It has an application in polymers and ethers synthesis. Its biosynthesis was carried out using *Saccharomyces cerevisiae* strains (307-12H120 and 307-12H60), *Meyerozyma guilliermondi* SC1103, *Escherichia coli* CCZU-K14, *Ganoderma sessile*, and *Burkholderia contaminans* NJPI-15. However, bioconversion of HMF to DHMF requires NAD(P)H as a cofactor, and NAD(P)H regeneration depends on the co-substrates used for the reaction. Glucose is the substrate widely used (He et al., 2014; Xu et al., 2018; Hou et al., 2020; Chang et al., 2021).

It is the precursor of 2,5-diacryloyloxymethylfuran (difunctional cross-linker increasing the tensile strength of acrylated epoxidized vegetable oils based polymer networks), side-chain functional polyesters, 2,5-bis-allyloxymethyl-furan, 2,5-bis[(2-oxrianylmethoxy)methyl]-furan (high performance epoxies preparation), 2,5-bis(chloromethyl)furan 2,5-bis(azidomethyl)furan, 2,5-bis(cyanomethyl)furan, and 2,5-bis(aminomethyl)furan (building block for polyamides) (Yang et al., 2021).

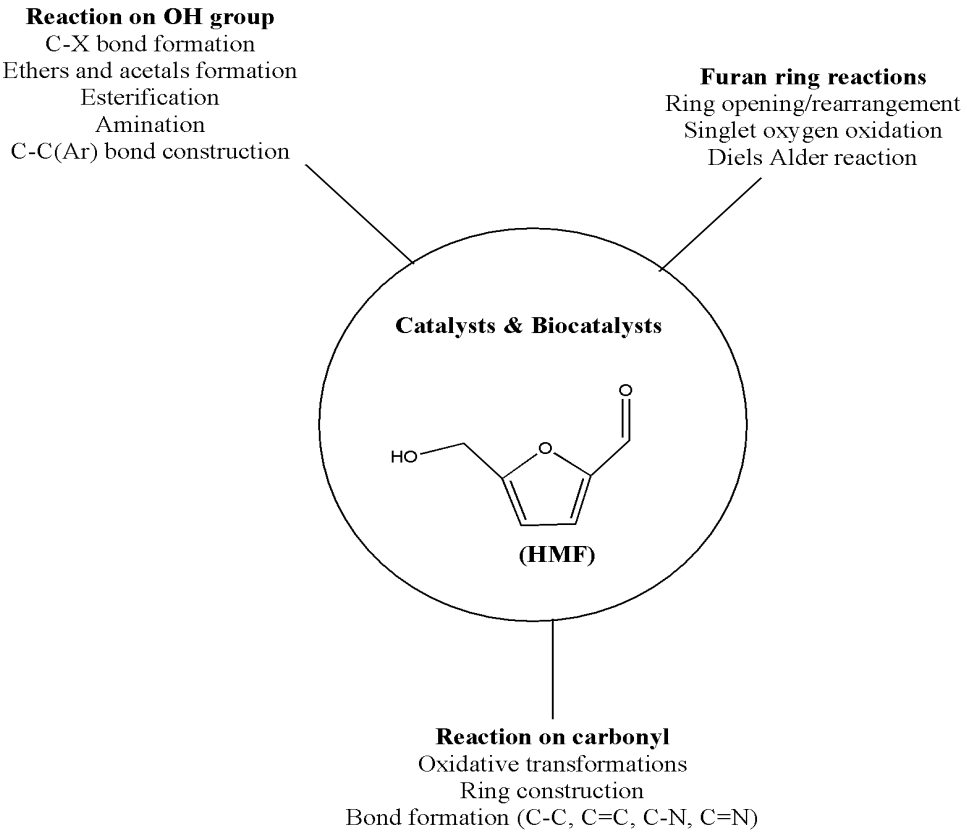

Figure 6. Overview of reactions leading to 5-hydroxymethylfurfural (HMF) derivatives.

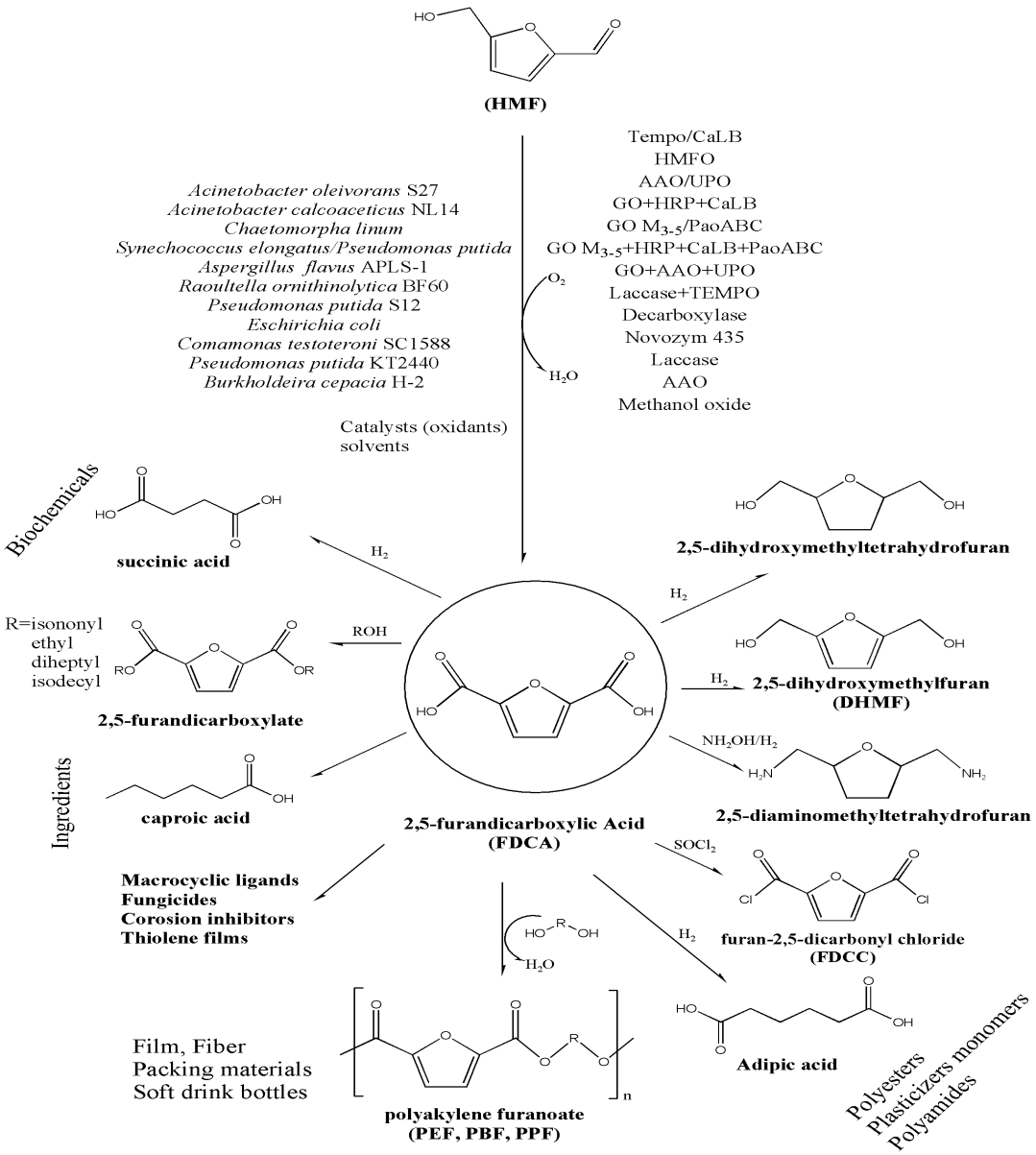

Figure 7. 5-hydroxymethylfurfural (HMF) bioconversion into 2,5-furandicarboxylic acid (FDCA) and its derivatives. TEMPO: 2,2,6,6-tetramethylpiperidine-1-oxyl; CaLB: Candida antartica lipase B; HMFO: HMF oxidase; AAO: aryl alcohol oxidase; UPO: unidentified peroxidase;GO: galactose oxidase; HRP: horseradish peroxidase; PaoABC: periplasmic aldehyde oxidase; PET: polyethylene terephthalate; PBF: poly(butylene2,5-furandicarboxylate); PPF: poly(propylene-2,5-furandicarboxylate).

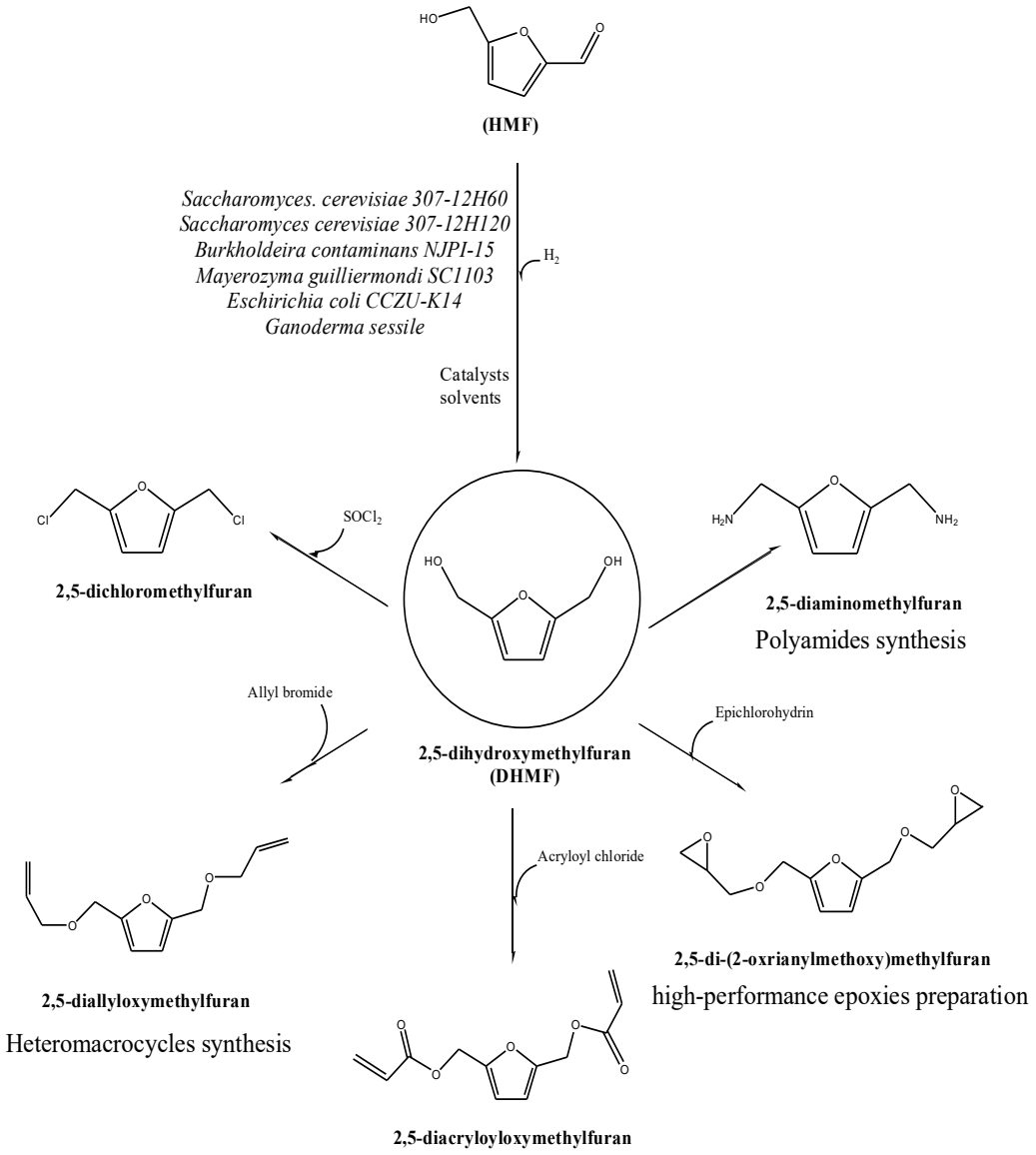

Figure 8. 5-hydroxymethylfurfural (HMF) bioconversion into 2,5-dihydroxymethylfuran (DHMF) and its derivatives

4.3.1.1.3. HMF to 2,5 Dimethylfuran (DMF)

DMF is a new-fashioned liquid biofuel for transportation because of its higher energy density, boiling point and octane number compared to bioethanol. It is insoluble in water, and its properties are more similar to those of gasoline than bioethanol. It is also used as a solvent in the pharmaceutical and cosmetic industries (Figure 9). Upgraded, DMF is used to produce p-xylene, the main industrial precursor for PET (Brandi et al., 2020). DMF is produced by hydrogenation/hydrodeoxygenation of HMF with catalysts such as ZrO_2-Cu/RuCu, Ru-Co/SiO_2, Ni-Fe/TiO_2, Pt/Co, Pt/activated carbon (AC), Pt/grahitized carbon (GC), Pt-Co/AC, and Pt-Co/GC (Esen et al., 2019; Brandi et al., 2020; Przydacz et al., 2020). Bio-metallic/bimetallic catalysts were also used: Bacillus benzeovorans-Pd, Desulfovibrio desulfuricans-Pd, Escherichia coli-Ru, and Escherichia coli-Ru/Pd (Gomez-Bolivar et al., 2019; Omajali et al., 2019).

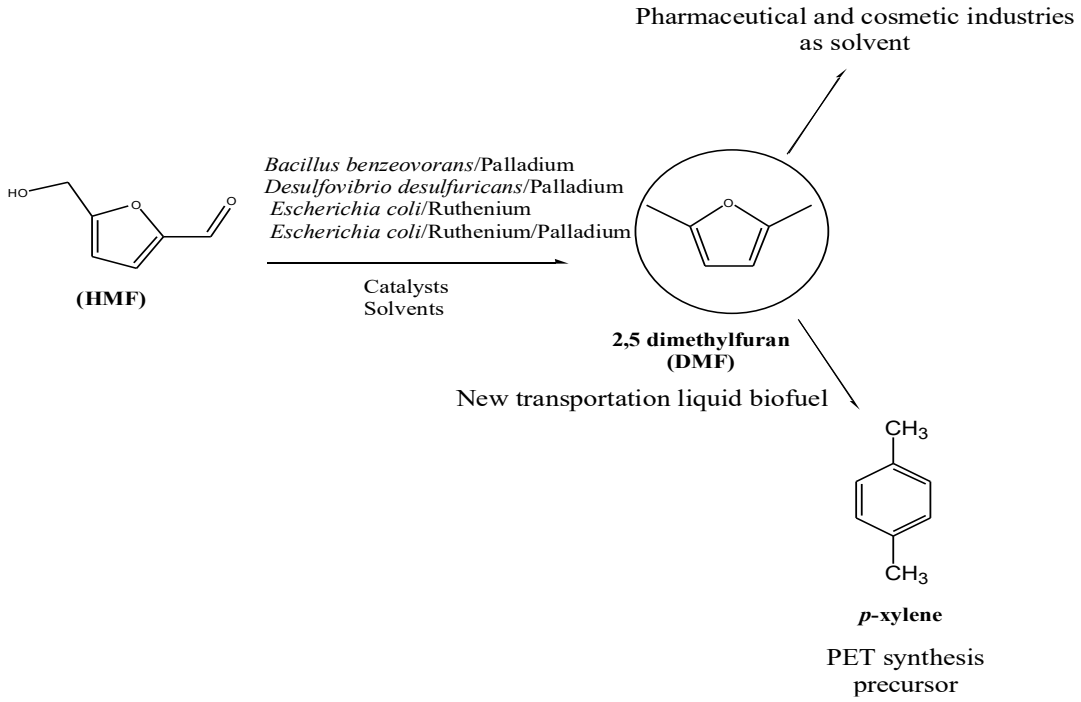

Figure 9. HMF bioconversion into DMF.

4.3.1.1.4. HMF to 2,5-Diformylfuran (DFF)

With two symmetrical aldehyde groups, DFF is a versatile chemical intermediate for pharmaceuticals, fungicides, furan-urea resins, and heterocyclic ligands (Yadav and Sharma, 2014). It is produced from HMF by oxidation using mainly Ru-, V-, Mn-, Cu-based catalysts. Although direct oxidation of HMF was successfully investigated with stoichiometric oxidants or electrophilic agents, its oxidation to DFF in water is a great challenge due to its poor selectivity and harsh reaction conditions. However, limited processes for metal-free oxidation of HMF were developed, reducing catalyst cost and avoiding metal contamination (use of chitosan and other substrates to prepare nitrogen-doped carbon materials). In addition, new technologies such as biocatalysis (chloroperoxidase, alcohol oxidase, catalase, GO, HRP), photocatalysis and electrocatalysis were used to produce DFF from HMF (Dai, 2021; Saikia et al., 2021). DFF is used to produce furan-2,5-dicarbonyl chloride (biofuel production), 2,5-diaminomethylfuran (polyamides) and 2,5-dihydroxymethyltetrahydrofuran (resins, polymers, artificial fibers). Maleic acid and maleic anhydride are also produced from DFF and are precursors of thermoplastic polyurethanes, elastane/spandex fibers, curing agents, adhesives, dispersants and corrosion inhibitors (Figure 10).

4.3.1.2. Unsymmetrically functional derivatives of HMF

Unsymmetrically functional monomers were prepared by selectively reacting hydroxyl or formyl groups of HMF.

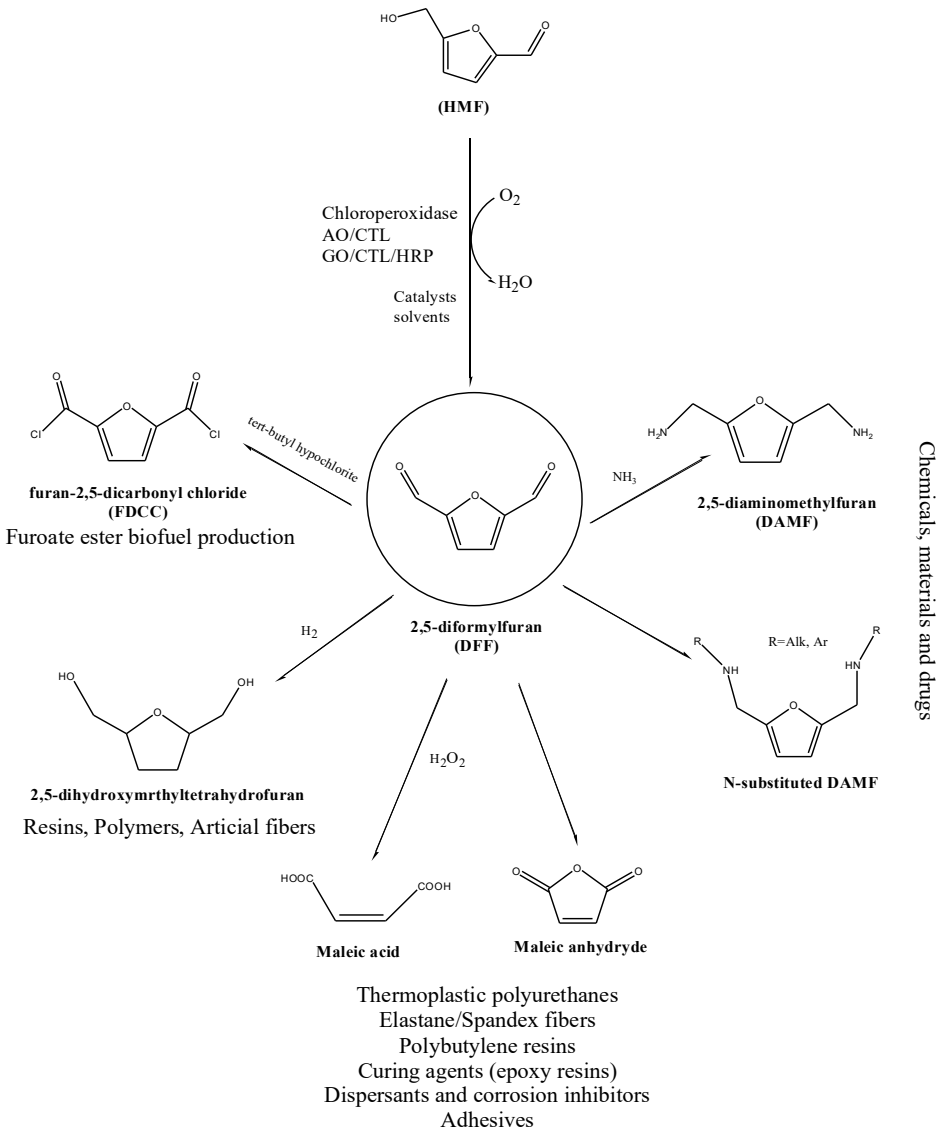

Figure 10. HMF bioconversion into DFF and its derivatives.

AO: Alcohol oxidase, CTL: Catalase, GO: Galactose oxidase, HRP: Horseradish peroxidase.

4.3.1.2.1. HMF to 5-hydroxymethyl-2-furancarboxylic acid (HMFCA)

The oxidation of the HMF aldehyde group leads to HMFCA, which is a precursor of FDCA and used to prepare polyesters as antitumor agents and interleukin inhibitors (Figure 11a). HMF oxidation was performed through photocatalysis, biocatalysis (*Serratia liquefaciens* LF14,

Comamonas testosteroni SC1588, *Gluconobacter oxydans*, *Serratia marcescens*, *Pseudomonas putida* KT2440, *Pseudomonas aeruginosa* PC-1, horse liver alcohol dehydrogenase, phenylacetone monooxygenase, xanthine oxidase, UPO, CaLB) and Cannizzaro reaction (Cang et al., 2019; Muñoz et al., 2020; Xu et al., 2020, Saikia et al., 2021) Catalytic systems (Ru, Cu) were used in Cannizzaro and aerobic reactions involving an excess of hydroxide in an aqueous solution at elevated temperatures.

4.3.1.2.2. HMF to Formylfurancarboxylic acid (FFCA)

FFCA is produced by the HMF partial oxidation using catalysts such as heteropolyacid (Fe-Anderson: $Na_3H_6FeMo_6O_{24}.5H_2O$), mixed metal oxides ($CuO{\cdot}CeO_2$ and $MgO{\cdot}CeO_2$) and transition metals (Fe_3O_4, Fe-Zr-O and Fe-organic porphyrin polymer support). FFCA is used in surfactants and resins synthesis (Pal et al., 2020). Biocatalytic strategies to produce FFCA are limited because it is selectively oxidized from HMF. Nonetheless, the use of some enzymes (CaLB, laccase, TEMPO, AAO and HMF oxidase) have enhanced its production (Saikia et al., 2021) (Figure 11b).

4.3.1.2.3. HMF to 5,5-bis(hydroxymethyl)furoin (BHMF)

BHMF is produced through HMF benzoin-type condensation. The reaction was promoted by catalysts (N-heterocycle carbene), enzymes (thiamine diphosphate-enzyme BAL, CaLB) and microbes (*Pseudomonas fluorescens*). It is a precursor of oxygenated diesel fuels and C_{12} linear alkanes obtained through catalytic hydrogenation and hydrodeoxygenation. It is also converted into bio-based polyesters and polyurethanes (Baraldi et al., 2017; Saikia et al., 2021) (Figure 11c).

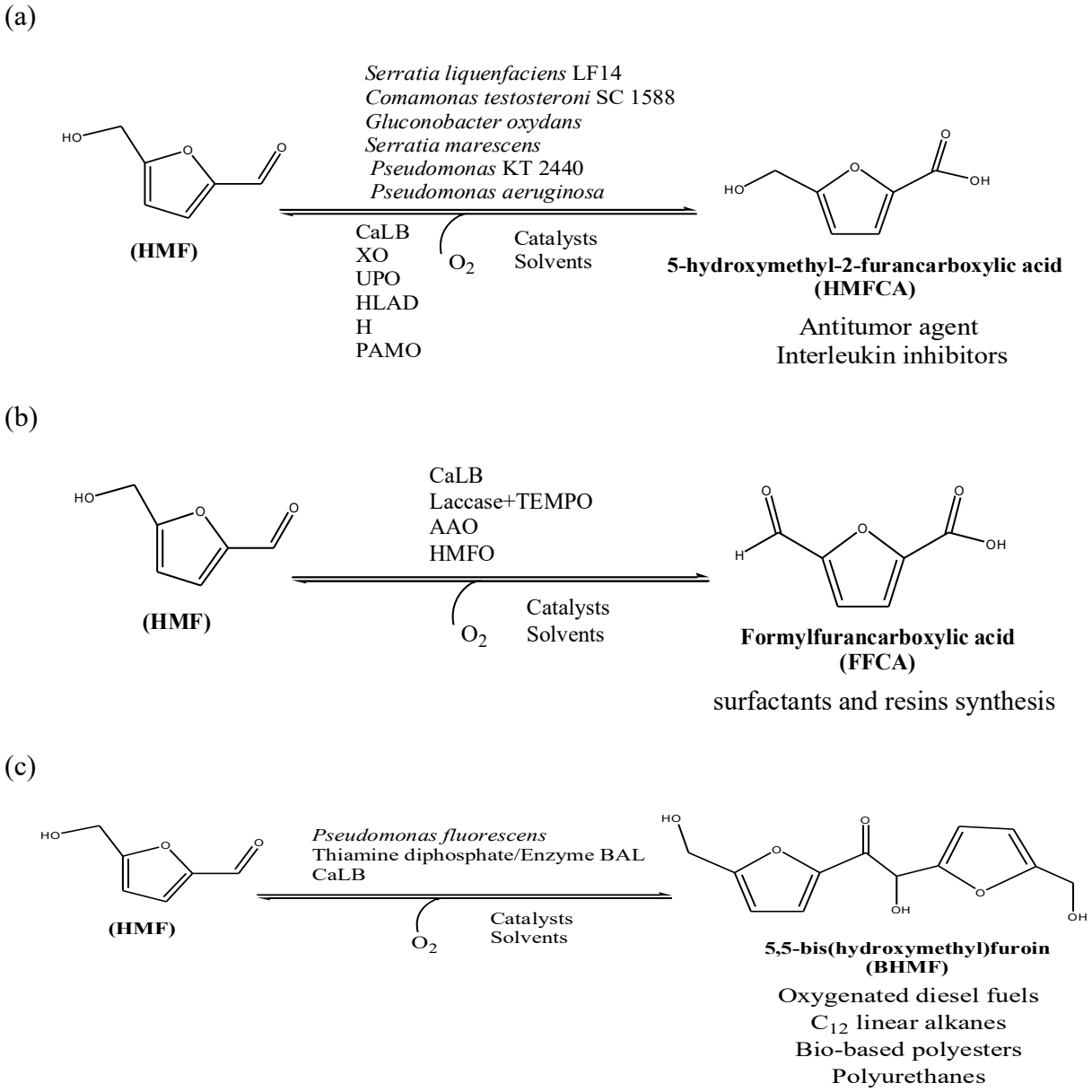

Figure 11. HMF bioconversion into HMFCA (a), FFCA (b) and BHMF (c).

CaLB: Candida antartica lipase B, TEMPO: 2,2,6,6-tetramethylpiperidine-1-oxyl, AAO: Aryl alcohol oxidase; HMFO: HMF oxidase; UPO: Unidentified peroxidase; XO: Xanthine oxidase; PAMO: Phenylacetone monooxygenase; HLADH: Horse liver alcohol dehydrogenase.

4.3.1.2.4. HMF to other chemicals

5-Hydroxymethylfurfurylamine (HMFA) is formed by the reductive amination of HMF supported with ruthenium nanoparticles or transaminase enzymes. It is applied for the preparation of antiseptic agents, antihypertensives and curing agents (Petri et al., 2018). 5-Hydroxymethyl-2-vinylfuran (HMVF) is formed by alkenylation of HMF. HMVF is a versatile adhesive that can be link to variable substrates (metal, glass, plastics, and rubber) under heating or acid treatment at room temperature by free radical polymerization. It also exerts cell adhesive property. HMVF is obtained by reductive amination of HMF (Han et al., 2017).

4.3.1.3. Derivatives of HMF from furan ring reactions

Most chemicals derived from the furan ring reaction are good biofuel candidates or precursors and were obtained by reactions with nucleophiles, electrophiles, oxidants, reductants, cycloaddition, metals, and metallic derivatives. These derivatives include:

(1) Maleic anhydride (MA): MA is formed by aerobic oxidation of HMF using catalysts such as heteropolyacids (phosphomolybdic acid, vanadium oxide and copper (II) nitrate). MA is used to synthesize unsaturated polyester resins as food and oil additives and in pharmaceuticals. Industrially, it is largely produced from petroleum-based n-butane and benzene oxidation in the gas phase (Li and Zhang, 2016; Lou et al., 2020).

(2) Levulinic acid (LA) and formic acid (FA): Rehydration of HMF directly generates LA and FA. The use of hydrotalcite, zeolites, metal oxides, ionic liquids, enzymes, or an aqueous base has increased their yields from glucose and fructose. LA is a platform chemical of interest in various fields of application such as pharmaceutical, biologically active material, corrosion inhibitors, adsorbents, personal care products, batteries, coating materials, polymers, anti-freezers,

electronics, photography, plasticizers, flavoring agents, antifouling compounds, fuels, herbicides and flavouring agents (Dutta et al., 2020). Among levulinic acid derivatives, levulinic esters are applicable as oxygenated fuel. Calcium levulinate is used in pills, capsules and injections production, while δ-aminolevulinic acid is a photoactivation weedicide. Sodium levulinate is a skin or food preservative and conditioning agent. Methyl tetrahydrofuran (MTHF), γ-valerolactone and ethyl levulinate are applicable in potential biofuel precursors preparation, while diphenolinic acid is used in polymeride and other materials. α-Methylene-γ-valerolactone is a new attractive acrylic monomer that bestows high thermal stability to polymers. Angelica lactone and 1,4-pentanediol are important biobased building blocks as monomers. Angelica lactone is used in UV-light induced, cationic and ring-opening polymerisations while 1,4-pentanediol is used to produce high strength biodegradable polyesters (Dell'Acqua et al., 2020; Simakova et al., 2020). Acetyl acrylate is a precursor for adhesives, plastics, emulsions, coatings and acrylic rubber. MTHF is also an electrolyte for lithium rechargeable batteries. Although being a low-cost product, FA has a very high potential to synthesize plasticizers, textiles, formalin, pharmaceuticals, rubber, fuel cells and hydrogen (Adeleye et al., 2019; Ajekwene, 2020; Zunita et al., 2021).

(3) ε-caprolactone (CLo), ε-caprolactam (CLa), 1,6-hexanediol and 2,5-tetrahydrofuran dimethanol: These chemicals were obtained by HMF reduction. They are used in the production of Nylon, dyeing, and polyesters. Copolymers of CLo and CLa through polyesterification lead to poly(ester amide)s (PEAs). PEAs combine the advantages of polyesters (biocompatibility and environmental degradability) and polyamides (excellent thermal and mechanical properties) and deeply impact biomaterials such as tissue engineering scaffolds, drug delivery systems and non-viral gene carriers (Zeng et al., 2020).

4.4. Concluding remarks and prospects

The glucose isomerase is a crucial enzyme in converting glucose into fructose, and its use is well established and highly optimized through enzyme engineering and bioprocess design. The engineering of GI could enhance *in vivo* enzyme performance in the engineered host organisms (S. cerevisiae etc.) and would be important for developing improved strains. Therefore, *in vivo* strategies for structure-based enzyme engineering are required. They should focus on the metal dependence of enzyme catalytic properties in the host cells because metal loading is a limiting factor for glucose metabolism that impacts *in vivo* performance. Combining enzyme rational and semi-random approaches (mutations around the active site) should be considered to optimize pH activity profile and metal specificity for better intracellular conditions of cell hosts. Studies on metal binding kinetics and thermodynamics could explain *in vivo* metal binding and elucidate its influence on activity. Also, the investigation of growth-based screening methods combined with semi-random mutagenesis (mutations around the metal-binding residues) would enhance cell host growth on glucose. The semi-random approach combined with *in vivo* selection could avoid uncertainties between *in vivo* and *in vitro* enzyme performance. Such selection could be done by mutations elsewhere in the host cell genome and not in the enzyme gene. In addition, enzyme rational engineering and *in vivo* mutant behavior characterization would improve mutant library design. The analysis of the cellular behavior of selected variants could explain bottlenecks between *in vitro* properties and *in vivo* performance of GI in glucose metabolism.

HMF and its derivatives are widely used in diverse industries. Various chemical conversion routes (hydrotalcite, zeolites and several metal oxides) were developed to produce furanic derivatives in recent years. However, there is an urgent need for biotransformation processes of HMF because of harsh reaction conditions of chemical routes and harmful by-product production.

Although these bioprocesses are promising, their commercial large-scale applications are limited. HMF is a toxic chemical and inhibits cell growth and enzyme activity. Other factors such as low substrate loading, insufficient selectivity, side-product formation, catalyst regeneration, low yield, and end-product complex recovery methodologies affect their industrial production. Various enzyme engineering strategies (recombinant enzyme, whole-cell system design, modification of structure and active enzyme sites) should be investigated with high industrial applications to overcome these limitations. The designed and immobilized robust biocatalysts could lead to their easy recovery. Downstream processing techniques should also be explored for easy furanic derivatives recovery with high purity and avoiding intermediate product accumulation.

5. References

Adeleye AT, Louis H, Akakuru OU, Joseph I, Enudi OC, Michael DP (2019). A Review on the conversion of levulinic acid and its esters to various useful chemicals. *AIMS Energy*, 7,165-185.

Adsul MG, Bastawdek B,Verma AJ, Gokhle DV (2007). Strain improvement of Penicillium janthenellum. *Bioresource Technol*, 98, 1467-1473.

Ahmed A, Bibi, A (2018). Fungal cellulase; production and applications: Minireview. *LIFE Int J Health Life Sci*, 4, 19-36.

Ajeje SB, Hu Y, Song G, Peter SB, Afful RG, Sun F, Asadollahi MA, Amiri H, Abdulkhani A, Sun H (2021). Thermostable cellulases/xylanases from thermophilic and hyperthermophilic microorganisms: Current perspective. *Front Bioeng Biotechnol*, 9, 794304.

Ajekwene KK (2020). Chapter 3: Properties and Applications of Acrylates. In Acrylate Polymers for Advanced Applications, Intechopen, London, pp. 35-46.

Al Mousa AA, Hassane AMA, Gomaa AE-RF, Aljuriss JA, Dahmash ND, Abo-Dahab NF (2022). Response-surface statistical optimization of submerged fermentation for pectinase and cellulase production by *Mucor circinelloides* and *M. hiemalis*. *Fermentation*, 8, 205.

Amadi OC, Egong EJ, Nwagu TN, Okpala G, Onwosi CO, Chukwu GC, Okolo BN, Agu RC, Moneke AN (2020). Process optimization for simultaneous production of cellulase, xylanase and ligninase by *Saccharomyces cerevisiae* SCPW 17 under solid state fermentation using Box-Behnken experimental design. *Heliyon*, 6, e04566.

Ando S, Ishida H, Kosugi Y, Ishikawa K (2002). Hyperthermostable endoglucanase from *Pyrococcus horikoshii*. *Appl Environ Microbiol*, 68, 430-433.

Ariff INM, Bahrin EK, Ramli N, Abd-Aziz S (2019). Direct use of spent mushroom substrate from *Pleurotus pulmonarius* as a readily delignifed feedstock for cellulase production. *Waste Biomass Valor*, 10, 839-850.

Asmare B (2014). Biotechnological advances for animal nutrition and feed improvement. *World J Agric Res*, 2, 115-118.

Bajar S, Singh A, Bishnoi NR (2020). Exploration of low-cost agro-industrial waste substrate for cellulase and xylanase production using *Aspergillus heteromorphus*. *Appl Water Sci*, 10, 153.

Banerjee S, Maiti TK, Roy RN (2020). Production, purification, and characterization of cellulase from *Acinetobacter junii* GAC 16.2, a novel cellulolytic gut isolate of *Gryllotalpa africana*, and its effects on cotton fiber and sawdust. *Ann Microbiol*, 70, 28.

Baraldi S, Fantin G, Di Carmine G, Ragno D, Brandolese A, Massi A, Bortolini O, Marchetti N, Giovannini PP (2019). Enzymatic synthesis of biobased aliphatic-aromatic oligoesters using 5,50- bis(hydroxymethyl)furoin as a building block. *RSC Adv*, 9, 29044.

Basso A, Serban S (2019). Industrial applications of immobilized enzymes—A review. *Mol Catal*, 479, 110607.

Beri D, Herring CD, Blahova S, Poudel S, Giannone RJ, Hettich RL, Lynd LR (2021). Coculture with hemicellulose-fermenting microbes reverses inhibition of corn fiber solubilization by *Clostridium thermocellum* at elevated solids loadings. *Biotechnol Biofuels*, 14, 24.

Beri D, York WS, Lynd LR, Peña MJ, Herring CD (2020). Development of a thermophilic coculture for corn fiber conversion to ethanol. *Nat Commun*, 11, 1937.

Biswas P, Bharti AK, Kadam A, Dutt D (2019). Wheat bran as substrate for enzyme production

and its application in the bio-deinking of mixed office waste (MOW) paper. *BioRes*, 14, 5788-5806.

Bittencourt GA, Vandenberghe LPdS, Valladares-Diestra KK, Soccol CR (2022). Soybean hull valorization for sugar production through the optimization of citric acid pretreatment and enzymatic hydrolysis. *Ind Crops Prod*, 186, 115178.

Bocarsly ME, Powell ES, Avena NM, Hoebel BG (2010). High-fructose corn syrup causes characteristics of obesity in rats: increased body weight, body fat and triglyceride levels. *Pharmacol Biochem Behav*, 97, 101-106.

Boisset C, Pétrequin C, Chanzy H, Henrissat B, Schülein M (2001). Optimized mixtures of recombinant *Humicola insolens* cellulases for the biodegradation of crystalline cellulose. *Biotechnol Bioeng*, 72, 339-345.

Brandi F, Bäumel M, Shekova I, Molinari V, Al-Naji M (2020). 5-Hydroxymethylfurfural hydrodeoxygenation to 2,5-dimethylfuran in continuous-flow system over Ni on nitrogen-doped Carbon. *Sustain Chem*, 1, 106-115.

Cacua A, Gelvez JJ, Rodríguez DC, Parra JW (2018). Production of bioethanol from rice husk pretreated with alkalis and hydrolyzed with acid cellulase at pilot scale. *J Phys: Conf Ser*, 1126 012034.

Cai J, He Y, Yu X, Banks SW, Yang Y, Zhang X, Yu Y, Liu R, Bridgwater AV (2017). Review of physicochemical properties and analytical characterization of lignocellulosic biomass. *Renew Sustain Energy Rev*, 76, 309-322.

Cai W, Chen Y, Zhang L, Fang X, Wang W (2022). A three-gene cluster in *Trichoderma reesei* reveals a potential role of dmm2 in DNA repair and cellulase production. *Biotechnol Biofuels*, 15, 34.

Cajnko MM, Novak U, Grilc M, Likozar B (2020). Enzymatic conversion reactions of 5-hydroxymethylfurfural (HMF) to bio-based 2,5-diformylfuran (DFF) and 2,5-furandicarboxylic acid (FDCA) with air: mechanisms, pathways and synthesis selectivity. *Biotechnol Biofuels*, 13, 66.

Cang R, Shen LQ. Yang G, Zhang ZD, Huang H, Zhang ZG (2019). Highly selective oxidation of 5-hydroxymethylfurfural to 5-hydroxymethyl-2-furancarboxylic acid by a robust whole-cell biocatalyst. *Catalysts*, 9, 526.

Chang S, He X, Li B, Pan X (2021). Improved biosynthesis of 2,5-bis(hydroxymethyl)furan by *Burkholderia contaminans* NJPI-15 with co-substrate. *Front Chem*, 9, 635191.

Chen Z, Pereira JH, Liu H, Tran HM, Hsu NS, Dibble D, Singh S, Adams PD, Sapra R, Hadi MZ (2013). Improved activity of a thermophilic cellulase, Cel5A, from *Thermotoga maritima* on ionic liquid pretreated switchgrass. *PLoS One*, 8, e79725.

Chownk M, Sangwan RS, Yadav SK (2019). A novel approach to produce glucose from the supernatant obtained upon the dilute acid pre-treatment of rice straw and synergistic action of hydrolytic enzymes producing microbes. *Braz J Microbiol*, 50, 395-404.

Chung D, Sarai NS, Knott BC, Hengge N, Russell JF, Yarbrough JM, Brunecky R, Young J, Supekar N, Wall TV, Sammond DW, Crowley MF, Szymanski CM, Wells L, Azadi P, Westpheling J, Himmel ME, Bomble YJ (2019). Glycosylation is vital for industrial performance of hyperactive cellulases. *ACS Sustainable Chem*, 7, 4792-4800.

Contreras F, Pramanik S, Rozhkova AM, Zorov IN, Korotkova O, Sinitsyn AP, Schwaneberg U, Davari MD (2020). Engineering robust cellulases for tailored lignocellulosic degradation cocktails. *Int J Mol Sci*, 21, 1589.

Dai C, Miao T, Hai J, Xiao Y, Li Y, Zhao J, Qiu H, Xu B (2020). A novel glucose isomerase from

Caldicellulosiruptor bescii with great potentials in the production of high-fructose corn syrup. *Biomed Res Int*, 13, 1871934.

Dai J (2021). Synthesis of 2,5-diformylfuran from renewable carbohydrates and its applications: A review. *Green Energy & Environment*, 6, 22-32.

Dai JY, Yang Y, Dong YS, Xiu ZL (2020). Solid-state co-cultivation of *Bacillus subtilis*, *Bacillus mucilaginosus*, and *Paecilomyces lilacinus* using tobacco waste residue. *Appl Biochem Biotechnol* 190, 1092-1105.

Dell'Acqua A, Stadler BM, Kirchhecker S, Tin S, de Vries JG (2020). Scalable synthesis and polymerisation of a β-angelica lactone derived monomer. *Green Chem*, 22, 5267-5273.

Desai SS, Gachhi DB, Hungund BS (2017). Glucose Isomerising Enzymes. In: Ray, R.C., & Rosell, C.M. (Eds.). Microbial Enzyme Technology in Food Applications (1st ed.). CRC Press.

Dey P, Singh J, Scaria J, Anand AP, Dey P (2018). Improved production of cellulase by *Trichoderma reesei* (MTCC 164) from coconut mesocarp-based lignocellulosic wastes under response surface-optimized condition. *3 Biotech*, 8, 402.

Dos Santos YQ, de Veras BO, de França AFJ, Gorlach-Lira K, Velasques J, Migliolo L, Dos Santos EA (2018). A new salt-tolerant thermostable cellulase from a marine *Bacillus* Sp Strain. J *Microbiol Biotechnol*, 28, 1078-1085.

Dutta S, Yu IKM, Tsang DCW, Su Z, Hu C, Wu KCW, Yip ACK, Ok YS, Poon CS (2020). Influence of green solvent on levulinic acid production from lignocellulosic paper waste. *Bioresour Technol*, 298, 122544.

Ega SL, Drendel G, Petrovski S, Egidi E, Franks AE, Muddada S (2020). Comparative analysis of

structural variations due to genome shuffling of *Bacillus Subtilis* VS15 for improved cellulase production. *Int J Mol Sci*, 21, 1299.

Eitner V, Lindorfer J (2016). Evaluation of technology structure based on energy yield from wheat straw for combined bioethanol and biomethane facility. *Renewable Energy*, 8, 193-202.

Ejaz U, Sohail M, Ghanemi A (2021). Cellulases: from bioactivity to a variety of industrial applications. *Biomimetics*, 6, 44.

Elegbede JA, Ajayi VA, Lateef A (2021). Microbial valorization of corncob: Novel route for biotechnological products for sustainable bioeconomy. *Environmental Technology and Innovation*, 24.

Esen M, Akmaz S, Koç SN, Gürkaynak MA (2019). The hydrogenation of 5-hydroxymethylfurfural (HMF) to 2,5-dimethylfuran (DMF) with sol–gel Ru-Co/SiO2 catalyst. *J Sol-Gel Sci Technol*, 91, 664-672.

Ezeilo UR, Wahab RA, Mahat NA (2020). Optimization studies on cellulase and xylanase production by *Rhizopus oryzae* UC2 using raw oil palm frond leaves as substrate under solid state fermentation. *Renewable Energy*, 156, 1301–1312.

Ezeilo UR, Lee CT, Huyop F, Zakaria II, Wahab RA (2019). Raw oil palm frond leaves as cost-efective substrate for cellulase and xylanase productions by *Trichoderma asperellum* UC1 under solid-state fermentation. *J Environ Manag*, 243, 206-217.

Fernandes P (2018). Enzymatic processing in the food industry, Reference Module in Food Science, Elsevier.

Garvey M, Klose H, Fischer R, Lambertz C, Commandeur U (2013). Cellulases for biomass degradation: comparing recombinant cellulase expression platforms. *Trends Biotechnol*, 31, 581-593.

Gomez-Bolivar J, Mikheenko IP, Orozco RL, Sharma S, Banerjee D, Walker M, Hand RA, Merroun ML, Macaskie LE (2019). Synthesis of Pd/Ru bimetallic nanoparticles by *Escherichia coli* and potential as a catalyst for upgrading 5-hydroxymethyl furfural into liquid fuel precursors. *Front Microbiol*, 10, 1276.

Gregorc A, Jurišić S, Sampson B (2020). Hydroxymethylfurfural affects caged honey bees (*Apis mellifera carnica*). *Diversity*, 12, 18.

Guerriero G, Hausman JF, Strauss J, Ertan H, Siddiqui KS (2016). Lignocellulosic biomass: Biosynthesis, degradation, and industrial utilization. *Eng Life Sci*, 16, 1-16.

Hajer HB, Dorra AZ, Monia M, Samir B, Nushin A (2014). Probing the role of helix α1 in the acid-tolerance and thermal stability of the *Streptomyces* sp. SK glucose isomerase by site-directed mutagenesis. *J Biotechnol*, 173, 1-6.

Han M, Liu X, Zhang X, Pang Y, Xu P, Guo J, Liu Y, Zhang S, Ji S (2017). 5-Hydroxymethyl-2-vinylfuran: a biomass-based solvent-free adhesive. *Green Chem*, 2017, 19722-19728.

He YC, Tao ZC, Zhang X, Yang ZX, Xu JH (2014). Highly efficient synthesis of ethyl (S)-4-chloro-3-hydroxybutanoate and its derivatives by a robust NADH-dependent reductase from *E. coli* CCZU-K14. *Bioresour. Technol*, 61, 461-464.

Herculano PN, Porto TS, Moreira KA, Pinto GA, Souza-Motta CM, Porto AL (2011). Cellulase production by *Aspergillus japonicus* URM5620 using waste from castor bean (*Ricinus communis* L.) under solid-state fermentation. *Appl Biochem Biotechnol*, 165, 1057-1067.

Herrero AE, Kratzer R, Luley-Goedl C, Müller CA, Pitzer J, Ribitsch D, Sauer M, Schm¨olzer K,

Schnitzhofer W, Sensen CW, Soh J, Steiner K, Winkler CK, Winkler M, Wriessnegger T (2020). Enzymes revolutionize the bioproduction of value-added compounds: from enzyme discovery to special applications. *Biotechnol Adv*, 40, 10752.

Hlima HB, Bejar S, Riguet J, Haser R, Aghajari N (2013). Identification of critical residues for the activity and thermostability of *Streptomyces* sp. SK glucose isomerase. Appl. *Microbiol Biotechnol*, 97, 9715-9726.

Hong J, Tamaki H, Kumagai H (2007). Cloning and functional expression of thermostable β-glucosidase gene from *Thermoascus aurantiacus*. *Appl Microbiol Biotechnol*, 73, 1331-1339.

Hou J, Qiu C, Shen Y, Li H, Bao X (2017). Engineering of Saccharomyces cerevisiae for the efficient co-utilization of glucose and xylose. *FEMS Yeast Res*, 1, 17.

Hou YN, Wang YR, Zheng CH, Feng K (2020). Biotransformation of 5-hydroxymethylfurfural into 2,5-dihydroxymethylfuran by *Ganoderma sessile* and toxicological assessment of both compounds. *AMB Express*, 10, 88.

Hu L, He A, Liu X, Xia J, Xu J, Zhou S, Xu J (2018). Biocatalytic transformation of 5-hydroxymethylfurfural into high-Value Derivatives: Recent advances and future aspects. *ACS Sustainable Chem Eng*, 6, 12, 15915-15935.

Ibrahim AM, Hamouda RA, El-Naggar NEA, Al-Shakankery FM (2021). Bioprocess development for enhanced endoglucanase production by newly isolated bacteria, purification, characterization and in-vitro efficacy as anti-biofilm of *Pseudomonas aeruginosa*. *Sci Rep*, 11, 9754.

Ibrahim M, Bonfiglio S, Schlögl M, Vinales KL, Piaggi P, Venti C, Walter M, Krakoff J, Thearle

MS (2018). Energy expenditure and hormone responses in humans after overeating High-fructose corn syrup versus whole-wheat foods. *Obesity (Silver Spring, Md.)*, 26, 141-149.

Infanzón-Rodríguez MI, Ragazzo-Sánchez JA, del Moral S, Calderón-Santoyo M, Gutiérrez-Rivera B, Aguilar-Uscanga MG (2020). Optimization of cellulase production by *Aspergillus niger* ITV 02 from sweet sorghum bagasse in submerged culture using a Box–Behnken design. *Sugar Tech*, 22, 266-273.

Ioelovich M (2008). Cellulose as a nanostructured polymer: a short review. *BioRes*, 3, 1403-1418.

Jalak J, Kurašin M, Teugjas H, Väljamäe P (2012). Endo-exo synergism in cellulose hydrolysis revisited. *J Biol Chem*, 287, 28802-28815.

Jeong D, Oh EJ, Ko JK, Nam JO, Park HS, Jin YS, Lee EJ, Kim SR (2020). Metabolic engineering considerations for the heterologous expression of xylose-catabolic pathways in *Saccharomyces cerevisiae*. *PloS one*, 15, e0236294.

Jin LQ, Xu Q, Liu ZQ, Jia DX, Liao CJ, Chen DS, Zheng YG (2017). Immobilization of recombinant glucose isomerase for efficient production of High fructose corn syrup. *Appl Biochem Biotechnol*, 183, 293-306.

Juturu V, Wu JC (2014). Microbial cellulases: Engineering, production and applications. *Renew Sustain Energy Rev*, 33, 188-203.

Kazeem M, Ajijolakewu K, Abdul Rahman N (2021). Cellulase production by co-culture of *Bacillus licheniformis* and *B. paralicheniformis* over monocultures on microcrystalline cellulose and chicken manure-supplemented rice bran media. *BioRes*, 16, 6850-6869.

Kazlauskas R (2018). Engineering more stable proteins. *Chem Soc Rev*, 47, 9026-9045.

Kosan B, Römhild K, Meister F, Pelenc V, Kühnel S, Gerhardt M (2020). Enzymatic pulp

modification: an excellent way to expand the raw material base for lyocell applications? *Cellulose*, 27, 6577-6590.

Kuhad RC, Gupta R, Singh A (2011). Microbial cellulases and their industrial applications. *Enzyme Res*, 2011, 280696.

Kumar VA, Kurup RSC, Snishamol C, Prabhu GN (2019). Role of cellulases in food, feed, and beverage industries. In Parameswaran B, Varjani S, Raveendran S (Eds.), Green Bioprocesses, Springer Singapore, pp. 323-343.

Lah TNT, Norulaini NAN, Shahadat M, Nagao H, Hossain MDS, Omar AKM (2016). Utilization of industrial waste for the production of cellulase by the cultivation of *Trichoderma* via solid state fermentation. *Environ Process*, 3, 803.

Lee M, Rozeboom HJ, de Waal PP, de Jong RM, Dudek HM, Janssen DB (2017). Metal dependence of the xylose isomerase from *Piromyces* sp. E2 explored by activity profiling and protein crystallography. *Biochemistry*, 56, 5991-6005.

Lee M, Rozeboom HJ, Keuning E, de Waal P, Janssen DB (2020). Structure-based directed evolution improves *S. cerevisiae* growth on xylose by influencing *in vivo* enzyme performance. *Biotechnol Biofuels*, 13, 5.

Lenting HB, Warmoeskerken MM (2001). Mechanism of interaction between cellulase action and applied shear force, an hypothesis. *J Biotechnol*, 89, 217-26.

Li H, Dou M, Wang X, Guo N, Kou P, Jiao J, Fu Y (2021). Optimization of cellulase production by a novel endophytic fungus *Penicillium oxalicum* R4 isolated from *Taxus cuspidata*. *Sustainability*, 13, 6006.

Li H, Xu M, Yao X, Wen Y, Lu S, Wang J, Sun B (2022). The promoted hydrolysis effect of

cellulase with ultrasound treatment is reflected on the sonicated rather than native brown rice. *Ultrason Sonochem*. 83, 105920.

Li X, Zhang Y (2016). The conversion of 5-hydroxymethyl furfural (HMF) to maleic anhydride with vanadium-based heterogeneous catalysts. *Green Chem*, 18, 643-647.

Liming X, Xueliang S (2004). High yield cellulase production by *Trichoderma reesei* ZU-02 on corn cob residue. *Bioresource Technol*, 91, 259-262.

Liu H, Zhang D, Zhang X, Zhou C, Zhou P, Zhi Y (2020). Medium optimization for spore production of a straw-cellulose degrading *Actinomyces* strain under solid-state fermentation using response surface method. *Sustainability*, 12, 8893.

Liu F, Wang Z, Manglekar RR, Geng A (2020). Enhanced cellulase production through random mutagenesis of *Talaromyces pinophilus* OPC4-1 and fermentation optimization. *Process Biochem*, 90, 12-22.

Liu T, Huang S, Geng A (2018). Recombinant diploid *Saccharomyces cerevisiae* strain development for rapid glucose and xylose co-fermentation. *Fermentation*, 4, 59.

Liu ZQ, Zheng W, Huang JF, Jin LQ, Jia DX, Zhou HY, Xu JM, Liao CJ, Cheng XP, Mao BX, Zheng YG (2015). Improvement and characterization of a hyperthermophilic glucose isomerase from *Thermoanaerobacter ethanolicus* and its application in production of high fructose corn syrup. *J Ind Microbiol Biotechnol*, 42, 1091-1103.

Lou Y, Marinkovic S, Estrine B, Qiang W, Enderin G (2020). Oxidation of furfural and furan derivatives to maleic acid in the presence of a simple catalyst system based on acetic acid and TS-1 and hydrogen peroxide. *ACS omega*, 5, 2561-2568.

Lu M, Li J, Han L, Xiao W (2020). High-solids enzymatic hydrolysis of ball-milled corn stover with reduced slurry viscosity and improved sugar yields. *Biotechnol Biofuels*, 13, 77.

Malgas S, Thoresen M, van Dyk JS, Pletschke BI (2017). Time dependence of enzyme synergism during the degradation of model and natural lignocellulosic substrates. *Enzym Microb Technol*, 103, 1-11.

Market Study Report (2019). Global 5-hydroxymethylfurfural (5-HMF) (CAS 67-47-0) Market 2019 by Manufacturers, Regions, Type and Application, Forecast to 2024. https://www.marketstudyreport.com/reports/global-5-hydroxymethylfurfural-5-hmf-cas-67-47-0-market-2019-by-manufacturers-regions-type-and-application-forecast-to-2024.

Maryana R, Wahono S, Rosyida V (2015). Effect of temperature and fermentation time of crude cellulase production by *Trichoderma reesei* on straw substrate. *Energy Procedia*, 65, 368-371.

Megías-Sayago C, Bonincontro D, Lolli A, Ivanova S, Albonetti S, Cavani F, Odriozola JA (2020). 5-Hydroxymethyl-2-furfural oxidation over Au/CexZr1-xO2 catalysts. *Front Chem*, 8, 461.

Mika LT, Cséfalvay E, Németh Á (2018). Catalytic conversion of carbohydrates to initial platform chemicals: chemistry and sustainability. *Chem Rev*, 118, 505-613.

Misra P, Shukla PK, Prasad RK, Ramteke PW (2019). Genetic engineering applications to improve cellulase production and efficiency: Part II, New and future developments in microbial biotechnology and bioengineering from cellulose to cellulase: Strategies to improve biofuel production, Elsevier, pp. 227-260.

Mock K, Lateef S, Benedito VA, Tou JC (2017). High-fructose corn syrup-55 consumption alters hepatic lipid metabolism and promotes triglyceride accumulation. *J Nutr Biochem*, 39, 32-39.

Mthembu LD, Gupta R, Deenadayalu N (2021). Conversion of cellulose into value-added

products. In: Sand, A., Banga, S., editors, Cellulose Science and Derivatives, IntechOpen, London.

Muñoz T, Rache LY, Rojas HA, Romanelli GP, Martinez JJ, Luque R (2020). Production of 5-hydroxymethyl-2-furan carboxylic acid by *Serratia marcescens* from crude 5-hydroxymethylfurfural. *Biochem Eng J*, 154, 107421.

Nair AS, Al-Battashi H, Al-Akzawi A, Annamalai N, Gujarathi A, Al-Bahry S, Dhillon GS, Sivakumar N (2018). Waste office paper: A potential feedstock for cellulase production by a novel strain *Bacillus velezensis* ASN1. *Waste Management*, 79, 491–500.

Nam KH (2022). Glucose isomerase: Functions, Structures, and Applications. *Appl Sci*, 12, 428.

Neifar S, BenHlima H, Mhiri S, Mezghani M, Bouacem K, Ibrahim AH, Jaouadi B, Bouanane-Darenfed A, Bejar S (2019). A novel thermostable and efficient Class II glucose isomerase from the thermophilic *Caldicoprobacter algeriensis*: Biochemical characterization, molecular investigation, and application in High Fructose Syrup production. *Int J Biol Macromol*, 129, 31-40.

Neifar S, Cervantes FV, Bouanane-Darenfed A, BenHlima H, Ballesteros AO, Plou FJ, Bejar S (2020). Immobilization of the glucose isomerase from *Caldicoprobacter algeriensis* on Sepabeads EC-HA and its efficient application in continuous High Fructose Syrup production using packed bed reactor. *Food Chem*, 309, 125710.

Ng IS, Li CW, Yeh YF, Chen PT, Chir JL, Ma CH, Yu SM, Ho TH, Tong CG (2009). A novel endo-glucanase from the thermophilic bacterium *Geobacillus* sp. 70PC53 with high activity and stability over a broad range of temperatures. *Extremophiles*, 13, 425-435.

Nordwald EM, Brunecky R, Himmel ME, Beckham GT, Kaar JL (2014). Charge engineering of

cellulases improves ionic liquid tolerance and reduces lignin inhibition. *Biotechnol Bioeng*, 111, 1541-1549.

Nugraha WD, Wafiroh H, Syafrudin, Junaidi, Budihardjo MA, Safitri RP (2021). The effect of amylase and cellulase enzymes on biogas production from rice husk waste using solid-state anaerobic digestion (SS-AD) method. *IOP Conf Ser: Earth Environ Sci*, 623, 012018.

Obeng EM, Adam SNN, Budiman C, Ongkudon CM, Maas R, Joseet J (2017). Lignocellulases: a review of emerging and developing enzymes, systems, and practices. *Bioresour Bioprocess*, 4, 16.

Ohara A, Santos JG, Angelotti JA, Barbosa PD, Dias FF, Bagagli MP, Sato HH, Castro RJ (2018). A multicomponent system based on a blend of agroindustrial wastes for the simultaneous production of industrially applicable enzymes by solid-state fermentation. *J Food Sci Technol*, 38, 131-137.

Olsen NJ, Heitmann BL (2009). Intake of calorically sweetened beverages and obesity. *Obes Rev*, 10, 68-75.

Omajali JB, Gomez-Bolivar J, Mikheenko IP, Sharma S, Kayode B, Al-Duri B, Banerjee D, Walker M, Merroun ML, Macaskie LE (2019). Novel catalytically active Pd/Ru bimetallic nanoparticles synthesized by *Bacillus benzeovorans*. *Sci Rep*, 9, 4715.

Ottenheim C, Nawrath M, Wu JC (2018). Microbial mutagenesis by atmospheric and room temperature plasma (ARTP): the latest development. *Bioresour Bioprocess*, 5, 12.

Ozkan H, Yakan A (2019). Dietary high calories from sunflower oil, sucrose and fructose sources alters lipogenic genes expression levels in liver and skeletal muscle in rats. *Ann Hepatol*, 18, 715-724.

Padmanabhan SK, Lionetto F, Nisi R, Stoppa M, Licciulli A (2022). Sustainable production of

stiff and crystalline bacterial cellulose from orange peel extract. *Sustainability*, 14, 2247.

Pal P, Kumar S, Devi MM, Saravanamurugan S (2020). Oxidation of 5-hydroxymethylfurfural to 5-formyl furan-2-carboxylic acid by non-precious transition metal oxide-based catalyst. *J Supercritical Fluids*, 160, 104812.

Paniagua AI, Diez-Antolinez R, Hijosa-Valsero M, Sanchez ME, Coca M (2016). Response surface optimization of dilute sulfuric acid pretreatment of switchgrass (*Panicum virgatum* l.) for fermentable sugars production. *Chemical Engineering Transactions*, 49, 223-228.

Papzan Z, Kowsari M, Javan-Nikkhah M, Gohari AM, Limón MC (2021). Strain improvement of *Trichoderma* spp. through two-step protoplast fusion for cellulase production enhancement. *Can J Microbiol*, 67, 406-414.

Park YJ, Jung BK, Hong SJ, Park GS, Ibal JC, Pham HQ, Shin JH (2018). Expression and characterization of calcium- and zinc-tolerant xylose isomerase from *Anoxybacillus kamchatkensis* G10. J *Microbiol Biotechnol*, 28, 606-612.

Patel AK, Singhania RR, Sim SJ, Pandey A (2019). Thermostable cellulases: Current status and perspectives. *Bioresour Technol*, 279, 385-392.

Pedersen S (1993.) Industrial aspects of immobilized glucose isomerase. *Bioprocess Technol*, 16, 185-208.

Pena CE Jr, Costa MGS, Batista PR (2020). Glycosylation effects on the structure and dynamics of a full-length Cel7A cellulase. *Biochim Biophys Acta Proteins Proteom*, 1868, 140248.

Peng ZQ, Li C, Lin Y, Wu SS, Gan LH, Liu J, Yang SL, Zeng XH, Lin L (2021). Cellulase production and efficient saccharification of biomass by a new mutant *Trichoderma afroharzianum* MEA-12. *Biotechnol Biofuels*, 14, 219.

Petri A, Masia G, Piccolo O (2018). Biocatalytic conversion of 5-hydroxymethylfurfural:

Synthesis of 2,5-bis(hydroxymethyl)furan and 5-(hydroxymethyl)furfurylamine. *Catal Commun*, 114, 15-18.

Phaneuf PV, Yurkovich JT, Heckmann D, Wu M, Sandberg TE, King ZA, Tan J, Palsson BO, Feist AM (2020). Causal mutations from adaptive laboratory evolution are outlined by multiple scales of genome annotations and condition-specificity. *BMC Genomics*, 21, 514.

Potprommanee L, Wang XQ, Han YJ, Nyobe D, Peng YP, Huang Q, Liu JY, Liao YL, Chang KL (2017). Characterization of a thermophilic cellulase from *Geobacillus* sp. HTA426, an efficient cellulase-producer on alkali pretreated of lignocellulosic biomass. *PLoS One*, 2017 12, e0175004.

Pottkämper J, Barthen P, Ilmberger N, Schwaneberg U, Schenk A, Schulte M, Ignatiev N, Streit WR (2009). Applying metagenomics for the identification of bacterial cellulases that are stable in ionic liquids. *Green Chem*, 11, 957-965.

Pramanik SK, Mahmud S, Paul GK, Jabin T, Naher K, Uddin MS, Zaman S, Saleh MA (2020). Fermentation optimization of cellulase production from sugarcane bagasse by *Bacillus pseudomycoides* and molecular modeling study of cellulase. *Curr Res Microb Sci*, 2, 100013.

Przydacz M, Jędrzejczyk M, Rogowski J, Szynkowska-Jóźwik M, Ruppert AM (2020). Highly efficient production of DMF from biomass-derived HMF on recyclable Ni-Fe/TiO2 catalysts. *Energies*, 13, 4660.

Qi X, Zha J, Liu GG, Zhang W, Li BZ, Yuan YJ (2015). Heterologous xylose isomerase pathway and evolutionary engineering improve xylose utilization in *Saccharomyces cerevisiae*. *Front Microbiol*, 6, 1165.

Rajesh RO, Godan TK, Sindhu R, Pandey A, Binod P (2020). Bioengineering advancements,

innovations and challenges on green synthesis of 2, 5-furan dicarboxylic acid. *Bioengineered*, 11, 19-38.

Ramesh, A., Devi, P. H., Chattopadhyay, S., & Kavitha, M. (2020). Commercial applications of microbial enzymes. In Arora NK, Mishra J & Mishra V (Eds.), Microbial enzymes: Roles and applications in industries, *Springer Nature*, 11, 137–184.

Raveendran S, Parameswaran B, Ummalyma SB, Abraham A, Mathew AK, Madhavan A, Rebello S, Pandey A (2018). Applications of microbial enzymes in food industry. *Food Technol Biotechnol*, 56, 16-30.

Rigoldi F, Donini S, Redaelli A, Parisini E, Gautieri A (2018). Review: Engineering of thermostable enzymes for industrial applications. *APL Bioeng*, 2, 011501.

Sadowska J, Rygielska M (2019). The effect of high fructose corn syrup on the plasma insulin and leptin concentration, body weight gain and fat accumulation in rat. *Adv Clin Exp Med*, 28, 879-884.

Sahoo K, Sahoo RK, Gaur M, Subudhi E (2018). Isolation of cellulase genes from thermophilies: A novel approach toward new gene discovery. In New and future developments in microbial biotechnology and bioengineering: Microbial genes biochemistry and applications, Elsevier, pp. 151-169.

Saikia K, Rathankumar AK, Kumar PS, Varjani S, Nizar M, Lenin R, George J, Vaidyanathan VK (2022). Recent advances in biotransformation of 5-hydroxymethylfurfural: challenges and future aspects. J Chem Technol Biotechnol, 97, 409-419.

Saini R, Saini JK, Adsul M, Patel AK, Mathur A, Tuli D, Singhania RR (2015).Enhanced cellulase production by *Penicillium oxalicum* for bio-ethanol application. *Bioresour Technol*, 188, 240-246.

Sajid M, Zhao X, Liu D (2018). Production of 2,5-furandicarboxylic acid (FDCA) from 5-hydroxymethylfurfural (HMF): recent progress focusing on the chemical-catalytic routes. *Green Chem*, 20, 5427-5453.

Sampathkumar K, Kumar V, Sivamani S, Sivakumar N (2019). An insight into fungal cellulases and their industrial applications. In Srivastava M, Srivastava N, Ramteke PW, Mishra PK (Eds.), Approaches to enhance industrial production of fungal cellulases, Springer, pp. 19-35).

Seike T, Kobayashi Y, Sahara T, Ohgiya S, Kamagata Y, Fujimori KE (2019). Molecular evolutionary engineering of xylose isomerase to improve its catalytic activity and performance of micro-aerobic glucose/xylose co-fermentation in *Saccharomyces cerevisiae*. *Biotechnol Biofuels*, 12, 139.

Shah F, Mishra S (2020). *In vitro* optimization for enhanced cellulose degrading enzyme from *Bacillus licheniformis* KY962963 associated with a microalgae *Chlorococcum* sp. using OVAT and statistical modeling. *SN Appl Sci*, 2, 1923.

Shapla UM, Solayman M, Alam N, Khalil MI, Gan SH (2018). 5-Hydroxymethylfurfural (HMF) levels in honey and other food products: effects on bees and human health. *Chem Cent J*, 12, 35.

Sharma A, Tewari R, Rana SS, Soni R, Soni SK (2016). Cellulases: classification, methods of determination and industrial applications. *Appl Biochem Biotechnol*, 179, 1346-1380.

Sharma S, Jha PK, Panwar A (2021). Production of bioethanol from wheat straw via optimization of co-culture conditions of *Bacillus licheniformis* and *Saccharomyces cerevisiae*. *Discov Energy*, 1, 5.

Sheng Y, Tan X, Zhou X, Xu Y (2020). Bioconversion of 5-hydroxymethylfurfural (HMF) to 2,5-

furandicarboxylic acid (FDCA) by a native obligate aerobic bacterium, *Acinetobacter calcoaceticus* NL14. *Appl Biochem Biotechnol*, 192, 455-465.

Sher H, Zeb N, Zeb S, Ali A, Aleem B, Iftikhar F, Rahman SU, Rashid MH (2021). Microbial cellulases: A Review on strain development, purification, characterization and their industrial applications. *J Bacteriol Mycol*, 8, 1180.

Shida Y, Furukawa T, Ogasawara W (2016). Deciphering the molecular mechanisms behind cellulase production in *Trichoderma reesei*, the hyper-cellulolytic flamentous fungus. *Biosci Biotechnol Biochem*, 80, 1712-1729.

Shokri Z, Seidi F, Karami S, Li C, Saeb MR, Xiao H (2021). Laccase immobilization onto natural polysaccharides for biosensing and biodegradation. *Carbohydr Polym*, 262, 117963.

Silva JCR, Salgado JCS, Vici AC, Ward RJ, Polizeli MLTM, Guimarães LHS, Furriel RPM, Jorge JA (2020). A novel *Trichoderma reesei* mutant RP698 with enhanced cellulase production. *Braz J Microbiol*, 51, 537-545.

Silva PC, Ceja-Navarro JA, Azevedo F, Karaoz U, Brodie EL, Johansson BA (2021). A novel D-xylose isomerase from the gut of the wood feeding beetle *Odontotaenius disjunctus* efficiently expressed in *Saccharomyces cerevisiae*. *Sci Rep*, 11, 4766.

Silva TP, Ferreira AN, de Albuquerque FS, Barros ACdeA, da Luz JMR, Gomes FS, Pereira HJV (2021). Box–Behnken experimental design for the optimization of enzymatic saccharification of wheat bran. *Biomass Conv Bioref*.

Simakova I, Demidova Y, Simonov M, Prikhod'ko S, Niphadkar P, Bokade V, Dhepe P, Murzin DY (2020). Heterogeneously catalyzed γ-valerolactone hydrogenation into 1,4-pentanediol in milder reaction conditions. *Reactions*, 1, 54-71.

Sindhu R, Binod P, Pandey A (2016). Biological pretreatment of lignocellulosic biomass – An

overview. *Bioresour Technol*, 199, 76-82.

Singhania RR, Adsul M, Pandey A, Patel AK (2017). Cellulases. In Pandey A, Negi S, Soccol CR (Eds.), Current developments in biotechnology and bioengineering - Production, isolation and purifcation of industrial products, Elsevier, pp. 73-101.

Singhania RR, Sukumaran RK, Pandey A (2007). Improved cellulase production by *Trichoderma reesei* RUT C30 under SSF through process optimization. Appl Biochem Biotechnol, 142, 60-70.

Sirohi R, Singh A, Tarafdar A, Shahi NC (2018). Application of genetic algorithm in modelling and optimization of cellulase production. *Bioresour Technol*, 270, 751-754.

Sirohi R, Singh A, Tarafdar AS, Sahi NC, Verma AK, Kushwaha A, Sirohi R (2019). Cellulase production from pre-treated pea hulls using *Trichoderma reesei* under submerged fermentation. *Waste Biomass Valor*, 10, 2651-2659.

Siva D, Srivethi G, Vasan PT, Rajesh D, Alfarhan A, Rajagopal R (2022). Enhanced cellulase enzyme production by Aspergillus niger using cellulase/iron oxide magnetic nano-composites. *J King Saud Univ Sci*, 34.

Soccol CR, Costa ESF, da Letti LAJ, Karp SG, Woiciechowski AL, Vandenberghe LPdeS (2017). Recent developments and innovations in solid state fermentation. *Biotechnol Res Innov*, 1, 52-71.

Socha AM, Parthasarathi R, Shi J, Pattathil S, Whyte D, Bergeron M, George A, Tran K, Stavila V, Venkatachalam S (2014). Efficient biomass pretreatment using ionic liquids derived from lignin and hemicellulose. *Proc Natl Acad Sci*, 111, E3587-E3595.

Soni SK, Sharma A, Soni R (2018). Cellulases: Role in lignocellulosic biomass utilization. In Lübeck M (Ed.), Cellulases, Humana Press, New York, 1796, pp. 3–23.

Souzanchi S, Nazari L, Rao KTV, Yuan Z, Tan Z, Xu C (2019). Catalytic isomerization of glucose to fructose using heterogeneous solid base catalysts in a continuous-flow tubular reactor: catalyst screening study. *Catal Today*, 319, 76-83.

Srivastava N, Srivastava M, Ramteke PW, Mishra PK (2019). Synthetic biology strategy for microbial cellulases: An overview, new and future developments in microbial biotechnology and bioengineering, microbial genes biochemistry and applications, Elsevier, pp. 229-238.

Sulyman AO, Igunnu A, Malomo SO (2020). Isolation, purification and characterization of cellulase produced by *Aspergillus niger* cultured on *Arachis hypogaea* shells. *Heliyon*, 6, e05668.

Sun X, Liang Y, Wang Y, Zhang H, Zhao T, Yao B, Luo H, Huang H, Su X (2022). Simultaneous manipulation of multiple genes within a same regulatory stage for iterative evolution of *Trichoderma reesei*. *Biotechnol Biofuels Bioprod*, 15, 26.

Thakkar A, Saraf M (2014). Application of statistically based experimental designs to optimize cellulase production and identification of gene. *Nat Prod Bioprospect*, 4, 341-351.

Tiwari S, Yadav J, Gaur R, Singh R,Verma T, Yadav JS, Pandey PK and Rath SK (2022). Multistep structural and chemical evaluation of sugarcane baggase, pretreated with alkali for enhancing the enzymatic saccharification by cellulase and xylanase of the *Pseudomonas* sp. CVB-10 (MK443365) and *Bacillus paramycoides* T4 (MN370035) mixculture system. *Front Energy Res*, 9, 726010.

Tongtummachat T, Akkarawatkhoosith N, Kaewchada A, Jaree A (2020). Conversion of glucose to 5-hydroxymethylfurfural in a microreactor. *Front Chem*, 7, 951.

Toushik SH, Lee KT, Lee JS, Kim KS (2017). Functional applications of lignocellulolytic enzymes

in the fruit and vegetable processing industries. *J Food Sci*, 82, 585-593.

Ursachi VF, Gutt G (2020). Production of cellulosic ethanol from enzymatically hydrolysed wheat straws. *Appl Sci*, 10, 7638.

Varghese LM, Agrawal S, Sharma D, Mandhan RP, Mahajan R (2017). Cost-effective screening and isolation of xylanocellulolytic positive microbes from termite gut and termitarium. *3 Biotech*, 7, 108.

Verma N, Kumar V (2020). Impact of process parameters and plant polysaccharide hydrolysates in cellulase production by *Trichoderma reesei* and *Neurospora crassa* under wheat bran based solid state fermentation. *Biotechnol Rep*, 25.

Verma N, Kumar V, Bansal MC (2021). Valorization of waste biomass in fermentative production of cellulases: A review. *Waste Biomass Valor*, 12, 613-640.

Voutilainen SP, Murray PG, Tuohy MG, Koivula A (2010). Expression of *Talaromyces emersonii* cellobiohydrolase Cel7A in *Saccharomyces cerevisiae* and rational mutagenesis to improve its thermostability and activity. *Protein Eng Des Sel*, 23, 69-79.

Vu V, Farkas C, Riyad O, Bujna E, Kilin A, Sipiczki G, Sharma M, Usmani Z, Gupta VK, Nguyen QD (2022). Enhancement of the enzymatic hydrolysis efficiency of wheat bran using the *Bacillus* strains and their consortium. *Bioresour Technol*, 343,126092.

Wang S, Dai G, Yang H, Luo Z (2017). Lignocellulosic biomass pyrolysis mechanism: A state-of-the-art review. *Prog Energy Combust Sci*, 62, 33-86.

Wang X, Deng Z, Liu T (2019). Marker-free system using ribosomal promoters enhanced xylose/glucose isomerase production in *Streptomyces rubiginosus*. *Biotechnol J*, 14, 1900114.

Weerathunga H, Sarina S, Zhu HY, Waclawik ER (2021). Oxidative Esterification of 5-

hydroxymethylfurfural into dimethyl 2,5-furandicarboxylate using gamma alumina-supported gold nanoparticles. *ACS Omega*, 6, 4740-4748.

Wiltschi B, Cernava T, Dennig A, Galindo CM, Geier M, Gruber S, Haberbauer M, Heidinger P, Xu Q, Zheng Z, Zou L, Zhang C, Yang F, Zhou K, Ouyang J (2020). A versatile *Pseudomonas putida* KT2440 with new ability: selective oxidation of 5-hydroxymethylfurfural to 5-hydroxymethyl-2-furancarboxylic acid. *Bioprocess Biosyst Eng*, 43, 67-73.

Winarsih S, Siskawardani DD (2020). Hydrolysis of corncobs using a mixture of crude enzymes from *Trichoderma reesei* and *Aspergillus niger* for bioethanol production. *Energy Reports*, 6, 256-262.

Wolski PW, Dana CM, Clark DS, Blanch HW (2016). Engineering ionic liquid-tolerant cellulases for biofuels production. *Protein Eng Des Sel*, 29, 117-122.

Wu X, Luo N, Xie S, Zhang H, Zhang Q, Wang F, Wang Y (2020). Photocatalytic transformations of lignocellulosic biomass into chemicals. *Chem Soc Rev*, 49, 6198-6223.

Xie M, Zhang J, Tschaplinski TJ, Tuskan GA, Chen JG, Muchero W (2018). Regulation of lignin biosynthesis and its role in growth-defense tradeoffs. *Front Plant Sci*, 9, 1427.

Xu ZH, Cheng AD, Xing XP, Zong MH, Bai YP, Li N (2018). Improved synthesis of 2,5-bis (hydroxymethyl) furan from 5-hydroxymethylfurfural using acclimatized whole cells entrapped in calcium alginate. *Bioresour Technol*, 262, 177-183.

Yadav GD, Sharma RV (2014). Biomass derived chemicals: environmentally benign process for oxidation of 5-hydroxymethylfurfural to 2, 5-diformylfuran by using nano-fibrous Ag-OMS-2-catalyst. *Appl Catal B: Environ*, 147, 293-301.

Yadav V, Wang Z, Wei C, Amo A, Ahmed B, Yang X, Zhang X (2020). Phenylpropanoid pathway

engineering: An emerging approach towards plant defense. *Pathogens*, 9, 312.

Yang Z, Zhang J, Qian G, Duan X, Zhou X (2021). Production of biomass-derived monomers throughcatalytic conversion of furfural and hydroxymethylfurfural. *GreenChE*, 2, 158-173.

Yao L, Yang H, Meng X, Ragauskas AJ (2022) Toward a fundamental understanding of the role of lignin in the biorefinery process. *Front Energy Res*, 9, 804086.

Yuan Y, Jiang B, Chen H, Wu W, Wu S, Jin Y, Xiao H (2021). Recent advances in understanding the effects of lignin structural characteristics on enzymatic hydrolysis. Biotechnol Biofuels, 14, 205.

Zapata YM, Galviz-Quezada A, Osorio-Echeverri VM (2018). Cellulases production on paper and sawdust using native *Trichoderma asperellum*. Univ Sci, 23, 419-436.

Zeng FR, Xu J, Sun LH, Ma J, Jiang H, Li ZL (2020). Copolymers of ε-caprolactone and ε-caprolactam via polyesterification: towards sequence-controlled poly(ester amide)s. *Polym Chem*, 11, 1211-1219.

Zhao HC, Liu X, Zhan T, He J (2018). Production of cellulase by *Trichoderma reesei* from pretreated straw and furfural residues. *RSC Adv*, 8, 36233-36238.

Zhong R, Cui D, Ye Z (2019). Secondary cell wall biosynthesis. *New Phytologist*, 221, 1703-1723.

Zunita M, Wahyuningrum D, Buchari, Bundjali B, Wenten IG, Boopathy R (2021). Conversion of glucose to 5-hydroxymethylfurfural, levulinic acid, and formic acid in 1,3-dibutyl-2-(2-butoxyphenyl)-4,5-diphenylimidazolium iodide-based ionic liquid. *Appl Sci*, 11, 989.

CHAPTER 2

Characterization of cellulose-degrading bacteria isolated from soil and the optimization of their culture conditions for cellulase production

Adapted from: Aristide Laurel Mokale Kognou[1], Chonlong Chio[1], Janak Raj Khatiwada[1], Sarita Shrestha[1], Xuantong Chen[1], Sihai Han[1,2], Hongwei Li[3], Zi-Hua Jiang[4], Chunbao (Charles) Xu[3], Wensheng Qin[1]*

Applied biochemistry and biotechnology, 2022

[1]Department of Biology, Lakehead University, Thunder Bay, Ontario, Canada

[2]College of Food and Bioengineering, Henan University of Science and Technology, Luoyang, China

[3]Department of Chemical and Biochemical Engineering, Western University, London, Ontario, Canada

[4]Department of Chemistry, Lakehead University, Thunder Bay, Ontario, Canada

*Corresponding author: Wensheng Qin

Abstract

The characterization of bacteria with hydrolytic potential significantly contributes to the industries. Six cellulose-degrading bacteria were isolated from mixture soil samples collected at Kingfisher Lake and the University of Manitoba campus by Congo red method using carboxymethyl cellulose agar medium and identified as *Paenarthrobacter* sp. MKAL1, *Hymenobacter* sp. MKAL2, *Mycobacterium* sp. MKAL3, *Stenotrophomonas* sp MKAL4, *Chryseobacterium* sp. MKAL5 and *Bacillus* sp. MKAL6. Their cellulase production was optimized by controlling different

environmental and nutritional factors such as pH, temperature, incubation period, substrate concentration, nitrogen and carbon sources using the dinitrosalicylic acid and response surface methods. Except for *Paenarthrobacter* sp. MKAL1, all strains are motile. Only *Bacillus* sp. MKAL6 was non-salt-tolerant and showed gelatinase activity. Sucrose enhanced higher cellulase activity of 78.87-190.30 U/mL in these strains at their optimum pH (5-6) and temperature (35-40°C). The molecular weights of these cellulases were about 25 kDa. These bacterial strains could be promising biocatalysts for converting cellulose into glucose for industrial purposes.

Keywords: Cellulolytic bacteria; soil; carboxymethylcellulose; cellulase; SDS-PAGE

1. Introduction

In the past, humans used cellulosic materials as fertilizers, fodder, and firewood. Nowadays, it has become a cost-effective raw material and its industrial applications have become more complex. These applications have created a vast platform based on cellulose research in multidisciplinary projects. Cellulose hydrolysis is one of the approaches catalyzed by cellulases. Cellulose is a linear polymer made up of D-glucopyranose units linked by β-(1-4) glycosidic linkage and constitutes practically inexhaustible carbon and renewable energy resource (Danalache et al., 2018). Cellulose offers the best prospects for reducing the production costs of many products due to its abundance and potentially lower price than other substrates, despite the complexity of the transformation processes (Silalertruksa and Gheewala, 2020). It constitutes a significant challenge in research, particularly in the field of bioproducts, biofuels and chemicals. Cellulose (crystalline and amorphous) forms with hemicellulose and lignin, a water-insoluble compact network structure that limits its degradation (Faria et al., 2020). Therefore, pretreatment

(physical, chemical and biological) is required to facilitate fermentable sugar release. Biological pretreatment (enzymes and cellulolytic microorganisms) remains the best approach to address this issue because it is eco-friendly (Sankaran et al., 2020).

Cellulase is a whole enzyme system composed of endoglucanase and exoglucanases including cellobiohydrolases and β-glucosidase (Paudel and Qin, 2015), which breaks down β-1,4-linkages in cellulose polymer to release glucose units. Many investigators have reported that aerobic and anaerobic bacteria (Singhania et al., 2017; Soni et al., 2018; Kumar et al., 2019; Sampathkumar et al., 2019), fungi and actinomycetes (Shida et al., 2016; Kumar et al., 2019; Ramesh et al., 2020) are good cellulase enzyme producers. These microbes secrete free or cell surface-bound cellulases and exhibit an efficient enzyme decomposition. Among different types of microbes, bacteria are the most efficient cellulose degraders because they grow fast and have high cellulase synergistic activity (Bilal and Iqbal, 2020). Cellulases are very successful in the industrial exploitation of the degradation of lignocellulosic biomass. Cellulases have a wide range of applications in several sectors such as chemicals, food and feed, pulp and paper, textiles, beverages, automobiles, electronics and, most importantly, energy (Cipolatti et al., 2019; De Souza and Kawaguti, 2021).

Recent data shows that the market demand for cellulase is 29.71% in animal feed, 26.37% in food and beverages, and 13.77% in the textile industry (Guerrand, 2018). Also, cellulase applications are drastically rising annually. They will reach 2300 million USD by the end of 2025, with a 5.5% of annual growth rate for the 2018-2025 period according to the Global cellulase (CAS 9012-54-8) market growth 2021-2026 report in 2021. However, few cellulases perform well on an industrial scale, and their production cost remains very high. Therefore, it is essential to search for new cellulases with interesting properties from an industrial point of view. In recent years much

work has been devoted to selecting cellulolytic microorganisms, genetic mutations for obtaining hyperproductive strains and the culture conditions of the microorganisms involved (Marques et al., 2018). Their cellulase yields depend on a combination of various factors such as pH, temperature, inoculum size, cellulose type, aeration, incubation time and inducers (Islam and Roy, 2018). In the present study, we have characterized six cellulose-degrading bacteria isolated from the soil samples collected at Kingfisher Lake (Thunder Bay, Canada) and the University of Manitoba campus (Winnipeg, Canada). The culture conditions for these bacterial strains were optimized to achieve maximum cellulase production.

2. Materials and Methods

2.1. Culture media

Different culture media were used for bacterial growth and cellulase production. These culture media include a) Reasoner's 2A (R2A) agar, b) Luria-Bertani (LB) broth, c) carboxymethylcellulose (CMC) agar, and d) CMC broth. Their compositions were as follows:

a) R2A agar: 0.5 g yeast extract, 0.5 g peptone, 0.5 g starch, 0.5 g $MgSO_4$, 0.5 g casein hydrolysate, 0.5 g glucose, 0.3 g K_2HPO_4, 15 g agar and distilled water up to 1 L;

b) LB broth:10 g peptone, 5 g yeast extract, 5 g NaCl and distilled water up to 1 L;

c) CMC agar: 5 g CMC, 1 g $NaNO_3$, 1 g K_2HPO_4, 1 g KCl, 0.5 g $MgSO_4$, 0.5 g yeast extract, 15 g agar and distilled water up to 1 L;

d) CMC broth: 5 g CMC, 1 g $NaNO_3$, 1 g K_2HPO_4, 1 g KCl, 0.5 g $MgSO_4$, 0.5 g yeast extract and distilled water up to 1 L.

2.2. Screening of cellulose-degrading bacteria

The soil samples were collected from Kingfisher Lake and the University of Manitoba campus. The topsoil was dug by a sterile spatula, kept in a clean zip lock bag, and transported to the laboratory. The samples were mixed for bacterial isolation by dilution method (Maki et al., 2011). The samples (0.5 g) were suspended in distilled water (50 mL) by vortexing for 2 min. A 10x dilution series was made and each dilution (5 µL) was plated onto R2A agar. All plates were incubated for 72 h at 28°C. Based on their morphological features (size, shape, and colour), forty-one bacterial colonies were selected. These colonies were streaked out in R2A agar Petri dishes. After incubation at 30°C for 48 h, these colonies were screened for their ability to produce cellulase using Congo red method (Cangelosi et al., 1999). For this purpose, the isolates (bacterial colonies, negative and positive controls) were grown in LB broth (10 mL) for 24 h shaking at 30°C. *Bacillus* sp. IM7 and *Escherichia coli* JM109 from Dr Qin's lab were used as positive and negative controls respectively. All broth cultures (5 µL) were singly dropped onto CMC agar plates and then incubated at 30°C for 48 h. After incubation, plates were stained with aqueous Congo red solution (0.1% w/v) as an indicator to visualize the cellulase activity. The appearance of a clear halo around the isolate confirms cellulase activity by the isolate. Halo diameters were measured using a ruler for a semi-qualitative comparison of cellulase activity among isolates. Plates were photographed, and six cellulose-degrading bacterial isolates (CDBs) were selected and stored for subsequent uses (Figure 1).

2.3. Characterization of cellulose-degrading bacteria

2.3.1. Morphological and biochemical characterization

CDBs were differentiated based on mobility, cell wall composition (Gram stain), vegetative cells and endospores (endospore stain), carbon source utilization and enzymatic activities by standard methods such as catalase production, gas production, starch hydrolysis, gelatin hydrolysis, DNA hydrolysis, urease test, bile esculin test, oxidase test, nitrate reduction, salt tolerance and sugar fermentation (Cowan and Steel, 2003).

2.3.2. Molecular identification by 16S rRNA gene sequencing

DNA was isolated from each CDB culture (LB broth, 24 h shaking and 30°C) using the Bacteria Genomic DNA Isolation Kit (Norgen Biotek Corporation, Canada). The resulting isolated DNA was used as a template in a PCR reaction to amplify a region of the 16S rRNA. Universal primers within conserved regions of the 16S rRNA, which amplify an approximately 796 bp fragment were used: forward primer HAD-1 (5′-GACTCCTACGGGAGGCAGCAGT) and reverse primer E1115R (5′-AGGGTTGCGCTCGTTGCGGG) (Giannino et al., 2009). The amplification system contains 2 × Taq PCR Master Mix of 10 μL (10 x Taq DNA polymerase buffer, 10 mM dNTPs, 25 mM of MgCl2, 1 U of Taq DNA polymerase), 1 μL of 10 μM forward and reverse primers respectively, 1 μL of the genomic DNA template, and 7 μL of distilled water making a total volume of 20 μL. The PCR methodology consisted of denaturation for 1 minute at 94°C, followed by 30 amplification cycles consisting of denaturing at 94°C for 30 s, annealing for 30 s at 58°C, and extension at 72°C for 1 min and 30 s. A final extension step was done at 72°C for 10 min. Then, PCR products were viewed on an agarose gel (1% w/v) to confirm size, quantity, and purity. They were extracted using Gel/PCR DNA Fragments Extraction Kit (Geneaid

FroggaBio, Canada). The resulting products were sequenced by Eurofins MWG Operon Inc., Canada. Sequencing results were individually imputed online using the Nucleotide Basic Local Alignment Search Tool (BLAST) through the National Center for Biotechnology Information (NCBI) database (http://www.ncbi.nlm.nih.gov/) to identify the genera of CDB. For molecular analyses, the available sequence data for all related species were downloaded from GenBank. Sequences were assembled and aligned using the Clustalw module in BioEdit v. 7.0.9.0 (Hall, 1999) with default settings. Phylogenetic analysis was conducted using the Neighbor-Joining (NJ) Tree with 1000 bootstrap using the program MEGA 7 (Kumar et al., 2016).

2.4. Quantification of cellulase activity

Quantitative cellulase activities of CDBs were determined by measuring the release of reducing sugars from CMC using the 3,5-dinitrosalicylic acid (DNS) method (Paudel and Qin, 2015). `CDBs were grown in 5 mL of LB broth (24 h, 30°C and 200 rpm). Five hundred microliters of each cultured isolate were centrifuged at 12,000 x g for 5 min and the cells were suspended in 0.05 M citrate buffer (pH 6). These bacterial samples were inoculated separately into a 250 mL Erlenmeyer flask containing CMC broth (50 mL, 1% CMC) prepared with citrate buffer (0.05 M, pH 6). Then, the flasks were incubated at 35°C and 200 rpm for 5 days. Cellulase assay was performed using the cell-free culture supernatant as an extracellular crude enzyme. Each crude enzyme was obtained by centrifugation of 500 µL of culture at 12,000 × g for 5 min. The reaction mixture containing crude enzyme (10 µL), 0.05 M citrate buffer pH 6 (20 µL) and 1% CMC (20 µL) was transferred into a 1 mL microcentrifuge tube and incubated in the water bath at 50°C for 15 min. The DNS solution (60 µL) was added to the reaction mixture and the tube was heated for 5 min to stop the reaction. The release of reducing sugars in reaction mixture was estimated using

glucose (1.1-2 mg/mL) as a standard for the calibration curve ($y = 0.6419x - 0.1021$; $r^2 = 0.9975$). Every 24 h for 120 h, reaction mixture and bacterial growth were respectively measured at 540 and 600 nm by using a microplate reader spectrophotometer (BioTek, USA). The bacterial growth was expressed in terms of biomass, whereas the cellulase activity was measured in U/mL (one unit of cellulase enzyme corresponds to the release of 1 μM of reducing sugar equivalent per minute from CMC) (Rahman et al., 2018).

2.5. Optimization of cellulase production

Cellulase production was optimized by varying some parameters such as incubation time, pH, temperature, CMC concentration, salts, surfactants, carbon, and nitrogen sources. CDBs were grown in LB broth (24 h, 30°C and 200 rpm). The culture medium was inoculated and incubated for 5 days and the cellulase amount produced was determined from the supernatant using the DNS method (Paudel and Qin, 2015).

2.5.1. Effect of temperature and incubation period on cellulase production

The CMC broth (50 mL) containing overnight cultured bacterial strain (500 μL) was incubated in a shaking incubator (200 rpm) at 30, 35, 40, 45 and 50°C for 5 days. The effect of temperature and incubation time on enzyme production was quantified by collecting culture solution (500 μL) every day.

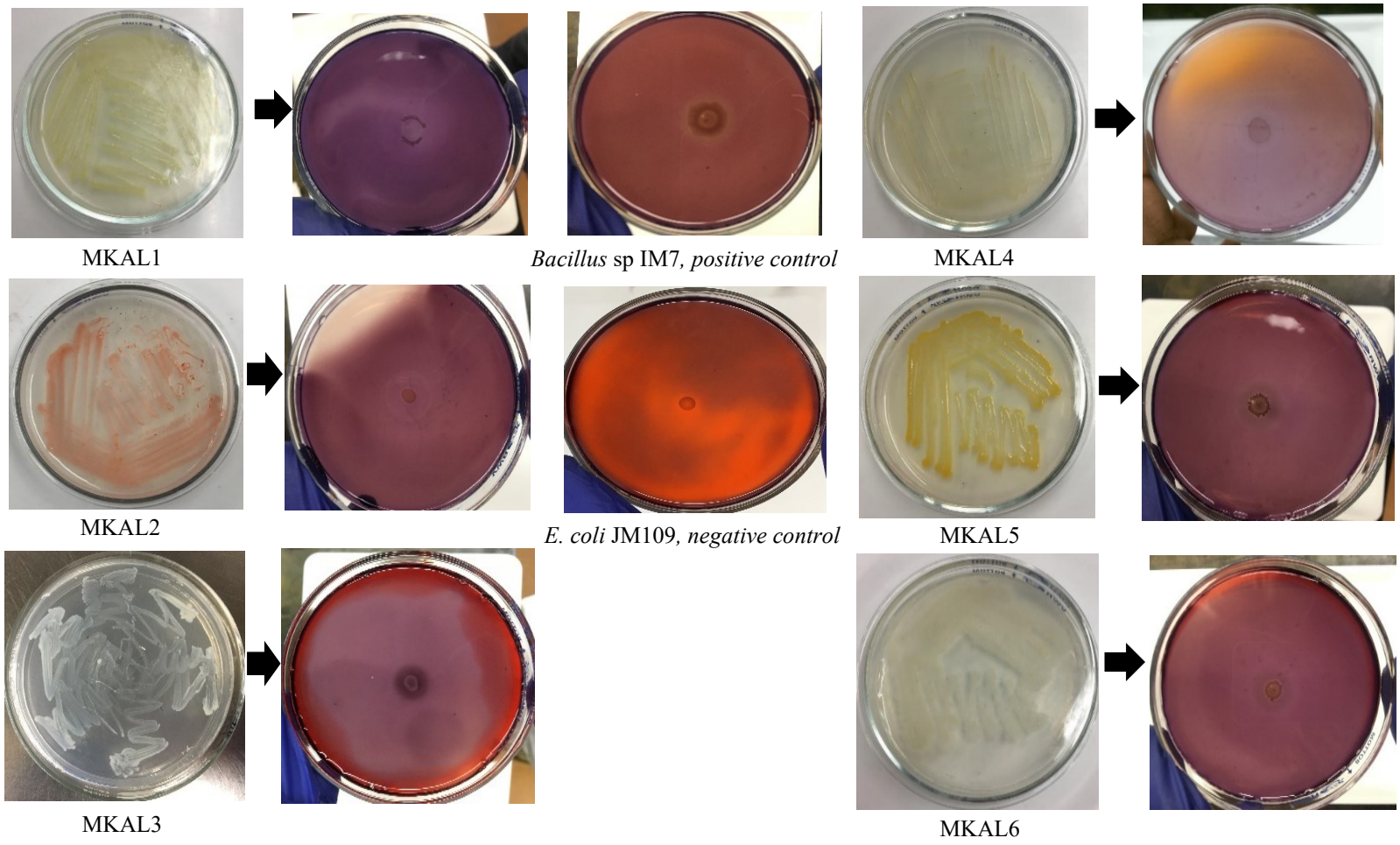

Figure 1. Cellulase activity characterized by the appearance of clear halos around bacterial strains.

2.5.2. Effect of pH on cellulase production

The CMC broth (50 mL) containing overnight cultured bacterial strain (500 µL) was incubated in a shaking incubator (200 rpm) in the pH ranges from 4 to 9. The effect of pH on enzyme production was investigated at the optimum temperature of each bacterial isolate.

2.5.3. Effect of CMC concentration on cellulase production

The bacterial strain was inoculated in the culture medium with CMC (0.5-2.5% w/v) at optimum pH and temperature and shaking at 200 rpm for 120 h.

2.5.4. Effect of carbon sources on cellulase production

The effect of carbon sources on enzyme production was performed by replacing CMC with other carbon sources such as pure cellulose, cellulose acetate, Poly(ethylene terephthalate) (PET), D-sucrose, D-glucose, D-fructose, D-sorbitol, D-mannitol and D-xylose. Bacterial strain was inoculated with a carbon source (0.5-2.5% w/v) in the production medium at the optimum temperature and pH and shaking at 200 rpm for 120 h.

2.5.5. Effect of nitrogen sources on cellulase production

Effect of various nitrogen sources such as yeast extract, malt extract, tryptone, casein hydrolysate, peptone, urea, ammonium chloride (NH_4Cl), ammonium sulfate ($(NH_4)_2SO_4$), and ammonium nitrate (NH_4NO_3) was examined. The bacterial strain was inoculated with a nitrogen source (0.05-2% w/v) in the culture medium at the optimum temperature and pH and shaking at 200 rpm for 120 h.

2.5.6. Effect of salts on cellulase production

The influence of salt supplementation was investigated by adding various salts such as potassium chloride, sodium chloride, calcium chloride, aluminum chloride, magnesium chloride, manganese chloride, cobalt chloride, nickel chloride, zinc chloride, chromium (III) chloride, lead chloride and barium chloride. The bacterial strain was inoculated with salt (0.5-5 mM) in the production medium at the optimum temperature and pH and shaking at 200 rpm for 120 h.

2.5.7. Effect of surfactants and EDTA on cellulase production

Effect of surfactant supplementation was performed by adding different surfactants such as tween 20, sodium dodecyl sulfate (SDS), triton X-100 (0.1-2.5% w/v) and a chelating agent, ethylenediaminetetraacetic acid (EDTA, 0.5-2.5 mM). The bacterial strain was inoculated with surfactant in the culture medium at the optimum temperature and pH and shaking at 200 rpm for 120 h.

2.6. Optimization of cellulase production using Response Surface Methodology (RSM)

Response surface methodology (RSM) was used to optimize the fermentation conditions to produce cellulase. The experiment was performed by Box–Behnken design (BBD) using the SYSTAT 12 software (SYSTAT Software Inc., San Jose, USA). The temperature (X1), initial pH (X2), and fermentation period (X3) were determined as independent variables based on the results of the preliminary single-factor experiments. Cellulase activity was used as a response value. The ranges and levels of these independent variables are presented in Table 1. BBD was used to generate the second-order response surface. The F-test at the 0.05 significance level, coefficient of determination (R2), and the lack of fit were used to measure the goodness of fit of the second-

order polynomial model. The fitted contour plots were obtained with the response surface methods-contour/surface program in SYSTAT 12 software.

2.7. SDS-Polyacrylamide gel electrophoresis and zymogram

The cellulase molecular weights were determined by sodium dodecyl sulfate-polyacrylamide gel electrophoresis (SDS-PAGE) analysis. The crude enzymes from CDBs (20 µL) were mixed with loading buffer (5 µL) and boiled (100°C) before electrophoresis. Enzymes samples and protein ladder were run in 15% acrylamide gel. A constant supply of 120 V was maintained throughout the experiment. After gel running, the gel was divided into two parts. One part was stained overnight in Coomassie Brillant Blue R-250, then de-stained with a de-stain solution. Protein bands present in the gel were compared with the protein ladder (BioRad, Canada) to estimate their molecular weights. Another part of the gel was soaked in Triton X-100 (1% v/v) for 30 min to remove SDS and allow activity. Then, the gel was submerged in Congo red solution (0.1% w/v) for 30 min and de-stained with NaCl solution (1 M) until the halos appeared. The reaction was stopped by dipping the gel in acetic acid solution (4% v/v).

3. Results and discussion

3.1. Morphological and biochemical characterization

Among forty-one bacterial isolates, only six were selected based on the appearance of a clear halo around confirming cellulase production by these bacteria. Morphological and biochemical characteristics of CDBs were presented in Table 2. Different shapes were observed among these strains. MKAL1 and MKAL3 are circular-shaped while MKAL2, MKAL4, MKAL5

and MKAL6 are rod-shaped. Strains MKAL2, MKAL4 and MKAL5 are negative Gram bacteria. MKAL1, MKAL3 and MKAL6 are positive Gram bacteria. MKAL1 and MKAL4 are pale coloured, while MKAL2, MKAL3, MKAL5 and MKAL6 are red, white, yellow, and creamy coloured respectively. All strains are non-endospore-forming bacteria. Except for MKAL1, all tested strains are motile. All strains did not produce indole, hydrogen sulfide, gas, phenylalanine deaminase, citrate permease, lysine decarboxylase and lysine deaminase. Except for MKAL3, all strains produced catalase and α-amylase and hydrolyzed malonate, DNA and esculin. Only MKAL6 was non-salt-tolerant and showed a gelatinase activity. All strains degraded most sugars tested. These six cellulose-degrading bacteria from soil samples belong to the genera *Bacillus*, *Hymenobacter*, *Chryseobacterium*, *Paenarthrobacter*, *Mycobacterium* and *Stenotrophomonas*. Many investigators reported cellulase activity of the members of these bacteria isolated from various sources (Van Wyk et al., 2017; Ye et al., 2017; Molina et al., 2018; Tan et al., 2018; Dai et al., 2020; Scarcella et al., 2021). Their cellulase production was influenced by growth parameters such as temperature, incubation period, pH, carbon and nitrogen sources, metal ions, surfactants, and incubation time.

3.2. Phylogenetic analysis

Based on phylogenetic analysis, S1.3, S2.1R, S2.1W, S2.2, S4.2 and S5.6 were identified as *Paenarthrobacter* sp. MKAL1, *Hymenobacter* sp. MKAL2, *Mycobacterium* sp. MKAL3, *Stenotrophomonas* sp. MKAL4, *Chryseobacterium* sp. MKAL5 and *Bacillus* sp. MKAL6 with the NCBI accession numbers ON442553, ON442554, ON442555, ON442556, ON442557 and ON442558 respectively (Figure 2).

Table 1. Box-Behnken design matrix for optimization of cellulase activity

Bacterial strains	Run	X_1 Temperature (°C)	X_2 pH value	X_3 Time (h)	Cellulase activity (U/mL)
Paenarthrobacter sp. MKAL1	1	-1 (30)	-1 (5)	0 (96)	0.00 ± 0.00
	2	1 (40)	-1	0	0.00 ± 0.00
	3	-1	1 (7)	0	0.00 ± 0.00
	4	1	1	0	5.52 ± 0.17
	5	-1	0 (6)	-1 (72)	0.00 ± 0.00
	6	1	0	-1	0.34 ± 0.01
	7	-1	0	1 (120)	0.00 ± 0.00
	8	1	0	1	4.83 ± 0.11
	9	0 (35)	-1	-1	0.00 ± 0.00
	10	0	1	-1	2.89 ± 0.06
	11	0	-1	1	0.00 ± 0.00
	12	0	1	1	4.27 ± 0.18
	13	0	0	0	12.27 ± 1.29
	14	0	0	0	14.52 ± 1.08
	15	0	0	0	12.90 ± 1.88
Hymenobacter sp. MKAL2	1	-1 (35)	-1 (5)	0 (96)	14.15 ± 2.91
	2	1 (45)	-1	0	0.00 ± 0.00
	3	-1	1 (7)	0	4.68 ± 0.25
	4	1	1	0	1.26 ± 0.00
	5	-1	0 (6)	-1 (72)	2.45 ± 0.03
	6	1	0	-1	1.78 ± 0.03
	7	-1	0	1 (120)	3.54 ± 0.10
	8	1	0	1	2.03 ± 0.05
	9	0 (40)	-1	-1	7.98 ± 1.29
	10	0	1	-1	3.08 ± 0.09
	11	0	-1	1	8.21 ± 1.79
	12	0	1	1	5.98 ± 0.99
	13	0	0	0	17.86 ± 2.77
	14	0	0	0	18.15 ± 3.07
	15	0	0	0	19.53 ± 3.35
Mycobacterium sp. MKAL3	1	-1 (30)	-1 (5)	0 (96)	0.00 ± 0.00
	2	1 (40)	-1	0	0.00 ± 0.00
	3	-1	1 (7)	0	0.00 ± 0.00
	4	1	1	0	0.00 ± 0.00
	5	-1	0 (6)	-1 (72)	0.00 ± 0.00
	6	1	0	-1	0.00 ± 0.00
	7	-1	0	1 (120)	0.00 ± 0.00
	8	1	0	1	0.00 ± 0.00
	9	0 (35)	-1	-1	0.00 ± 0.00
	10	0	1	-1	0.00 ± 0.00
	11	0	-1	1	0.00 ± 0.00
	12	0	1	1	0.00 ± 0.00
	13	0	0	0	9.70 ± 0.49
	14	0	0	0	9.47 ± 0.80
	15	0	0	0	9.37 ± 0.97

Table 1. (continued) Box-Behnken design matrix for optimization of cellulase activity.

Bacterial strains	Run	X_1 Temperature (°C)	X_2 pH value	X_3 Time (h)	Cellulase activity (U/mL)
Stenotrophomonas sp. MKAL4	1	-1 (30)	-1 (5)	0 (96)	0.00 ± 0.00
	2	1 (40)	-1	0	0.00 ± 0.00
	3	-1	1 (7)	0	0.00 ± 0.00
	4	1	1	0	3.60 ± 0.05
	5	-1	0 (6)	-1 (72)	0.00 ± 0.00
	6	1	0	-1	3.08 ± 0.01
	7	-1	0	1 (120)	0.00 ± 0.00
	8	1	0	1	2.71 ± 0.04
	9	0 (35)	-1	-1	0.00 ± 0.00
	10	0	1	-1	3.01 ± 0.15
	11	0	-1	1	0.00 ± 0.00
	12	0	1	1	4.99 ± 0.72
	13	0	0	0	10.56 ± 1.38
	14	0	0	0	10.67 ± 1.08
	15	0	0	0	11.33 ± 0.76
Chryseobacterium sp. MKAL5	1	-1 (30)	-1 (5)	0 (96)	0.00 ± 0.00
	2	1 (40)	-1	0	0.00 ± 0.00
	3	-1	1 (7)	0	0.00 ± 0.00
	4	1	1	0	4.83 ± 0.52
	5	-1	0 (6)	-1 (72)	0.00 ± 0.00
	6	1	0	-1	2.82 ± 0.05
	7	-1	0	1 (120)	0.00 ± 0.00
	8	1	0	1	5.52 ± 0.67
	9	0 (35)	-1	-1	0.00 ± 0.00
	10	0	1	-1	3.01 ± 0.07
	11	0	-1	1	0.00 ± 0.00
	12	0	1	1	4.35 ± 0.08
	13	0	0	0	10.56 ± 1.75
	14	0	0	0	11.67 ± 1.78
	15	0	0	0	11.33 ± 1.91
Bacillus sp. MKAL6	1	-1 (30)	-1 (4)	0 (96)	0.00 ± 0.00
	2	1 (40)	-1	0	0.00 ± 0.00
	3	-1	1 (6)	0	0.00 ± 0.00
	4	1	1	0	12.86 ± 0.61
	5	-1	0 (5)	-1 (72)	0.00 ± 0.00
	6	1	0	-1	12.97 ± 0.11
	7	-1	0	1 (120)	0.00 ± 0.00
	8	1	0	1	13.98 ± 0.35
	9	0 (35)	-1	-1	0.00 ± 0.00
	10	0	1	-1	13.65 ± 0.71
	11	0	-1	1	0.00 ± 0.00
	12	0	1	1	14.59 ± 0.09
	13	0	0	0	18.73 ± 1.09
	14	0	0	0	18.78 ± 1.50
	15	0	0	0	19.01 ± 1.17

3.3. Effect of temperature and incubation period on cellulase production

Each microorganism needs optimum temperature for enzyme production stabilization. The effect of different temperatures was evaluated on the enzymatic activity and growth rate of isolates. Bacterial isolates were separately cultured in 250 mL conical flasks containing CMC broth (50 mL) for 5 days at 30, 35, 40, 45, and 50°C. The results are presented in Figure 3. All strains did not produce cellulase at 30 and 50°C and no cell growth was observed at these temperatures. Enzyme inactivation at these temperatures would be due to weak intermolecular interactions on the enzyme structure stability, decreasing enzyme catalytic abilities. At lower temperatures, substrate transport across the cell is suppressed, while at a higher temperature, the enzyme is unfolded and inactivated (thermal denaturation) (Ibrahim et al., 2021). However, some researchers revealed cellulase production by *Paenibacillus* sp. IM7, *Bacillus* sp., *Bacillus wiedmannii* and *Chryseobacterium* sp. at 30 and 50°C (Nkohla et al., 2017; Almuharef et al., 2020; Steiner and Margesin, 2020; Bhagat and Kokitkar, 2021; Indumathi et al., 2022). MKAL3 showed cellulase activity only at 35°C. Strains MKAL1, MKAL4, MKAL5 and MKAL6 exhibited maximum activity at 35°C while the optimum temperature of MKAL2 for cellulase production occurred at 40°C. *Bacillus subtilis* subsp. subtilis JJBS300 (Anu et al., 2021), *Bacillus velezensis* (Li et al., 2020), *Bacillus subtilis* Strain MU S1 (Sreena and Sebastian, 2018) were reported to produce higher cellulase yield at 35°C. Some other bacteria such as *Bacillus pacificus*, *Pseudomonas mucidolens* (Krishnaswamy et al., 2022), *Bacillus pseudomycoides* (Pramanik et al., 2020) and *Streptomyces thermocoprophilus* Strain TC13W (Sinjaroonsak et al., 2019) showed higher cellulase activity at 40°C. The cell growth of isolates increased until the optimum temperatures and then declined. All strains exerted optimum cellulase production after 96 h of incubation. Beyond, enzyme activity decreased. (Figure 4). This occurred due to nutrient depletion in the

fermentation medium, inhibition by end-products, or by-products production. Nutrient depletion causes bacterial stress leading to enzyme secretion inactivation and cell death (Ariffin et al., 2006). *Micrococcus* sp. SAMRC-UFH3 (Mmango-Kaseke et al., 2016), *Bacillus amyloliquefaciens* AK9 (Irfan et al., 2017) and *Bacillus albus* (Abada et al., 2021) were reported to produce maximum cellulase after 96 h of incubation.

3.4. Effect of pH on cellulase production

Medium pH is an essential factor for enzyme production and enzyme stability. The effect of pH on cellulase production and bacterial growth was studied by adjusting the pH of the culture medium between 4 and 9. No cellulase activity and cell growth of strains were observed at pH 4 (Figure 5). Only MKAL2 and MKAL6 produced cellulase at pH 5. MKAL3 exhibited cellulase activity only at pH 6. The optimum pH of MKAL6 for cellulase production was 5 while MKAL1, MKAL2, MKAL3, MKAL4 and MKAL5 showed maximum activity at pH 6. Similar optimum pH of 5 to 6 was reported in *Chryseobacterium* sp. (Nkohla et al., 2017), *Stenotrophomonas maltophilia* (Molina et al., 2018) and *Bacillus albus* (Abada et al., 2021). However, MKAL1, MKAL2, MKAL4 and MKAL6 also exerted cellulase production in the broader pH ranges from 6 to 8. These results were also recorded for different bacterial cellulases (Potprommanee et al., 2017; Herrera et al., 2019; Pramanik et al., 2020; Steiner and Margesin, 2020; Thapa et al., 2020; Bhagat and Kokitkar, 2021; Ibarahim et al., 2021). We observed a decrease in enzyme activity that may be due to ionization groups change at the enzyme active site or conformational change of the enzyme slowing or preventing the enzyme-substrate complex formation (Ibrahim et al., 2021).

3.5. Effect of CMC concentration on cellulase production

CMC is widely used to produce microbial cellulase because it is a soluble cellulose derivative with a high degree of polymerization. Its concentration in the culture influences enzyme production (da Silva et al., 2021). The effects of CMC concentration on cell growth and cellulase production are presented in Figure 6. No cellulase production was observed at 0.5% CMC. However, isolates showed cellulase activity at a range of CMC concentrations from 1-2.5% except for MKAL3 which exerted cellulase activity only at 1% CMC (9.66 U/mL). MKAL1 (13.22 U/mL) and MKAL5 (11.51 U/mL) showed optimum cellulase production at 1.5% CMC while MKAL2 (16.50 U/mL), MKAL4 (10.93 U/mL) and MKAL6 (18.06 U/mL) exhibited maximum activity at 2% CMC. MKAL6 exhibited cellulase activity of 6.27 U/mL at 1% CMC. Malik and Javed (2021) reported cellulase activity of 2.4 U/mL in *Bacillus subtilis* CD001 at 1% CMC.

3.6. Effect of carbon sources on cellulase production

The effect of carbon sources on enzyme production was determined by replacing CMC in the culture medium with various carbon sources (0-2.5%). All tested carbon sources boosted cellulase production at different concentrations except for pure cellulose, cellulose acetate and PET (Figure 7, Appendix 1). Some carbohydrates enhanced cellulase production by strains compared to CMC (9.66- 18.06 U/mL). MKAL1 exhibited maximum activity at 1% sucrose (158.27 U/mL); 1.5% fructose (21.16 U/mL), 1.5% xylose (25.56 U/mL), 2% sorbitol (33.34 U/mL) and 2% mannitol (44.22 U/mL). MKAL2 showed higher activity at 1.5% sorbitol (34.01 U/mL); 2% sucrose (78.87 U/mL), 2% mannitol (40.20 U/mL) and 2% xylose (26.57 U/mL). MKAL3 exhibited maximum activity at 1.5% sucrose (100.82 U/mL), 1.5% glucose (15.40 U/mL),1.5% mannitol (39.72 U/mL) and 2% sorbitol (44.01 U/mL). MKAL4 showed higher activity at 2% of sucrose (190.30 U/mL),

fructose (39.44 U/mL), sorbitol (56.96 U/mL) and mannitol (27.25 U/mL). Higher cellulase production by MKAL5 was found only at 1.5% sucrose (134.76 U/mL). Maximum cellulase activity by MKAL6 occurred at 1.5% sucrose (186.54 U/mL), 1.5% sorbitol (27.48 U/mL), 1.5% mannitol (44.99 U/mL), 2% glucose (34.90 U/mL), 2% fructose (23.33 U/mL) and 2% xylose (48.52 U/mL). However, sucrose was the best cellulase production inducer by these bacterial strains. Sugars act as inducers or repressors for enzyme production. Sucrose enhanced higher production, which suggested the negligible requirement of this sugar for appropriate enzyme induction. Hussain et al. (2017) showed that *Bacillus amyloliquefaciens* SA5, *Bacillus subtilis* BTN7A, *Bacillus megaterium* BMS4 and *Anoxybacillus flavithermus* BTN7B exhibited maximum cellulase production when sucrose was used as sole carbon source in the culture medium. Pure cellulose, cellulose acetate and PET didn't stimulate enzyme production because of their structural complexity and insolubility.

3.7. Effect of nitrogen sources on cellulase production

The cellulase production was highly affected by various nitrogen sources. The effect of each nitrogen source (0.05-2% w/v) on enzyme production by strains was investigated at their optimum pH (5 and 6) and temperature (35 and 40°C). Except for MKAL6, all tested bacterial isolates cannot degrade CMC without a nitrogen source in the culture medium. Thus, nitrogen sources are essential for cellulase production. No cellulase production and cell growth by MKAL1, MKAL2, MKAL3 and MKAL4 were observed with urea. Also, ammonium nitrate inhibited cellulase production by MKAL6 while ammonium chloride and ammonium sulfate inhibited cellulase activity of MKAL2 (Figure 8, Appendix 2). The results showed higher cellulase production when yeast extract (MKAL2 and MKAL6), casein hydrolysate (MKAL1, MKAL4 and

MKAL5) and tryptone (MKAL3) were used. MKAL2 (20.50 U/mL) and MKAL6 (26.60 U/mL) exerted maximum activity at 0.5 and 1.5% yeast extract respectively. Maximum cellulase production by MKAL1 (19.62 U/mL), MKAL5 (17.75 U/mL) and MKAL4 (21.80 U/mL) occurred at 1 and 1.5% casein hydrolysate respectively. The highest cellulase activity in MKAL3 (14.00 U/mL) was observed when 1.5% tryptone was used. Other investigators recorded similar results (Pramanik et al., 2020; Sharma et al., 2020). Organic nitrogen sources have stimulated higher production than inorganic nitrogen sources because their metabolism contributes to culture medium acidification, affecting cellulase production. However, other studies revealed that inorganic nitrogen sources such as urea and ammonium chloride promoted maximum cellulase production by *Bacillus licheniformis* 2D55 (Kazeem et al., 2016) and *Aneurinibacillus aneurinilyticus* BKT-9 (Ahmad et al., 2020).

3.8. Effect of salts on cellulase production

Metal ions play a vital role in enzyme catalysis by binding directly or indirectly to the enzyme active site (Gundupalli et al., 2021). The effect of salts (0.5-5 mM) on enzyme production by strains was performed at their optimum pH (5 and 6) and temperature (35 and 40°C). Except for MKAL3, all bacterial strains stimulated cellulase production in a non-salt supplemented culture medium (Figure 9, Appendix 3 and 4). Some salts enhanced cellulase production by strains compared to control (0.09-10.92 U/mL). MKAL4 (24.38 U/mL), MKAL6 (28.71 U/mL) and MKAL2 (23.23 U/mL) exhibited maximum activity at 1 and 2.5 mM $CoCl_2$ respectively. The optimum enzyme production by MKAL1 (21.15 U/mL) and MKAL3 (16.39 U/mL) occurred at 2.5 mM KCl while maximum production by MKAL5 (20.05 U/mL) was at 2.5 mM $MgCl_2$. Other reports showed these salts enhanced higher cellulase activity in *Bacillus tequilensis* S28 (Sharma

et al., 2015), *Bacillus cereus* (Tabssum et al., 2018) and *Bacillus amyloliquefaciens* (Pham et al., 2022).

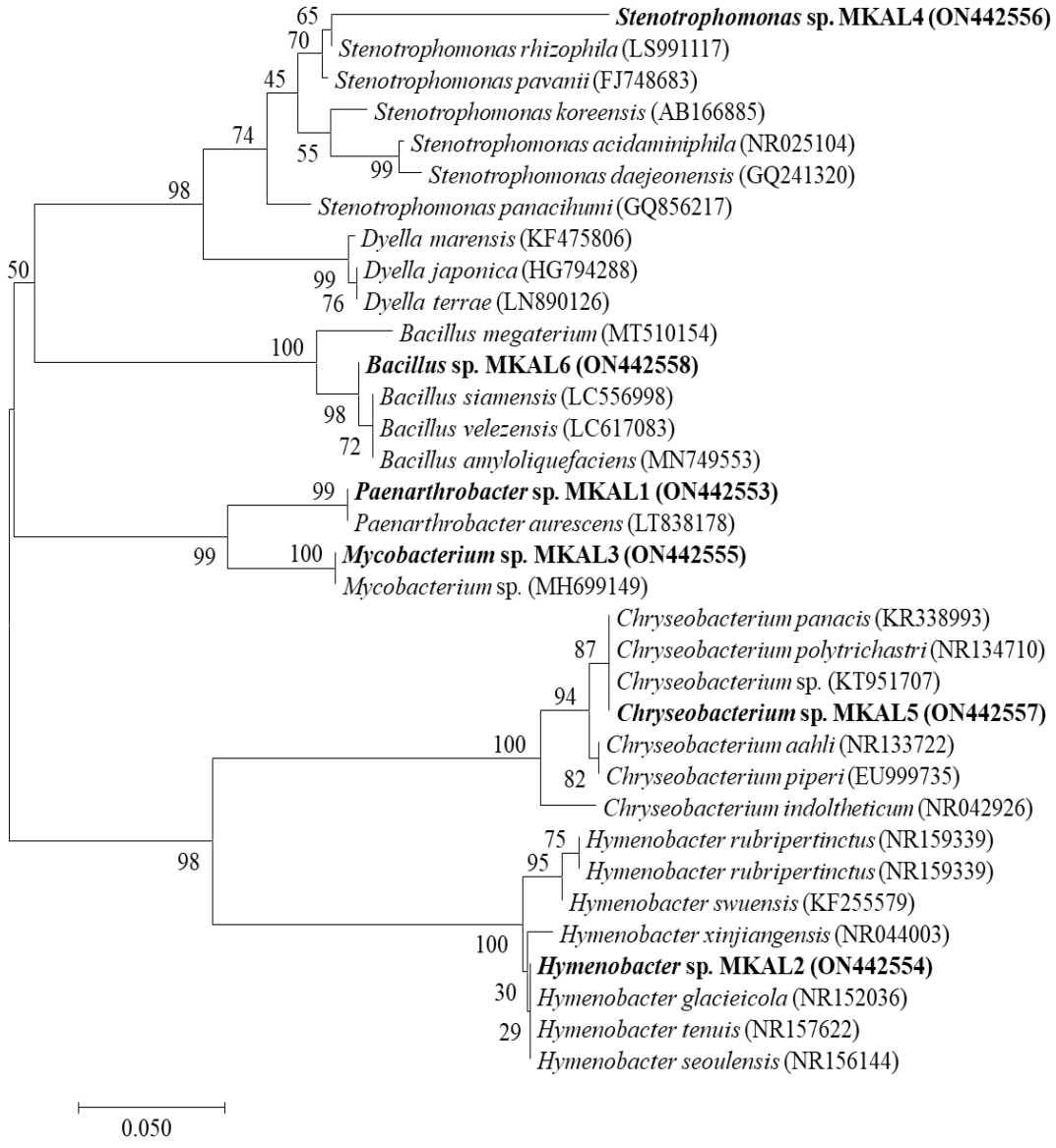

Figure 2. Phylogenetic tree of the CDB and related bacterial strains based on the neighbor-joining tree of the 16S rRNA sequences. Bootstrap values are shown as percentages of 1000 replicates. The bar (0.005) at the bottom of the tree indicates the substitution per nucleotide position.

Table 2. Biochemical and enzymatic characteristics of cellulose-degrading bacteria

Tests	Characteristics					
	MKAL1	MKAL2	MKAL3	MKAL4	MKAL5	MKAL6
Motility	non-motile	motile	motile	motile	motile	motile
Gram stain	$Gram^+$	$Gram^-$	$Gram^+$	$Gram^-$	$Gram^-$	$Gram^+$
Shape	Circular	Rod	Circular	Rod	Rod	Rod
Pigmentation	Pale	Red	White	Pale	Yellow	Creamy
Endospore stain	-	-	-	-	-	-
D-xylose	+	+	+	+	+	+
D-arabinose	-	-	-	-	-	+
D-glucose	+	+	+	+	+	+
D-fructose	+	+	+	+	+	+
D-galactose	-	-	-	-	-	+
D-mannitol	+	+	+	+	+	+
D-sorbitol	+	+	+	+	+	+
Inositol	-	-	-	-	-	+
D-rhamnose	+	-	-	-	-	+
Dulcitol	-	-	-	-	-	+
D-sucrose	+	+	+	+	+	+
D-lactose	-	-	+	+	+	+
Cellobiose	+	+	+	+	+	+
D-raffinose	-	+	-	-	-	+
Pectinase	-	+	+	-	-	-
Xylanase	+	-	-	-	+	-
Acetate	+	-	-	-	+	-
Malonate	+	+	-	+	+	+
Bile esculin	+	+	-	+	+	+
α- amylase	+	+	-	+	+	+
DNase	+	+	-	+	+	+
Phenylalanine deaminase	-	-	-	-	-	-
Lysine deaminase	-	-	-	-	-	-
Lysine decarboxylase	-	-	-	-	-	-
Ornithine decarboxylase	+	-	-	+	-	+
Urease	+	+	+	-	-	+
Gelatinase	-	-	-	-	-	+
Nitrate reductase	-	-	+	+	+	-
Citrate permease	-	-	-	-	-	-
Catalase	+	+	-	+	+	+
Oxidase	-	-	-	-	-	-
H_2S	-	-	-	-	-	-
Gas	-	-	-	-	-	-
Indole	-	-	-	-	-	-
Salt tolerance (6.5%)	+	+	+	+	+	-

+: production/degradation/tolerant, -: no production/no degradation/no tolerant.

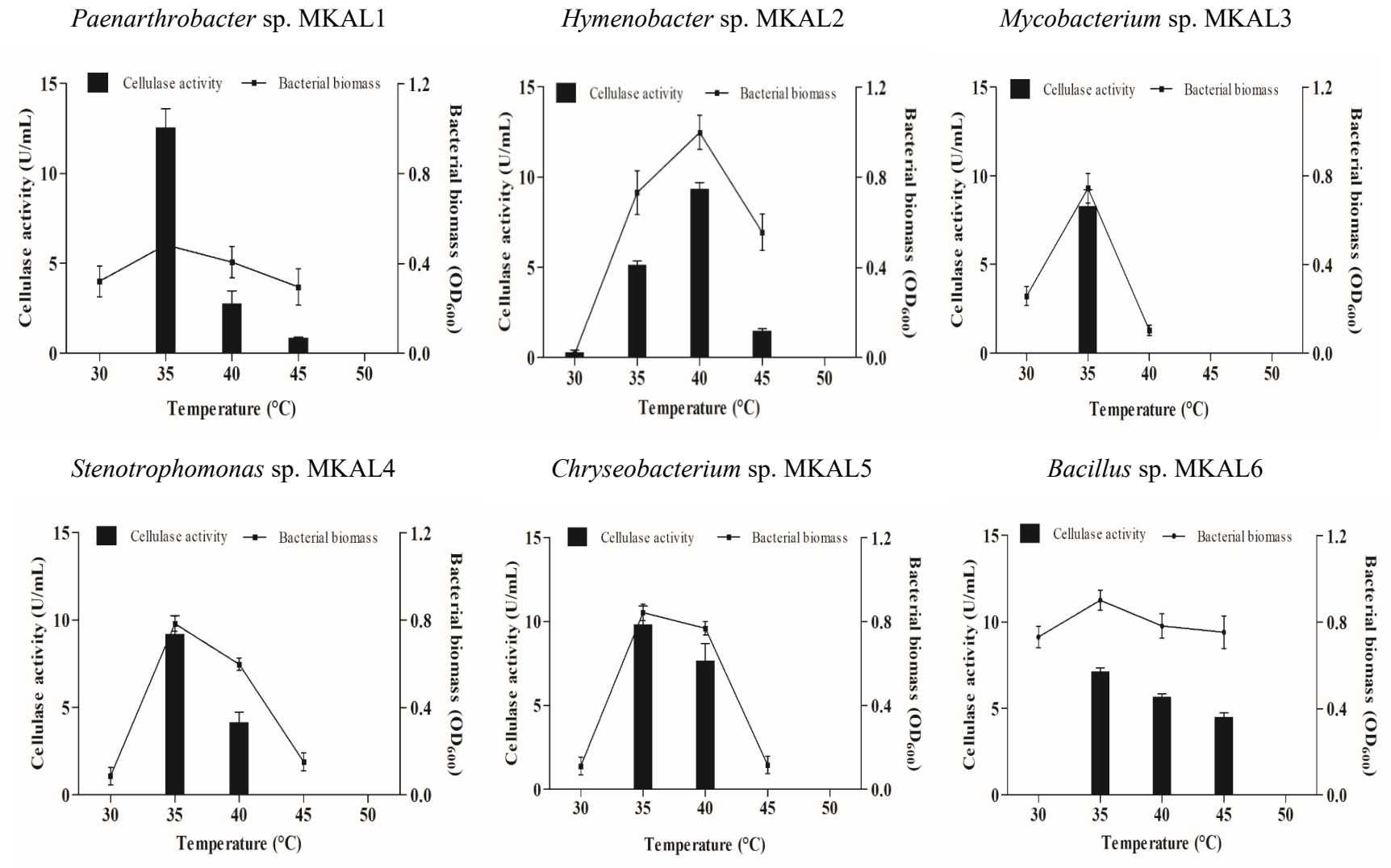

Figure 3. Effect of temperature on cellulase production by strains MKAL1, MKAL2, MKAL3, MKAL4, MKAL5 and MKAL6.

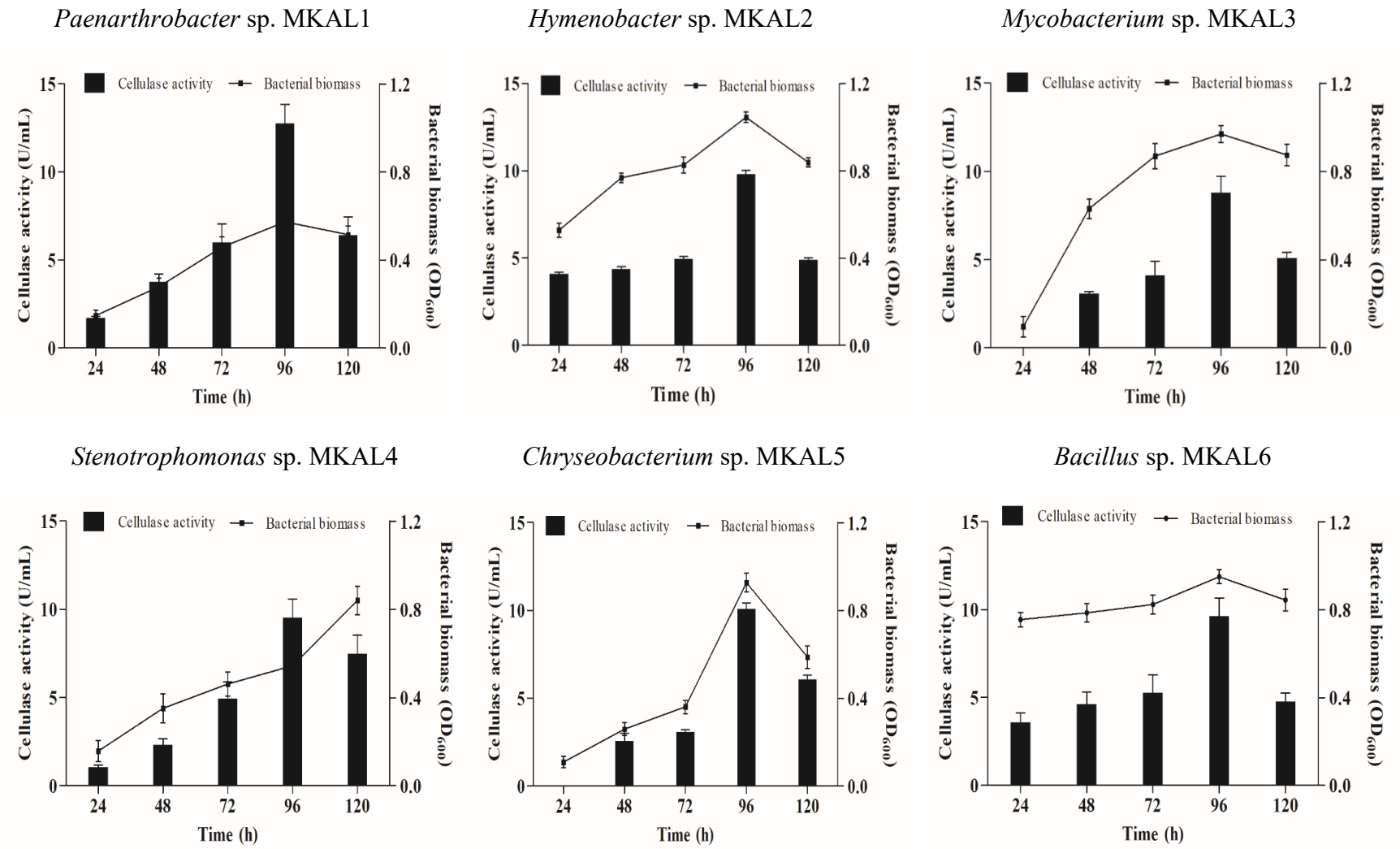

Figure 4. Effect of incubation period on cellulase production by strains MKAL1, MKAL2, MKAL3, MKAL4, MKAL5 and MKAL6.

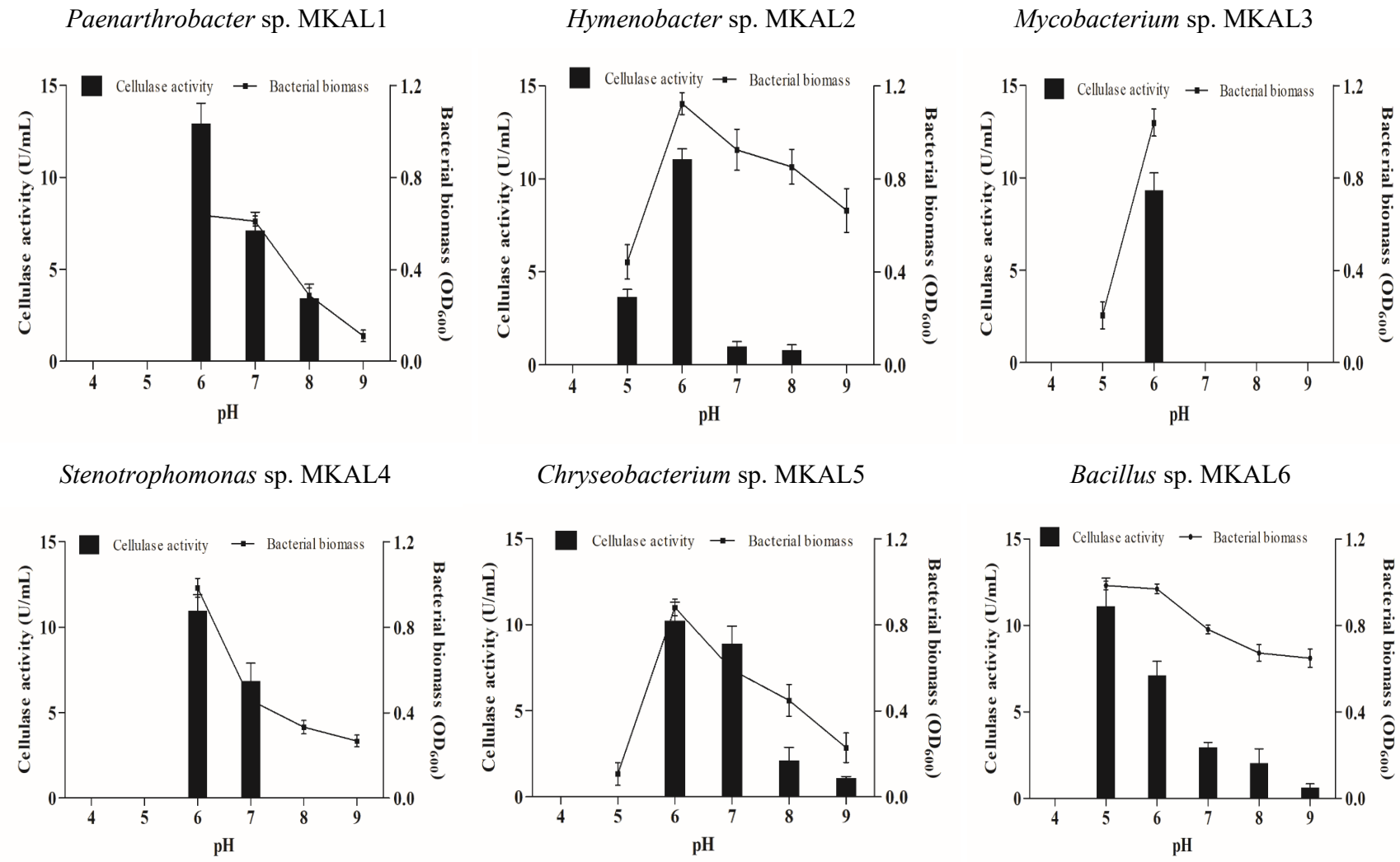

Figure 5. Effect of pH on cellulase production by strains MKAL1, MKAL2, MKAL3, MKAL4, MKAL5 and MKAL6.

Paenarthrobacter sp. MKAL1 *Hymenobacter* sp. MKAL2 *Mycobacterium* sp. MKAL3

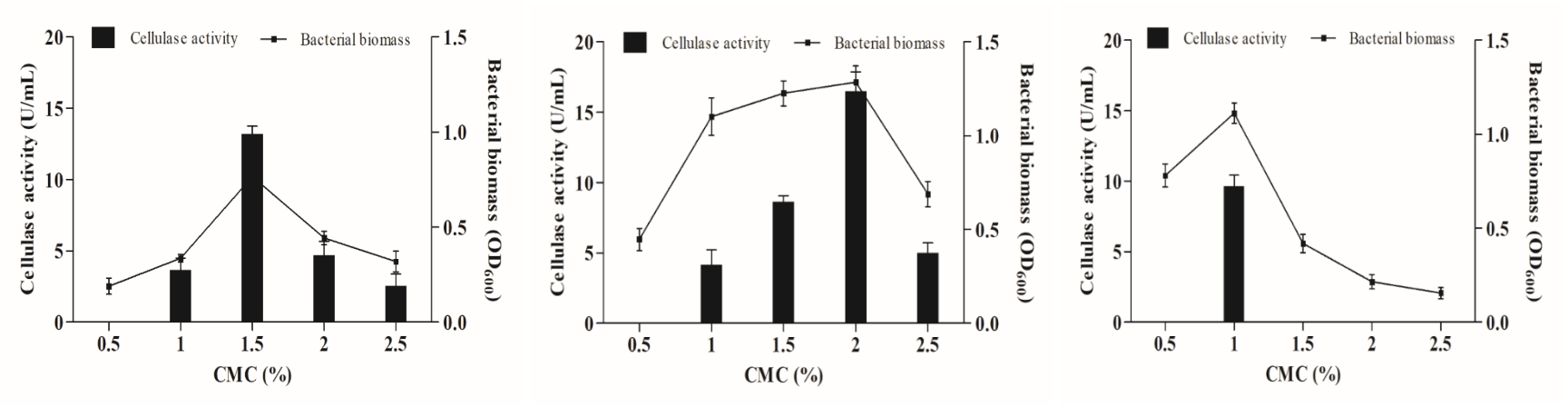

Stenotrophomonas sp. MKAL4 *Chryseobacterium* sp. MKAL5 *Bacillus* sp. MKAL6

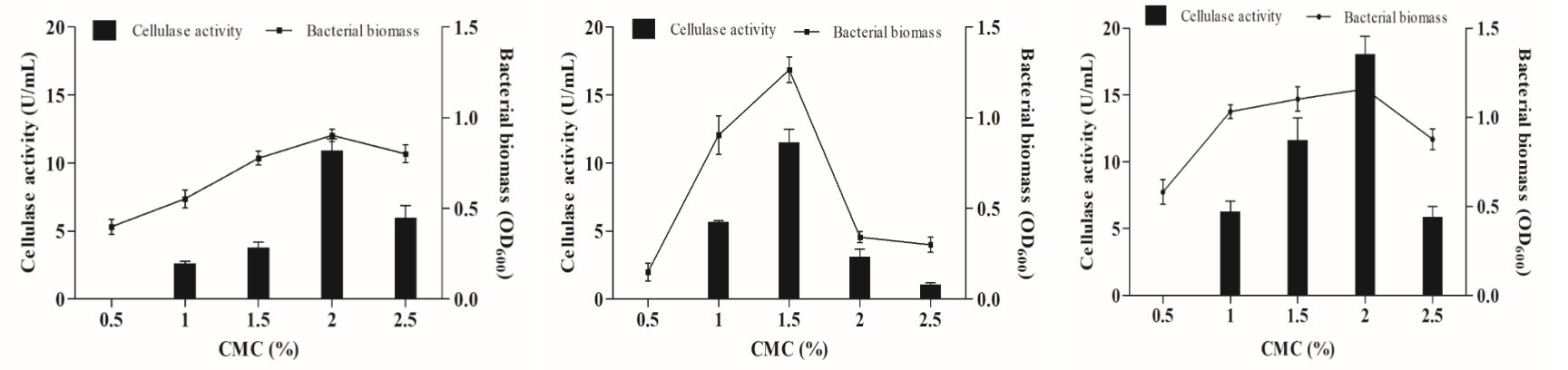

Figure 6. Effect of CMC concentration on cellulase production by strains MKAL1, MKAL2, MKAL3, MKAL4, MKAL5 and MKAL6.

3.9. Effect of surfactants and EDTA on cellulase production

No cellulase production was observed with triton X-100, SDS and EDTA. The presence of tween 20 in the culture medium enhanced cellulase production by MKAL2 (27.87-31.72 U/mL), MKAL4 (28.93-32.00 U/mL) and MKAL6 (33.99-35.91 U/mL) compared to control (23.23-28.71 U/mL) (Figure 10). This cellulase production gradually increased with an increase in tween 20 concentration and reached a maximum production at 1% (w/v) concentration in the medium and then declined. This trend was also observed in bacterial growth. Bhagia et al. (2019) revealed that even nonionic surfactants at high concentrations such as tween 20 could negatively affect enzymatic hydrolysis.

3.10. Optimization of fermentation

The Box–Behnken design was used to optimize the fermentation conditions. Results were presented in Table 3. Cellulase was the response variable, while temperature (X_1), pH (X_2) and fermentation time (X_3) were independent variables. Quadratic equations showing the linear relationship between response and independent variables were:

(1) MKAL1: Cellulase (U/mL)$= -\ 6.174X_1^2 -\ 5.676X_2^2 - 5.764X_3^2 + 1.380X_1X_2 + 0.345X_2X_3 + 1.123X_1X_3 + 1.336X_1 + 1.585X_2 + 0.734X_3 + 13.230$

(2) MKAL2: Cellulase (U/mL)$= -\ 8.677X_1^2 -\ 4.814X_2^2 - 7.387X_3^2 + 2.682X_1X_2 + 0.667X_2X_3 - 0.210X_1X_3 - 2.469X_1 - 1.918X_2 + 0.559X_3 + 18.513$

(3) MKAL3: Cellulase (U/mL)$= -\ 4.757X_1^2 -\ 4.757X_2^2 - 4.757X_3^2 + 1.208X_1X_2 + 0.335X_2X_3 + 0.675X_1X_3 + 9.513$

(4) MKAL4: Cellulase (U/mL)$= -\ 5.253X_1^2 -\ 4.700X_2^2 - 4.153X_3^2 + 0.900X_1X_2 + 0.495X_2X_3 - 0.093X_1X_3 + 1.174X_1 + 1.450X_2 + 0.201X_3 + 10.853$

(5) MKAL5: Cellulase (U/mL)$= -\ 4.867X_1^2 -\ 5.112X_2^2 - 4.235X_3^2 + 1.208X_1X_2 + 0.335X_2X_3 + 0.675X_1X_3 + 1.646X_1 + 1.524X_2 + 0.505X_3 + 11.187$

(6) MKAL6: Cellulase (U/mL)$= -\ 7.974X_1^2 -\ 7.651X_2^2 - 4.129X_3^2 + 3.215X_1X_2 + 0.235X_2X_3 + 0.252X_1X_3 + 4.976X_1 + 5.138X_2 + 0.244X_3 + 18.840$

The analysis of variance revealed that *p*-values of regression and lack of fit were 0.000-0.009 ($p < 0.05$) and 0.074-0.778 ($p > 0.05$) respectively for strains MKAL1, MKAL2, MKAL4 and MKAL5 (Table S4). This indicates that the built quadratic equation is relatively credible for the evaluation of cellulase activity of these bacterial strains. However, the *p*-value of the lack of fit was 0.001 ($p < 0.05$) respectively for MKAL3 and MKAL6. This suggests that the relationship between parameters is not significant, or the response surface quadratic model doesn't fit well for the assessment of enzyme activity of those two bacteria. Contour plots were produced based on the fitted model to estimate response surface shape. All contour plots appeared as ellipses, suggesting interactions between temperature, pH, and fermentation time. These variables affect cellulase activity and optimum conditions for maximum enzyme production yield were in the design range (Appendix 5). The optimal responses, 13.474, 18.982, 11.052 and 11.502 U/mL with a 95% confidence interval were obtained by canonical analysis for MKAL1, MKAL2, MKAL4 and MKAL5 respectively. The coded factor values for the stationary point were:

(1) MKAL1: $0.133\ (X_1), 0.158\ (X_2), 0.081\ (X_3)$, with corresponding experimental conditions: temperature 35.67°C, pH 6.16, and fermentation time 97.94 h.

(2) MKAL2: $-0.181\ (X_1), -0.248\ (X_2), 0.029\ (X_3)$, with corresponding experimental conditions: temperature 39.10°C, pH 5.75, and fermentation time 96.70 h.

(3) MKAL4: $0.126\ (X_1), 0.168\ (X_2), 0.033\ (X_3)$, with corresponding experimental conditions: temperature 35.63°C, pH 6.17, and fermentation time 96.79 h.

(4) MKAL5: $0.197\ (X_1), 0.175\ (X_2), 0.082\ (X_3)$, with corresponding experimental conditions: temperature 35.99°C, pH 6.18, and fermentation time 97.97 h.

The fitness of the model was checked by performing triplicate experiments under predicted optimum fermentation conditions. Experimental values were 13.303, 18.817, 10.89 and 11.381 U/mL for MKAL1, MKAL2, MKAL4 and MKAL5, respectively. This demonstrates reliable goodness of fit to predict cellulase production yield during the fermentation process with these bacterial strains.

3.11. Molecular weight determination and Zymogram

Protein bands of cellulases were observed in 15% acrylamide gel. Multiple bands were observed in the gel. However, the bands with hydrolytic zone correspond to 25 kDa (Figure 11) confirming the presence of cellulase. Cellulase bands in the range of 24.4-185 kDa have been estimated from SDS-PAGE (Sriariyanun et al., 2016; Barbosa et al., 2020; Mafa et al., 2021; Shankar et al., 2021). A similar molecular weight of 25 kDa has been reported in *Bacillus licheniformis* SVD1 (Van Dyk et al., 2009), *Bacillus subtilis* MA139 (Qiao et al., 2009), *Penicillium verruculosum* (Morozova et al., 2010) and *Novosphingobium* sp. Cm1 (Goswami et al., 2022).

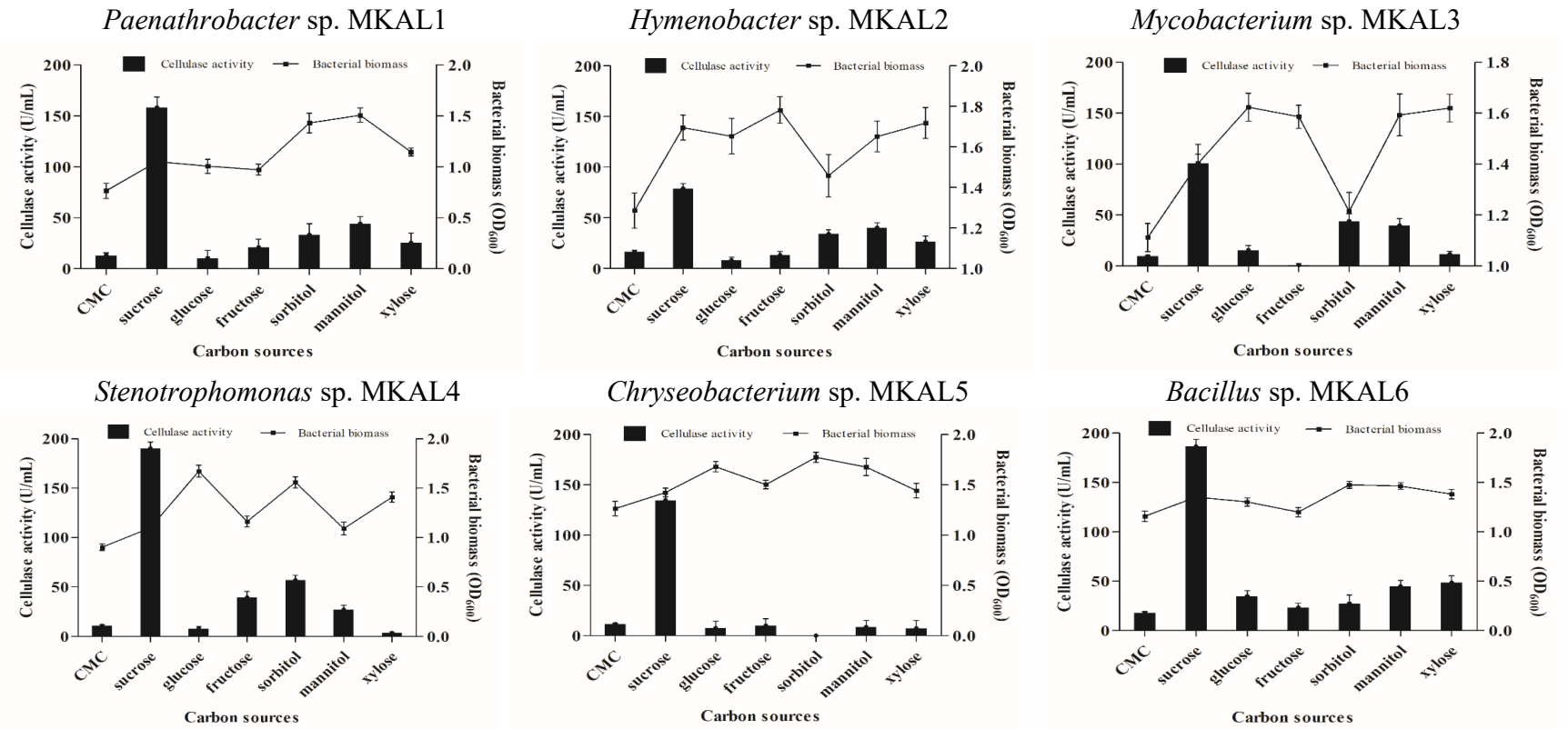

Figure 7. Effect of carbon sources on cellulase production by strains MKAL1, MKAL2, MKAL3, MKAL4, MKAL5 and MKAL6. Carbon sources enhanced cellulase production at different concentrations: MKAL1 (1% sucrose, 1.5% CMC, 1.5% glucose, 1.5% fructose, 1.5% xylose, 2% sorbitol and 2% mannitol), MKAL2 (1.5% sorbitol, 2% CMC, 2% sucrose, 2% glucose, 2% fructose, 2% mannitol and 2% xylose), MKAL3 (1% CMC; 1.5% sucrose, 1.5% glucose, 1.5% mannitol, 2% fructose, 2% sorbitol and 2% xylose), MKAL4 (2% of all tested carbon sources), MKAL5 (1% xylose, 1.5% CMC, sucrose, 1.5% fructose, 2% glucose and 2% mannitol) and MKAL6 (1.5% sucrose, 1.5% sorbitol, 1.5% mannitol, 2% CMC, 2% glucose, 2% fructose and 2% xylose). CMC: carboxymethylcellulose.

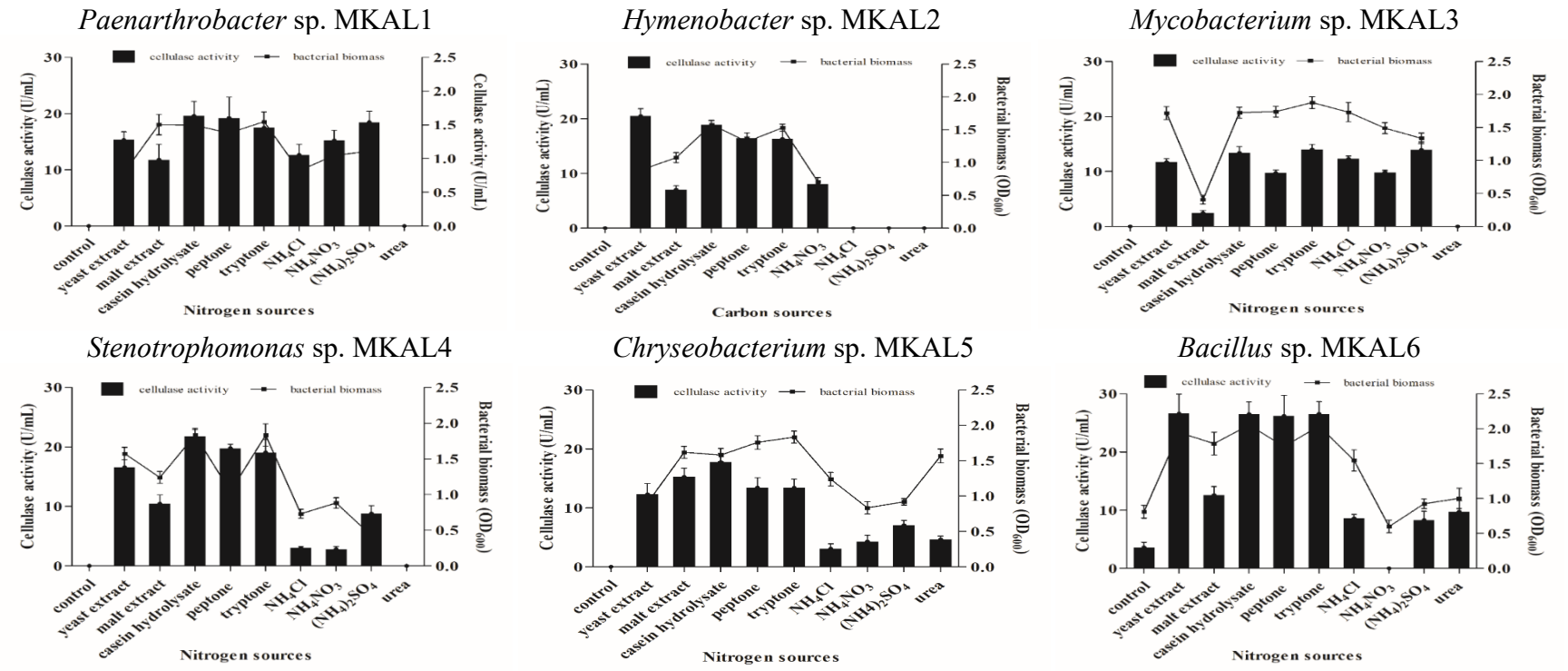

Figure 8. Effect of nitrogen sources on cellulase production by strains MKAL1, MKAL2, MKAL3, MKAL4, MKAL5 and MKAL6. Nitrogen sources enhanced cellulase production at different concentrations: MKAL1 (1% of all tested nitrogen sources except for urea), MKAL2 (0.5% yeast extract, 0.5% malt extract, 0.5% NH_4NO_3, 1.5% casein hydrolysate, 1.5% peptone and 1.5% tryptone), MKAL3 (0.5% malt extract, 1% NH_4Cl, 1% NH_4NO_3, 1.5% yeast extract, 1.5% casein hydrolysate, 1.5% peptone, 1.5% tryptone and 1.5% $(NH_4)_2SO_4$), MKAL4 (0.5% malt extract, 0.5% NH_4Cl, 0.5% NH_4NO_3, 1% $(NH_4)_2SO_4$, 1.5% yeast extract, 1.5% casein hydrolysate, 1.5% peptone and 1.5% tryptone), MKAL5 (0.5% NH_4Cl, 0.5% NH_4NO_3, 0.5% urea, 1% yeast extract, 1% malt extract, 1% casein hydrolysate, 1.5% peptone, 1.5% tryptone and 1.5% $(NH_4)_2SO_4$) and MKAL6 (0.5% NH_4Cl, 0.5% $(NH_4)_2SO_4$, 0.5% urea; 1% malt extract, 1.5% yeast extract, 1.5% casein hydrolysate, 1.5% peptone and 1.5% tryptone).

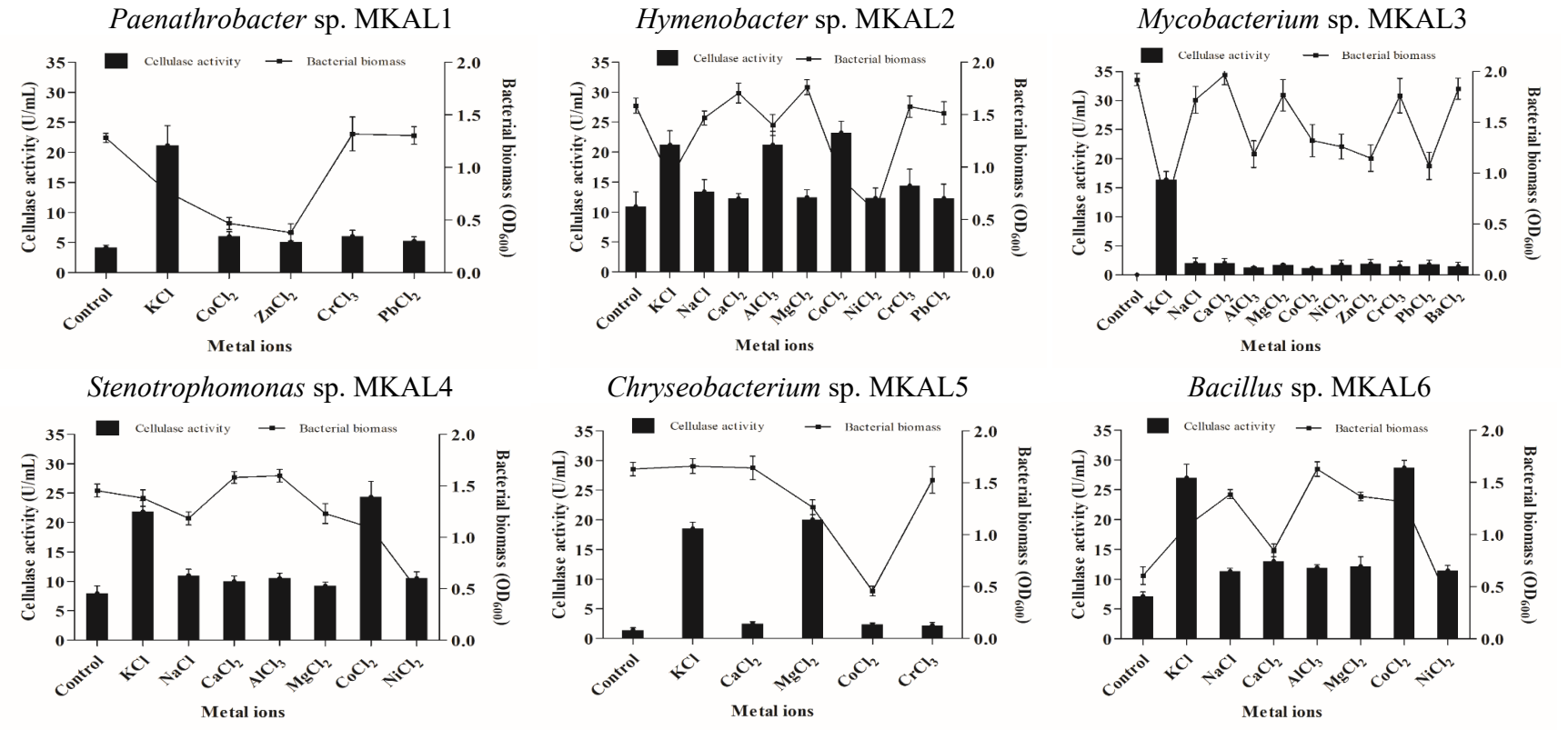

Figure 9. Effect of salts on cellulase production by strains MKAL1, MKAL2, MKAL3, MKAL4, MKAL5 and MKAL6. Salts enhanced cellulase production at different concentrations: MKAL1 (1 mM $CoCl_2$, 1 mM $ZnCl_2$, 1 mM $PbCl_2$, 2.5 mM KCl and 2.5 mM $CrCl_3$), MKAL2 (1 mM NaCl, 1 mM $CaCl_2$, 1 mM $CrCl_3$, 1 mM $PbCl_2$, 2.5 mM KCl, 2.5 mM $AlCl_3$, 2.5 mM $MgCl_2$, 2.5 mM $CoCl_2$ and 2.5 mM $NiCl_2$), MKAL3 (1 mM NaCl, 1 mM $CaCl_2$, 1 mM $AlCl_3$, 1 mM $MgCl_2$, 1 mM $CoCl_2$, 1 mM $CrCl_3$, 1 mM $PbCl_2$, 1 mM $BaCl_2$, 2.5 mM KCl, 2.5 mM $NiCl_2$ and 2.5 mM $ZnCl_2$), MKAL4 (1 mM KCl, 1 mM $CaCl_2$, 1 mM $AlCl_3$, 1 mM $MgCl_2$, 1 mM $CoCl_2$, 2.5 mM NaCl and 2.5 mM $NiCl_2$), MKAL5 (1 mM $CaCl_2$, 1 mM $CrCl_3$, 2.5 mM KCl, 2.5 mM $MgCl_2$ and 2.5 mM $CoCl_2$) and MKAL6 (1 mM NaCl, 1 mM $CaCl_2$, 1 mM $AlCl_3$, 1 mM $MgCl_2$, 1 mM $CoCl_2$, 2.5 mM KCl and 2.5 mM $NiCl_2$).

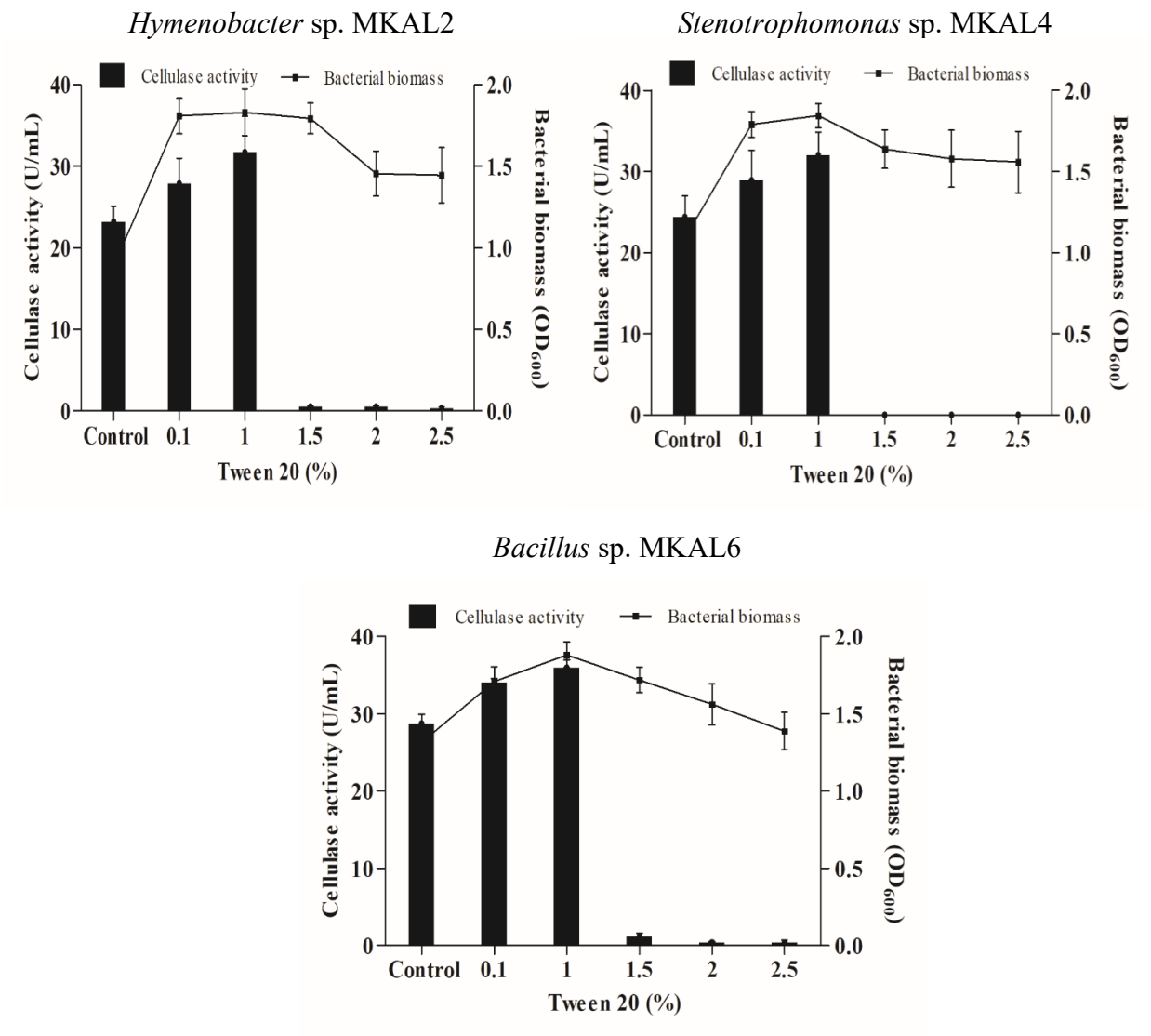

Figure 10. Effect of tween 20 on cellulase production by strains MKAL2, MKAL4 and MKAL6.

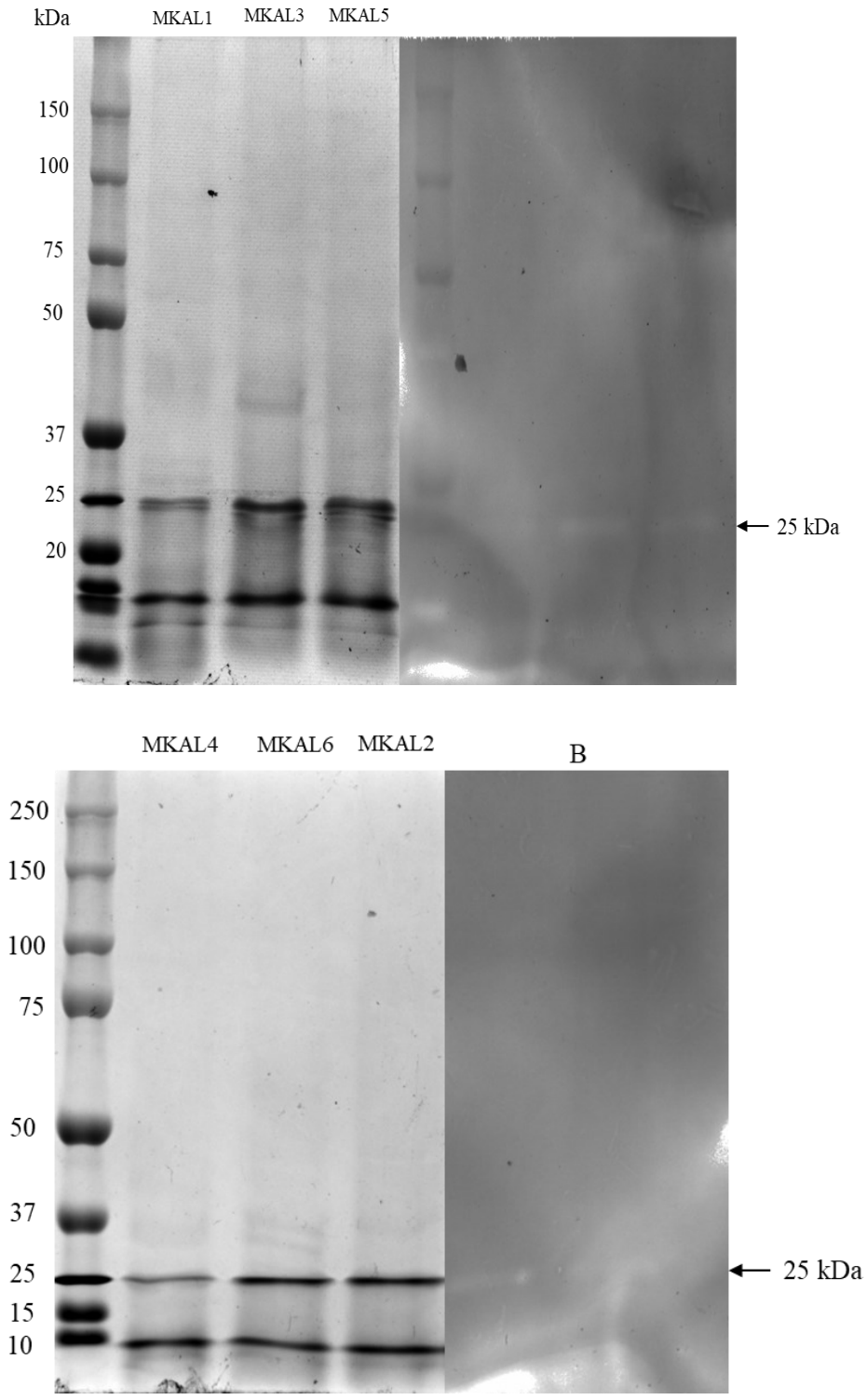

Figure 11. SDS-PAGE of crude cellulase from strains MKAL1, MKAL2, MKAL3, MKAL4, MKAL5 and MKAL6. A and B: hydrolytic bands in zymogram.

Table 3. Analysis of variance and lack of fit test for the response surface quadratic model

Bacterial strains	source	df	SS	Mean squares	F-ratio	*p*-value
Paenarthrobacter sp. MKAL1	Regression	9	383.315	42.591	50.046	0.000
	Squared Multiple R	0.989				
	Lack of fit	3	1.561	0.520	0.386	0.778
Hymenobacter sp. MKAL2	Regression	9	607.274	67.475	10.628	0.009
	Squared Multiple R	0.950				
	Lack of fit	3	30.153	10.051	12.623	0.074
Mycobacterium sp. MKAL3	Regression	9	217.208	24.134	2107.183	0.000
	Squared Multiple R	1.000				
	Lack of fit	3	0.000	0.000	0.000	
Stenotrophomonas sp. MKAL4	Regression	9	247.092	27.455	33.839	0.001
	Squared Multiple R	0.987				
	Lack of fit	3	3.710	1.237	7.130	0.125
Chryseobacterium sp. MKAL5	Regression	9	267.539	29.727	46.185	0.000
	Squared Multiple R	0.988				
	Lack of fit	3	2.571	0.857	2.650	0.286
Bacillus sp. MKAL6	Regression	9	904.171	100.463	9.229	0.012
	Squared Multiple R	0.943				
	Lack of fit	3	54.385	18.128	812.925	0.001

4. Conclusions

This study aimed to characterize cellulose-degrading bacteria and optimize their cellulase production. Six CDBs were isolated from soil samples showing that soil is a vast cellulolytic bacteria untapped reservoir and identified as *Paenarthrobacter* sp. MKAL1, *Hymenobacter* sp. MKAL2, *Mycobacterium* sp. MKAL3, *Stenotrophomonas* sp MKAL4, *Chryseobacterium* sp. MKAL5 and *Bacillus* sp. MKAL6. The higher cellulase production in these strains occurred at the culture conditions of 35-40°C, pH 5-6, 1-2% CMC and 96 h of incubation. The presence of yeast extract, casein hydrolysate, Tryptone, sucrose, potassium chloride, cobalt chloride, magnesium chloride and tween 20 boosted their cellulase production. Response surface quadratic model was reliable to predict cellulase production during the fermentation process with strains MKAL1,

MKAL2, MKAL4 and MKAL5. The purification of these cellulases for hydrolysis and saccharification of lignocellulosic biomasses are being studied.

5. References

Abada EA, Elbaz RM, Sonbol H, korany SM (2021). Optimization of Cellulase Production from *Bacillus albus* (MN755587) and Its Involvement in Bioethanol Production. *Polish J Environ Stud*, 30, 2459-2466.

Ahmad T, Sharma A, Gupta G, Mansoor S, Jan S, Kaur B, Paray BA, Ahmad A (2020). Response surface optimization of cellulase production from *Aneurinibacillus aneurinilyticus* BKT-9: an isolate of urban Himalayan freshwater. *Saudi J Biol Sci*, 27, 2333-2343.

Almuharef I, Rahman MS, Qin W (2020). High production of cellulase by a newly isolated strain *Paenibacillus* sp. IM7. *Waste Biomass Valor*, 11, 6085-6094.

Anu, Kumar S, Kumar A, Kumar V, Singh B (2021). Optimization of cellulase production by *Bacillus subtilis* subsp. subtilis JJBS300 and biocatalytic potential in saccharification of alkaline pretreated rice straw. *Prep Biochem Biotechnol*, 51, 697-704.

Ariffin HN, Abdullah MS, Umi Kalsom Y, Shirai, Hassan MA (2006). Production and characterisation of cellulase by *Bacillus pumilus* EB3. *International Journal of Engineering & Technology*, 3, 47-53.

Barbosa KL, Malta VRDS, Machado SS, Leal JGA, da Silva APV, Almeida RMRG, da Luz JMR (2020). Bacterial cellulase from the intestinal tract of the sugarcane borer. *Int J Biol Macromol*, 161, 441-448.

Bhagat SA, Kokitkar SS (2021). Isolation and identification of bacteria with cellulose-degrading

potential from soil and optimization of cellulase production. *J appl biol biotechnol*, 9, 154-161.

Bhagia S, Wyman CE, Kumar R (2019). Impacts of cellulase deactivation at the moving air-liquid interface on cellulose conversions at low enzyme loadings. *Biotechnol Biofuels*, 12, 96.

Bilal M, Iqbal HM (2020). State-of-the-art strategies and applied perspectives of enzyme biocatalysis in food sector—current status and future trends. *Crit Rev Food Sci Nutr*, 60, 2052-2066.

Cangelosi GA, Palermo CO, Laurent JP, Hamlin AM, Brabant W H (1999). Colony morphotypes on Congo red agar segregate along species and drug susceptibility lines in the *Mycobacterium* avium-intracellulare complex. *Microbiology*, 145, 1317-1324.

Cipolatti EP, Cerqueira PMCC, Henriques RO, da Silva Pinto JCC, de Castro AM, Freire DMG, Manoel EA (2019). Enzymes in green chemistry: The state of the art in chemical transformations (In Singh R.S., Singhania R.R., Pandey A. & Larroche C., ed.), Advances in Enzyme Technology, Elsevier, pp. 137-151.

Cowan ST, Steel KJ (2003). Manual for the Identification of Medical Bacteria (G.I. Barrow and R.K.A., ed.), Cambridge University Press, pp. 188-238.

da Silva RN, Melo LFDA, Luna FCL (2021). Optimization of the Cultivation Conditions of *Bacillus Licheniformis* BCLLNF-01 for Cellulase Production. *Biotechnol Rep (Amst)*, 29, e00599.

Dai J, Dong A, Xiong G, Liu Y, Hossain MS, Liu S, Gao N, Li,S, Wang J, Qiu D (2020). Production of highly active extracellular amylase and cellulase from *Bacillus subtilis* ZIM3 and a recombinant strain with a potential application in tobacco fermentation. *Front Microbiol*, 11, 1539.

Danalache F, Mata P, Alves V D, Moldão-Martins M (2018). Chapter 10: Enzyme-assisted extraction of fruit juices (In Rajauria G. & Tiwari B.K., ed.), Academic Press, pp. 183-200.

De Souza TSP, Kawaguti HY (2021). Cellulases, Hemicellulases, and Pectinases: Applications in the Food and Beverage Industry. *Food Bioprocess Technol*, 14, 1446-1477.

Faria SP, de Melo GR, Cintra LC, Ramos LP, Amorim JRS, Ulhoa CJ, de Faria FP (2020). Production of cellulases and xylanases by *Humicolagrisea var. thermoidea* and application in sugarcane bagasse arabinoxylan hydrolysis. *Ind Crops Prod*, 158, 112968.

Giannino ML, Aliprandi M, Feligini M, Vanoni L, Brasca M, Fracchetti F (2009). A DNA array-based assay for the characterization of microbial community in raw milk. *J Microbiol Methods*, 78, 181-188.

Global Cellulase (CAS 9012-54-8) Market Growth 2021-2026 (2021). Available from: https://www.360researchreports.com/global-cellulase-cas-9012-54-8-sales-market-16610450. Accessed October 30, 2020.

Goswami K, Deka BHP, Saikia R (2022). Purification and characterization of cellulase produced by *Novosphingobium* sp. Cm1 and its waste hydrolysis efficiency and bio-stoning potential. *J Appl Microbiol*, 132, 3618-3628.

Guerrand D (2018). Economics of food and feed enzymes: Status and prospectives (In Nunes C. & Kumar V., ed.), Enzymes in Human and Animal Nutrition. Elsevier, pp. 487-514.

Gundupalli PM, Sahithi STA, Cheng YS, Tantayotai P, Sriariyanun M (2021). Differential effects of inorganic salts on cellulase kinetics in enzymatic saccharification of cellulose and lignocellulosic biomass. *Bioprocess Biosyst Eng*, 44, 2331-2344.

Hall TA (1999). BioEdit: a user-friendly biological sequence alignment editor and analysis

program for Windows 95/98/NT, Nucleic acids symposium series, 95-98.

Herrera LM, Braña V, Franco FL, Castro-Sowinski S (2019). Characterization of the cellulase-secretome produced by the Antarctic *bacterium Flavobacterium* sp. AUG42. *Microbiol Res*, 223-225, 13-21.

Hussain AA, Abdel-Salam MS, Abo-Ghalia HH, Hegazy WK, Hafez SS (2017). Optimization and molecular identification of novel cellulose degrading bacteria isolated from Egyptian environment. *J Genet Eng Biotechnol*, 15, 77-85.

Ibrahim AM, Hamouda RA, El-Naggar NEA, Al-Shakankery FM (2021). Bioprocess development for enhanced endoglucanase production by newly isolated bacteria, purification, characterization and *in-vitro* efficacy as anti-biofilm of *Pseudomonas aeruginosa*. *Sci Rep*, 11, 9754.

Indumathi T, Jayaraj R, Kumar PS, Sonali JMI, Krishnaswamy VG, Ghfar AA, Govindaraju S (2022). Biological approach in deinking of waste paper using bacterial cellulase as an effective enzyme catalyst. *Chemosphere*, 287, 132088.

Irfan M, Tayyab A, Hasan F, Khan S, Badshah M, Shah AA (2017). Production and characterization of organic solvent-tolerant cellulase from *Bacillus amyloliquefaciens* AK9 isolated from hot spring. *Appl Biochem Biotechnol*, 182, 1390-1402.

Islam F, Roy N (2018). Screening, purification and characterization of cellulase from cellulose producing bacteria in molasses. *BMC Res Notes*, 11, 445-451.

Kazeem MO, Shah UKM, Baharuddin AS, Rahman NA (2016). Enhanced cellulase production by a novel thermophilic *Bacillus licheniformis* 2D55: Characterization and application in lignocellulosic saccharification. *BioResources*, 11, 5404-5423.

Krishnaswamy VG, Sridharan R, Kumar PS, Fathima MJ (2022). Cellulase enzyme catalyst

producing bacterial strains from vermico post and its application in low-density polyethylene degradation. *Chemosphere*, 288, 132552.

Kumar S, Stecher G, Tamura K (2016). MEGA7: Molecular Evolutionary Genetics Analysis Version 7.0 for Bigger Datasets. *Mol Biol Evol*, 33, 1870-1874.

Kumar VA, Kurup RSC, Snishamol C, Prabhu GN (2019). Role of cellulases in food, feed, and beverage industries (In Parameswaran B., Varjani S., & Raveendran S., ed.), Green Bioprocesses: Enzymes in Industrial Food Processing, Springer Singapore, pp. 323-343.

Li F, Xie Y, Gao X, Shan M, Sun C, Niu YD, Shan A (2020). Screening of Cellulose Degradation Bacteria from Min Pigs and Optimization of its Cellulase Production. *Electron J Biotechnol*, 48, 29-35.

Mafa MS, Pletschke BI, Malgas S (2021). Defining the frontiers of synergism between cellulolytic enzymes for improved hydrolysis of lignocellulosic feedstocks. *Catalysts*, 11, 1343.

Maki ML, Broere M, Leung KT, Qin W (2011). Characterization of some efficient cellulase producing bacteria isolated from paper mill sludges and organic fertilizers. *Int J Biochem Mol Biol*, 2, 146-154.

Malik WA, Javed S (2021). Biochemical characterization of cellulase from *Bacillus subtilis* strain and its effect on digestibility and structural modifications of lignocellulose rich biomass. *Front Bioeng Biotechnol*, 9, 800265.

Marques NP, de Cassia Pereira J, Gomes E, da Silva R, Araújo AR, Ferreira H, Rodrigues A, Dussan KJ, Bocchini DA (2018). Cellulases and xylanases production by endophytic fungi by solid state fermentation using lignocellulosic substrates and enzymatic saccharification of pretreated sugarcane bagasse. *Ind Crops Prod*, 122, 66-75.

Mmango-Kaseke Z, Okaiyeto K, Nwodo UU, Mabinya LV, Okoh AI (2016). Optimization of

cellulase and xylanase production by *Micrococcus* species under submerged fermentation. *Sustainability*, 8, 1168.

Molina GCE, de la Rosa G, Gonzalez CJ, Sánchez Y, Castillo-Michel H, Valdez-Vazquez I, Balcazar E, Salmerón I (2018). Optimization of culture conditions for production of cellulase by *Stenotrophomonas maltophilia*. *BioResources*, 13, 8358-8372.

Morozova VV, Gusakov AV, Andrianov RM, Pravilnikov AG, Osipov DO, Sinitsyn AP (2010). Cellulases of *Penicillium verruculosum*. *Biotechnol J*, 5, 871-880.

Nkohla A, Okaiyeto K, Nwodo UU, Mabinya LV, Okoh AI (2017). Endoglucanase and xylanase production by *Chryseobacterium* species isolated from decaying biomass. *Polish J Environ Stud*, 26, 2651-2660.

Paudel PY, Qin W (2015). Characterization of novel cellulase-producing bacteria isolated from rotting wood samples. *Appl Biochem Biotechnol,* 177, 1186-1198.

Pham VHT, Kim J, Shim J, Chang S, Chung W (2022). Coconut Mesocarp-Based LignocellulosicWaste as a Substrate for Cellulase Production from High Promising Multienzyme-Producing *Bacillus amyloliquefaciens* FW2 without Pretreatments. *Microorganisms*, 10, 327.

Potprommanee L, Wang XQ, Han YJ, Nyobe D, Peng YP, Huang Q, Liu JY, Liao YL, Chang KL (2017). Characterization of a thermophilic cellulase from *Geobacillus* sp. HTA426, an efficient cellulase-producer on alkali pretreated of lignocellulosic biomass. *PloS one*, 12, e0175004.

Pramanik SK, Mahmud S, Paul GK, Jabin T, Naher K, Uddin MS, Zaman S, Saleh MA (2020).

Fermentation optimization of cellulase production from sugarcane bagasse by *Bacillus pseudomycoides* and molecular modeling study of cellulase. *Curr Res Microb Sci*, 2, 100013.

Qiao J, Dong B, Li Y, Zhang B, Cao Y (2009). Cloning of a beta-1,3-1,4-glucanase gene from *Bacillus subtilis* MA139 and its functional expression in *Escherichia coli*. *Appl Biochem Biotechnol*, 152, 334-342.

Rahman MS, Fernando S, Ross B, Wu J, Qin W (2018). Endoglucanase (EG) Activity Assays (In: Lübeck M., ed.), Cellulases, Methods in Molecular Biology, Humana Press, New York.

Ramesh A, Devi PH, Chattopadhyay S, Kavitha M (2020). Commercial applications of microbial enzymes (In Arora N.K., Mishra J., & Mishra V., ed.), Microbial enzymes: Roles and applications in industries, Springer Nature, pp. 137-184.

Sampathkumar K, Kumar V, Sivamani S, Sivakumar N (2019). An insight into fungal cellulases and their industrial applications (In Srivastava M., Srivastava N., Ramteke P.W., & Mishra P.K., ed.), Approaches to Enhance Industrial Production of Fungal Cellulases, Springer International Publishing, pp. 19-35.

Sankaran R, Parra CRA, Pakalapati H, Show PL, Ling TC, Chen WH, Tao Y (2020). Recent advances in the pretreatment of microalgal and lignocellulosic biomass: a comprehensive review. *Bioresour Technol,* 298, 122476.

Scarcella ASDA, Pasin TM, de Oliveira TB, de Lucas RC, Ferreira-Nozawa MS, Freitas EN, Polizeli MDLTDM (2021). Saccharification of different sugarcane bagasse varieties by enzymatic cocktails produced by *Mycothermusthermophilus* and *Trichodermareesei* RP698 cultures in agro-industrial residues. *Energy*, 226, 120360.

Shankar T, Sankaralingam S, Balachandran C, Chinnathambi A, Nasif O, Alharbi SA, Park S,

Baskar K (2021). Purifcation and characterization of carboxymethylcellulase from *Bacillus pumilus* EWBCM1 isolated from earthworm gut (Eudrilus eugeniae). *J King Saud Univ Sci*, 33, 1-8.

Sharma A, Tewari R, Soni S (2015). Application of statistical approach for optimizing CMCase production by *Bacillus tequilensis* S28 strain via submerged fermentation using wheat bran as carbon source. *World Academy of Science, Engineering and Technology International Journal of Biotechnology and Bioengineering*, 9, 76-86.

Sharma HK, Xu CC, Qin W (2020). Co-culturing of novel *Bacillus* species isolated from Municipal Sludge and Gut of Red Wiggler Worm for improving CMCase activity. *Waste Biomass Valor*, 11, 2047-2058.

Shida Y, Furukawa T, Ogasawara W (2016). Deciphering the molecular mechanisms behind cellulase production in *Trichoderma reesei*, the hyper-cellulolytic filamentous fungus. *Biosci Biotechnol Biochem*, 80, 1712-1729.

Silalertruksa T, Gheewala SH (2020). Competitive use of sugarcane for food, fuel, and biochemical through the environmental and economic factors. *Int J Life Cycle Assess*, 25, 1343-1355.

Singhania RR, Adsul M, Pandey A, Patel AK (2017). Cellulases (In Pandey A., Negi S., Soccol C. R., ed.), Current developments in biotechnology and bioengineering-Production, isolation and purification of industrial products, Elsevier, pp. 73-101.

Sinjaroonsak S, Chaiyaso T, Kittikun HA (2019). Optimization of cellulase and xylanase productions by *Streptomyces thermocoprophilus* Strain TC13W using oil palm empty fruit bunch and tuna condensate as substrates. *Appl Biochem Biotechnol*,189, 76-86.

Soni SK, Sharma A, Soni R (2018). Cellulases: Role in lignocellulosic biomass utilization (In

Lübeck M., ed.), Cellulases, Humana Press, New York, pp. 3-23.

Sreena CP, Sebastian D (2018). Augmented cellulase production by *Bacillus subtilis* strain MUS1 using different statistical experimental designs. *J Genet Eng Biotechnol*, 16, 9-16.

Sriariyanun M, Tantayotai P, Yasurin P, Pornwongthong P, Cheenkachorn K (2016). Production, purification and characterization of an ionic liquid tolerant cellulase from *Bacillus* sp. isolated from rice paddy field soil. *Electron J Biotechnol*, 19, 23-28.

Steiner E, Margesin R (2020). Production and partial characterization of a crude cold-active cellulase (CMCase) from *Bacillus mycoides* AR20-61 isolated from an Alpine forest site. *Ann Microbiol*, 70, 67.

Tabssum F, Irfan M, Shakir HA, Qazi JI (2018). RSM based optimization of nutritional conditions for cellulase mediated Saccharification by *Bacillus cereus*. *J Biol Eng*, 12, 7.

Tan H, Miao R, Liu T, Yang L, Yang Y, Chen C, Lei J, Li Y, He J, Sun Q, Peng W, Gan B, Huang Z (2018). A bifunctional cellulase-xylanase of a new *Chryseobacterium* strain isolated from the dung of a straw-fed cattle. *Microb Biotechnol*, 11, 381-398.

Thapa S, Mishra J, Arora N, Mishra P, Li H, O′Hair J, Bhatti S, Zhou S (2020). Microbial cellulolytic enzymes: diversity and biotechnology with reference to lignocellulosic biomass degradation. *Rev Environ Sci Biotechnol*, 19, 621-648.

Van Dyk JS, Sakka M, Sakka K, Pletschke BI (2009). The cellulolytic and hemi-cellulolytic system of *Bacillus licheniformis* SVD1 and the evidence for production of a large multi-enzyme complex. *Enzyme Microb Technol*, 45, 372-378.

Van Wyk N, Navarro D, Blaise M, Berrin JG, Henrissat B, Drancourt M, Kremer L (2017). Characterization of a mycobacterial cellulase and its impact on biofilm- and drug-induced cellulose production. *Glycobiology*, 27, 392-399.

Ye M, Sun L, Yang R, Wang Z, Qi KZ (2017). The optimization of fermentation conditions for producing cellulase of *Bacillus amyloliquefaciens* and its application to goose feed. *R Soc Open Sci*, 4, 171012.

CHAPTER 3

Characterization of glucose isomerase-producing bacteria and optimization of fermentation conditions for producing glucose isomerase using biomass

Adapted from: Aristide Laurel Mokale Kognou[1], Chonlong Chio[1], Janak Raj Khatiwada[1], Sarita Shrestha[1], Xuantong Chen[1], Hongwei Li[2], Yuen Zhu[1,3], Zi-Hua Jiang[4], Chunbao (Charles) Xu[2], Wensheng Qin[1*]

Green Chemical Engineering, 2022

[1]Department of Biology, Lakehead University, Thunder Bay, Ontario, Canada

[2]Department of Chemical and Biochemical Engineering, Western University, London, Ontario, Canada

[3]School of Environment and Resources, Shanxi University, Taiyuan, China

[4]Department of Chemistry, Lakehead University, Thunder Bay, Ontario, Canada

*Corresponding author: Wensheng Qin

Abstract

Glucose isomerase (GI) is an enzyme with high potential applications. Characterization of glucose isomerase producing bacteria with interesting properties from an industrial point of view is essential. *Paenarthrobacter* sp. MKAL1, *Hymenobacter* sp. MKAL2, *Mycobacterium* sp. MKAL3, *Stenotrophomonas* sp. MKAL4, *Chryseobacterium* sp. MKAL5 and *Bacillus* sp. MKAL6 were isolated from soil samples. Optimization of enzyme production yield was investigated in various fermentation conditions using response surface methodology. All isolates exhibited maximum GI activity at 40°C, pH 6-8 after 4 days of incubation. A mixture of

peptone/yeast extract or tryptone/peptone enhanced higher enzyme production. The same trend was observed in fermentation medium containing 1% xylose or 2-2.5% wheat straw. This study advanced the knowledge of these bacterial isolates in promoting wheat straw as feedstock for the bio-based industry.

Keywords: Cellulolytic bacteria, glucose/xylose isomerase, biomass conversion

1. Introduction

Glucose isomerase (GI) is an enzyme that catalyzes the isomerization of glucose to fructose. It has a wide range of applications in the baking, food, canning, pharmaceutical, and fuel sectors (Zargaraan et al., 2016; Sahin et al., 2019; Saikia et al., 2022). It is one of the three most-produced industrial enzymes, along with amylase and protease (Al-Dhabi et al., 2020; Nam, 2022). The glucose isomerase world market is approximately one billion US dollars (Singh et al., 2020). The largest glucose isomerase applications rely on the high fructose corn syrups (HFCS) and crystalline fructose. HFCS are derived from corn and its formulations contain different fructose amounts known as HFCS 90 (90% fructose and 10% glucose), HFCS 42 (42% fructose and 58% glucose), and HFCS 55 (55% fructose and 45% glucose) (Singh et al., 2018). HFCS improves the flavour, freshness, texture, stability, colour, consistency and flowability of different products. These properties were attributed either to fructose or to the interaction of fructose with other systems (Singh et al., 2020). According to the Food and Agricultural Organization of the United Nations, sugar and HFCS represent respectively 80% and 10% of the sweetener market (OECD/FAO, 2019). Recently, there has been a growing interest in the production of 5-

hydroxymethylfurfural (5-HMF) from fructose and HFCS. 5-HMF is a versatile chemical platform that provides various synthesis possibilities, hence a precious and renewable chemical fundamental element. It is the precursor of several industrial interest chemicals, biofuels and biobased polymers (Saikia et al., 2022). The global 5-HMF market is expected to reach around 61 million USD in 2024 compared to 56 million USD in 2019 (Market Study Report, 2019).

Fructose can be obtained from various feedstocks, including lignocellulosic biomass and agricultural wastes, via multiple processes using glucose isomerase (Philippini et al., 2020). This is due to their availability, low cost and rich lignocellulosic composition (Zhou et al., 2011). Their use reduces the production costs of bioprocesses and has a positive environmental impact (Domingues et al., 2021). Several investigators have reported glucose isomerase production from agricultural wastes (Chanitnun and Pinphanichakarn, 2012; Thi Nguyen and Tran, 2018; Singh et al., 2020).

The glucose isomerase is widely distributed in microorganisms (Givry and Duchiron, 2008; Liu et al., 2015; Jia et al., 2017; Dai et al., 2020; Nam, 2022). The cost of GI production from bacteria is low compared to other microbes because bacteria grow more rapidly and have higher applicability. However, enzyme production yields depend on a complex relationship involving various factors such as the size of the inoculum, carbon and nitrogen sources, pH, temperature, inducers, additives, aeration and growth time. Also, substrate particle size affects GI production (Thi Nguyen and Tran, 2018). Soils have been documented to contain bacteria with various metabolic properties (Rengasamy et al., 2020; Singh et al., 2020). Tolerating extreme conditions, bacteria represent an excellent source for searching and isolating new glucose isomerases.

The present study aimed to characterize glucose isomerase producing bacteria from soil samples collected from Kingfisher Lake (Thunder Bay, Ontario, Canada) and the University of

Manitoba campus (Winnipeg, Manitoba, Canada). Optimization of enzyme production was also investigated in various physicochemical conditions and by response surface methodology.

2. Materials and methods

2.1. Characterization of glucose isomerase producing bacteria

Bacterial isolates were isolated from soil samples collected in Kingfisher Lake and the University of Manitoba campus by dilution method. The screening of glucose isomerase producing bacteria was performed in a xylose agar plate using 2,3,5-triphenyltetrazolium as the indicator of D-xylulose, the product of D-xylose isomerization. This method is based on the capacity of D-xylulose to oxidize colorless 2,3,5-triphenyltetrazolium chloride in an alkaline medium with the formation of formazan having a dark pink color. Bacterial isolates (5 μL) were inoculated in a xylose agar and plates were incubated at 37°C for 5 days to screen for glucose isomerase activity. The xylose agar medium was composed of D-xylose (15 g/L), $NaNO_3$ (1 g/L), K_2HPO_4 (1 g/L), KCl (1 g/L), $MgSO_4.7H_2O$ (0.5 g/L) and agar (11.5 g/L). The enzyme activity was characterized by the development of a pinkish red colored hydrolysis zone around the bacteria (Sapunova et al., 2004). Six bacterial isolates showing a positive result with a zone of clearance in plate assay were selected and photographed (Figure 1). These selected isolates were cultured in 10 mL of Luria-Bertani (LB) broth (containing 10 g peptone, 5 g yeast extract, 5 g NaCl and distilled water up to 1 L) for subsequent uses. These bacteria were identified as *Paenarthrobacter* sp. MKAL1, *Hymenobacter* sp. MKAL2, *Mycobacterium* sp. MKAL3, *Stenotrophomonas* sp. MKAL4, *Chryseobacterium* sp. MKAL5 and *Bacillus* sp. MKAL6 with the NCBI accession numbers ON442553, ON442554, ON442555, ON442556, ON442557 and ON442558 respectively.

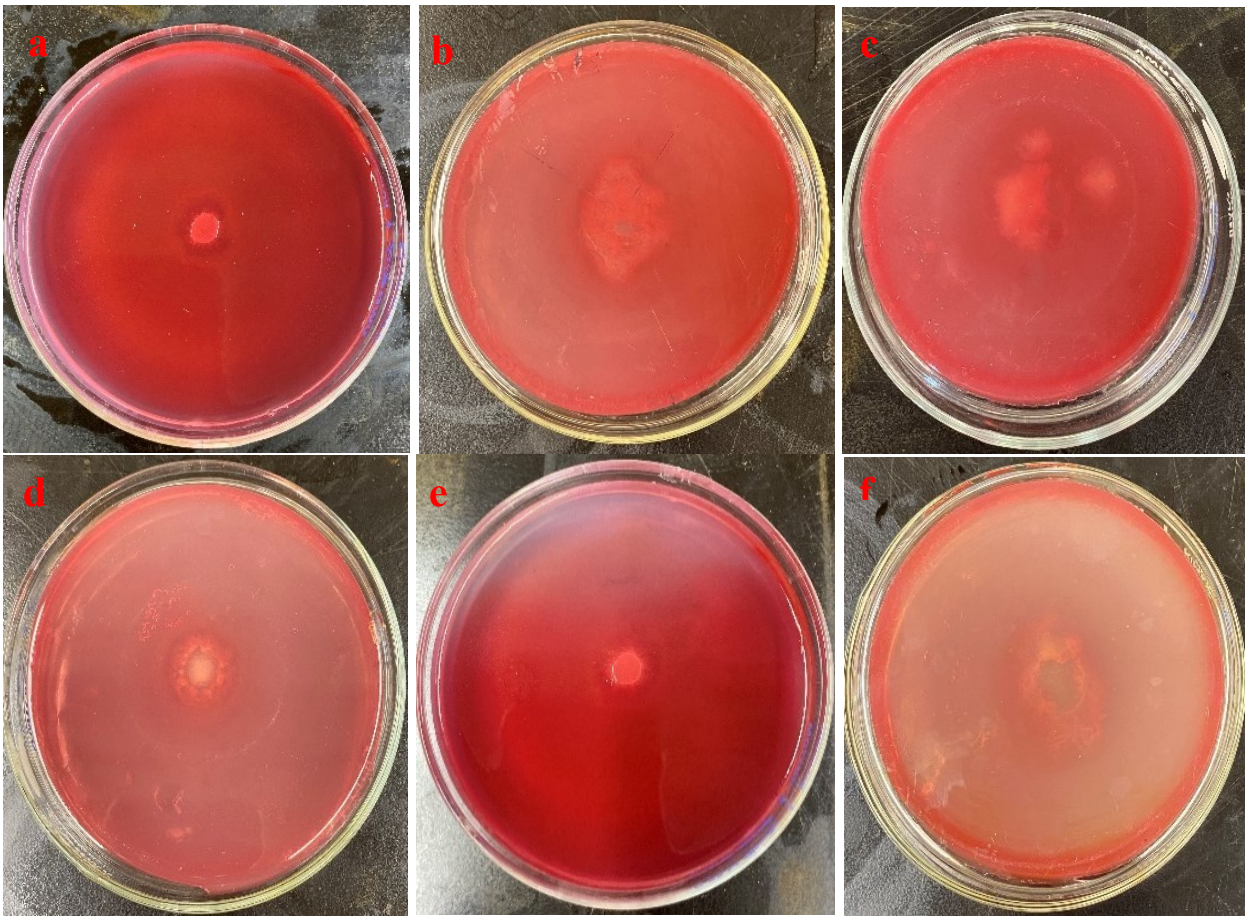

Figure 1. Glucose isomerase activity characterized by the appearance of clear halos around bacterial isolate. (a) *Paenarthrobacter* sp. MKAL1, (b) *Bacillus* sp. MKAL6, (c) *Hymenobacter* sp. MKAL2, (d) *Mycobacterium* sp. MKAL3, (e) *Stenotrophomonas* sp. MKAL4 and (f) *Chryseobacterium* sp. MKAL5.

2.2. Quantification of glucose isomerase activity

The quantification of GI was carried out using the Cysteine-Carbazole method (Tsumura and Sato, 1965). The xylose broth medium (10 g/L D-xylose, 1.5 g/L peptone, 1.5 g/L yeast extract, 1 g/L K_2HPO_4, 0.1 g/L $MnCl_2$.4H2O, 1 g/L $MgSO_4$.7H_2O) was used for glucose isomerase (GI) production. The overnight bacterial culture (500 mL) was inoculated in 250 mL Erlenmeyer flasks

containing 50 mL of xylose broth. Flasks were incubated in a shaking incubator (200 rpm) throughout the experiments. The bacterial production of extracellular glucose isomerase was optimized by varying temperature, incubation period, pH, carbon sources and nitrogen sources in the culture medium. After incubation, the culture medium (500 µL) was collected each day for 5 days and centrifuged (12,000×g, 3 min). the supernatant containing extracellular crude enzyme was further analyzed for enzyme activity at 540 nm using a microplate reader spectrophotometer (BioTek, USA). The bacterial growth was also determined in terms of biomass at 600 nm. The GI activity was estimated by measuring fructose yield after the isomerization reaction. The mixture reaction was composed of an aliquot of supernatant (200 µL), 0.5 M D-glucose solution (100 µL), 0.2 M K-Na-Phosphate buffer (75 µL, pH 7.8), 0.1 M $MgSO_4 \cdot 7H_2O$ (25 µL) and 0.01 M $CoCl_2$ (25 µL). The reaction mixture was incubated in the water bath (70°C, 1 h) for isomerization and the reaction was ended by adding 0.2 N HCl (10 µL). After cooling down in ice-cold water for 5 min, 1.5% (w/v) cysteine hydrochloride solution (50 µL), 50 µL of 0.12% (w/v) alcoholic carbazole solution (prepared in 99% ethanol) and 70% (v/v) H_2SO_4 (1 mL) were added in the mixture solution. Then, the solution was vigorously mixed and kept in the water bath (50ºC, 30 min). The purple color development in the solution represents the presence of fructose after the isomerization reaction. The GI activity was estimated using the fructose standard curve ($y = 0.0602x + 0.1179$; $r^2 = 0.9949$) and expressed in units per milliliter (U/mL), where one unit of enzyme corresponds to the release of 1 µmole of fructose equivalent per minute from the substrate.

2.2.1. Effect of temperature and incubation period on glucose isomerase production

The xylose broth medium (50 mL) containing overnight cultured bacterial isolate (500 µL) was incubated in a shaking incubator (200 rpm) at 25, 30, 35, 40, 45 and 50°C for five days. The

effect of temperature on enzyme production was quantified by collecting 500 µL of culture solution every day.

2.2.2. Effect of pH on glucose isomerase production

The xylose broth medium (50 mL) containing overnight cultured bacterial isolate (500 µL) was incubated in a shaking incubator (200 rpm) in the pH ranges from 5 to 10. The effect of pH on enzyme production was investigated at the optimum temperature of each bacterial isolate.

2.2.3. Effect of carbon sources on glucose isomerase production

The effect of carbon sources on enzyme production was performed by replacing the xylose with different carbon sources at various concentrations (0.5-3%) such as carboxymethylcellulose, glucose and thirteen lignocellulosic biomasses (oat straw, barley straw, wheat straw, wild rice, corn cob, hay, sawdust, wood dust, wheat bran, ginkgo leaves, rice hulls, barley grain split and pine tree) in the production medium at the optimum temperature, pH and incubation time of each bacterial isolate. The lignocellulosic biomasses were collected from different locations. They were ground and filtered in a filter/screen of mesh size of 200 micrometers to obtain powders. Then, powders were macerated thrice in hot water (100°C), 95% ethanol and the pretreated residues were dried at room temperature for one week. The effect of the pretreated residues was also evaluated on enzyme production. Agricultural residues were collected after five days of bacterial treatment and kept in glutaraldehyde at 4°C for subsequent scanning electron microscope (SEM) analysis.

2.2.4. Effect of nitrogen sources on glucose isomerase production

The effect of different nitrogen sources, namely peptone, tryptone, casein, yeast extract and mixtures of nitrogen sources (peptone/yeast extract, casein/peptone, casein/tryptone, casein/yeast extract, tryptone/peptone and tryptone/yeast extract) in the production medium at different concentrations was investigated at the optimum temperature, pH and incubation time of each bacterial isolate.

2.3. Optimization of glucose isomerase using Response Surface Methodology (RSM)

Response surface methodology (RSM) was used to optimize the fermentation conditions to produce glucose isomerase. The experiment was performed by Box–Behnken design (BBD) using the SYSTAT 12 software (SYSTAT Software Inc., San Jose, USA). The temperature (X_1), initial pH (X_2), and fermentation time (X_3) were determined as independent variables based on the results of the preliminary single-factor experiments. GI activity was used as a response value. The ranges and levels of these independent variables are presented in Table 1. BBD was used to generate the second-order response surface. The F-test at the 0.05 significance level, coefficient of determination (R^2), and the lack of fit were used to measure the goodness of fit of the second-order polynomial model. The fitted contour plots were obtained with the response surface methods-contour/surface program in SYSTAT 12 software.

Table 1. Box-Behnken design matrix for optimization of glucose isomerase (GI) activity

Bacterial isolates	Run	X1 Temperature (°C)	X2 pH value	X3 Time (h)	GI activity (U/mL)
Bacillus sp. MKAL6	1	-1 (35)	-1 (7)	0 (96)	9.479 ± 0.038
	2	1 (45)	-1	0	0.858 ± 0.004
	3	-1	1 (9)	0	6.841 ± 0.076
	4	1	1	0	1.517 ± 0.004
	5	-1	0 (8)	-1 (72)	3.509 ± 0.104
	6	1	0	-1	0.974 ± 0.026
	7	-1	0	1 (120)	12.025 ± 0.093
	8	1	0	1	0.920 ± 0.017
	9	0 (40)	-1	-1	4.114 ± 0.176
	10	0	1	-1	7.274 ± 1.641
	11	0	-1	1	1.578 ± 0.015
	12	0	1	1	2.332 ± 0.073
	13	0	0	0	18.848 ± 0.999
	14	0	0	0	19.786 ± 0.108
	15	0	0	0	20.846 ± 0.097
Hymenobacter sp. MKAL2	1	-1 (35)	-1 (5)	0 (96)	6.114 ± 0.217
	2	1 (45)	-1	0	0.780 ± 0.000
	3	-1	1 (7)	0	10.903 ± 0.029
	4	1	1	0	1.596 ± 0.029
	5	-1	0 (6)	-1 (72)	3.385 ± 0.011
	6	1	0	-1	1.109 ± 0.089
	7	-1	0	1 (120)	9.294 ± 0.108
	8	1	0	1	1.162 ± 0.004
	9	0 (40)	-1	-1	11.139 ± 0.252
	10	0	1	-1	3.650 ± 0.190
	11	0	-1	1	6.393 ± 0.047
	12	0	1	1	1.301 ± 0.008
	13	0	0	0	16.279 ± 0.070
	14	0	0	0	16.585 ± 0.068
	15	0	0	0	16.637 ± 0.057
Stenotrophomonas sp. MKAL4	1	-1 (35)	-1 (5)	0 (96)	6.672 ± 0.046
	2	1 (45)	-1	0	0.870 ± 0.000
	3	-1	1 (7)	0	11.672 ± 0.245
	4	1	1	0	1.829 ± 0.015
	5	-1	0 (6)	-1 (72)	8.543 ± 0.234
	6	1	0	-1	1.278 ± 0.056
	7	-1	0	1 (120)	10.830 ± 0.343
	8	1	0	1	1.818 ± 0.004
	9	0 (40)	-1	-1	18.321 ± 0.111
	10	0	1	-1	4.733 ± 0.234
	11	0	-1	1	6.203 ± 0.111
	12	0	1	1	1.578 ± 0.029
	13	0	0	0	19.778 ± 0.150
	14	0	0	0	20.984 ± 0.080
	15	0	0	0	20.738 ± 0.109

Table 1 (continued). Box-Behnken design matrix for optimization of glucose isomerase (GI) activity

Bacterial isolates	Run	X1 Temperature (°C)	X2 pH value	X3 Time (h)	GI activity (U/mL)
Paenarthrobacter sp. MKAL1	1	-1 (35)	-1 (7)	0 (96)	10.885 ± 0.245
	2	1 (45)	-1	0	7.896 ± 0.035
	3	-1	1 (9)	0	11.088 ± 0.129
	4	1	1	0	8.946 ± 0.026
	5	-1	0 (8)	-1 (72)	10.066 ± 0.026
	6	1	0	-1	7.801 ± 0.111
	7	-1	0	1 (120)	10.299 ± 0.046
	8	1	0	1	6.752 ± 0.046
	9	0 (40)	-1	-1	9.441 ± 0.213
	10	0	1	-1	16.546 ± 0.183
	11	0	-1	1	12.151 ± 0.023
	12	0	1	1	6.951 ± 0.023
	13	0	0	0	17.265 ± 0.157
	14	0	0	0	17.857 ± 0.183
	15	0	0	0	17.341 ± 0.201
Chryseobacterium sp. MKAL5	1	-1 (35)	-1 (7)	0 (96)	11.564 ± 0.088
	2	1 (45)	-1	0	9.798 ± 0.048
	3	-1	1 (9)	0	12.231 ± 0.011
	4	1	1	0	10.727 ± 0.020
	5	-1	0 (8)	-1 (72)	11.549 ± 0.095
	6	1	0	-1	9.386 ± 0.051
	7	-1	0	1 (120)	10.149 ± 0.115
	8	1	0	1	10.624 ± 0.058
	9	0 (40)	-1	-1	11.866 ± 0.037
	10	0	1	-1	12.484 ± 0.170
	11	0	-1	1	10.583 ± 0.046
	12	0	1	1	9.649 ± 0.013
	13	0	0	0	18.733 ± 1.051
	14	0	0	0	19.204 ± 2.189
	15	0	0	0	19.809 ± 1.178
Mycobacterium sp. MKAL3	1	-1 (35)	-1 (5)	0 (96)	11.505 ± 0.191
	2	1 (45)	-1	0	10.080 ± 0.000
	3	-1	1 (7)	0	12.094 ± 0.068
	4	1	1	0	10.557 ± 0.101
	5	-1	0 (6)	-1 (72)	13.069 ± 0.098
	6	1	0	-1	9.945 ± 0.060
	7	-1	0	1 (120)	10.059 ± 0.104
	8	1	0	1	9.652 ± 0.104
	9	0 (40)	-1	-1	11.600 ± 0.000
	10	0	1	-1	13.321 ± 0.159
	11	0	-1	1	10.412 ± 0.000
	12	0	1	1	9.632 ± 0.091
	13	0	0	0	16.151 ± 2.156
	14	0	0	0	16.473 ± 1.580
	15	0	0	0	16.080 ± 1.677

3. Results and discussion

3.1. Effect of temperature and incubation time on glucose isomerase production

The ideal temperature and incubation period for high enzyme production by a microorganism differ from species to species. Bacterial isolates were grown in a xylose broth medium at different temperatures of 25, 30, 35, 40, 45 and 50°C for 5 days. All isolates produced an extracellular GI in a broader temperature range from 35 to 50°C. However, they exhibited maximum GI activity at 40°C (6.70-9.14 U/mL) (Figure 2) after 4 days of incubation (Figure 3). The glucose isomerase production by all isolates declined above 40°C. This resulted in decreased cell growth. Similar, maximum GI activity from *Serratia marcescens* HK2 was recorded at 40°C after 96 h of incubation (Sharma et al., 2021). *Streptomyces lividans* RSU26 showed higher enzyme activity at 37.5°C and 96 h of incubation (Rengasamy et al., 2020). *Bacillus megaterium* and *Escherichia coli* strain BL21 achieved maximum GI activity at 37°C after 48 h (Thi Nguyen and Tran, 2018; Fatima and Javed, 2020). However, the optimum temperature for GI production in *Thermoanaerobacter xylanolyticum*, *Thermus oshimai*, *Geobacillus thermocatenulatus and Thermoanaerobacter siderophilus* reached 85°C (Jia et al., 2017).

3.2. Effect of pH on glucose isomerase production

The pH ranges have highly influenced glucose isomerase production. The pH of the xylose broth medium was adjusted to 5, 6, 7, 8, 9 and 10 using 2 N KOH and 2 N HCl. All isolates exerted a GI activity at the pH tested. Optimum pH for the GI production by *Bacillus* sp. (6.83 U/mL), *Paenarthrobacter* sp. (9.29 U/mL) and *Chryseobacterium* sp. (8.29 U/mL) occurred at pH 8 while *Hymenobacter* sp. (8.85 U/mL), *Mycobacterium* sp. (6.70 U/mL) and *Stenotrophomonas* sp. (9.49

U/mL) were at pH 6 (Figure 4). Cell growth raised until the optimum pH and then decreased progressively. Similar findings were revealed by Sharma et al. (2021) in *Serratia marcescens* HK2. Other investigators reported optimum pH for GI production at pH 7-7.5 (Thi Nguyen and Tran, 2018; Fatima and Javed, 2020; Rengasamy et al., 2020).

3.3. Effect of carbon sources on glucose isomerase production

All isolates have used CMC, glucose, xylose and various lignocellulosic biomasses as a carbon source for GI production. Each isolate was grown in xylose broth containing 0.5-3% carbon sources. Xylose (8.35-11.92 U/mL) induced higher GI production compared to CMC (3.28-5.82 U/mL) and glucose (1.88-3.82 U/mL). However, 1% xylose boosted maximum enzyme activity in all isolates (8.35-11.92 U/mL). Higher xylose concentration inhibited enzyme production and bacterial cell growth (Figures 5 and 6). Similar, higher enzyme yield by *Bacillus megaterium* (Thi Nguyen and Tran, 2018), *Escherichia coli strain* BL21 (Fatima and Javed, 2020) and *Parageobacillus thermantarcticus* (Finore et al., 2019) were obtained in the fermentation medium with 1% xylose. *Serratia marcescens* HK2 exerted maximum GI activity in the culture medium with 1.5% xylose (Sharma et al., 2021). However, pretreated biomass (2.22-10.12 U/mL) stimulated enzyme production better than crude biomass (1.12-8.23 U/mL) at 1%. This resulted in increased cell growth. Wheat straw promoted higher glucose isomerase production. *Chryseobacterium* sp. (12.40 U/mL) exhibited maximum GI activity at 2% wheat straw while *Bacillus* sp. (15.00 U/mL), *Paenarthrobacter* sp. (11.51 U/mL), *Hymenobacter* sp. (9.81 U/mL), *Mycobacterium* sp. (11.23 U/mL) and *Stenotrophomonas* sp. (13.90 U/mL) exerted higher activity at 2.5% wheat straw (Figures 7 and 8). Sharma et al. (2021) showed that *Serratia marcescens* HK2 exhibited higher GI production at 2% barley straw. Corn husk (2.5%) (Chanitnun and

Pinphanichakarn, 2012), corn cob and wheat dusk (Bhasin and Modi, 2012) promoted higher GI yield from *Streptomyces* sp. CH7 and *Streptomyces* sp. SB-P1, respectively. SEM analysis was performed to observe morphological changes in wheat straw. Morphological characteristics of raw, pretreated and enzyme-hydrolyzed wheat straw are shown in figure 7. Raw wheat straw showed a smooth, nonporous, and compact surface (Figure 9a) which impedes nutrient access by bacterial isolates. The obstacle for microorganisms to degrade wheat straw is the presence of lignin and hemicellulose. However, hot water/ethanol pretreatment (Figure 9b) caused minimal changes on the surface (less compact surface, fibers cohesion disappearance and internal cell wall exposure), which could consist of the low-efficiency removal of hemicellulose and lignin. The sample surface was destroyed after bacterial treatment (cracks, pores, and wall erosion), resulting in the exposal of internal structures (Figure 9c-d). This suggests that lignin and hemicellulose of the pretreated wheat straw sample became loose or were partially removed and broken, making accessible essential nutrients (carbohydrates) to bacteria for their growth and enzyme production. These findings demonstrated that bacterial treatment of pretreated wheat straw could destroy the hemicellulose-lignin network, thereby removing some fibers and exposing internal structures to bacteria and thus accelerating the biodegradation process.

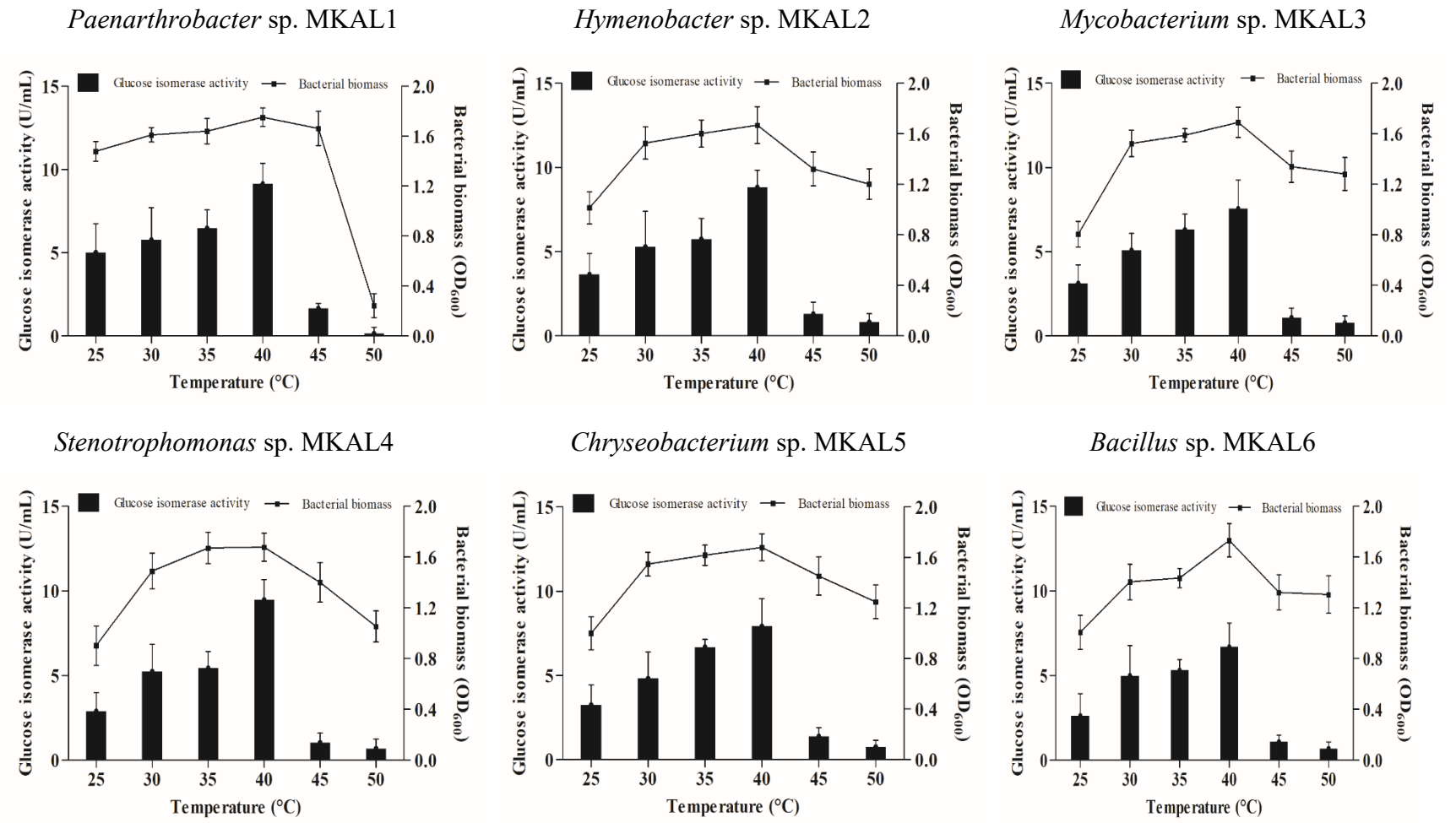

Figure 2. Effect of temperature on bacterial biomass and glucose isomerase production by *Paenarthrobacter* sp. MKAL1, *Hymenobacter* sp. MKAL2, *Mycobacterium* sp. MKAL3, *Stenotrophomonas* sp. MKAL4, *Chryseobacterium* sp. MKAL5 and *Bacillus* sp. MKAL6.

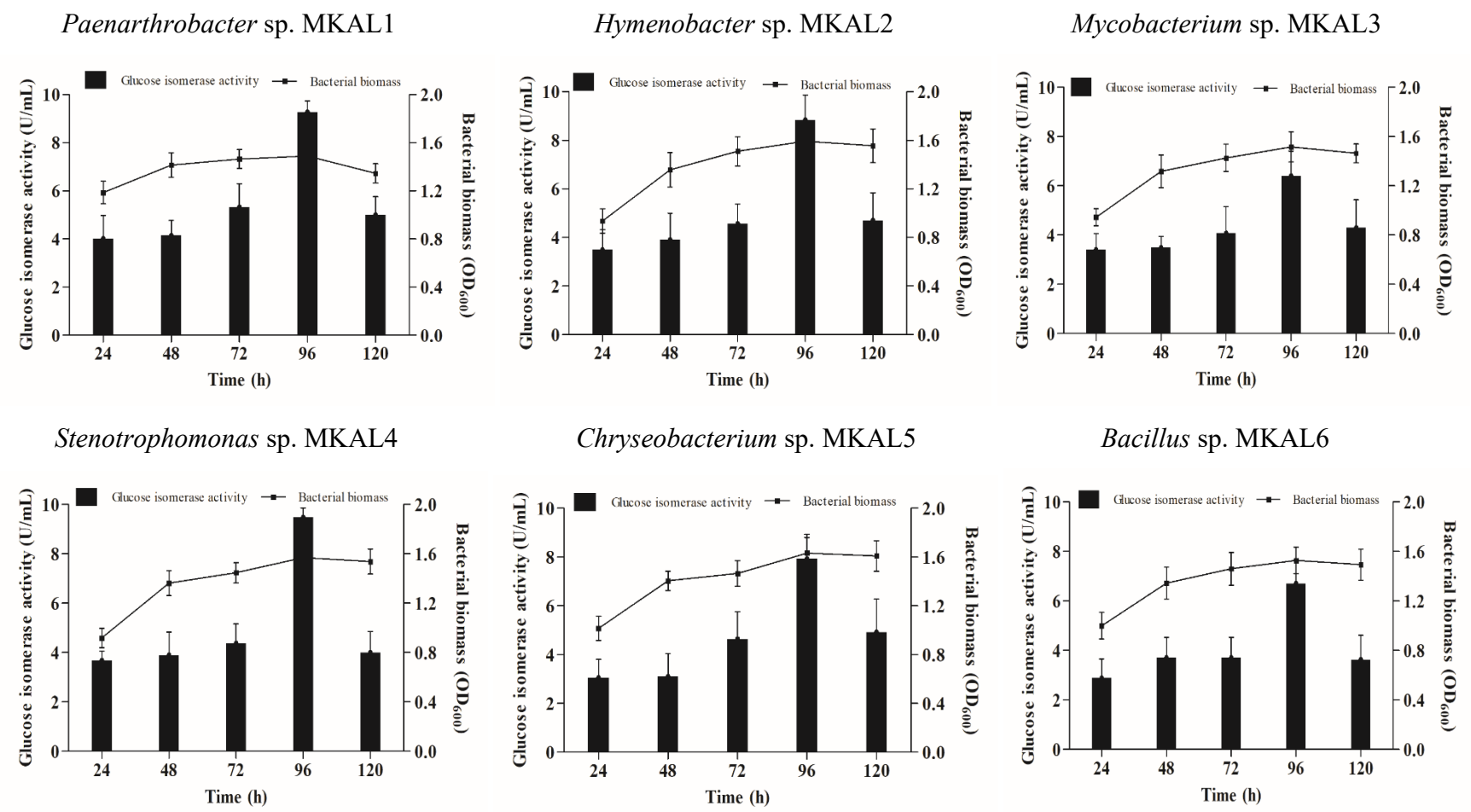

Figure 3. Effect of incubation period on bacterial biomass and glucose isomerase production by *Paenarthrobacter* sp. MKAL1, *Hymenobacter* sp. MKAL2, *Mycobacterium* sp. MKAL3, *Stenotrophomonas* sp. MKAL4, *Chryseobacterium* sp. MKAL5 and *Bacillus* sp. MKAL6.

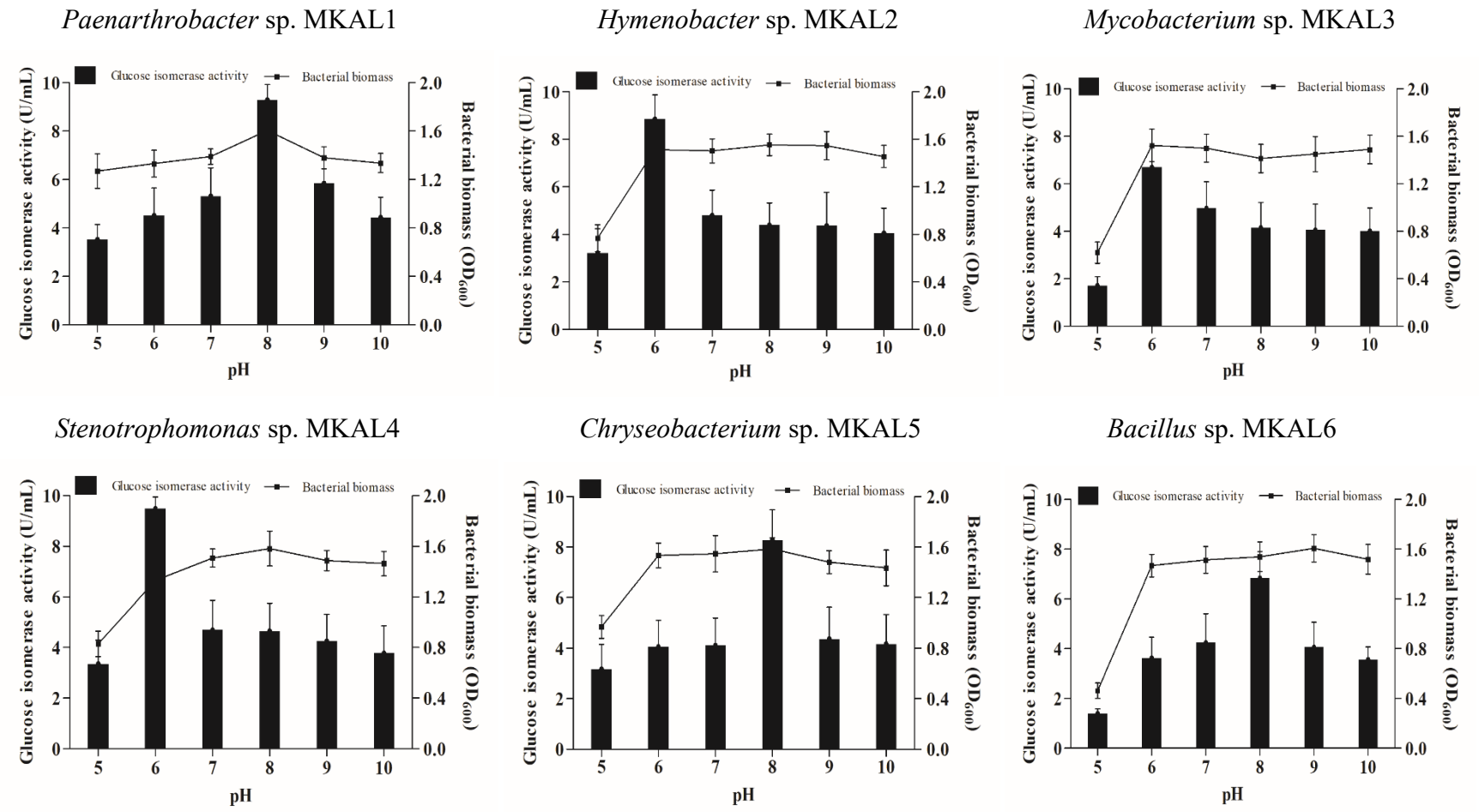

Figure 4. Effect of pH on bacterial biomass and glucose isomerase production by *Paenarthrobacter* sp. MKAL1, *Hymenobacter* sp. MKAL2, *Mycobacterium* sp. MKAL3, *Stenotrophomonas* sp. MKAL4, *Chryseobacterium* sp. MKAL5 and *Bacillus* sp. MKAL6.

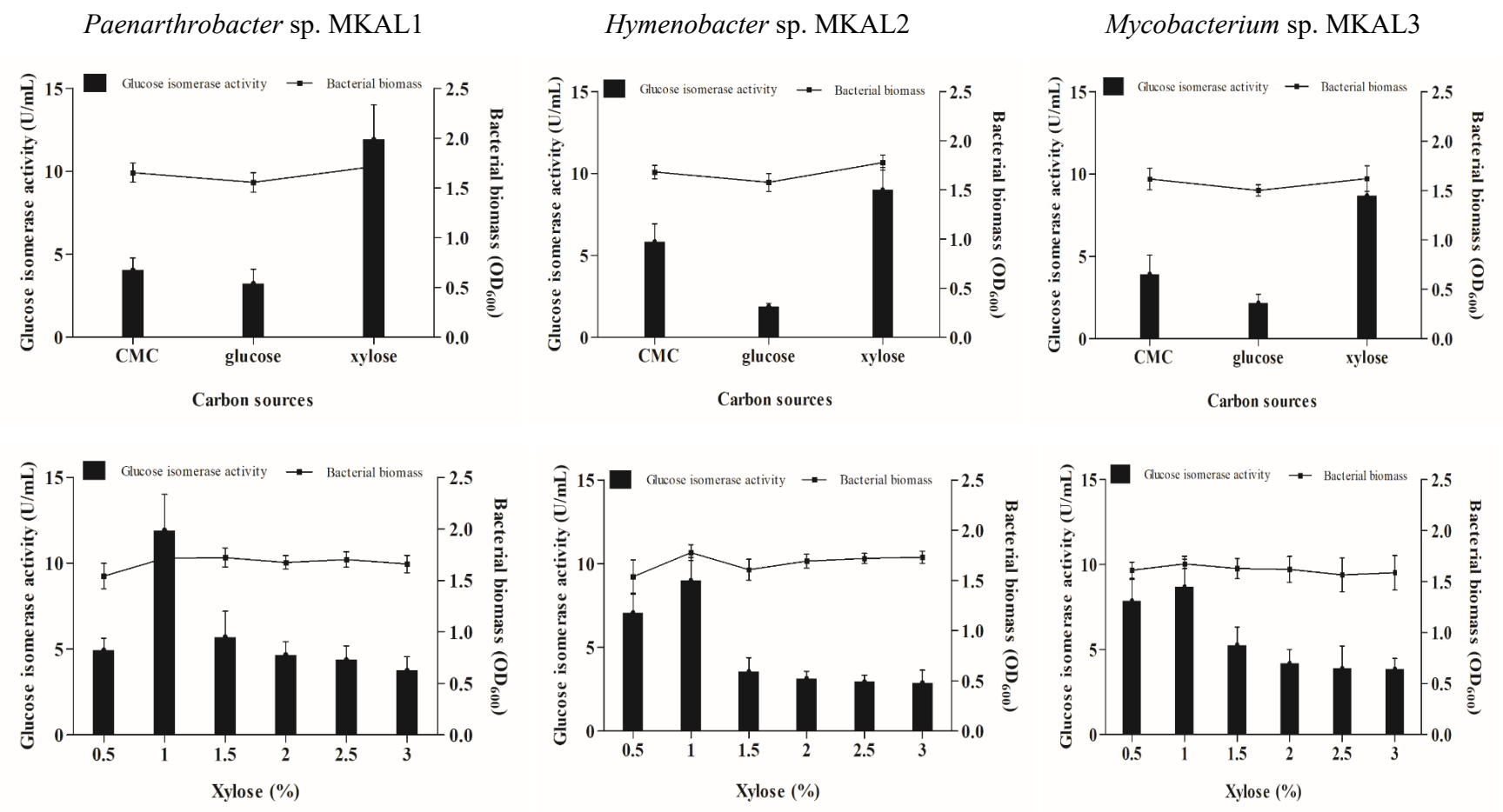

Figure 5. Effect of carbon sources and xylose concentration on bacterial biomass and glucose isomerase production by *Paenarthrobacter* sp. MKAL1, *Hymenobacter* sp. MKAL2 and *Mycobacterium* sp. MKAL3.

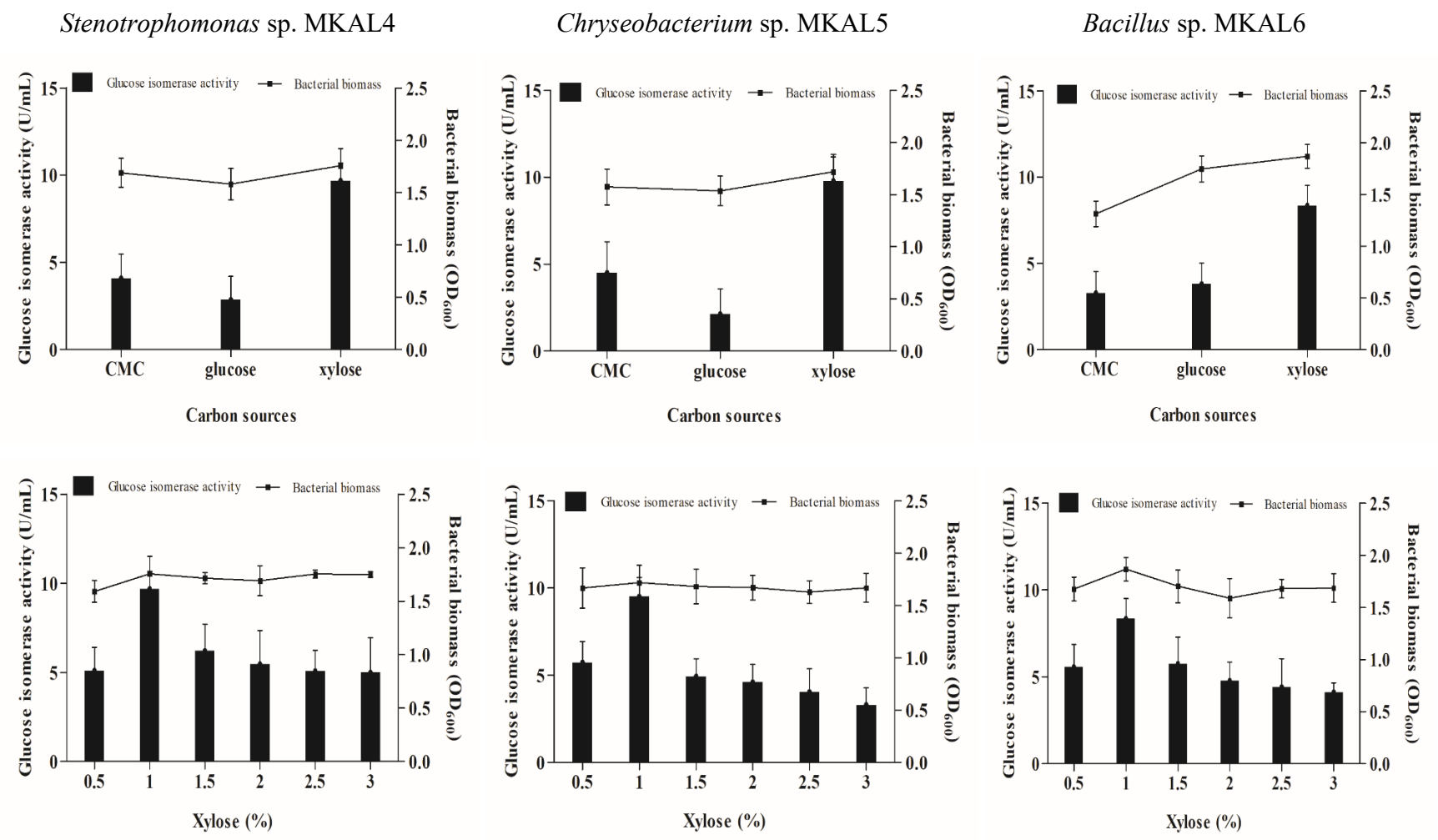

Figure 6. Effect of carbon sources and xylose concentration on bacterial biomass and glucose isomerase production by *Stenotrophomonas* sp. MKAL4, *Chryseobacterium* sp. MKAL5 and *Bacillus* sp. MKAL6.

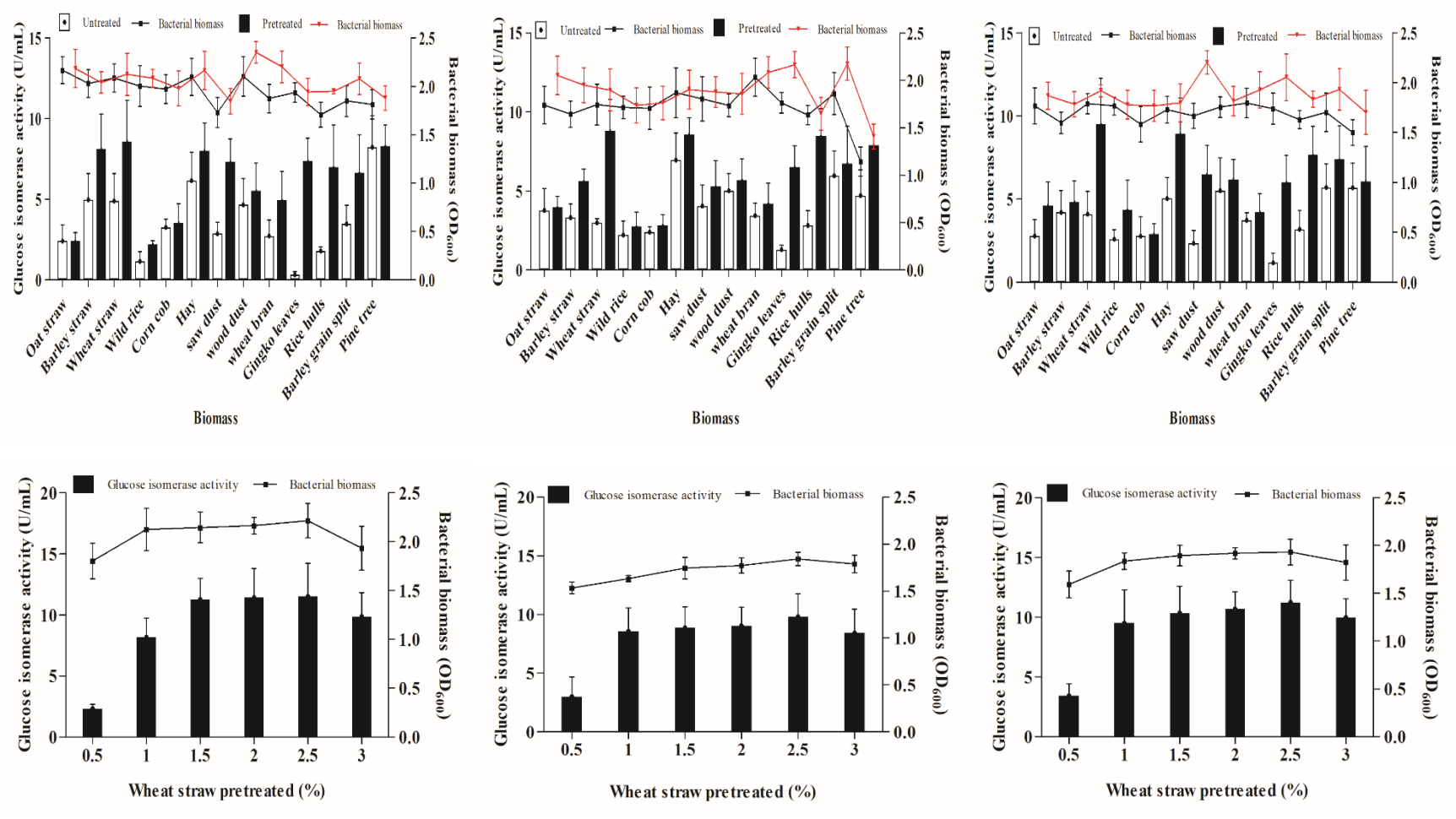

Figure 7. Effect of different lignocellulosic biomass and wheat straw concentration on bacterial biomass and glucose isomerase production by *Paenarthrobacter* sp. MKAL1, *Hymenobacter* sp. MKAL2 and *Mycobacterium* sp. MKAL3.

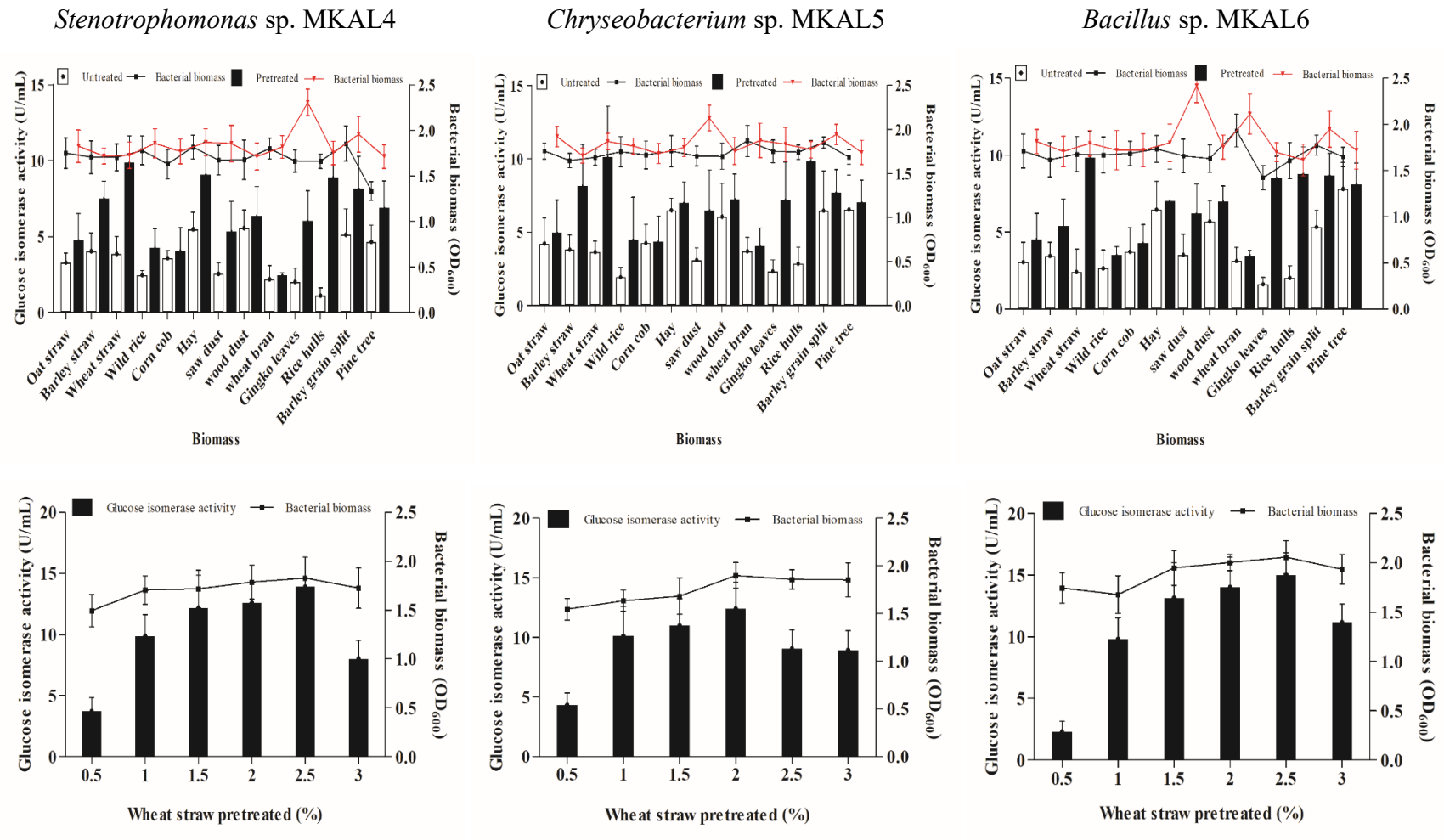

Figure 8. Effect of different lignocellulosic biomass and wheat straw concentration on bacterial biomass and glucose isomerase production by *Stenotrophomonas* sp. MKAL4, *Chryseobacterium* sp. MKAL5 and *Bacillus* sp. MKAL6.

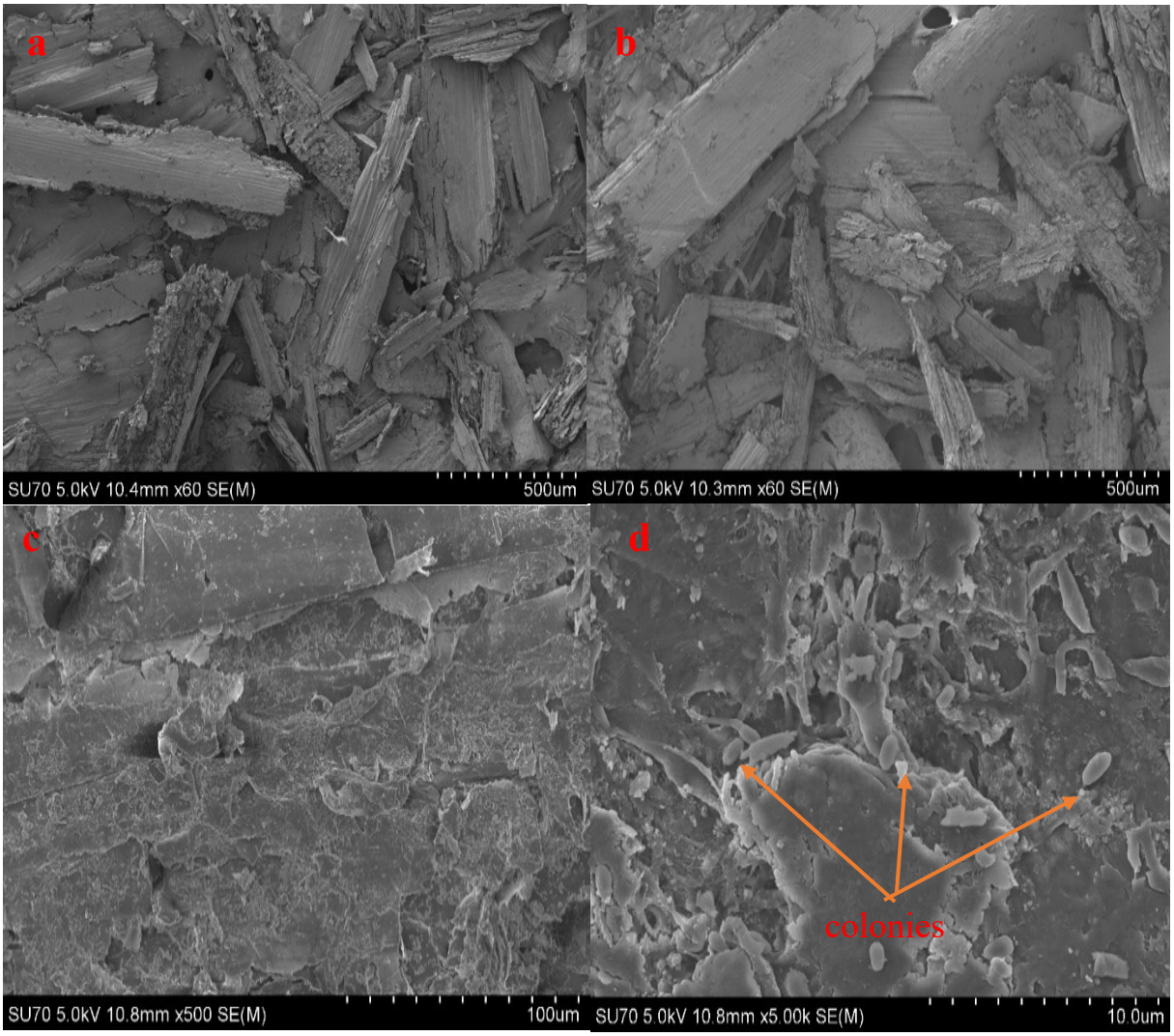

Figure 9. SEM micrographs of the treated and non-treated wheat straw (a) Raw wheat straw; (b) Pretreated wheat straw (washing with hot water and 95% ethanol); (c) Pretreated wheat straw after degradation by *Bacillus* sp. MKAL6 for 5 days; (d) Adhesion of *Bacillus* sp. MKAL6 to the exterior surface of pretreated wheat straw.

3.4. Effect of nitrogen sources on glucose isomerase production

The experiment was performed on various nitrogen sources. Bacterial isolates showed variable enzyme activities depending on the type of nitrogen sources (Figures 10 and 11). Fermentation medium non-supplemented by nitrogen sources could not promote GI production by

isolates. Peptone, tryptone, casein and yeast extract enhanced the least enzyme activity when used separately in the fermentation medium. However, GI activity increased when both were used in the same culture medium. *Paenarthrobacter* sp. (11.92 U/mL), *Chryseobacterium* sp. (9.50 U/mL), *Hymenobacter* sp. (8.59 U/mL), *Mycobacterium* sp. (8.95 U/mL) and *Stenotrophomonas* sp. (9.57 U/mL) exhibited higher GI activity in mixed peptone and yeast extract, while *Bacillus* sp. (9.80 U/mL) showed better activity in a mixture of tryptone and peptone. The highest GI production in *Paenarthrobacter* sp. (15.37 U/mL), *Chryseobacterium* sp. (22.78 U/mL), *Hymenobacter* sp. (17.37 U/mL), *Mycobacterium* sp. (12.65 U/mL) and *Bacillus* sp. (14.67 U/mL) was observed in a 2:1 ratio of peptone and yeast extract or tryptone and peptone, respectively. However, maximum enzyme production in *Stenotrophomonas* sp. occurred at a 1:2 ratio of peptone and yeast extract (14.08 U/mL). Similarly, Sharma et al. (2021) revealed a mixture of organic nitrogen sources highly boosted glucose isomerase activity in *Serratia marcescens* HK2 and the highest activity occurred at a 1:3 ratio of peptone and yeast extract.

3.5. Optimization of fermentation

The Box–Behnken design was used to optimize the fermentation of pretreated wheat straw. Results were presented in table 2. Glucose isomerase was the response variable, while temperature (X_1), pH (X_2) and fermentation time (X_3) were independent variables. Quadratic equations showing the linear relationship between response and independent variables were:

(1) *Bacillus* sp.: GI (U/mL)= $-\ 7.310X_1^2 - 7.843X_2^2 - 8.159X_3^2 + 0.824X_1X_2 - 0.602X_2X_3 - 2.143X_1X_3 - 3.448X_1 + 0.242X_2 + 0.123X_3 + 19.827$

(2) *Paenathrobacter* sp.: GI (U/mL)= $-\ 5.163X_1^2 - 2.621X_2^2 - 3.595X_3^2 + 0.212X_1X_2 - 3.076X_2X_3 - 0.320X_1X_3 - 1.368X_1 + 0.395X_2 - 0.963X_3 + 17.488$

(3) *Chryseobacterium* sp.: GI (U/mL)$= -\ 4.444X_1^2 -\ 3.725X_2^2 - 4.378X_3^2 + 0.066X_1X_2 - 0.388X_2X_3 + 0.660X_1X_3 - 0.620X_1 + 0.160X_2 - 0.535X_3 + 19.249$

(4) *Hymenobacter* sp.: GI (U/mL)$= -\ 6.768X_1^2 -\ 4.884X_2^2 - 5.995X_3^2 - 0.993X_1X_2 + 0.599X_2X_3 - 1.464X_1X_3 - 3.131X_1 - 0.872X_2 - 0.142X_3 + 16.500$

(5) *Mycobacterium* sp.: GI (U/mL)$= -\ 2.868X_1^2 -\ 2.308X_2^2 - 2.686X_3^2 - 0.028X_1X_2 - 0.625X_2X_3 + 0.679X_1X_3 - 0.812X_1 + 0.251X_2 - 1.023X_3 + 16.235$

(6) *Stenotrophomonas* sp.: GI (U/mL)$= -\ 8.665X_1^2 -\ 6.574X_2^2 - 6.217X_3^2 - 1.010X_1X_2 + 2.241X_2X_3 - 0.437X_1X_3 - 3.990X_1 - 1.532X_2 - 1.556X_3 + 20.500$

The analysis of variance revealed that *p*-values of regression and lack of fit were 0.000-0.01 ($p < 0.05$) and 0.063-0.284 ($p > 0.05$) respectively for Bacillus sp., *Paenarthrobacter* sp., *Chryseobacterium* sp. and *Mycobacterium* sp. (Table 2). This indicates that the built quadratic equation is relatively credible for the evaluation of glucose isomerase activity of these isolates. However, *p*-values of regression and lack of fit were 0.080-0.097 ($p > 0.05$) and 0.002-0.011 ($p < 0.05$) respectively for *Hymenobacter* sp. and *Stenotrophomonas* sp. This suggests that the relationship between parameters is not significant, or the response surface quadratic model doesn't fit well for the assessment of enzyme activity of those two bacteria (Han et al., 2021). Contour plots were produced based on the fitted model to estimate response surface shape. All contour plots appeared as ellipses, suggesting interactions between temperature, pH, and fermentation time. These variables affect glucose isomerase and optimum conditions for maximum enzyme production yield were in the design range (Appendix 6). The optimal responses, 20.246, 19.292, 17.711 and 16.427 U/mL with a 95% confidence interval were obtained by canonical analysis for *Bacillus* sp., *Chryseobacterium* sp., *Paenarthrobacter* sp. and *Mycobacterium* sp. respectively. The coded factor values for the stationary point were:

(1) *Bacillus* sp.: $-0.242\ (X_1), 0.001(X_2), 0.039\ (X_3)$, with corresponding experimental conditions: temperature 38.79°C, pH 8.00, and fermentation time 96.94 h.

(2) *Chryseobacterium* sp.: $-0.075\ (X_1), 0.024(X_2), -0.068\ (X_3)$, with corresponding experimental conditions: temperature 39.65°C, pH 8.02, and fermentation time 94.37 h.

(3) *Paenarthrobacter* sp.: $-0.122\ (X_1), 0.195(X_2), -0.212\ (X_3)$, with corresponding experimental conditions: temperature 39.39°C, pH 8.20, and fermentation time 90.91 h.

(4) *Mycobacterium* sp.: $-0.168\ (X_1), 0.085(X_2), -0.222\ (X_3)$, with corresponding experimental conditions: temperature 39.16°C, pH 6.09, and fermentation time 90.67 h.

The fitness of the model was checked by performing triplicate experiments under predicted optimum fermentation conditions. Experimental values were 20.128, 19.188, 17.633 and 16.379 U/mL for *Bacillus* sp., *Chryseobacterium* sp*., Paenarthrobacter* sp. and *Mycobacterium* sp., respectively. This demonstrates reliable goodness of fit to predict glucose isomerase production yield during the fermentation process with these bacterial isolates.

4. Conclusion

This study aimed to characterize glucose isomerase producing bacterial isolates and optimize their enzyme production. Six bacteria were isolated from soil samples (*Paenarthrobacter* sp MKAL1, *Hymenobacter* sp. MKAL2, *Mycobacterium* sp. MKAL3, *Stenotrophomonas* sp. MKAL4, *Chryseobacterium* sp. MKAL5 and *Bacillus* sp. MKAL6). Maximum GI production in these isolates occurred at the culture conditions of 40°C, pH 6-8 and 96 h of incubation. A mixture of peptone/yeast extract or tryptone/peptone enhanced higher enzyme production. The same trend was observed in fermentation medium containing 1% xylose or 2-2.5% wheat straw. Response surface quadratic model was reliable to predict glucose isomerase production during the

fermentation process with *Bacillus* sp., *Chryseobacterium* sp., *Paenarthrobacter* sp. and *Mycobacterium* sp. These bacterial isolates could be promising wheat straw degraders in bio-based industries. The purification of these glucose isomerases for hydrolysis and saccharification of lignocellulosic biomasses are being studied.

Table 2. Analysis of variance and lack of fit test for the response surface quadratic model.

Bacterial isolates	source	df	SS	Mean squares	F-ratio	*p*-value
Hymenobacter sp. MKAL2	Regression	9	437.988	48.665	3.745	0.080
	Squared Multiple R	0.871				
	Lack of fit	3	64.892	21.631	578.090	0.002
Stenotrophomonas sp. MKAL4	Regression	9	695.510	77.279	3.364	0.097
	Squared Multiple R	0.858				
	Lack of fit	3	114.037	38.012	93.605	0.011
Bacillus sp. MKAL6	Regression	9	699.403	77.711	10.195	0.010
	Squared Multiple R	0.948				
	Lack of fit	3	36.113	12.038	12.047	0.078
Paenarthrobacter sp. MKAL1	Regression	9	213.346	23.705	24.077	0.001
	Squared Multiple R	0.977				
	Lack of fit	3	4.715	1.572	15.149	0.063
Chryseobacterium sp. MKAL5	Regression	9	177.105	19.678	29.744	0.001
	Squared Multiple R	0.982				
	Lack of fit	3	2.726	0.909	3.123	0.252
Mycobacterium sp. MKAL3	Regression	9	84.122	9.347	106.255	0.000
	Squared Multiple R	0.995				
	Lack of fit	3	0.352	0.117	2.676	0.284

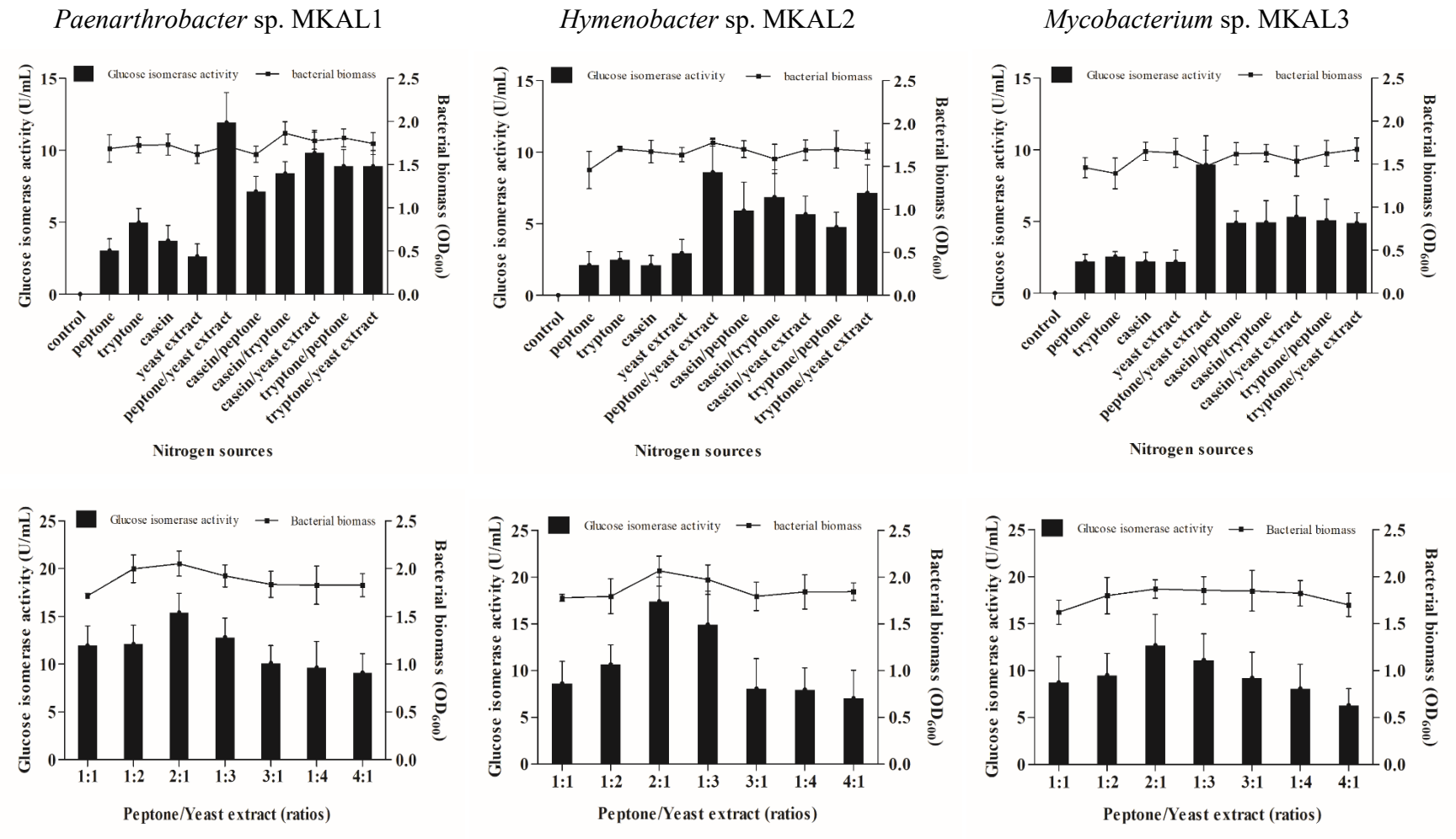

Figure 10. Effect of nitrogen sources and proportion of their mixture on bacterial biomass and glucose isomerase production by *Paenarthrobacter* sp. MKAL1, *Hymenobacter* sp. MKAL2 and *Mycobacterium* sp. MKAL3.

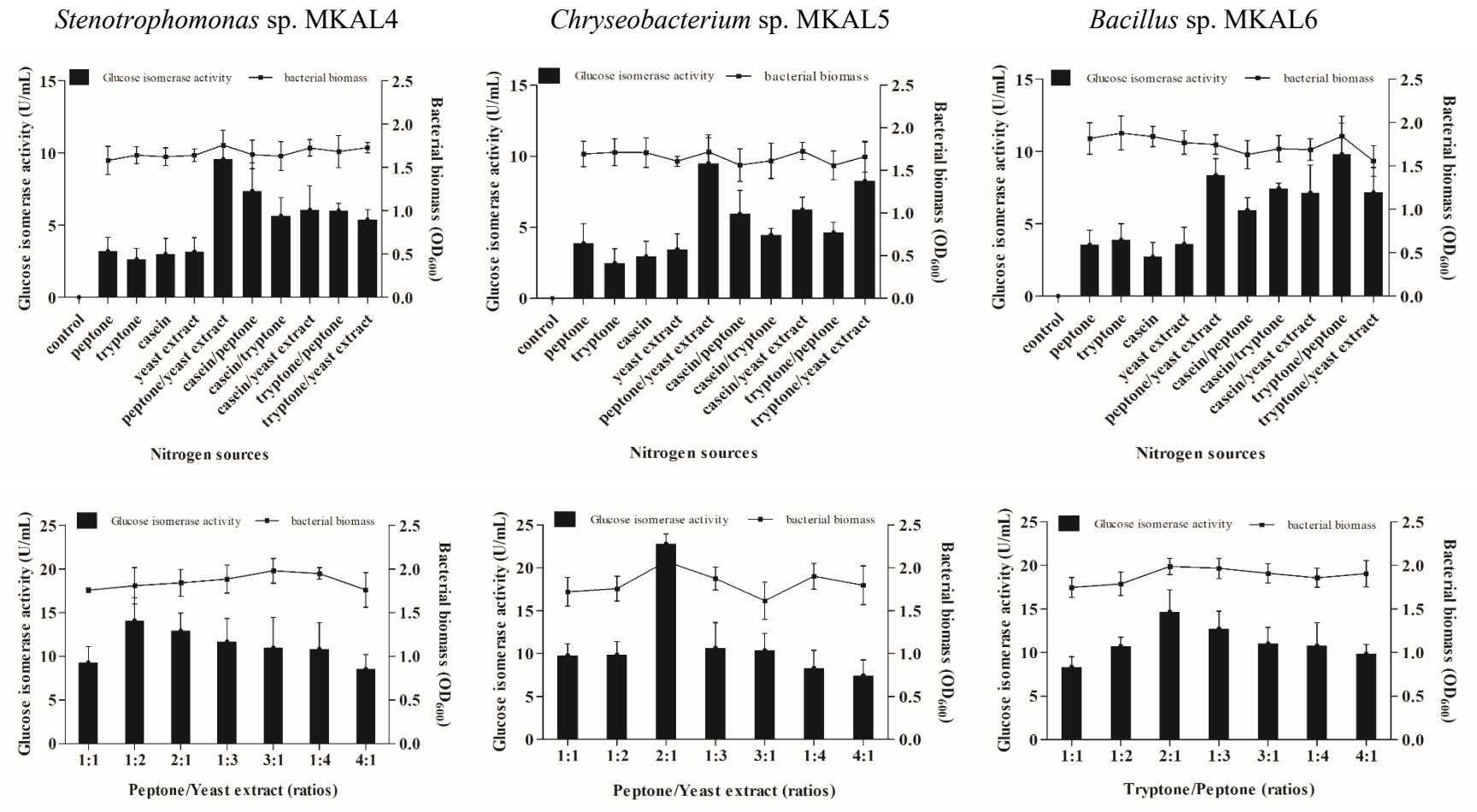

Figure 11. Effect of nitrogen sources and proportion of their mixture on bacterial biomass and glucose isomerase production by *Stenotrophomonas* sp. MKAL4, *Chryseobacterium* sp. MKAL5 and *Bacillus* sp. MKAL6.

5. References

Al-Dhabi NA, Esmail GA, Ghilan AKM, Arasu MV (2020). Isolation and screening of *Streptomyces* sp.Al-Dhabi-49 from the environment of Saudi Arabia with concomitant production of lipase and protease in submerged fermentation. *Saudi J Biol Sci*, 27, 474-479.

Bhasin S, Modi H (2012). Optimization of fermentation medium for the production of glucose isomerase using *Streptomyces* sp. SB-P1. Biotechnol Res Int, 2012, 1-10.

Chanitnun K, Pinphanichakarn P (2012). Glucose(xylose) isomerase production by *Streptomyces* sp. CH7 grown on agricultural residues. *Braz J Microbiol*, 43, 1084-1093.

Dai C, Miao T, Hai J, Xiao Y, Li Y, Zhao J, Qiu H, Xu B (2020). A novel glucose isomerase from *Caldicellulosiruptor bescii* with great potentials in the production of high-fructose corn syrup. *Biomed Res Int*, 2020, 1871934.

Domingues R, Bondar M, Palolo I, Queirós O, de Almeida CD, Cesário MT (2021). Xylose metabolism in bacteria—Opportunities and challenges towards efficient lignocellulosic biomass-based biorefineries. *Appl Sci*, 11, 8112.

Fatima B, Javed MM (2020). Production, purification and physicochemical characterization of D-xylose/glucose isomerase from *Escherichia coli* strain BL21. *3 Biotech*, 10, 39.

Finore I, Lama L, Di Donato P, Romano I, Tramice A, Leone L, Nicolaus B, Poli A (2019). *Parageobacillus thermantarcticus*, an antarctic cell factory: from crop residue valorization by green chemistry to astrobiology studies. *Diversity*, 11, 128.

Givry S and Duchiron F (2008). Optimization of culture medium and growth conditions for production of L-arabinose isomerase and D-xylose isomerase by *Lactobacillus bifermentans*. *Microbiology*, 77, 281-287.

Han S, Chio C, Ma T, Mokale Kognou AL, Shrestha S, Chen F, Qin W (2021). Extracting flavonoid from Ginkgo biloba using lignocellulolytic bacteria *Paenarthrobacter* sp. and optimized via response surface methodology. *Biofuels Bioprod Bioref*, 15, 867-878.

Jia DX, Zhou L, Zheng YG (2017). Properties of a novel thermostable glucose isomerase mined from *Thermus oshimai* and its application to preparation of high fructose corn syrup. *Enzym Microb Technol*, 99, 1-8.

Liu ZQ, Zheng W, Huang JF, Jin LQ, Jia DX, Zhou, HY, Xu JM, Liao CJ, Cheng XP, Mao BX, Zheng YG (2015). Improvement and characterization of a hyperthermophilic glucose isomerase from *Thermoanaerobacter ethanolicus* and its application in production of high fructose corn syrup. *J Ind Microbiol Biotechnol,* 42, 1091-1103.

Market Study Report (2019). Global 5-hydroxymethylfurfural (5-HMF) (CAS 67-47-0) Market 2019 by manufacturers, regions, type and application, forecast to 2024, https://www.marketstudyreport.com/reports/global-5-hydroxymethylfurfural-5-hmf-cas-67-47-0-market-2019-by-manufacturers-regions-type-and-application-forecast-to-2024.

Nam KH (2022). Glucose isomerase: Functions, Structures, and Applications. *Appl Sci*, 12, 428.

OECD/FAO (2019). OECD-FAO Agricultural Outlook 2018-2027, https://www.oecd-ilibrary.org/agriculture-and-food/data/oecd-agriculture-statistics_agr-data-en.

Philippini RR, Martiniano SE, Ingle AP, Franco Marcelino PR, Silva GM, Barbosa FG, dos Santos JC, da Silva SS (2020). Agroindustrial byproducts for the generation of biobased products: Alternatives for sustainable biorefineries. *Front Energ Res*, 8, 152.

Rengasamy S, Subramanian MR, Perumal V, Ganeshan S, Al Khulaifi MM, Al-Shwaiman HA, Elgorban AM, Syed A, Thangaprakasam U (2020). Purification and kinetic behavior of glucose isomerase from *Streptomyces lividans* RSU26, *Saudi J Biol Sci*, 27, 1117-1123.

Sahin AW, Zannini E, Coffey A, Arendt EK (2019). Sugar reduction in bakery products: Current strategies and sourdough technology as a potential novel approach. *Food Res Int*, 126, 108583.

Saikia K, Rathankumar AK, Kumar PS, Varjani S, Nizar M, Lenin R, George J, Vaidyanathan VK (2022). Recent advances in biotransformation of 5-Hydroxymethylfurfural: challenges and future aspects. *J Chem Technol Biotechnol*, 97, 409-419.

Sapunova LI, Lobanok AG, Kazakevich IO, Evtushenkov AN (2004). Chashechnyĭ metod skrininga mikroorganizmov--produtsentov ksilozoizomerazy [A plate method to screen for microorganisms producing xylose isomerase]. *Mikrobiologiia*, 73, 126-132.

Sharma HK, Xu C, Qin W (2021). Isolation of bacterial strain with xylanase and xylose/glucose Isomerase (GI) activity and whole cell immobilization for improved enzyme production. *Waste Biomass Valor*, 12, 833-845.

Singh RS, Chauhan K, Pandey A, Larroche C (2018). Biocatalytic strategies for the production of high fructose syrup from inulin. *Bioresour Technol*, 260, 395-403.

Singh TA, Jajoo A, Bhasin S (2020). Production and application of glucose isomerase from *Streptomyces enissocaesilis* and amylase from *Streptomyces* sp. for the synthesis of high fructose corn syrup. *SN Appl Sci*, 2, 1968.

Thi Nguyen HY, Tran GB (2018). Optimization of fermentation conditions and media for production of glucose isomerase from *Bacillus megaterium* using response surface methodology. *Scientifica (Cairo)*, 2018, 6842843.

Tsumura N, Sato T (1965). Enzymatic conversion of D-glucose to D-fructose part V: partial purifcation and properties of the enzyme from Aerobacter cloacae. *Agric Biol Chem*, 29, 1123-1128.

Zargaraan A, Kamaliroosta L, Yaghoubi AS, Mirmoghtadaie L (2016). Effect of substitution of sugar by high fructose corn syrup on the physicochemical properties of bakery and dairy products: A review. *Nutr Food Sci*, 3, 3-11.

Zhou CH, Xia X, Lin CX, Tong DS, Beltramini J (2011). Catalytic conversion of lignocellulosic biomass to fine chemicals and fuels. *Chem Soc Rev*, 40, 5588-5617.

CHAPTER 4

Coculture and whole-cell immobilization of cellulolytic soil bacteria for enhanced glucose isomerase production from wheat straw

Aristide Laurel Mokale Kognou[1], Chonlong Chio[1], Janak Raj Khatiwada[1], Sarita Shrestha[1], Xuantong Chen[1], Yuen Zhu[2], Rosalie Anne Ngono Ngane[3], Gabriel Agbor Agbor[4], Zi-Hua Jiang[5], Chunbao (Charles) Xu[6], Wensheng Qin[1]

[1]Department of Biology, Lakehead University, Thunder Bay, Canada

[2]School of Environment and Resources, Shanxi University, Taiyuan, China

[3]Department of Biochemistry, Faculty of Science, The University of Douala, Douala, Cameroon

[4]Centre for Research on Medicinal Plants and Traditional Medicine, Institute of Medical Research and Medicinal Plants Studies Cameroon, Yaounde, Cameroon

[5]Department of Chemistry, Lakehead University, Thunder Bay, Canada

[6]Department of Chemical and Biochemical Engineering, Western University, London, Ontario, Canada

*Corresponding author: Wensheng Qin

Abstract

Coculture and whole-cell immobilization find myriad applications in industries for enhancing enzyme production. Using pretreated wheat straw as the sole carbon source, improving glucose isomerase production and cell growth by synthetic bacterial consortia was investigated. Thirteen cocultures were constructed based on their performance and antagonistic activities of monocultures from six cellulolytic soil bacteria. The performance of monocultures immobilized

with calcium alginate was also tested. Only five cocultures (A, B, C, G and J) exhibited cell growth and enzyme production synergies. The highest level of synergism (15.17 U/mL) was found in coculture J composed of *Mycobacterium* sp. MKAL3 (4.06 U/mL) and *Stenotrophomonas* sp. MKAL4 (3.37 U/mL) with a synergism degree of 2.04. The synergism was unique to growth on wheat straw as it was completely absent in xylose-grown cocultures. The wheat straw degradation synergism could rely on specific compounds released by strain MKAL3 that promote the strain MKAL4 activity and vice versa. However, immobilized strain MKAL1, MKAL2, MKAL3, MKAL4 and MKAL5 improved glucose isomerase production in the wheat straw fermentation process at different sodium alginate concentrations. The immobilization studies of purified glucose isomerases for hydrolysis and saccharification of wheat straw are being studied.

Keywords: cellulolytic bacteria, glucose isomerase, coculture, entrapment, sodium alginate, wheat straw

1. Introduction

Designing and constructing microbial consortia and whole-cell immobilization became important for improving enzyme production from low-cost agricultural residues to minimize the cost of down streaming processing. Bacteria interact dynamically with other bacteria, but these interactions are still poorly studied. The suggested predominant interactions are the competition for resources among bacterial species (Deng and Wang, 2017) and lacking some key metabolic pathways in some species which others can supplement (Cortes-Tolalpa et al., 2017). In nature, one bacterium competes with other species by producing antibiotic-like substances due to the limited labile nutrients (Sarkar et al., 2021; Chhetri et al., 2022).

Although competitive interactions among bacterial species are ubiquitous, many investigations showed their importance in metabolic complementarity by synergistic cooperation of bacterial partners in key metabolite exchanges or niche partitioning for lignocellulosic biomass degradation. Several mechanisms and dynamism that play a role in the wheat straw microbial attack have been reported (Cortes-Tolalpa et al., 2017, Cortes-Tolalpa et al., 2018; Kong et al., 2018; Lazuka et al., 2018; Bremond et al., 2022; Kabaivanova et al., 2022). Globally, about 734 million tons of wheat straw are produced yearly (Serrano et al., 2020) and are widely used as raw material for enzymes, fuels, and value-added compounds production (Tomás-Pejó et al., 2017; Lozano and Lozano, 2018). Its composition depends on plant age, collecting season, local growth conditions and soil quality used for cultivation. The obstacle to its utilization is its recalcitrant nature due to its complex chemical complex related to linkages between cellulose, lignin and hemicellulose (Ruiz et al., 2013; Domínguez-Robles et al., 2017). Also, cellulose crystallinity and polymerization degrees influence its degradability. Bacteria could form consortia to achieve a better degradation synergistically. The cooperative interactions could depend on wheat straw complexity.

However, enhanced enzyme production can also be obtained by immobilizing the enzyme or whole-cell using carriers from natural origin matrixes (agarose spheres or beads, glyoxyl- and octyl-agarose, novel affinity tag ChBD-AB from *Chitinolyticbacter meiyuanensis*, *Pichia pastoris*, chitin and alginate) to artificial synthetic materials (porous, polymeric, nanostructured, or magnetic materials) (Lou et al., 2021). A high-molecular-weight extracellular copolymer, natural alginate can bind divalent cations and water (Jin et al., 2016). It has been applied to the immobilization of *Serratia marcescens* HK2 producing glucose isomerase (Sharma et al., 2021), *Bacillus amyloliquens* MBL27 producing antimicrobial (Kumaravel and Gopal, 2010),

Escherichia coli producing β-galactosidase (Lee et al., 2013) and D-hydantoinase-engineered *Escherichia coli* for D-carbamoyl-p-hydroxyphenylglycine biosynthesis (Jin et al., 2016).

Six bacteria with cellulolytic properties were previously isolated from a mixture of soil samples collected at Kingfisher Lake (Thunder Bay, Ontario) and the University of Manitoba campus (Winnipeg, Manitoba). These bacteria grown on pretreated wheat straw showed glucose isomerase (GI) activity and repeated growth. This study investigated the effect of bacterial coculture and whole-cell immobilization on GI production from pretreated wheat straw. Two hypotheses were also examined, namely (1) substrate complexity has mediated bacterial interaction and (2) released compounds were the synergism basis.

2. Materials and methods

2.1. Strains, culture media, and biomass pretreatment

Six glucose-producing bacteria were isolated from a mixture of soil samples collected from Kingfisher Lake (Thunder Bay, Ontario) and the University of Manitoba campus (Winnipeg, Manitoba). These bacteria were identified as *Paenarthrobacter* sp. MKAL1, *Hymenobacter* sp. MKAL2, *Mycobacterium* sp. MKAL3, *Stenotrophomonas* sp. MKAL4, *Chryseobacterium* sp. MKAL5 and *Bacillus* sp. MKAL6 with the NCBI accession numbers ON442553, ON442554, ON442555, ON442556, ON442557 and ON442558 respectively (Mokale et al., 2022a; Mokale et al., 2022b). Bacterial strains were cultured in Luria-Bertani (LB) broth (containing 10 g peptone, 5 g yeast extract, 5 g NaCl and distilled water up to 1 L) for subsequent uses. The wheat straw was ground and filtered in a filter/screen of mesh size of 200 micrometers to obtain a powder. Then, the powder was macerated thrice in hot water (100 °C), 95% ethanol, and the pretreated residue

was dried at room temperature for one week. Bacterial strains were cultured in the pretreated wheat straw broth medium (3% pretreated wheat straw, 1.5 g/L peptone, 1.5 g/L yeast extract, 1 g/L K_2HPO_4, 0.1 g/L $MnCl_2.4H_2O$, 1 g/L $MgSO_4.7H_2O$ and 0.05 M citrate buffer pH 8 up to 1 L) for glucose isomerase (GI) production.

2.2. Antagonistic Interaction Assays

Burkholder's 'spot-on-lawn' method investigated antagonistic interactions between strains (Burkholder et al., 1966). A complete interaction matrix of strains was obtained by confronting each other in a set-up. Overnight strain cultures (optical density 0.5 at 600 nm) were mixed and inoculated onto the surface of Mueller Hinton agar Petri dishes. Following solidification, overnight cultures of selected bacterial strains were added on top. After incubation for 48 h at 30°C, Petri dishes were inspected for inhibition halos around the growth of the test isolates. The broad-spectrum antibiotic erythromycin was used as a control.

2.3. Monocultures and cocultures

A monoculture refers to the microbial strains growing alone in a flask, while a coculture refers to combined strains growing in a flask. The selection of strains for constructing the synthetic pairs was based on enzyme activity and antagonism assay data. Six bacterial strains were selected to examine the behavior in cocultures, and thus 13 cocultures were formed (Table 1).

Table 1. Bacterial composition of the cocultures in this study.

Coculture	Taxonomy affiliation		
	Strain code	Strain 1	Strain 2
A	MKAL1, MKAL2	*Paenarthrobacter* sp. MKAL1	*Hymenobacter* sp. MKAL2
B	MKAL1, MKAL3	*Paenarthrobacter* sp. MKAL1	*Mycobacterium* sp. MKAL3
C	MKAL1, MKAL4	*Paenarthrobacter* sp. MKAL1	*Stenotrophomonas* sp. MKAL4
D	MKAL1, MKAL5	*Paenarthrobacter* sp. MKAL1	*Chryseobacterium* sp. MKAL5
E	MKAL1, MKAL6	*Paenarthrobacter* sp. MKAL1	*Bacillus* sp. MKAL6
F	MKAL2, MKAL3	*Hymenobacter* sp. MKAL2	*Mycobacterium* sp. MKAL3
G	MKAL2, MKAL4	*Hymenobacter* sp. MKAL2	*Stenotrophomonas* sp. MKAL4
H	MKAL2, MKAL5	*Hymenobacter* sp. MKAL2	*Chryseobacterium* sp. MKAL5
I	MKAL2, MKAL6	*Hymenobacter* sp. MKAL2	*Bacillus* sp. MKAL6
J	MKAL3, MKAL4	*Mycobacterium* sp. MKAL3	*Stenotrophomonas* sp. MKAL4
K	MKAL3, MKAL5	*Mycobacterium* sp. MKAL3	*Chryseobacterium* sp. MKAL5
L	MKAL3, MKAL6	*Mycobacterium* sp. MKAL3	*Bacillus* sp. MKAL6
M	MKAL4, MKAL5	*Stenotrophomonas* sp. MKAL4	*Chryseobacterium* sp. MKAL5

2.4. Glucose isomerase activity assay

The quantification of GI was carried out using the Cysteine-Carbazole method (Tsumura et al., 1965). The overnight bacterial culture (500 mL) was inoculated in 250 mL Erlenmeyer flasks containing 50 mL of pretreated wheat straw broth, and flasks were incubated in a shaking incubator (200 rpm) throughout the experiments. The GI production by bacterial cultures was monitored at 24, 48, 72, and 96 h. It was optimized by varying pH from 5 to 10 in the fermentation medium at the culture conditions of 3% wheat straw, 40°C and 5 days incubation period. After incubation, 500 µL of culture medium was collected, centrifuged (12,000×g, 3 min), and supernatant (containing extracellular GI) was analyzed at 540 nm using a microplate reader spectrophotometer (BioTek, USA). The bacterial growth was also determined in terms of biomass at 600 nm. As previously described, the GI activity was estimated by measuring fructose yield after the isomerization reaction. The GI activity was calculated using the fructose standard curve ($y = 0.0602x + 0.1179$; $r^2 = 0.9949$) and expressed in units per milliliter (U/mL), where one unit of enzyme corresponds to the release of 1 µmole of fructose equivalent per minute from the substrate.

The enzymatic synergism degree (DS) was calculated by dividing the coculture enzyme activity by the sum of individual activities from respective monocultures (Van Dyk et al., 2013). The coculture with the highest DS was selected for induction assay. Experiments were done in triplicate.

2.5. Induction assay

The coculture J exerted the highest enzyme synergistic activity. Monocultures of strains *Mycobacterium* sp. MKAL3 and *Stenotrophomonas* sp. MKAL4 were prepared as described above using xylose or pretreated wheat straw as a carbon source at a concentration of 3%. The induction assay was performed as Cortes-Tolalpa et al. (2017) described. After five days of incubation, supernatants were collected and filtered (Whatman filter paper No 1), and bacterial cell absence in supernatants was checked. For induction of MKAL3, a final volume of MKAL4 (10%) was to the MKAL3 culture and incubated for 5 days. The strain MKAL4 was also treated reciprocally. Controls were composed of strains growing with 10% medium adding. Then, cell growth and enzyme activities were monitored over time and compared with their respective controls. Assays were done in triplicate.

2.5. Effect of whole-cell immobilization on GI Activity

Bacterial strains were immobilised in calcium alginate beads using the entrapment method with some modifications (Anisha and Prema, 2008). Briefly, sodium alginate (0.25 g) was prepared in distilled water (5 mL), and overnight, LB broth cell culture (5 mL) was added to the sodium alginate solution. The mixture was collected in a syringe and dropped from 15 cm height in $CaCl_2$ solution (1.5g of 0.2M $CaCl_2$ in 100 mL distilled water) with continuous steering until small

calcium alginate beads were formed. The beads were left for 20 min in $CaCl_2$ solution to become hardened. Bacterial cultures entrapped in calcium alginate beads were washed with autoclaved distilled water. These beads were used for GI production in the fermentation medium (50 mL) in optimum culture conditions (40°C, pH 6 for strains MKAL2, MKAL3 and MKAL4, pH 8 for strains MKAL1, MKAL5 and MKAL6 for 5 days of incubation). The inoculum size of immobilized strain was maintained equivalent to the seed culture inoculum size of free strain used in all other experiments. Experiments were performed in triplicate.

3. Results and Discussion

3.1. Antagonistic Interaction

Antagonistic interactions between *Bacillus* sp. MKAL6 and two other strains (*Stenotrophomonas* sp. MKAL4 and *Chryseobacterium* sp. MKAL 5) were observed (Figure 1). This suggests that strains MKAL4 and MKAL5 produced antibiotic-like compounds that inhibited cell growth MKAL6 strain. Antimicrobial activities were reported in *Stenotrophomonas maltophilia* INA 01133, *Stenotrophomonas maltophilia* INA 01134, *Stenotrophomonas rhizophila* sp. nov. INA 01137 (Efimenko et al., 2016), *Stenotrophomonas* sp. (Sarkar et al., 2021), *Chryseobacterium antibioticum* (Dahal et al., 2021) and *Chryseobacterium tagetis* (Chhetri et al., 2022).

3.2. Degradation potential in cocultures

The tested Cocultures stimulated glucose isomerase production in a pH and time-dependent manner (Appendix 7 and 8), indicating mutual effects of strains in enzyme production. Among 13

cocultures tested, only 5 cocultures (A, B, C, G and J) exhibited synergism in cell growth and enzyme production. Thus, specific combinations of bacteria are essential because the physiological or metabolic responses of a bacteria depend on its partner in the coculture. Enzyme production in cocultures A (19.62 U/mL), B (20.09 U/mL), C (18.11 U/mL), G (16.03 U/mL) and J (15.17 U/mL) exceeded those found in corresponding monocultures (Figure 2A). These cocultures exhibited synergistic enzyme activity with DS of 1.32, 1.44, 1.37, 1.90 and 2.04, respectively, for cocultures A, B, C, G and J. These synergistic interactions could be due to the metabolic complementary of the component strains (Rafieenia et al., 2022). For instance, in the most synergistic coculture (coculture J), *Mycobacterium* sp. MKAL3 and *Stenotrophomonas* sp. MKAL4 differ widely in their metabolic properties. *Mycobacterium* sp. is a Gram-positive bacteria belonging to the *Mycobacteriaceae* family and produces urease, pectinase and protease. It cannot produce DNase, catalase, and α-amylase. *Stenotrophomonas* sp. is a Gram-negative bacteria belonging to the *Xanthomonadaceae* family and produces DNase, catalase and α-amylase. It cannot secrete urease, pectinase and protease. Both can degrade cellobiose. However, no synergistic enzyme activity was observed in cocultures D, E, F, H, I, K, L and M. Of 13 cocultures, only cocultures A, B, C, G and J enhanced cell growth compared to the respective monocultures suggesting that each strain benefited from the other in the coculture (Figure 2 B).

3.3. Influence of the carbon source on collaboration between *Mycobacterium* sp. MKAL3 and *Stenotrophomonas* sp. MKAL4

The influence of carbon source complexity on the collaborative relationship in cocultures was investigated using the most synergistic coculture (Coculture J: MKAL3/MKAL in a 3:2 ratio). Growth experiments were recorded in mono- and coculture on carbon sources with increasing

complexity and degradability levels, namely xylose and pretreated wheat straw and results were presented in figure 3. No synergistic relationship was observed in xylose-grown coculture (Figure 3A and Appendix 9). Coculture cell growth was similar to those of respective monocultures. This suggests the dominance of a negative interaction or competition among monocultures when grown on a xylose medium (Deng and Wang, 2016). Published studies support the concept that substrate complexity regulates the type of bacterial interaction (Deng and Wang, 2017; Li et al., 2017; Rafieenia et al., 2018; Tshikantwa et al., 2018; Zheng et al., 2019; Markakiou et al., 2020; Blair et al., 2021; Romero et al., 2021; Xu et al., 2021). For example, Deng and Wang (2017) revealed that reliance on complex carbohydrates reduced bacterial antagonism frequency. They found that growth inhibition among bacteria grown on glucose was twice that of bacteria grown on carboxymethylcellulose-xylan (CMC-xylan). They explained that glucose promoted faster cell growth and antibiotics that inhibit the competing bacteria growth. On the contrary, challenging to break down, CMC and xylan need multiple lignocellulolytic enzymes to make accessible simple sugars. So, bacteria in mixed cultures devote a more significant energy proportion to producing enzymes for substrate degradation and less energy for antibiotic-like component production. There is a strong relationship in pretreated wheat straw-grown coculture, suggesting a collaborative interaction level in the system. This results in increased cell growth from 24 h during the incubation period. Consequently, synergistic bacterial growth depends on carbon source structural complexity and substrate complexity may increase cooperative interactions, including division of labour and reduce the competition for resources (Rafieenia et al., 2022).

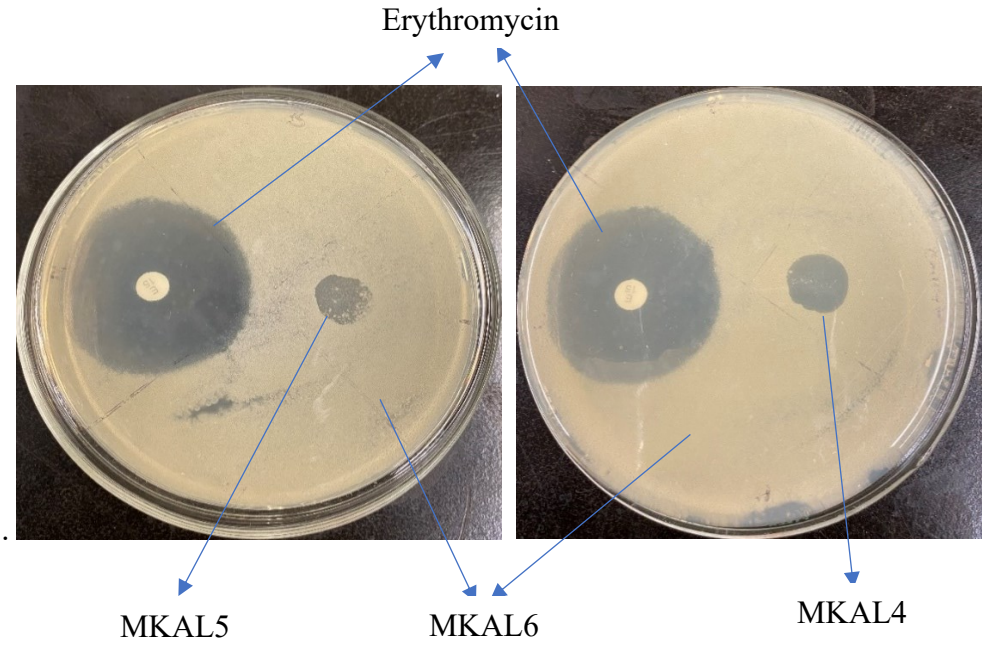

Figure 1. Antagonistic interactions between *Bacillus* sp. MKAL6 and two other strains (*Stenotrophomonas* sp. MKAL4 and *Chryseobacterium* sp. MKAL 5) characterized by inhibition zones.

3.4. Basis of synergism: compounds released

Coculture J was selected to explore the relative mechanism involved in the synergism. Monocultures were treated with collected supernatants of their partner strain under two conditions. First, supernatant donor strains were cultured on pretreated wheat straw and then on xylose. Both partner strains exhibited enhanced cell growth from 24 h when treated with supernatants from the partner strain cultured in pretreated wheat straw. This suggests bacteria in coculture can continue to grow by using metabolites produced by their partners. However, no enhanced growth was observed with strains grown on xylose (Figure 4).

(A)

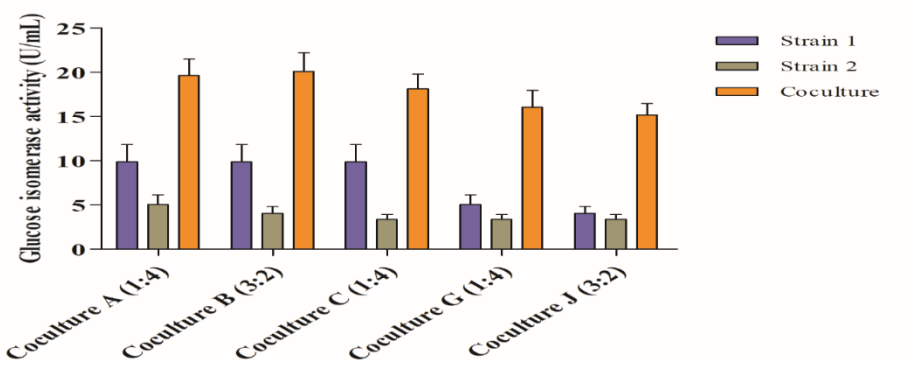

(B)

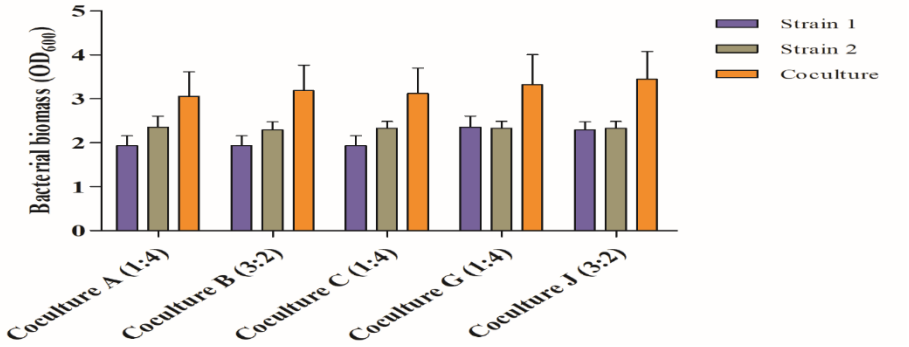

Figure 2. Characterization of synergistic cocultures. (A) Synergistic glucose isomerase production in the supernatant from synergistic cocultures. Only cocultures A (1:4), B (3:2), C (1:4), G (1:4) and J (3:2) showed synergistic enzyme activities. (B) Cell growth after 120 h. Coculture A is a mixture of strains *Paenarthrobacter* sp. MKAL1 and *Hymenobacter* sp. MKAL2 in a 1:4 ratio. Coculture B is a mixture of strains *Paenarthrobacter* sp. MKAL 1 and *Mycobacterium* sp. MKAL3 in a 3:2 ratio. Coculture C is a mixture of strains *Paenarthrobacter* sp. MKAL 1 and *Stenotrophomonas* sp. MKAL4 in a 1:4 ratio. Coculture G is a mixture of strains *Hymenobacter* sp. MKAL2 and *Stenotrophomonas* sp. MKAL4 in a 1:4 ratio and coculture J is a mixture of strains *Mycobacterium* sp. MKAL3 and *Stenotrophomonas* sp. MKAL4 in a 3:2 ratio. Enzyme activity data were recorded at 40°C and pH 8 for 5 days of incubation. Data are shown as mean values from triplicates with corresponding standard error bars

(A) Xylose

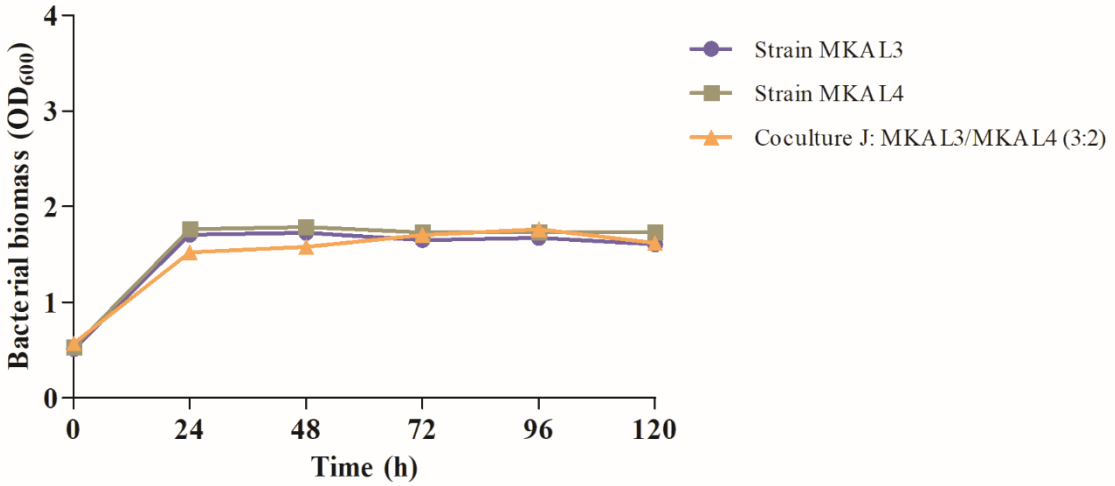

(B) Pretreated wheat straw

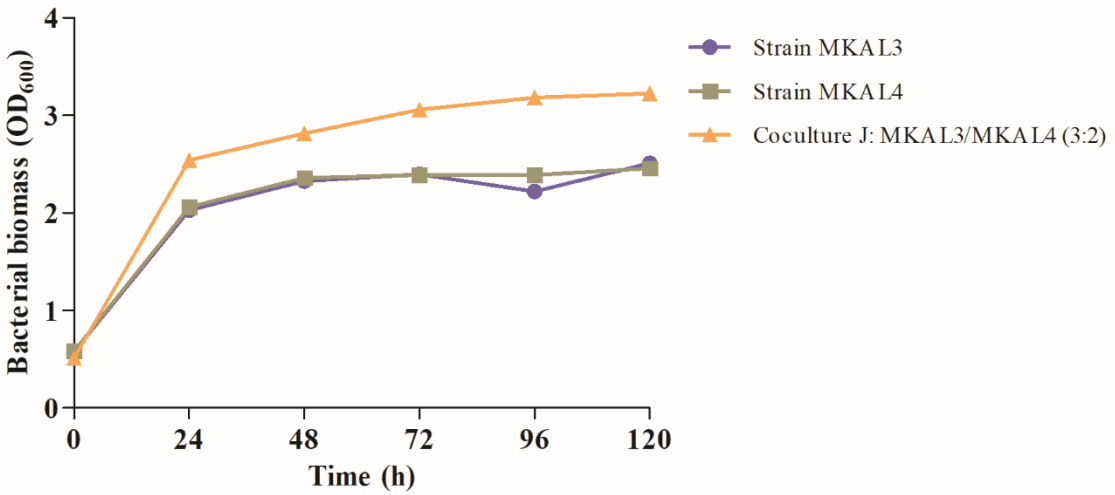

Figure 3. Effect of carbon source complexity on collaborative relationship between the most synergistic bacterial strain pair (*Mycobacterium* sp. MKAL3/*Stenotrophomonas* sp. MKAL4 in a 3:2 ratio). Strains MKAL3 and MKAL4 were grown in monoculture and coculture on 3% carbon sources: xylose (A) and pretreated wheat straw (B).

(A) *Mycobacterium* sp. MKAL3

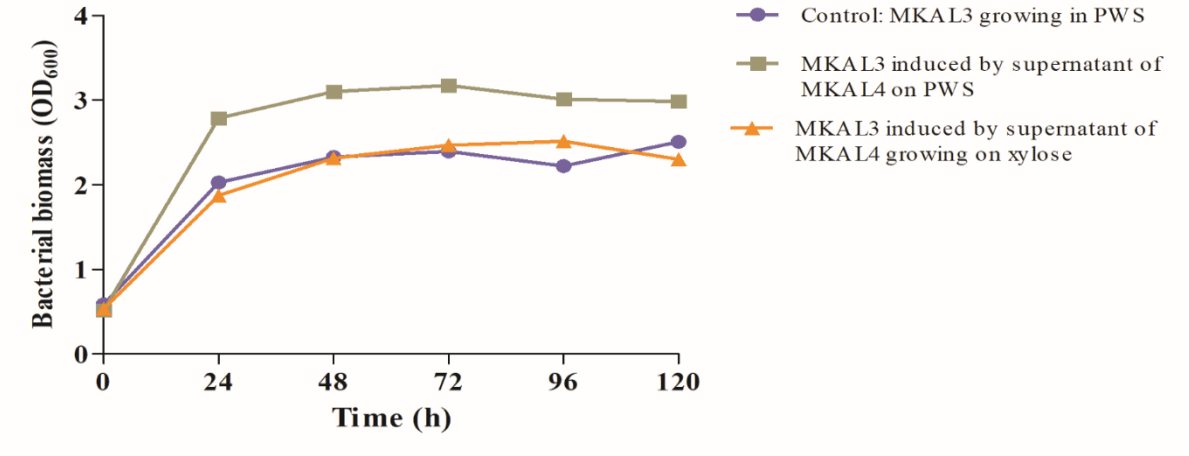

(B) *Stenotrophomonas* sp. MKAL4

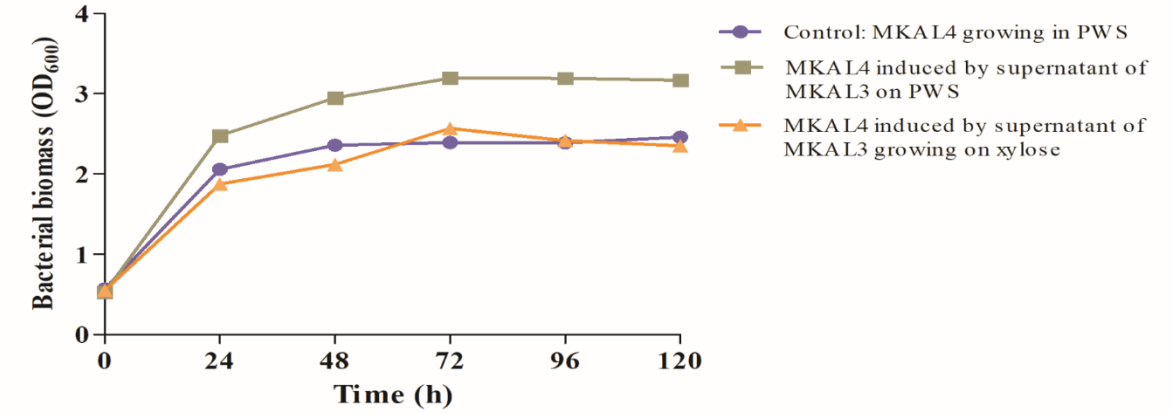

Figure 4. Induction experiment: effect of supernatant from *Mycobacterium* sp. MKAL3 growing on pretreated wheat straw (PWS) or xylose on the growth of *Stenotrophomonas* sp. MKAL4 and vice versa. (A) strain MKAL3 is the recipient while MKAL4 is the donor grown in monoculture on PWS or xylose. (B) strain MKAL4 is the recipient while MKAL3 is the donor grown in monoculture on PWS or xylose.

3.5. Whole-cell immobilization

Overnight strain cultures were immobilized and transferred to the fermentation medium flasks for efficient GI production. The extracellular GI was measured from supernatants at the optimum culture conditions of each strain for 5 days. Immobilized strains exhibited GI production

at different sodium alginate concentrations (Figure 5). Alginate is widely used for cell immobilization because of its non-toxicity and inexpensiveness (Jin et al., 2016). The efficiency of enzyme production in immobilized cells is affected by porosity, gel strength and alginate bead size depending on sodium alginate and calcium chloride concentrations (Zhu, 2007, Jobanputra et al., 2011). Overall, we observed a decrease in enzyme activity below and above a sodium alginate concentration range of 2 to 3%. So, beads with higher sodium alginate concentration decreased enzyme production due to a more robust surface and lower enzyme diffusion. However, beads were so fragile with lower sodium alginate concentrations that most were broken during fermentation. Immobilized strains MKAL1 (10.92 U/mL) and MKAL2 (9.45 U/mL) enhanced enzyme activity at 3% sodium alginate compared to control (9.85 and 8.42 U/mL, respectively). Enzyme productions in immobilized strains MKAL4 (8.50 U/mL) and MKAL5 (9.69 U/mL) were higher than those of free cells (8.01 and 8.92 U/mL, respectively) at 2% sodium alginate. The enhanced GI activity in immobilized strain MKAL3 (12.01 U/mL) was found at 2.5% sodium alginate compared to the control (9.96 U/mL). Cell entrapment provided higher cell density and cellular interaction at these concentrations, creating a favourable environment and increased enzyme production. Similar improved GI production has been reported in the whole-cell immobilization of *Thermus oshimai* (Jia et al., 2018) and *Serratia marcescens* HK2 (Sharma et al., 2021). However, immobilized strain MKAL6 (0-6.21 U/mL) did not improve enzyme activity at all sodium alginate concentrations tested compared to the free cells (11.18 U/mL). Also, cell growth was lower than free cells, suggesting that calcium alginate beads were unsuitable for GI diffusion and production in strain MKAL6.

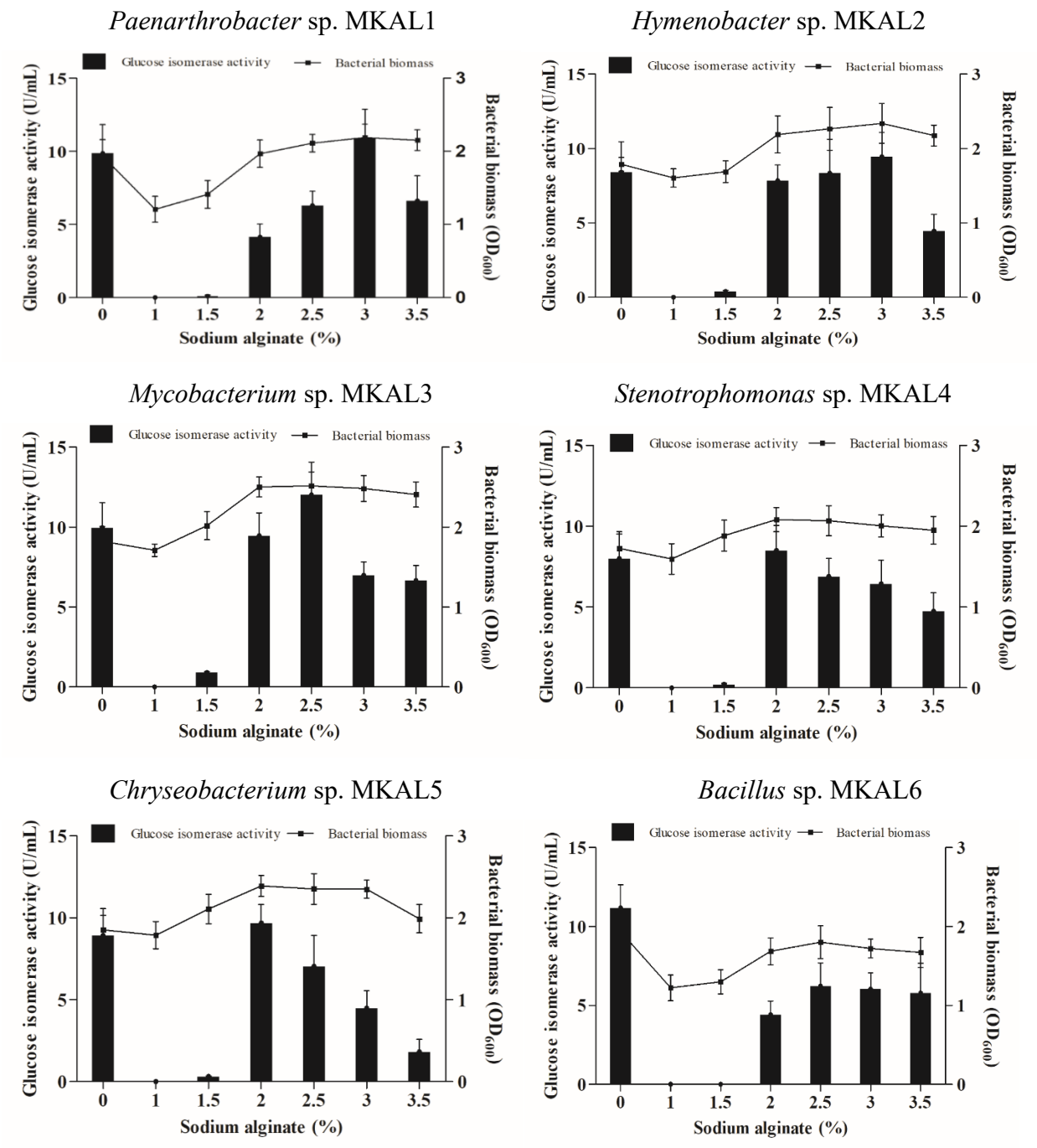

Figure 5. Effect of sodium alginate concentration on glucose isomerase production. 0 % alginate (control) represents free cells in the fermentation medium. Enzyme activity data were recorded at 40°C and pH 8 for 5 days of incubation. Data are shown as mean values from triplicates with corresponding standard error bars

4. Conclusions

This study investigated the coculturing and whole-cell immobilization effect of cellulolytic soil bacteria (*Paenarthrobacter* sp. MKAL1, *Hymenobacter* sp. MKAL2, *Mycobacterium* sp. MKAL3, *Stenotrophomonas* sp. MKAL4, *Chryseobacterium* sp. MKAL5 and *Bacillus* sp. MKAL6) for improved glucose isomerase production from wheat straw. Cocultures A, B, C, G and J enhanced performance over respective monocultures for glucose isomerase production. These cocultures showed cell growth synergism depending on the substrate complexity. When used as a carbon source, the bacterial partners in cocultures interacted synergistically to degrade wheat straw (complex substrate). However, they competed when xylose was used, resulting in antagonistic interaction predominance. The basis of synergism would be compounds released from each bacterial partner. Additional investigations are required because it's unclear how bacterial partners contribute to the coculture. A partner could produce enzymes that degrade specific compounds of wheat straw, while another one could produce stimulatory exudates or quorum-sensing molecules that coordinate bacterial interactions. The studies on the division of labour (relationship between substrate chemical complexity and bacterial enzymes produced by each partner) will help better understand the mechanism. Also, immobilized strains MKAL1, MKAL2 (3% sodium alginate), MKAL3 (2.5% sodium alginate), MKAL4 and MKAL5 (2% sodium alginate) improved enzyme production in the wheat straw fermentation process. The immobilization studies of purified glucose isomerases for hydrolysis and saccharification of wheat straw are being studied.

5. References

Anisha GS, Prema P (2008). Cell immobilization technique for the enhanced production of α-galactosidase by *Streptomyces griseoloalbus*. *Bioresour Technol*, 99, 3325-3330.

Blair EM, Dickson KL, O'Malley MA (2021). Microbial communities and their enzymes facilitate degradation of recalcitrant polymers in anaerobic digestion. *Curr Opin Microbiol*, 64, 100-108.

Brémond U, Bertrandias A, Hamelin J, Milferstedt K, Bru-Adan V, Steyer J-P, Bernet N, Carrere H (2022). Screening and application of ligninolytic microbial consortia to enhance aerobic degradation of solid digestate. *Microorganisms*, 10, 277.

Burkholder PR, Pfister RM, Leitz FH (1966). Production of a pyrrole antibiotic by a marine bacterium1. *Appl Microbiol*, 14, 649-653.

Chhetri G, Kim I, Kim J, So Y, Seo T (2022). *Chryseobacterium tagetis* sp. nov., a plant growth promoting bacterium with an antimicrobial activity isolated from the roots of medicinal plant (Tagetes patula). *J Antibiot*, 75, 312-320.

Cortes-Tolalpa L, Norder J, van Elsas JD, Salles JF (2018). Halotolerant microbial consortia able to degrade highly recalcitrant plant biomass substrate. *Appl Microbiol Biotechnol*, 102, 2913-2927.

Cortes-Tolalpa L, Salles JF, van Elsas JD (2017) Bacterial synergism in lignocellulose biomass degradation – complementary roles of degraders as influenced by complexity of the carbon source. *Front Microbiol*, 8, 1628.

Dahal RH, Chaudhary DK, Kim DU, Pandey RP, Kim J (2021). *Chryseobacterium antibioticum* sp. nov. with antimicrobial activity against Gram-negative bacteria, isolated from Arctic soil. *J Antibiot (Tokyo)*, 74, 115-123.

Deng YJ, Wang SY (2016). Synergistic growth in bacteria depends on substrate complexity. *J Microbiol*, 54, 23-30.

Deng YJ, Wang SY (2017). Complex carbohydrates reduce the frequency of antagonistic interactions among bacteria degrading cellulose and xylan. *FEMS Microbiol Lett*, 364.

Domínguez-Robles J, Sánchez R, Díaz-Carrasco P, Espinosa E, García-Domínguez M, Rodríguez A (2017). Isolation and characterization of lignins from wheat straw: Application as binder in lithium batteries. *Int J Biol Macromol*, 104, 909-918.

Efimenko TA, Malanicheva IA, Vasil'eva BF, Glukhova AA, Sumarukova IG, Boikova YV, Malkina ND, Terekhova LP, Efremenkova OV (2016). Antibiotic activity of bacterial endobionts of basidiomycete fruit bodies. *Microbiology*, 85, 752-758.

Jia DX, Wang T, Liu ZJ, Jin LQ, Li JJ, Liao CJ, Chen DS, Zheng YG (2018). Whole cell immobilization of refractory glucose isomerase using tris(hydroxymethyl)phosphine as crosslinker for preparation of high fructose corn syrup at elevated temperature. *J Biosci Bioeng*, 126:176-182.

Jin YY, Li YD, Sun W, Fan S, Feng XZ, Wang KY, He WQ, Yang ZY (2016). The whole-cell immobilization of D-hydantoinase-engineered Escherichia coli for D-CpHPG biosynthesis. *Electron J Biotechnol*, 19, 43-48.

Jobanputra AH, Karode BA, Chincholkar SB (2011). Calcium alginate as supporting material for the immobilization of rifamycin oxidase from *Chryseobacterium* species. *Biotechnol Bioinf Bioeng*, 1, 529-535.

Kabaivanova L, Hubenov V, Dimitrova L, Simeonov I, Wang H, Petrova P (2022). Archaeal and bacterial content in a two-stage anaerobic system for efficient energy production from agricultural wastes. *Molecules*, 27, 1512.

Kong X, Du J, Ye X, Xi Y, Jin H, Zhang M, Guo D (2018). Enhanced methane production from wheat straw with the assistance of lignocellulolytic microbial consortium TC-5. *Bioresour Technol*, 263, 33-39.

Kumaravel V, Gopal SR (2010). Immobilization of *Bacillus amyloliquefaciens* MBL27 cells for enhanced antimicrobial protein production using calcium alginate beads. *Biotechnol Appl Biochem*, 57, 97-103.

Lazuka A, Auer L, O'Donohue M, Hernandez-Raquet G (2018). Anaerobic lignocellulolytic microbial consortium derived from termite gut: enrichment, lignocellulose degradation and community dynamics. *Biotechnol Biofuels*, 11, 284.

Lee SE, Lee HY, Jung KH (2013). Production of chlorphenesin galactoside by whole cells of β-galactosidase containing *Escherichia coli*. *J Microbiol Biotechnol*, 23, 826-832.

Li X, Meng D, Li J, Yin H, Liu H, Liu X, Cheng C, Xiao Y, Liu Z, Yan M (2017). Response of soil microbial communities and microbial interactions to long-term heavy metal contamination. *Environ Pollut*, 231, 908-917.

Lou WY, Fernández-Lucas J, Ge J, Wu C (2021). Editorial: Enzyme or whole cell immobilization for efficient biocatalysis: Focusing on novel supporting platforms and immobilization techniques. *Front Bioeng Biotechnol*, 9, 620292.

Lozano FJ, Lozano R (2018). Assessing the potential sustainability benefits of agricultural residues: Biomass conversion to syngas for energy generation or to chemicals production. *J Clean Prod*, 172, 4162-4169.

Markakiou S, Gaspar P, Johansen E, Zeidan AA, Neves AR (2020). Harnessing the metabolic potential of *Streptococcus thermophilus* for new biotechnological applications. *Curr Opin Biotechnol*, 61,142-152.

Rafieenia R, Atkinson E, Ledesma-Amaro R (2022). Division of labor for substrate utilization in natural and synthetic microbial communities. *Curr Opin Biotechnol*, 75, 102706.

Rafieenia R, Pivato A, Lavagnolo MC (2018). Effect of inoculum pretreatment on mesophilic hydrogen and methane production from food waste using two-stage anaerobic digestion. *Int J Hydrogen Energy*, 43, 12013-12022.

Romero MAD, Yao T, Chen M-H, Oles RE, Lindemann SR (2021). Fine carbohydrate structure governs the structure and function of human gut microbiota independently of variation in glycosyl residue composition. *bioRxiv*, 2021.

Ruiz HA, Cerqueira MA, Silva HD, Rodríguez-Jasso RM, Vicente AA, Teixeira JA (2013). Biorefinery valorization of autohydrolysis wheat straw hemicellulose to be applied in a polymer-blend film. *Carbohydr Polym*, 92, 2154-2162.

Sarkar D, Nanda S, Poddar K, Sarkar A (2021). Isolation and characterization of an antibacterial compound producing *Stenotrophomonas* strain from sewage water, production optimization, and its antibiotic potential evaluation. *Environmental Quality Management*, 1– 12.

Serrano L, Rincón E, García A, Rodríguez J, Briones R (2020). Biodegradable polyurethane foams produced by liquefied polyol from wheat straw biomass. *Polymers*, 12, 2646.

Sharma HK, Xu C, Qin, W (2021). Isolation of bacterial strain with xylanase and xylose/glucose isomerase (GI) activity and whole cell immobilization for improved enzyme production. *Waste Biomass Valor*, 12, 833-845.

Tomás-Pejó E, Fermoso J, Herrador E, Hernando H, Jiménez-Sánchez S, Ballesteros M, González-Fernández C, Serrano D (2017). Valorization of steam-exploded wheat straw through a biorefinery approach: Bioethanol and bio-oil co-production. *Fuel*, 199, 403-412.

Tshikantwa TS, Ullah MW, He F, Yang G (2018). Current trends and potential applications of microbial interactions for human welfare. *Front Microbiol*, 9.

Tsumura N, Sato T (1965). Enzymatic conversion of D-glucose to D-fructose part V: partial purifcation and properties of the enzyme from *Aerobacter cloacae*. *Agric Biol Chem*, 29, 1123-1128.

Van Dyk JS, Gama R, Morrison D, Swart S, Pletschke BI (2013). Food processing waste: problems, current management and prospects for utilisation of the lignocellulose component through enzyme synergistic degradation. *Renew Sustain Energy Rev*, 26, 521-531.

Xu Z, Lu Z, Soteyome T, Ye Y, Huang T, Liu J, Harro JM, Kjellerup BV, Peters BM (2021). Polymicrobial interaction between *Lactobacillus* and *Saccharomyces cerevisiae*: coexistence relevant mechanisms. *Crit Rev Microbiol*, 47, 386-396.

Zheng H, Perreau J, Powell JE, Han B, Zhang Z, Kwong WK, Tringe SG, Moran NA (2019). Division of labor in honey bee gut microbiota for plant polysaccharide digestion. *Proc Natl Acad Sci U S A*, 116, 25909-25916.

Zhu Y (2007). Immobilized cell fermentation for production of chemicals and fuels. In: Bioprocessing for Value-Added Products from Renewable Resources, Elsevier, pp. 373-396.

CHAPTER 5

Soil lignocellulolytic bacteria: Characterization through putative virulence factors, antibiotics and heavy metals resistance, solvent adhesion and biofilm-forming capabilities

Aristide Laurel Mokale Kognou[1], Chonlong Chio[1], Janak Raj Khatiwada[1], Sarita Shrestha[1], Xuantong Chen[1], Yuen Zhu[2], Rosalie Anne Ngono Ngane[3], Gabriel Agbor Agbor[4], Zi-Hua Jiang[5], Chunbao (Charles) Xu[6], Wensheng Qin[1]

[1]Department of Biology, Lakehead University, Thunder Bay, Ontario, Canada

[2]School of Environment and Resources, Shanxi University, Taiyuan, China

[3]Department of Biochemistry, Faculty of Science, The University of Douala, Douala, Cameroon

[4]Centre for Research on Medicinal Plants and Traditional Medicine, Institute of Medical Research and Medicinal Plants Studies Cameroon, Yaounde, Cameroon

[5]Department of Chemistry, Lakehead University, Thunder Bay, Ontario, Canada

[6]Department of Chemical and Biochemical Engineering, Western University, London, Ontario, Canada

*Corresponding author: Wensheng Qin

Abstract

Soil bacteria participate in self-immobilization processes for survival in crucial parameters such as autoaggregation, cell surface hydrophobicity, biofilm formation, and antibiotic and heavy metal resistance. This study investigated putative virulence factors, antibiotics and heavy metals resistance, solvent adhesion, and biofilm-forming capabilities of six cellulolytic bacteria isolated

from soil samples: *Paenarthrobacter* sp. MKAL1, *Hymenobacter* sp. MKAL2, *Mycobacterium* sp. MKAL3, *Stenotrophomonas* sp. MKAL4, *Chryseobacterium* sp. MKAL5 and *Bacillus* sp. MKAL6. Strains were subjected to the phenotypic methods including heavy metal and antibiotic susceptibility and virulence factors (protease, lipase, capsule production, autoaggregation, hydrophobicity and biofilm formation). The action mechanism of ciprofloxacin was also investigated against strains. Strains MKAL2, MKAL5 and MKAL6 exhibited proteolytic and lipase activities, while only MKAL6 produced capsules. All strains were capable of aggregating, forming biofilm and adhering to solvents. They accumulated chromium, lead, zinc, nickel and manganese and were resistant to lincomycin. Ciprofloxacin exhibited bactericidal activity against these strains. This study showed that some strains exhibited phenotypic virulence factors. Further in-depth genetic studies of virulence, antibiotic and heavy metal resistance genes of these bacteria are required and currently underway in our lab.

Keywords: cellulolytic bacteria, virulence factors, antibiotic susceptibility, heavy metal susceptibility, action mechanism

1. Introduction

Bacteria grow in the soil systems as aggregates but rarely live as planktonic cells (Rumbaugh and Sauer 2020). However, they participate in self-immobilization processes in crucial parameters are autoaggregation, cell surface hydrophobicity, biofilm formation, and antibiotic and heavy metal resistance (Ning et al., 2021).

In autoaggregation, bacteria (same type) form multicellular clumps, generally mediated by self-recognizing surface structures such as exopolysaccharides and proteins. This phenomenon

protects bacteria against environmental stresses (oxygen availability and temperature change) or host responses (Trunk et al., 2018). A surface-attached community of bacterial cells embedded in a self-produced polymeric matrix including polysaccharides, extracellular DNA, proteins and lipids are often among the first steps in forming biofilms. (Wolska et al., 2016). This matrix is central to biofilm structure and integrity and is a shield protector for cells inside biofilms. Biofilms can form on biotic and abiotic surfaces and liquid-air interfaces in several stages beginning with an initial attachment depending on attractive and repulsive forces (electrostatic and hydrophobic interactions) between the microorganism and the contact surface; followed by bacterial division and extracellular matrix production, and, finally, matrix disassembly and bacteria dispersion. It also requires motility property generated by flagella for movement and direction (Penesyan et al., 2020). Cell hydrophobicity can influence the bacterial adhesion propensity depending on the surface type. More hydrophobic cells adhere more strongly to hydrophobic cells while hydrophilic cells firmly adhere to hydrophilic surfaces (Mirani et al., 2018). Biofilm is one of the significant causes for increased bacterial resistance to various heavy metals and antibiotics. These resistance abilities are sometime encoded in their plasmid genes facilitating the transfer of toxic metal resistance from one cell to another. (Lodha et al., 2022).

Derived from natural products, several antibiotics are found in environmental ecosystems. Therefore, bacteria have adapted through strategies to overcome toxic antibiotic effects. Also, bacteria have used them as signals for developing physiological responses, which provide them with an ecological advantage by increasing their survival (Penesyan et al., 2020, Shin et al., 2021).

The presence of heavy metal in the wastes induces heavy metal-resistant soil bacteria to emerge. This bacterial resistance is attributed to detoxifying mechanisms developed by resistant bacteria (exopolysaccharide complexation, metal reduction, metal efflux and binding with

bacterial cell envelope) (Masindi and Muedi, 2018). Multiple metal tolerances are typical among heavy metal-resistant bacteria because heavy metals are all similar in their toxic mechanism (Presentato et al., 2020). Heavy metal-resistant bacteria can be potential agents for the bioremediation of heavy metal pollution (Alotaibi et al., 2021).

While bacteria have developed strategies to better survive in their environment, they can become more harmful to humans in infection development and lead to higher medical costs, prolonged hospital stays, and increased mortality rates (Mogrovejo et al., 2020). Bacteria can produce various virulence factors, mainly depending on environmental conditions. In such circumstances, they exhibit their pathogenicity through several mechanisms such as (1) contribution of pili/flagella/fimbrial/adhesins to adherence, autoaggregation, biotic and abiotic surface colonization; (2) role of outer membrane lipopolysaccharide (LPS) in biofilm formation, resistance to antibiotics and heavy metals and complement-mediated cell killing; (3) role of diffusible signal factor in quorum sensing that mediates extracellular enzyme production, LPS synthesis, microcolony formation, antibiotic and heavy metal tolerance; and (4) extracellular enzyme production (protease, esterase, DNase, RNase, lipase, hemolysin, gelatinase and fibrinolysin) (Abbott et al., 2011; Brooke, 2012; Kalidasan et al., 2018, Odeyemi and Sani, 2019; Rhen, 2019). Therefore, this study investigated putative virulence factors, antibiotics and heavy metals resistance, solvent adhesion and biofilm-forming capabilities of six cellulolytic bacteria isolated from soil samples. The mechanism action of ciprofloxacin against these bacteria was also studied.

2. Materials and Methods

2.1. Microorganisms

Six bacterial isolates with cellulolytic properties (cellulase and glucose isomerase activities) were characterized from soil samples collected from Kingfisher Lake and the University of Manitoba campus. These isolates were identified as *Paenathrobacter* sp. MKAL1, *Hymenobacter* sp. MKAL2, *Mycobacterium* sp. MKAL3, *Stenotrophomonas* sp. MKAL4, *Chryseobacterium* sp. MKAL5 and *Bacillus* sp. MKAL6 with the NCBI accession numbers ON442553, ON442554, ON442555, ON442556, ON442557 and ON442558 respectively. Bacteria were maintained in Tryptic soy broth (TSB) at 30ºC for subsequent tests.

2.2. Hemolysin, protease and lipase production

Hemolytic, proteolytic and lipase activities were screened using blood agar, skim milk agar and tween80 agar, respectively (Vranova et al., 2013; Ahmed et al., 2010). Overnight bacterial cultures were inoculated on blood agar, skim milk agar and tween80 agar in sterile Petri dishes, then allowed to solidify and incubated at 30ºC for 48 h. After incubation, a clear zone of hydrolysis around bacterial isolate indicated the presence of proteolytic and lipase activities. A greenish-grey or brownish discoloration around the colony revealed α-hemolysis (α-hemolysin production), while the clear zone appearance around the colony showed β-hemolysis (β-hemolysin production). The absence of coloration change or zone appearance indicated γ-hemolysin production (no cell blood lysis).

2.3. Capsule production

Screening for capsule production was performed using Congo red agar (36 g sucrose, 0.8g Congo red in 1 L of tryptic soy agar supplemented with 1% NaCl) (Lamari et al., 2018). Overnight bacterial cultures were inoculated on Congo red agar Petri dishes and incubated at 30ºC for 24 h. After incubation, black colonies were capsule producers, while red colonies were non-capsule producers.

2.4. Autoaggregration capacity

Autoaggregation assay was performed according to Escamilla-Montes et al. (2015). Overnight bacterial cultures were collected, centrifuged at 5000×g for 15 min, washed twice, and suspended in phosphate-buffered saline (PBS, pH 7.4). Cell density was adjusted to the optical density of 0.55-0.60 at 600 nm (A_0). Bacterial cell suspensions (4 mL) were mixed by vortexing for 10 s and incubated at room temperature for 24 h. After 3, 6 and 24 h, 0.1 mL of the upper suspension was transferred to another 3.9 mL of PBS and absorbance was measured at 600 nm. PBS was used as a blank.

Autoaggregation (%) = $1 - (A_t/A_0) \times 100$, where A_t represented the absorbance at time t = 3, 6 or 24 h and A_0 the absorbance at t = 0.

2.5. Adhesion to solvents

Bacterial adherence to hydrocarbons (BATH) test was used to assess the bacterial hydrophobicity (Borghi et al., 2011). This test analyzed microbial linkage to n-octane (apolar solvent), chloroform (polar acid solvent) and ethyl acetate (basic polar solvent). Bacterial strains

were grown in TSB at 30ºC for 24 h. The bacterial culture was centrifuged at 5000 rpm for 15 min, the supernatant discarded, and pellets washed twice with PBS (pH 7.4). The density of cells was adjusted to the optical density of 0.55-0.60 at 600 nm (A_0). The test mixture was composed of cell suspension (4 mL) and 1 mL of n-octane, chloroform, and ethyl acetate in individual glass tubes and then vortexed for 1 min. The mixture was decanted into two phases at room temperature for 30 min. The supernatant was discarded, and absorbance was read at 600 nm (A_1). Hydrophobicity ability was estimated according to the formula:

Hydrophobicity (%) = $(A_0 - A_1)/A0 \times 100$, and isolate is classified into three categories: Not hydrophobic (< 20%), Moderate (20-50%), and strong (> 50%).

2.6. Resistance to heavy metals

Resistance of the isolates to heavy metals (Co^{2+}, Cd^{2+}, Cr^{3+}, Zn^{2+}, Hg^{2+}, Cu^{2+}, Mn^{2+}, Ni^{2+}, Ba^{2+} and Pb^{2+}) were carried out by inoculating overnight bacterial culture on Tryptic soy agar Petri dishes containing various concentrations of metal (50, 150, 300, 450, 600 and 750 µg/mL) (Marzan et al., 2017). Visible growth of isolates was observed for 24 and 48 h at 30ºC. Minimum inhibitory concentration (MIC) was noted as the lowest concentration that inhibited bacterial growth.

2.7. Biofilm-forming capacity

The biofilm-forming capacity of bacterial strains was carried out by adhesion to polystyrene (Chaieb et al., 2011). Isolates were grown in TSB at 30ºC and then diluted to 1:100 w/v (in TSB with 2% glucose). Aliquots of cell suspensions (200 µL) were transferred to 96-well microtiter plates and incubated at 35ºC for 24 h. Plates were washed twice with PBS and dried.

The well with sterile TSB alone was used as a control. Adherent strains were fixed with ethanol (95%) and stained with 100 µL crystal violet (1% w/v) solution for 5 min. Microplates were washed and air-dried. Biofilm forming ability was measured at 570 nm. The experiment was done in triplicate. Biofilm formation was interpreted as follows: Highly positive ($OD570 \geq 1$), moderately to weakly positive ($0.1 \leq OD570 < 1$), or negative ($OD570 \leq 0.1$).

2.8. Resistance to antibiotics

2.8.1. Agar-Well Diffusion Method

The bacterial susceptibility to antibiotics was investigated by determining the diameter of inhibition zones using the agar disc diffusion method (CLSI, 2008). Bacterial cell suspensions were prepared at 1.5×10^8 colony-forming units per mL (CFU/mL) corresponding to the McFarland 0.5 turbidity standard and then were seeded onto Mueller-Hinton agar (MHA) Petri dishes. Antibiotic discs were dropped on the surface of MHA plates and diffused for 15 min before incubation at 35º C for 24 h. Antibiotics tested were ampicillin (10 µg), novobiocin (30 µg), bacitracin, tetracycline (30 µg), erythromycin (15 µg), chloramphenicol (30 µg), penicillin (10 units), hygromycin B (50 µg), lincomycin (15 µg), phleomycin (50 µg), kanamycin (30 µg), trimethoprim (15 µg), and ciprofloxacin (15 µg). Dishes without antibiotics were used as blank.

2.8.2. Broth Microdilution Method

The bacterial sensibility to antibiotics was also carried out by determining minimum inhibitory concentrations (MICs) using Mueller Hinton Broth (MHB) by microdilution method (CLSI, 2008). A two-fold dilution of antibiotics (v/v medium, inoculum and water-soluble

antibiotics) and negative control (v/v medium and inoculum) were included. Each well of a 96-well sterile microtiter plate received MHB (100 µL), antibiotic (100 µL) and bacterial inoculum (1.5×10^8 CFU/mL) and plates were covered and incubated at 35ºC for 24 h. After incubation, 50 µL of aqueous p-iodonitrotetrazolium violet (INT, bacterial growth indicator) were added to the wells and incubated for 30 min. The MIC value was considered the lowest concentration of antibiotics that completely inhibited cell growth (when the solution remained clear in the well after incubation with INT). Ampicillin, chloramphenicol, ciprofloxacin, trimethoprim, kanamycin, and lincomycin were used at a concentration ranging between 128 and 1 µg/mL. MIC values were used to investigate the relative action mechanisms of antibiotics on bacterial isolates.

2.9. Action mechanisms of antibiotics on bacterial isolates

Ciprofloxacin (most active) was used for action mechanism studies against bacterial isolates.

2.9.1. Time-kill kinetic assay

The antimicrobial efficacy testing was performed to evaluate the inhibitory effect of ciprofloxacin over time (Tsuji et al., 2008). Concentrations of ciprofloxacin equal to MIC, 2MIC and 4MIC were prepared and transferred in test tubes containing MHB. Bacterial inoculum adjusted to 5×10^6 CFU/mL was added, and tubes were incubated at 35ºC. Aliquots of medium (1 mL) were collected at 0, 2, 4, 6, 12, 24 h, streaked aseptically into MHA Petri dishes and incubated at 35ºC for 24 h. A control test was carried out without the antibiotic. The number of viable organisms was counted as colony-forming units (CFU). Graphs of the log CFU/mL were plotted against time.

2.9.2. Action on cell membrane integrity: measurement of intracellular components (DNA/RNA)

The effect of ciprofloxacin on cell membrane integrity was conducted using the protocol described by Devi et al. (2010). Overnight bacterial cultures were centrifuged (5000xg, 15 min), and the supernatant was discarded. Pellets were washed twice using sterile distilled water and then suspended in PBS (pH 7.4) to obtain a cell density of 0.55-0.60 at 600 nm. Different concentrations of ciprofloxacin (MIC and 4MIC) were added to cell suspensions. Cell suspensions without antibiotic treatment were used as negative controls. All samples were incubated at 35ºC for 1 h under agitation (200 rpm). Experiments were done in triplicate. After incubation, samples were centrifuged (12,000xg, 15 min) and supernatants were read at 260 nm. Recordings were expressed as percentages of the extracellular UV-absorbing materials released by cells.

2.9.3. Action on membrane permeability

The effect of ciprofloxacin on membrane permeability was investigated using crystal violet according to the method described by Devi et al. (2010). Overnight bacterial cultures were centrifuged (5000xg, 15 min), and the supernatant was discarded. Pellets were washed twice using sterile distilled water and then suspended in PBS (pH 7.4) to obtain a cells density of 0.55-0.60 at 600 nm. Cell suspensions were treated with ciprofloxacin (MIC and 4MIC) followed by incubation at 35ºC for 30 min. Likewise, control samples were prepared similarly without antibiotic treatment. After incubation, samples were centrifuged, and cells resuspended in PBS containing crystal violet (10 µg/mL). Cell suspensions were incubated again for 10 min at 35ºC, followed by centrifugation (12,000xg, 15 min), and supernatants were measured at 590 nm. The percentage of crystal violet (CV) uptake of samples was calculated using the following formula:

CV uptake (%) = [OD value of the sample/OD value of crystal violet solution] × 100

2.9.4. Action on biofilm formation

The effect of ciprofloxacin on biofilm formation was performed using 96-well microtitre plates by crystal violet method (Nowak et al., 2015). A two-fold dilution of the antibiotic from 8MIC to 1/16 MIC (v/v TSB, inoculum and water-soluble antibiotic), growth control (v/v TSB and inoculum) and media control (only TSB) were included. Plates were incubated at 35ºC for 24 h. Upon well content was discarded, wells were washed with PBS (pH 7.4) and stained with 1% (w/v) crystal violet, followed by incubation at room temperature for 20 min. Biofilms were fixed with 30% (v/v) acetic acid (200 µL) and read at 595 nm. The percentage of biofilm inhibition was calculated using the following formula:

Biofilm inhibition (%) = [OD growth control − OD sample/OD growth control] × 100

2.10. Statistical analysis

All experiments were performed in triplicate. Data were expressed as mean±SD. Statistical analysis was carried out using one-way analysis of variance (ANOVA) followed by Student-Newman-Keuls Multiple comparison tests using GraphPad Prism 5 Windows software. Differences between values were considered significant at $p < 0.05$.

3. Results and Discussion

3.1. Screening for protease lipase, hemolysin and capsule production

Among the six bacterial isolates studied, only Bacillus sp. produced capsules (Table 1). Some investigators revealed capsules produced by *Bacillus* strains such as *Bacillus cereus*, *Bacillus anthracis* and *Bacillus* spp. (Beesley et al., 2010; Baldwin, 2020). Most capsules function in microbial pathogenesis by protecting the microbe against host immune mechanisms, although the capsular structures can serve as adhesins for some. *Hymenobacter* sp., *Mycobacterium* sp., *Chryseobacterium* sp. and *Bacillus* sp. exhibited proteolytic activities. *Hymenobacter* sp., *Chryseobacterium* sp. and *Bacillus* sp. showed lipase activity. Many strains of *Bacillus* (*Bacillus cereus*, *Bacillus* spp., *Bacillus* sp. AM1, *Bacillus methylotrophicus* PS3), *Chryseobacterium* (*Chryseobacterium polytrichastri* ERMR1:04, *Chryseobacterium schmidteae*, *Chryseobacterium gleum*, *Chryseobacterium aquifrigidense* FANN1), *Hymenobacter* (*Hymenobacter setariae* sp. nov.) and *Mycobacterium* (*Mycobacterium smegmatis* and *Mycobacterium tuberculosis*) exhibited lipase (Sharma et al., 2017; Hassan et al., 2018; Chhetri et al., 2020; Shart and Elkhalil, 2020; Kumar et al., 2020; Kangale et al., 2021; López-Moreno et al., 2021) and protease (Matsui et al., 2017; Marizcurrena et al., 2019; Nagpal et al., 2019; Danilova and Sharipova, 2020; Babin et al., 2021; Bokveld et al., 2021; Aktayeva et al., 2022) activities. No hemolytic properties were observed (Table 1). However, previous studies on hemolytic activities of *Bacillus* (Dabiré et al., 2022), *Chryseobacterium* (Sud et al., 2020), *Mycobacterium* (Augenstreich et al., 2020) and *Stenotrophomonas* genera (Peters et al., 2020) were reported. *Bacillus* sp. MKAL6 exhibited gelatinase and DNase activities.

3.2. Autoaggregation

The autoaggregation ability of bacterial isolates tested increased with incubation time (Figure 1). The aggregation potential increased from 31.09-56.36%, 26.18-59.95%, 33.30-58.87%, 21.11-53.16%, 18.13-46.30% and 29.11-55.11% for *Bacillus* sp. MKAL6, *Hymenobacter* sp. MKAL2, *Chryseobacterium* sp. MKAL5, *Paenarthrobacter* sp. MKAL1, *Mycobacterium* sp. MKAL3 and *Stenotrophomonas* sp. MKAL4, respectively. *Hymenobacter* sp. showed the highest auto-aggregation potential (59.95%) at 24 h, while *Mycobacterium* sp. showed the lowest ability (46.30%). Similarly, Nwagu et al. (2020) reported about 53.37% of autoaggregation in *Bacillus cereus* KY746353.1. isolated from *Parkia biglobosa* (traditional fermented African locust bean seeds). However, the autoaggregation ability of *Bacillus subtilis* P223 isolated from Kimichi (Korean food) was 93.42% after 24 h of incubation (Jeon et al., 2017). Manhar et al. (2015) reported the highest autoaggregation potential of *Bacillus amyloliquefaciens* AMS1 isolated from traditional fermented soybean (Churpi) was 75.5% after 24 h. Benladghem et al. (2020) revealed that *Stenotrophomonas maltophilia* had a low capacity to form cellular aggregates (26.13%) after 24 h. Both environmental and pathogenic bacteria have autoaggregation ability mediated by self-recognising surface structures (proteins and exopolysaccharides). This potential provides a gateway to colonizing abiotic and biotic surfaces. Depending on bacterial species, the autoaggregation phenotype may be constitutive or induced under some conditions (stress oxygen availability or a temperature change) (Nath et al., 2020).

Table 1. Capsule, protease and lipase production of bacterial isolates.

Isolates	Capsule production		Protease production	Lipase production	Hemolysis
	Phenotypes	Index			
Paenarthrobacter sp. MKAL1	Pinkish red	Capsule non-producer	-	-	-
Hymenobacter sp. MKAL2	Pinkish red	Capsule non-producer	+	+	-
Mycobacterium sp. MKAL3	Pinkish red	Capsule non-producer	+	-	-
Stenotrophomonas sp. MKAL4	Pinkish red	Capsule non-producer	-	-	-
Chryseobacterium sp. MKAL5	Pinkish red	Capsule non-producer	+	+	-
Bacillus sp. MKAL6	Black	Capsule producer	+	+	-

Black colony : capsule production; Pinkish red colony : no capsule production; +: production/hemolysis; - : no production/no hemolysis.

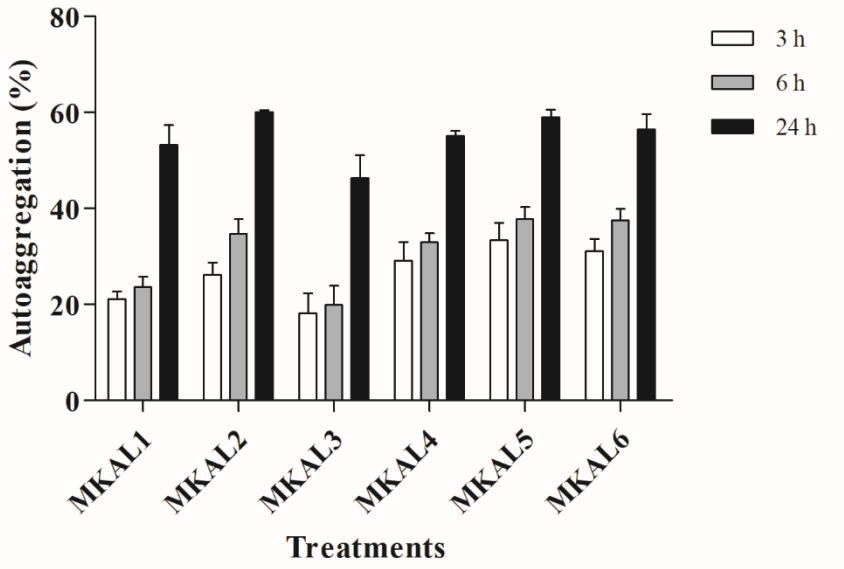

Figure 1. Quantitative estimation autoaggregation of *Paenarthrobacter* sp. MKAL1, *Hymenobacter* sp. MKAL2, *Mycobacterium* sp. MKAL3, *Stenotrophomonas* sp. MKAL4, *Chryseobacterium* sp. MKAL5 and *Bacillus* sp. MKAL6.

3.3. Adhesion to solvents

Cell surface hydrophobicity of bacterial isolates was characterized by BATH assay. This test analyzed microbial linkage to n-octane (apolar solvent), chloroform (polar acid solvent) and ethyl acetate (basic polar solvent). Hydrophobic cell surface showed adherence to n-octane (6.66-31.08%), chloroform (19.88-45.58%), and ethyl acetate (8.57-58.16%) (Figure 2). The cell hydrophobicity varied with the isolates tested. The differences in affinity may be due to the capsular material, appendages on the cell surface or composition and content of different lipopolysaccharides (Ning et al., 2021). The hydrophobicity ability of *Bacillus* sp. increased with solvent polarity while that of *Mycobacterium* sp. decreased with solvent polarity. All isolates showed a moderate hydrophobicity to chloroform except for *Hymenobacter* sp (19.88%). *Chryseobacterium* sp., *Paenarthrobacter* sp. and *Stenotrophomonas* sp. exhibited the highest hydrophobicity ability to chloroform, while *Hymenobacter* sp. and *Mycobacterium* sp. showed the highest adhesion effect to n-octane. However, *Bacillus* sp, a capsule producer, exhibited a strong hydrophobicity for ethyl acetate (58.16%). This indicates these bacterial isolates had an affinity for electron acceptance (ethyl acetate) and electron donation (chloroform). The hydrophobicity capabilities of *Bacillus* sp. in this study were comparatively lower than those reported by Kuebutornye et al. (2019). Also, Amenyogbe et al. (2021) revealed the adhesion of *Bacillus* sp. RCS1 (97.2%) and *Bacillus cereus* (97.1%) isolated from Cobia Fish (Rachycentron canadum) to xylene, chloroform and ethyl acetate were strong. Adhesion is the first stage in microbial colonization, and cell surface hydrophobicity increases microbial cell propensity to adhere to surfaces (Nwagu et al., 2020).

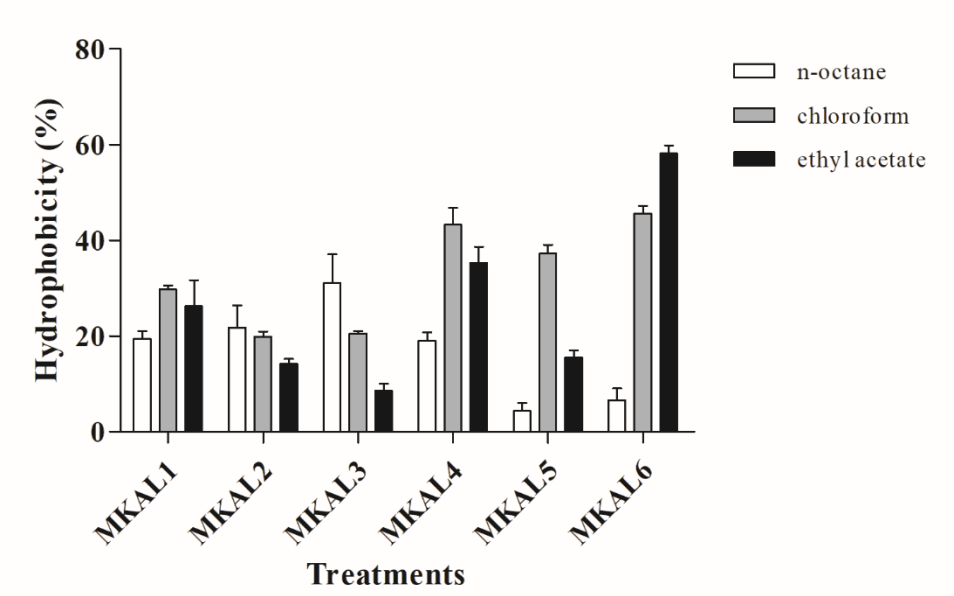

Figure 2. Quantitative estimation of adhesion of bacterial strains to solvents. *Paenarthrobacter* sp. MKAL1, *Hymenobacter* sp. MKAL2, *Mycobacterium* sp. MKAL3, *Stenotrophomonas* sp. MKAL4, *Chryseobacterium* sp. MKAL5 and *Bacillus* sp. MKAL6 were classified into three categories: Not hydrophobic (< 20%), Moderate (20-50%), Strong (> 50%)

3.3. Resistance to heavy metals

Resistance of isolates to heavy metals (Co^{2+}, Cd^{2+}, Cr^{3+}, Zn^{2+}, Hg^{2+}, Cu^{2+}, Mn^{2+}, Ni^{2+} and Pb^{2+}) were carried out at the concentrations of 50, 150, 300, 450, 600 and 750 µg/mL. Visible growth of isolates was observed for 24 hours, and 48 h at 30º C. Minimum inhibitory concentration (MIC) was noted as the lowest concentration inhibiting bacterial growth. The tested isolates showed variable degrees of resistance to different heavy metals (Table 2). Cadmium inhibited bacterial growth at the lowest concentration tested (50 µg/mL). Except for *stenotrophomonas* sp (50 µg/mL), cobalt inhibited isolate growth at the highest concentration tested (750 µg/mL). Copper and mercury inhibited the growth of all isolates tested with MICs ranging from 50-450 µg/mL. Many bacteria isolated from diverse sources, such as *Bacillus* sp. (Glibota et al., 2020;

Nath et al., 2020; Alotaibi et al., 2021); *Stenotrophomonas* sp. (Agarwal et al., 2019; Nath et al., 2020), *Chryseobacterium* sp. (Glibota et al., 2020), *Arthrobacter* sp. (Pathak et al., 2020) and *Mycobacterium* sp. (Sepehri et al., 2017) were reported to tolerate high levels of heavy metals and possess heavy metal resistance determinants. Also, *Paenarthrobacter* sp. was reported to evolve self-protective mechanisms for survival and prosperity in various stressful environments (stress responses to osmotic pressure, carbon starvation, oxygen radicals, and toxic chemicals) (Cao et al., 2019). Chromium, lead, zinc, nickel and manganese did not inhibit the bacterial growth except for *stenotrophomonas* sp at 600 µg/mL. This suggests that these bacterial isolates can grow under high concentration of chromium, lead, zinc, nickel and manganese.

Table 2. Resistance of bacterial strains to heavy metals.

Heavy metals	Minimum inhibitory concentration (µg/mL)					
	MKAL1	MKAL2	MKAL3	MKAL4	MKAL5	MKAL6
Cadmium	50	50	50	50	50	50
Chromium	-	-	-	-	-	-
Cobalt	750	750	750	50	750	750
Lead	-	-	-	-	-	-
Nickel	-	-	-	-	-	-
Manganese	-	-	-	600	-	-
Mercury	50	50	50	150	150	50
Zinc	-	-	-	-	-	-
Copper	50	50	50	450	150	50

-: growth at all tested concentrations, MKAL1: *Paenarthrobacter* sp. MKAL1, MKAL2: *Hymenobacter* sp. MKAL2, MKAL3: *Mycobacterium* sp. MKAL3, MKAL4: *Stenotrophomonas* sp. MKAL4, MKAL5: *Chryseobacterium* sp. MKAL5, MKAL6: *Bacillus* sp. MKAL6

3.4. Biofilm-forming capacity

The biofilm-forming capacity of isolates was estimated by adhesion to polystyrene. *Paenarthrobacter* sp., *Hymenobacter* sp., *Mycobacterium* sp., *Stenotrophomonas* sp. and *Bacillus* sp. showed strong biofilm-forming capacity, while *Chryseobacterium* sp. exhibited moderate ability (Figure 3). Many investigators revealed the biofilm-forming ability of these bacteria species

(Esteban and García-Coca, 2018; Kim et al., 2020; Bostanghadiri et al., 2021; Sornchuer et al., 2022). It was reported that there was a correlation between cell surface hydrophobicity and biofilm formation. Bacteria with high hydrophobic surface affinity displayed a high biofilm-forming ability (Ning et al., 2021). In our study, *Bacillus* sp., which exhibited higher hydrophobic ability, adhered more to polystyrene.

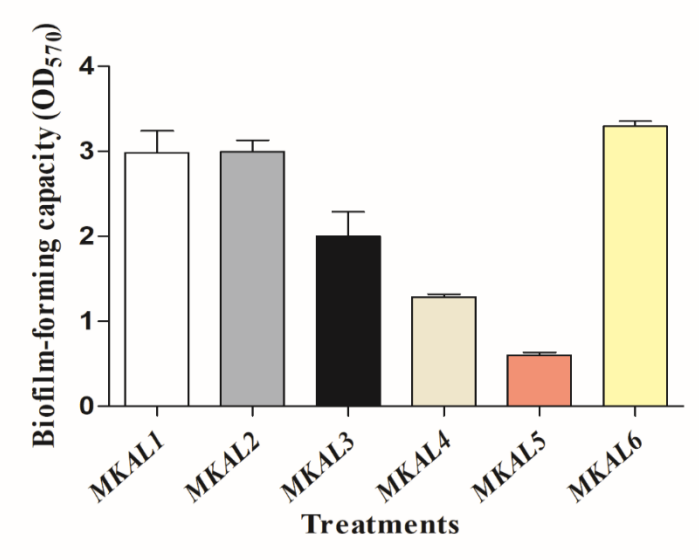

Figure 3. Biofilm-forming capacity of *Paenarthrobacter* sp. MKAL1, *Hymenobacter* sp. MKAL2, *Mycobacterium* sp. MKAL3, *Stenotrophomonas* sp. MKAL4, *Chryseobacterium* sp. MKAL5 and *Bacillus* sp. MKAL6. Adhesion ability of strains was interpreted as strong (OD ≥ 1), moderate (0.1 ≤ OD595 < 1) or weak (OD595 < 0.1).

3.5. Antibiotics resistance

Bacterial susceptibility to antibiotics was investigated by determining the diameter of inhibition zones. All isolates were resistant to lincomycin (0.0-18.6 mm). *Hymenobacter* sp. was resistant to novobiocin (9.6 mm), bacitracin (0.0 mm) and tetracycline (10.1 mm), while *Mycobacterium* sp. (8.3 mm) was intermediate to bacitracin (Table 3, Figure S1). Kang et al.

(2018) showed that *Hymenobacter defluvii* sp. nov., isolated from wastewater, was resistant to amikacin (30 µg), gentamicin (10 µg) and kanamycin (30 µg). Then, MICs of six different classes of antibiotics were investigated using Mueller Hinton Broth (MHB) by the microdilution method. All antibiotics exerted inhibitory effect against bacteria isolates with MIC ranging from 0.25-512 µg/mL. Ciprofloxacin exhibited the highest inhibitory activity (0.25-0.5 µg/mL), while kanamycin exhibited the lowest activity (4-512 µg/mL). *Paenarthrobacter* sp. (0.25-128 µg/mL), *Mycobacterium* sp. (0.25-256 µg/mL), *Hymenobacter* sp. (0.25-512 µg/mL), *Stenotrophomonas* sp. (0.5-512 µg/mL), *Chryseobacterium* sp. (0.5-512 µg/mL) and *Bacillus* sp. (0.5-256 µg/mL) exhibited variable susceptibilities to antibiotics. Differences in susceptibility could be due to the differences in cell wall composition and/or genetic content of plasmids that can be easily transferred among isolates (Kowalska-Krochmal and Dudek-Wicher, 2021). All isolates, resistant to lincomycin on agar Petri dishes, were sensitive to this antibiotic in the liquid medium. This is explained by the fact that in a solid medium, the antibiotic must diffuse, while in a liquid medium, it is directly in contact with the bacterial isolate (Mokale et al., 2011).

3.6. Antibacterial Action Mechanisms

3.6.1. Antimicrobial Efficacy Testing

Ciprofloxacin was tested for antibacterial efficacy over time (24 h) at different concentrations (MIC, 2MIC, and 4MIC). The time-kill kinetics profile of ciprofloxacin against bacterial isolates showed a reduction in viable cell number over 24 h compared to the control (non-treated cells). Viable cell number decreased with increasing antibiotic concentrations. Ciprofloxacin exhibited the highest inhibitory effect against *Bacillus* sp. and *Chryseobacterium* sp. at the concentration of 4MIC. The overall effect of ciprofloxacin was bactericidal at all tested

concentrations. Grillon et al. (2016) showed that ciprofloxacin exhibited a bacteriostatic effect on some strains of *Stenotrophomonas maltophilia* up to 6 h, followed by a regrowth at 24 h.

Table 3. Bacterial susceptibility to antibiotics.

Antibiotics	Diameter of inhibition zones (mm)					
	MKAL1	MKAL2	MKAL3	MKAL4	MKAL5	MKAL6
Ampi	32.0 ± 2.0	21.3 ± 0.5	24.3 ± 1.1	26.6 ± 1.1	31.0 ± 1.7	33.3 ± 1.5
Novo	27.0 ± 3.6	9.6 ± 0.5	20.3 ± 2.0	29.3 ± 1.1	33.6 ± 1.1	27.6 ± 1.1
Baci	11.6 ± 1.5	0.0 ± 0.0	8.3 ± 0.5	9.6 ± 0.5	16.6 ± 3.0	12.3 ± 0.5
Tetra	22.6 ± 0.5	10.1 ± 0.2	18.3 ± 1.1	21.0 ± 2.6	36.0 ± 0.0	21.0 ± 0.0
Eryt	30.6 ± 1.1	31.6 ± 2.5	30.3 ± 0.5	35.8 ± 0.2	26.3 ± 0.5	30.6 ± 0.5
Chlor	25.3 ± 0.5	30.0 ± 1.7	27.3 ± 2.0	35.6 ± 0.5	38.6 ± 1.5	34.3 ± 0.5
Peni	27.3 ± 2.5	29.6 ± 2.0	21.3 ± 0.5	31.0 ± 1.0	30.3 ± 0.5	32.3 ± 0.5
Linco	8.0 ± 0.0	10.0 ± 0.0	0.0 ± 0.0	18.6 ± 0.5	13.0 ± 1.7	8.3 ± 0.5
Phleo	15.1 ± 1.0	17.6 ± 1.5	18.0 ± 1.0	18.3 ± 0.2	19.3 ± 1.5	18.0 ± 1.0
Kana	16.3 ± 0.5	17.0 ± 1.0	16.6 ± 0.5	17.6 ± 0.5	14.3 ± 1.1	15.3 ± 0.5
Trime	30.6 ± 1.1	32.3 ± 0.5	31.6 ± 1.5	29.6 ± 0.5	35.0 ± 1.0	33.0 ± 2.6
Cipro	26.0 ± 1.7	29.0 ± 1.0	25.6 ± 0.5	25.1 ± 0.2	33.0 ± 1.0	25.6 ± 0.5

Ampi: Ampicillin; Novo: Novobiocin; Baci: Bacitracin; Tetra: Tetracyclin; Eryth: Erythromycin; Chlor: Chloramphenicol; Peni:Penicillin; Linco: Lincomycin; Phleo: Phleomycin; Kana: Kanamycin; Trime: Trimethoprim; Cipro: Ciprofloxacin; MKAL1: *Paenarthrobacter* sp. MKAL1; MKAL2: *Hymenobacter* sp. MKAL2; MKAL3: *Mycobacterium* sp. MKAL3; MKAL4: *Stenotrophomonas* sp. MKAL4; MKAL5: *Chryseobacterium* sp. MKAL5; MKAL6: *Bacillus* sp. MKAL6; Bacterial sensibility was interpreted as Ampicillin: resistant (DI ≤ 11 mm), intermediate (12 ≤ DI < 13) or susceptible (DI ≥ 14 mm); Novobiocin: resistant (DI ≤ 12 mm), intermediate (13 ≤ DI < 15) or susceptible (DI ≥ 16 mm); Bacitracin: resistant (DI ≤ 6 mm), intermediate (7 ≤ DI < 10) or susceptible (DI ≥ 11 mm); Tetracycline: resistant (DI ≤ 14 mm), intermediate (15 ≤ DI < 18) or susceptible (DI ≥ 19 mm); Erythromycin: resistant (DI ≤ 13 mm), intermediate (14 ≤ DI < 22) or susceptible (DI ≥ 23 mm); Chloramphenicol: resistant (DI ≤ 12 mm), intermediate (13 ≤ DI < 17) or susceptible (DI ≥ 18 mm); Penicillin: resistant (DI ≤ 28 mm), or susceptible (DI ≥ 29mm); Lincomycin: resistant (DI ≤ 22 mm), intermediate (23 ≤ DI < 25) or susceptible (DI ≥ 26 mm); Kanamycin: resistant (DI ≤ 13 mm), intermediate (14 ≤ DI < 17) or susceptible (DI ≥ 18 mm); Trimethoprim: resistant (DI ≤ 10 mm), intermediate (11 ≤ DI < 15) or susceptible (DI ≥ 16 mm); Ciprofloxacin: resistant (DI ≤ 15 mm), intermediate (16 ≤ DI < 20) or susceptible (DI ≥ 21 mm)

Table 4. Minimum inhibition concentrations (MIC) of antibiotics.

Antibiotic	Minimum Inhibition Concentrations (µg/mL)					
	MKAL1	MKAL2	MKAL3	MKAL4	MKAL5	MKAL6
Ampicillin	128	64	128	0.5	16	4
Chloramphenicol	4	1	8	4	4	4
Ciprofloxacin	0.25	0.25	0.25	0.5	0.5	0.5
Trimethoprim	0.25	0.5	0.5	0.5	0.5	0.5
Kanamycin	4	512	256	512	512	256
Lincomycin	32	32	128	64	32	64

MKAL1: *Paenarthrobacter* sp. MKAL1, MKAL2: *Hymenobacter* sp. MKAL2, MKAL3: *Mycobacterium* sp. MKAL3, MKAL4: *Stenotrophomonas* sp. MKAL4, MKAL5: *Chryseobacterium* sp. MKAL5, MKAL6: *Bacillus* sp. MKAL6

3.6.2. Action on cell membrane

The action of ciprofloxacin on the bacterial cell membrane was performed by quantifying the release of UV-absorbing materials (OD_{260}), an index of membrane integrity damage and loss. The results are presented in figure 5A. After treatment with ciprofloxacin at MIC and 4MIC, a slight increase in OD was observed in *Bacillus* sp. (0.139-0.176 and 0.139-0.185), *Chryseobacterium* sp. (0.140-0.162 and 0.140-0.169), *Paenarthrobacter* sp. (0.144-0.174 and 0.144-0.177) and *Mycobacterium* sp. (0.140-0.165 and 0.140-0.184). This suggests that ciprofloxacin weakly damaged the cytoplasmic membrane resulting in low leakage of bacterial isolates intracellular constituents (proteins and nucleic acids). However, no change in OD was observed in *Hymenobacter* sp. MKAL2 and *Stenotrophomonas* sp. MKAL4 suggesting that ciprofloxacin didn't affect the membrane integrity of these isolates. The action of ciprofloxacin on bacterial cell membrane permeability is shown in figure 5B. Crystal violet uptake significantly ($p < 0.001$) increased after treatment with ciprofloxacin at MIC and 4MIC in *Stenotrophomonas* sp. MKAL4 (62.06 and 62.87%), *Chryseobacterium* sp. MKAL5 (41.90 and 46.56%) and *Bacillus* sp.

MKAL6 (50.43 and 52.89%)compared to untreated cells (23.87, 32.56 and 52.35% respectively).The increase in crystal violet uptake might be attributed to the change in permeability and structure of the bacterial cell wall layer (Seukep et al., 2020).

3.6.3. Action on biofilm formation

Ciprofloxacin was tested for biofilm formation inhibition capability at different concentrations (8MIC-MIC/16). This experiment targeted peptidoglycan synthesis and modulated the quorum sensing (QS), a whole gene involved in the regulation of biofilm formation. QS regulates various functions in bacteria, including biofilm formation, antibiotic resistance, and induction of bacterial diseases (Seukep et al., 2020). Ciprofloxacin significantly ($p < 0.001$) inhibited the biofilm formation in *Bacillus* sp. (69.27-39.58%), *Hymenobacter* sp. (76.13-55.13%), *Chryseobacterium* sp. (96.98-75.96%), *Paenarthrobacter* sp. (71.90-38.75%), *Mycobacterium* sp. (80.07-60.38%) and *Stenotrophomonas* sp. (86.54-68.03%). Biofilm formation inhibition of bacterial isolates by ciprofloxacin could be due to its ability to inhibit QS signalling pathways involved in biofilm formation.

4. Conclusions

This study investigated putative virulence factors, antibiotics and heavy metals resistance, solvent adhesion and biofilm-forming capabilities in cellulolytic bacteria isolated from soil samples: *Paenarthrobacter* sp. MKAL1, *Hymenobacter* sp. MKAL2, *Mycobacterium* sp. MKAL3, *Stenotrophomonas* sp. MKAL4, *Chryseobacterium* sp. MKAL5 and *Bacillus* sp. MKAL6. Some bacterial strains phenotypically expressed virulence factors. Strains MKAL2, MKAL5 and MKAL6 exhibited proteolytic and lipase activities, while only MKAL6 produced capsules. All strains were capable of aggregating, forming biofilm and adhering to organic

solvents. All strains tolerated a high amount of chromium, lead, zinc, nickel and manganese. They were resistant to lincomycin. Also, MKAL2 was resistant to novobiocin, bacitracin and tetracycline. Ciprofloxacin exhibited bactericidal activity against these strains. Although some strains showed phenotypic virulence factors, an in-depth genetic study of virulence, antibiotic and heavy metal resistance genes is underway.

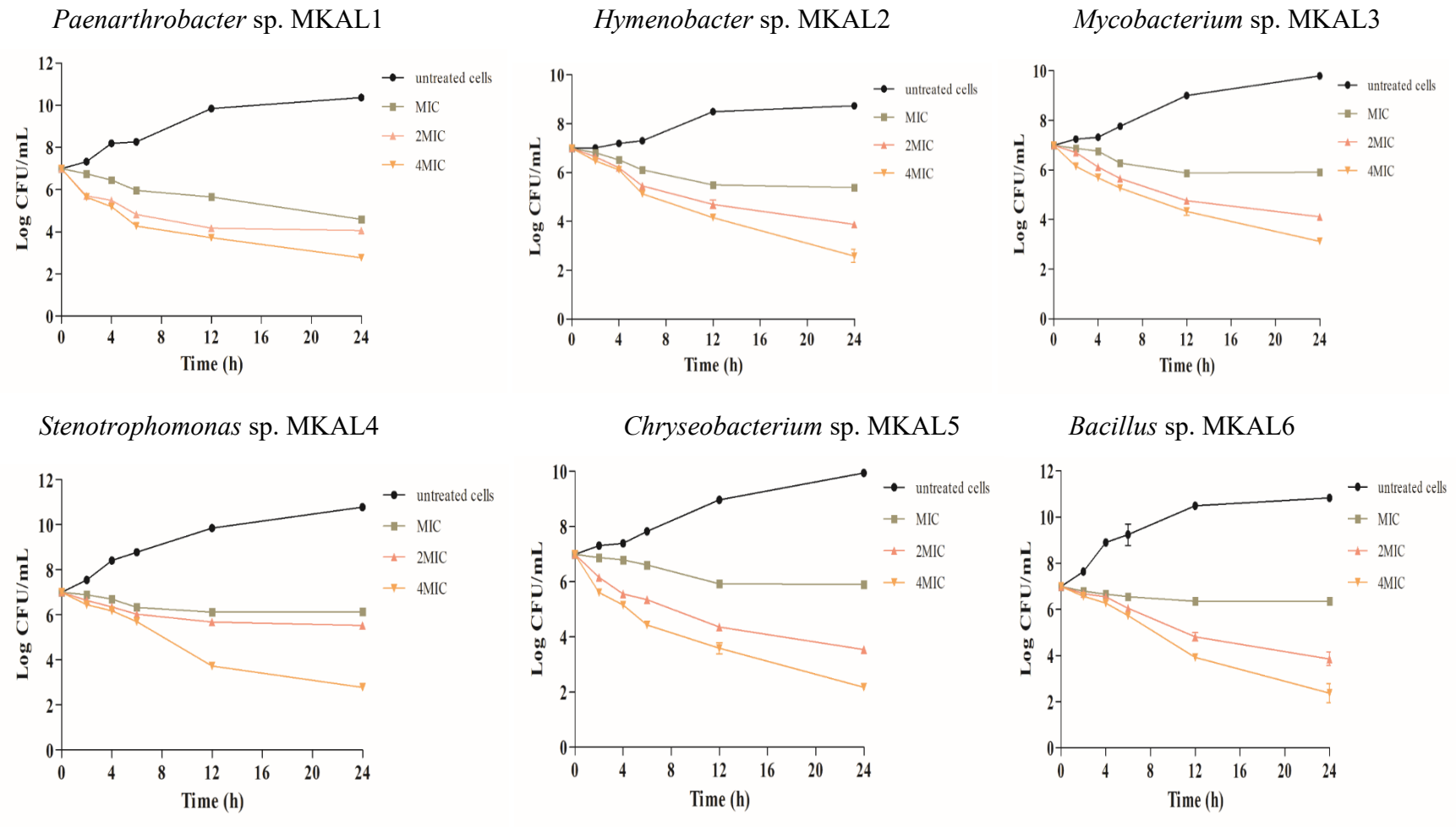

Figure 4. Antibacterial efficacy testing of ciprofloxacin on *Paenarthrobacter* sp. MKAL1, *Hymenobacter* sp. MKAL2, *Mycobacterium* sp. MKAL3, *Stenotrophomonas* sp. MKAL4, *Chryseobacterium* sp. MKAL5 and *Bacillus* sp. MKAL6. Time intervals: 0, 2, 4, 6, 12, and 24 h. MIC: minimum inhibitory concentration.

(A)

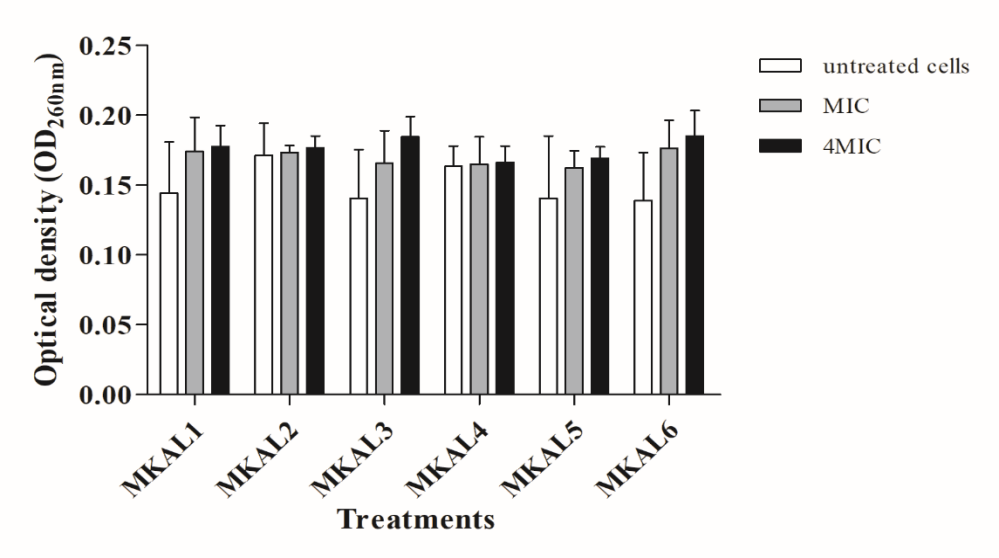

(B)

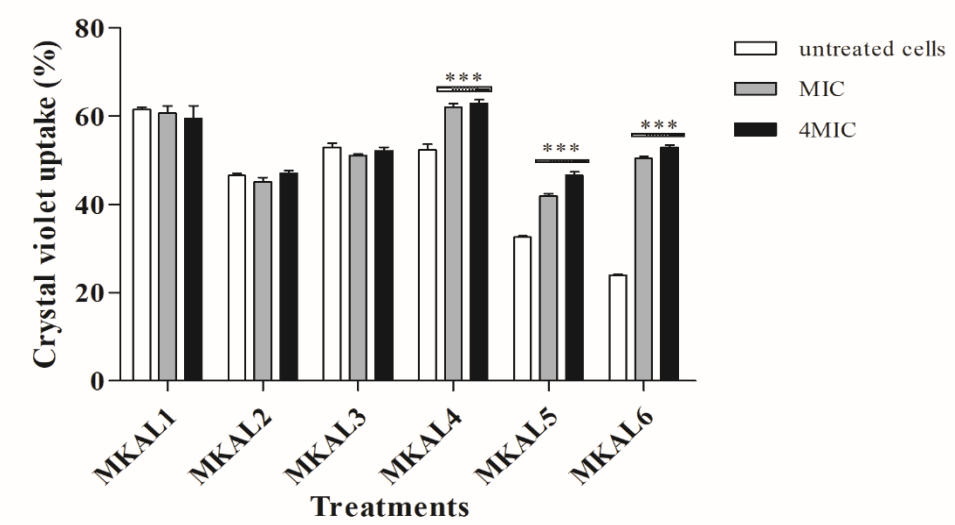

Figure 5. Effect of ciprofloxacin on cell membrane of *Paenarthrobacter* sp. MKAL1, *Hymenobacter* sp. MKAL2, *Mycobacterium* sp. MKAL3, *Stenotrophomonas* sp. MKAL4, *Chryseobacterium* sp. MKAL5 and *Bacillus* sp. MKAL6. (A) Action on cell membrane integrity: Absorbance measurement of intracellular components (DNA, RNA) at 260 nm after 1 h of incubation. (B) Action on membrane permeability. MIC: minimum inhibitory concentration. ***$p < 0.001$ compared to untreated cells (Student-Newman-Keuls).

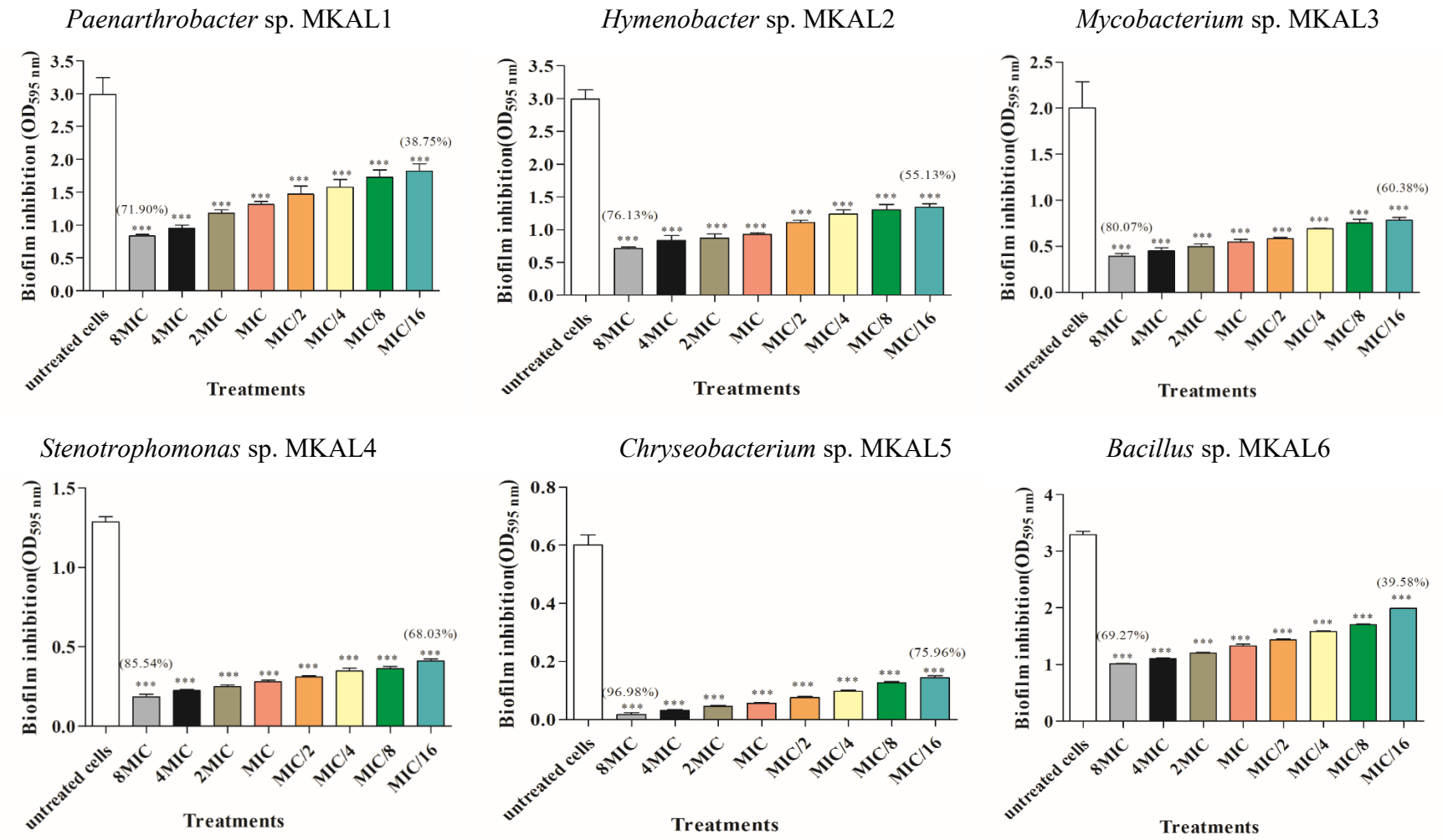

Figure 6. Effect of ciprofloxacin on biofilm formation in *Paenarthrobacter* sp. MKAL1, *Hymenobacter* sp. MKAL2, *Mycobacterium* sp. MKAL3, *Stenotrophomonas* sp. MKAL4, *Chryseobacterium* sp. MKAL5 and *Bacillus* sp. MKAL6. MIC: minimum inhibitory concentration. ***$p < 0.001$ compared to untreated cells (Student-Newman-Keuls).

5. References

Abbott IJ, Slavin MA, Turnidge JD, Thursky KA, Worth LJ (2011). *Stenotrophomonas maltophilia*: emerging disease patterns and challenges for treatment. *Expert Rev Anti Infect Ther*, 9, 471-488.

Agarwal M, Rathore RS, Jagoe C, Chauhan A (2019). Multiple lines of evidences reveal mechanisms underpinning mercury resistance and volatilization by *Stenotrophomonas* sp. MA5 isolated from the Savannah River Site (SRS), USA. *Cells*, 8, 309.

Ahmed ET, Raghavendra D, Madamwar (2010). An alkaline lipase from organic solvent tolerant *Acinetobacter* sp. EH28: application for ethyl caprylate synthesis. *Bioresour Technol*, 101, 3628-3634.

Aktayeva S, Baltin K, Kiribayeva A, Akishev Z, Silayev D, Ramankulov Y, Khassenov B (2022). Isolation of *Bacillus* sp. A5.3 Strain with keratinolytic activity. *Biology*, 11, 244.

Alotaibi BS, Khan M, Shamim S (2021). Unraveling the underlying heavy metal detoxification mechanisms of *Bacillus* Species. *Microorganisms*, 9, 1628.

Amenyogbe E, Huang JS, Chen G, Wang WZ (2021). Probiotic potential of indigenous (*Bacillus* sp. RCS1, *Pantoea agglomerans* RCS2, and *Bacillus cereus* strain RCS3) isolated from cobia fish (*Rachycentron canadum*) and their antagonistic effects on the growth of pathogenic *Vibrio alginolyticus*, *Vibrio harveyi*, *Streptococcus iniae*, and *Streptococcus agalactiae*. *Front Mar Sci*, 8, 672213.

Augenstreich J, Haanappel E, Sayes F, Simeone R, Guillet V, Mazeres S, Chalut C, Mourey L, Brosch R, Guilhot C, Astarie-Dequeker C (2020). Phthiocerol Dimycocerosates from *Mycobacterium tuberculosis* increase the membrane activity of bacterial effectors and host receptors. *Front Cell Infect Microbiol*, 10, 420.

Babin BM, Fernandez-Cuervo G, Sheng J, Green O, Ordonez AA, Turner ML, Keller LJ, Jain SK, Shabat D, Bogyo M (2021). Chemiluminescent protease probe for rapid, sensitive, and inexpensive detection of live *Mycobacterium tuberculosis*. *ACS Cent Sci*, 7, 803-814.

Baldwin VM (2020). You can't *B. cereus* - A review of *Bacillus cereus* strains that cause anthrax-like disease. *Front Microbiol*, 11, 1731.

Beesley CA, Vanner CL, Helsel LO, Gee JE (2010). Hoffmaster AR. Identification and characterization of clinical *Bacillus* spp. isolates phenotypically similar to *Bacillus anthracis*. *FEMS Microbiol Lett*, 313, 47-53.

Benladghem Z, Seddiki SML, Mahdad YM (2020). Identification of bacterial biofilms on desalination reverse osmosis membranes from the mediterranean sea. *Biofouling*, 36, 1065-1073.

Bokveld A, Nnolim NE, Nwodo UU (2021). *Chryseobacterium aquifrigidense* FANN1 produced detergent-stable metallokeratinase and amino acids through the abasement of chicken feathers. *Front Bioeng Biotechnol*, 9, 720176.

Borghi E, Sciota R, Biassoni C, Cirasola D, Cappelletti L, Vizzini L, Boracchi P, Morace G (2011). Cell surface hydrophobicity: a predictor of biofilm production in Candida isolates? *J Med Microbiol*, 60, 689-690.

Bostanghadiri N, Ardebili A, Ghalavand Z, Teymouri S, Mirzarazi M, Goudarzi M, Ghasemi E, Hashemi A (2021). Antibiotic resistance, biofilm formation, and biofilm-associated genes among *Stenotrophomonas maltophilia* clinical isolates. *BMC Res Notes*, 14, 151.

Brooke JS (2012). *Stenotrophomonas maltophilia*: an emerging global opportunistic pathogen. *Clin Microbiol Rev*, 25, 2-41.

Cao L, Zhang J, Zhao R, Deng Y, Liu J, Fu W, Lei Y, Zhang T, Li X, Li B (2019). Genomic

characterization, kinetics, and pathways of sulfamethazine biodegradation by *Paenarthrobacter* sp. A01. *Environ Int*, 131, 104961.

Chaieb K, Zmantar T, Souiden Y, Mahdouani K, Bakhrouf A (2011). XTT assay for evaluating the effect of alcohols, hydrogen peroxide and benzalkonium chloride on biofilm formation of *Staphylococcus epidermidis*. *Microb Pathog*, 50, 1-5.

Chhetri G, Kim J, Kim I, Kim H, Seo T (2020). *Hymenobacter setariae* sp. nov., isolated from the ubiquitous weedy grass *Setaria viridis*. *Int J Syst Evol Microbiol*, 70, 3724-3730.

CLSI (2008). Reference method for broth dilution antifungal susceptibility testing of yeasts: CLSI guideline M27 and A3. Wayne, PA, USA: Clinical and Laboratory Standards Instituts.

Dabiré Y, Somda NS, Somda MK, Mogmenga I, Traoré AK, Ezeogu LI, Traoré AS, Ugwuanyi JO, Dicko MH (2022). Molecular identification and safety assessment of *Bacillus* strains isolated from Burkinabe traditional condiment "soumbala". *Ann Microbiol*, 72, 10.

Danilova I, haripova M (2020). The practical potential of *Bacilli* and their enzymes for industrial production. *Front Microbiol*, 11, 1782.

Devi KP, Nisha SA, Sakthivel R, Pandian SK (2010). Eugenol (an essential oil of clove) acts as an antibacterial agent against *Salmonella typhi* by disrupting the cellular membrane. *J Ethnopharmacol*, 130, 107-115.

Escamilla-Montes R, Luna-González A, Flores-Miranda M, del C, Álvarez-Ruiz P, Fierro-Coronado JA, Sánchez-Ortiz AC, Ávila-Leal J (2015). Isolation and characterization of potential probiotic bacteria suitable for mollusk larvae cultures. *The Thai Journal of Veterinary Medicine*, 45, 11-21

Esteban J, García-Coca M (2018). *Mycobacterium* Biofilms. *Front Microbiol*, 8, 2651.

Glibota N, Grande MJ, Galvez A, Ortega E (2020). Genetic determinants for metal tolerance and

antimicrobial resistance detected in bacteria isolated from soils of olive tree farms. *Antibiotics (Basel)*, 9, 476.

Grillon A, Schramm F, Kleinberg M, Jehl F (2016) Comparative activity of ciprofloxacin, levofloxacin and moxifloxacin against *Klebsiella pneumoniae*, *Pseudomonas aeruginosa* and *Stenotrophomonas maltophilia* assessed by minimum inhibitory concentrations and time-kill studies. *PLoS ONE*, 11, e0156690.

Hassan SWM, Abd El Latif HH and Ali SM (2018). Production of cold-active lipase by free and immobilized marine *Bacillus cereus* HSS: Application in wastewater treatment. *Front Microbiol*, 9, 2377.

Jeon H, Lee N, Yang S, Kim W, Pak H (2017). Probiotic characterization of *Bacillus subtilis* P223 isolated from Kimchi. *Food Sc Biotechnol*, 26, 1641-1648.

Kalidasan V, Joseph N, Kumar S, Awang Hamat R, Neela VK (2018). Iron and virulence in *Stenotrophomonas Maltophilia*: All we know so far. *Front Cell Infect Microbiol*, 8, 401.

Kang JW, Choi S, Choe HN, Seong CN (2018). *Hymenobacter defluvii* sp. nov., isolated from wastewater of an acidic water neutralization facility. *Int J Syst Evol Microbiol*, 68, 277-282.

Kangale LJ, Raoult D, Ghigo E, Fournier PE (2021). *Chryseobacterium schmidteae* sp. nov. a novel bacterial species isolated from planarian *Schmidtea mediterranea*. *Sci Rep*, 11, 11002.

Kim SG, Giri SS, Kim SW, Kwon J, Lee SB, Park SC (2020). First isolation and characterization of *Chryseobacterium cucumeris* SKNUCL01, isolated from diseased pond loach (*Misgurnus anguillicaudatus*) in Korea. *Pathogens*, 2020, 9, 397.

Kowalska-Krochmal B, Dudek-Wicher R (2021). The minimum inhibitory concentration of

antibiotics: Methods, interpretation, clinical relevance. *Pathogens*, 10, 165.

Kuebutornye FKA, Lu Y, Abarike ED, Wang Z, Li Y, Sakyi ME (2019). *In vitro* Assessment of the probiotic characteristics of three *Bacillus* species from the gut of nile tilapia, *Oreochromis niloticus*. *Probiot Antimicrob Prot*, 12, 412-424.

Kumar A, Mukhia S, Kumar N, Acharya V, Kumar S and Kumar R (2020). A broad temperature active lipase purified from a psychrotrophic bacterium of Sikkim Himalaya with potential application in detergent formulation. *Front Bioeng Biotechnol*, 8, 642.

Lamari F, Khouadja S, Rtimi S (2018). Interaction of *vibrio* to biotic and abiotic surfaces: Relationship between hydrophobicity, cell Adherence, biofilm production, and cytotoxic activity. *Surfaces*, 1, 187-201.

Lodha D, Karolia R, Sharma S, Joseph J, Das T, Dave VP (2022). Biofilm formation and its effect on the management of culture-positive bacterial endophthalmitis. *Indian J Ophthalmol*, 70, 472-476.

López-Moreno A, Torres-Sánchez A, Acuña I, Suárez A, Aguilera M (2021). Representative *Bacillus* sp. AM1 from gut microbiota harbor versatile molecular pathways for bisphenol a biodegradation. *Int J Mol Sci*, 22, 4952.

Manhar AK, Saikia D, Bashir Y, Mech RK, Nath D, Konwar BK, Mandal M (2015). *In vitro* evaluation of celluloytic *Bacillus amyloliquefaciens* AMS1 isolated from traditional fermented soybean (Churpi) as an animal probiotic. *Res Vet Sc*, 99, 149-156.

Marizcurrena JJ, Herrera LM, Costábile A, Morales D, Villadóniga C, Eizmendi A, Davyt D, Castro-Sowinski S (2019). Validating biochemical features at the genome level in the Antarctic bacterium *Hymenobacter* sp. strain UV11. *FEMS Microbiol Lett*, 366, fnz177.

Marzan LW, Hossain M, Mina SA, Akter Y, Chowdhury AMMA (2017). Isolation and

biochemical characterization of heavy-metal resistant bacteria from tannery effluent in Chittagong city, Bangladesh: bioremediation viewpoint. *Egypt J Aquat Res*, 43, 65-74.

Masindi V, Muedi KL (2018). Environmental contamination by heavy metals. In Heavy Metals; Saleh, HED, Aglan RF, Eds. IntechOpen Publishers: London, UK, pp. 115-132.

Matsui M, Kawamata A, Kosugi M, Imura S, Kurosawa N (2017). Diversity of proteolytic microbes isolated from Antarctic freshwater lakes and characteristics of their cold-active proteases. *Polar Sci*, 13:82-90.

Mirani ZA, Fatima A, Urooj S, Aziz M, Khan MN, Abbas T (2018). Relationship of cell surface hydrophobicity with biofilm formation and growth rate: A study on *Pseudomonas aeruginosa*, *Staphylococcus aureus*, and *Escherichia coli*. *Iranian journal of basic medical sciences*, 21, 760-769.

Mogrovejo DC, Perini L, Gostinčar C, Sepčić K, Turk M, Ambrožič-Avguštin J, Brill FHH, Gunde-Cimerman N (2020). Prevalence of antimicrobial resistance and hemolytic phenotypes in culturable arctic bacteria. *Front Microbiol*, 11:570.

Mokale KAL, Ngono NRA, Kuiate JR, Koanga MML, Tchinda TA, Mouokeu RS, Biyiti L, Amvam ZPH (2011). Antibacterial and antioxidant properties of the methanolic extract of the stem bark of *Pteleopsis hylodendron* (Combretaceae). *Chemother Res Pract*, 2011, 218750.

Nagpal J, Paxman JJ, Zammit JE, Alhuwaider A, Truscott KN, Heras B, Dougan DA (2019). Molecular and structural insights into an asymmetric proteolytic complex (ClpP1P2) from *Mycobacterium smegmatis*. *Sci Rep*, 9, 18019.

Nath S, Sinha A, Singha YS, Dey A, Bhattacharjee N, Deb B (2020). Prevalence of antibiotic-

resistant, toxic metal-tolerant and biofilm-forming bacteria in hospital surroundings. *Environ Anal Health Toxicol*, 35, e2020018.

Ning Z, Xue B, Wang H (2021). Evaluation of the adhesive potential of bacteria isolated from meat-related sources. *Appl Sci*, 11, 10652.

Nowak J, Cruz CD, Palmer J, Fletcher GC, Flint S (2015). Biofilm formation of the *L. monocytogenes* strain 15G01 is influenced by changes in environmental conditions. *J Microbiol Methods*, 119, 189-195.

Nwagu TN, Ugwuodo CJ, Onwosi CO, Inyima O, Uchendu OC, Akpuru C (2020). Evaluation of the probiotic attributes of Bacillus strains isolated from traditional fermented African locust bean seeds (Parkia biglobosa), "daddawa". *Ann Microbiol*, 70, 20.

Odeyemi OA, Abdullah Sani N (2019). Antibiotic resistance, putative virulence factors and curli fimbrination among *Cronobacter* species. *Microb Pathog*, 136, 103665.

Pathak A, Jaswal R and Chauhan A (2020). Genomic characterization of a mercury resistant *Arthrobacter* sp. H-02-3 reveals the presence of heavy metal and antibiotic resistance determinants. *Front Microbiol*, 10, 3039.

Penesyan A, Paulsen IT, Gillings MR, Kjelleberg S, Manefield MJ (2020). Secondary effects of antibiotics on microbial biofilms. *Front Microbiol*, 11, 2109.

Peters DL, McCutcheon JG and Dennis JJ (2020). Characterization of novel broad-host-range bacteriophage DLP3 specific to *Stenotrophomonas maltophilia* as a potential therapeutic agent. *Front Microbiol*, 11, 1358.

Presentato A, Piacenza E, Turner RJ, Zannoni D, Cappelletti M (2020). Processing of metals and metalloids by Actinobacteria: Cell resistance mechanisms and synthesis of metal(loid)-based nanostructures. *Microorganisms*, 8, 2027.

Rhen M (2019). *Salmonella* and Reactive oxygen species: A love-hate relationship. *J Innate Immun*, 11, 216-226.

Rumbaugh KP, Sauer K (2020). Bioflm dispersion. *Nat Rev Microbiol*, 18, 571–586.

Sepehri Z, Mirzaei N, Sargazi A, Sargazi A, Mishkar AP, Kiani Z, Oskoee HO, Arefi D, Ghavami S (2017). Essential and toxic metals in serum of individuals with active pulmonary tuberculosis in an endemic region. *J Clin Tuberc Other Mycobact Dis*, 6, 8-13.

Seukep AJ, Fan M, Sarker SD, Kuete V, Guo MQ (2020). *Plukenetia huayllabambana* Fruits: Analysis of bioactive compounds, antibacterial activity and relative action mechanisms. *Plants*, 9, 1111.

Sharma P, Sharma N, Pathania S, Handa S (2017). Purification and characterization of lipase by *Bacillus methylotrophicus* PS3 under submerged fermentation and its application in detergent industry. *J Genet Eng Biotechnol*, 15, 369-377.

Shart AOB and Elkhalil EAI (2020). Biochemical characterization of lipase produced by *Bacillus* spp. isolated from soil and oil effluent. *Advances in Enzyme Research*, 8, 39-48.

Shin HJ, Yang S, Lim Y (2021). Antibiotic susceptibility of *Staphylococcus aureus* with different degrees of biofilm formation. *J Anal Sci Technol*, 12, 41.

Sornchuer P, Saninjuk K, Prathaphan P, Tiengtip R, Wattanaphansak S (2022). Antimicrobial susceptibility profile and whole-genome analysis of a strong biofilm-forming *Bacillus* Sp. B87 strain isolated from food. *Microorganisms,* 10, 252.

Sud A, Chaudhary M, Baveja CP, Pandey PN (2020). Rare case of meningitis due to an emerging pathogen *Chryseobacterium indologenes*. *SAGE open medical case reports*, 8, 2050313X20936098.

Trunk T, Khalil HS, Leo JC (2018). Bacterial autoaggregation. *AIMS Microbiol*, 4, 140-164.

Tsuji BT, Yang JC, Forrest A, Kelchlin PA, Smith PF (2008). *In vitro* pharmacodynamics of novel rifamycin ABI-0043 against *Staphylococcus aureus*. *J Antimicrob Chemother*, 62, 156-160.

Vranova V, Rejsek K, Formanek P (2013). Proteolytic activity in soil: a review. *Appl Soil Ecol*, 70, 23-32.

Wolska KI, Grudniak AM, Rudnicka Z, Markowska K (2016). Genetic control of bacterial biofilms. *J Appl Genet*, 57, 225-238.

CHAPTER 6

General discussion, summary of major contributions and recommendations of future research

The commercial production of fructose relies on the multienzyme hydrolysis of cellulose into two steps based on cellulases (endocellulase, exocellulase, ß-glucosidase) and glucose isomerase (Souzanchi et al., 2019). Cellulases catalyze the cellulose conversion to glucose, while glucose isomerase is a critical enzyme that catalyzes the isomerization of glucose to fructose. These enzymes are widely used in many applications and are currently produced by microbial fermentation. However, most reported cellulases and glucose isomerases to have enzyme activities limited. Presently, obtaining these enzymes with high activity is crucial. Soil bacteria are considered natural sources of potential enzymes for industrial applications. Therefore, this study aimed to characterize novel cellulases and glucose isomerase-producing bacteria from soil samples and optimize their enzyme production. Coculturing and whole-cell immobilization for glucose isomerase and bacterial resistance to environmental factors were also investigated.

Based on their morphological features (size, shape, and color), we isolated forty-one bacterial isolates from the soil mixture samples collected from Kingfisher Lake and the University of Manitoba campus. The qualitative screening of isolates for cellulase production was carried out by Congo red method using a carboxymethyl cellulose (CMC) agar medium. Only six isolates showed cellulase production based on the appearance of the halo zone around bacteria. Then they were selected for further characterization using 16S rRNA gene sequence analysis and morphological and biochemical methods. These isolates were differentiated based on mobility, cell wall composition (Gram stain), vegetative cells and endospores (endospore stain), carbon source utilization, and enzymatic activities by standard methods such as catalase production, gas

production, starch hydrolysis, gelatin hydrolysis, DNA hydrolysis, urease test, bile esculin test, oxidase test, nitrate reduction, salt tolerance, and sugar fermentation. They were identified as *Paenarthrobacter* sp. MKAL1, *Hymenobacter* sp. MKAL2, *Mycobacterium* sp. MKAL3, *Stenotrophomonas* sp. MKAL4, *Chryseobacterium* sp. MKAL5, and *Bacillus* sp. MKAL6. These strains are novel cellulose-degrading bacteria because no cellulase activity studies were reported on their closest strains in the phylogenetic tree. However, several studies reported cellulase production in some members of these bacteria isolated from various sources (Van Wyk et al., 2017; Ye et al., 2017, Molina et al., 2018; Tan et al., 2018; Dai et al., 2020). Their cellulase activities were quantified and optimized by varying pH, temperature, incubation period, substrate concentration, nitrogen, and carbon sources using the dinitrosalicylic acid (DNS) and response surface methods. The higher cellulase production in these strains occurred at the culture conditions of 35-40°C, pH 5-6, 1-2% CMC, and 96 h of incubation. These optimum culture conditions for higher yield enzyme production were observed in *Chryseobacterium* sp. (Nkohla et al., 2017), *Bacillus subtilis* Strain MU S1 (Sreena and Sebastian, 2018), *Stenotrophomonas maltophilia* (Molina et al., 2018), *Streptomyces thermocoprophilus* Strain TC13W (Sinjaroonsak et al., 2019), *Bacillus pseudomycoides* (Pramanik et al., 2020), *Bacillus velezensis* (Li et al., 2020), *Bacillus albus* (Abada et al., 2021), *Bacillus subtilis subsp. subtilis* JJBS300 (Anu et al., 2021), *Bacillus pacificus* and *Pseudomonas mucidolens* (Krishnaswamy et al., 2022). All strains preferred sucrose as a carbon source for significant increase in cellulase production, which suggested the negligible requirement of this sugar for appropriate enzyme induction. *Bacillus amyloliquefaciens* SA5, *Bacillus subtilis* BTN7A, *Bacillus megaterium* BMS4 and *Anoxybacillus flavithermus* BTN7B (Hussain et al., 2017) were reported exhibiting maximum cellulase production when sucrose was used as sole carbon in the culture medium. Organic nitrogen sources stimulated higher production

than inorganic nitrogen sources. This may be due to their metabolism that contributes to culture medium acidification, affecting cellulase production. However higher cellulase production in *Bacillus licheniformis* 2D55 (Kazeem et al., 2016) and *Aneurinibacillus aneurinilyticus* BKT-9 (Ahmad et al., 2020) was found inorganic nitrogen as urea and ammonium chloride were used. Unlike strains MKAL3 and MKAL6, the response surface quadratic model was reliable for predicting cellulase production during the fermentation process with strains MKAL1, MKAL2, MKAL4, and MKAL5. The SDS-PAGE and zymogram analysis showed the cellulase molecular weights of 25 kDa similar to those reported in *Bacillus licheniformis* SVD1 (Van Dyk et al., 2009), *Bacillus subtilis* MA139 (Qiao et al., 2009), *Penicillium verruculosum* (Morozova et al., 2010) and *Novosphingobium* sp. Cm1 (Goswami et al., 2022).

Glucose and xylose promoted cellulase production in the bacterial strains. Thus, strains were screened for their glucose isomerase (GI) production. Strains showed GI activity on xylose agar plates using 2,3,5-triphenyltetrazolium in an alkaline medium (halo appearance around bacteria). The GI production quantification was performed by the cysteine-carbazole method. Strains preferred the culture conditions of 40°C, pH 6-8 and 96 of incubation period for optimum GI production. Similar, Sharma et al. (2021) reported that maximum GI activity from *Serratia marcescens* HK2 occurred at 40°C, pH 8, after 96 h of incubation (Sharma et al., 2021). A mixture of peptone/yeast extract or tryptone/peptone and 1% xylose enhanced enzyme production in all strains. Higher enzyme yields by *Bacillus megaterium* (Thi Nguyen and Tran, 2018), *Parageobacillus thermantarcticus* (Finore et al., 2019) and *Escherichia coli* strain BL21 (Fatima and Javed, 2020) were obtained with 1% xylose. Sharma et al. (2021) revealed that a mixture of organic nitrogen sources highly boosted glucose isomerase activity in *Serratia marcescens* HK2. The highest activity occurred at a 1:3 ratio of peptone and yeast extract. Also, the GI activity was

optimized by the response surface method. The strains *Hymenobacter* sp. MKAL2 and *Stenotrophomonas* sp. MKAL4 did not pass the lack of fit test ($p < 0.05$); therefore, the RSM is not well established and explains the potential reason why the lack of fit is not passed. It could be that the relationship is not that strong, the difference in the GI activity is not well explained by the fermentation conditions, or the difference is too small. However, pretreated biomass with hot water and 95% ethanol stimulated enzyme production better than crude biomass. This resulted in increased cell growth. Generally, biomass pretreatment enhances sample digestibility. Besides the lignocellulose, the lignocellulosic biomass usually contains a significant amount of non-structural components. Some are well-known as inhibitors, such as acetic acid, furfural, and ash (metal ions). A study from Lu et al. (2010) indicated that washing corn stover biomass with water can effectively remove acetic acid and furfural and significantly enhance the breakdown of cellulose and fermentation. Similarly, Deng et al. (2013) indicated that washing with water could increase the volatile matter (mostly carbohydrates) ratio and lower the metal ions, sulfurs, and chloride. Washing the biomass with water and the organic solvent is also helpful in removing water-soluble and liposoluble substances. Liu et al. (2016) and Zhang et al. (2020) also showed that the pretreatment of the water and ethanol could significantly improve the cellulose and hemicellulose conversion rate. This is one of the approaches used in industries before entering the fermentation broth. The pretreated wheat straw promoted higher glucose isomerase production in all strains, and SEM analysis was carried out to observe its morphological changes. The sample surface was destroyed after bacterial treatment (cracks, pores, and wall erosion), resulting in the exposal of internal structures. This suggests that lignin and hemicellulose of the pretreated wheat straw sample became loose or were partially removed and broken, making accessible essential nutrients (carbohydrates) to bacteria for their growth and enzyme production. These findings demonstrated

that bacterial treatment of pretreated wheat straw could destroy the hemicellulose-lignin network, thereby removing some fibers and exposing internal structures to bacteria and thus accelerating the biodegradation process.

The use of cocultures or consortia and enzymes or cells immobilized in lignocellulosic biomass bioprocess industries is excellent of interest. Enhancing glucose isomerase production and cell growth by bacterial cocultures was investigated using pretreated wheat straw as the sole carbon source in the optimum culture conditions. Bacterial cocultures were constructed based on enzyme production and antagonism assay data. The cooperation between individual bacterial cells from cocultures and the influence of carbon source complexity were also studied. We observed a bacterial synergism in glucose isomerase production and cell growth in cocultures A, B, C, G and J. Also, there was a relationship between bacterial strains depending on carbon source complexity. This suggests metabolic cooperation between bacterial strains and synergistic action of secreted enzymes allowed for increased glucose isomerase production yields and consequently an efficient wheat straw degradation. Microbial consortia were reported as critical agents in wheat straw degradation (Deng and Wang, 2016; Ghosh et al., 2016; Jia et al., 2016; Cortes-Tolalpa et al., 2017). The most promising synergistic pair was the coculture J composed of *Mycobacterium* sp. MKAL3 and *Stenotrophomonas* sp. MKAL4. This coculture presented the highest cell growth compared to the respective monocultures with synergistic glucose isomerase activities, whereas strains MKAL3 and MKAL4 have different morphological, biochemical and enzyme profiles. Wheat straw promoted synergistic interactions between strains MKAL3 and MKAL4 compared to xylose used as the sole carbon source. This could be due to the heterogeneous composition of wheat straw, suggesting that the carbon source complexity can strongly modify the relationship between degrader strains. Many studies reported that carbon source complexity influences

heterotrophic organism metabolism (Deng and Wang, 2016; Deng and Wang, 2017; Blair et al., 2021; Romero et al., 2021; Xu et al., 2021). A cell growth increase in monocultures MKAL3 and MKAL4 was observed when they were treated with the wheat straw-grown partner strain supernatant, confirming that synergistic interactions happen when growing on wheat straw. Furthermore, strains were immobilized in calcium alginate beads and tested for GI production in optimum culture conditions. We observed a decrease in enzyme activity below and above a sodium alginate concentration range of 2 to 3%. So, beads with higher sodium alginate concentration decreased enzyme production due to a more robust surface and lower enzyme diffusion. However, beads were so fragile with lower sodium alginate concentrations that most were broken during fermentation.

Soil bacteria adhere to diverse surfaces and promote biofilm formation in a protective and self-produced matrix responsible for disease emergence and resurgence (Ning et al., 2021). Consequently, putative virulence factors, antibiotics and heavy metals resistance, solvent adhesion and biofilm-forming capabilities in these strains were investigated. *Bacillus* sp. MKAL6 exhibited DNase and gelatinase activities and produced capsules. Capsular structures can serve as adhesins in microbial pathogenesis by protecting the microorganism against host immune mechanisms. All strains showed higher autoaggregation properties, providing a gateway to colonizing abiotic and biotic surfaces. The hydrophobicity capability of *Bacillus* sp. MKAL6 increased with solvent polarity while that of *Mycobacterium* sp. MKAL3 decreased with solvent polarity. *Bacillus* sp. MKAL6 exhibited higher hydrophobic ability and adhered more to polystyrene. Cell surface hydrophobicity increases microbial cell propensity to adhere to surfaces (Nwagu et al., 2020). Ning et al. (2021) reported that bacteria with high hydrophobic surface affinity displayed a high biofilm-forming ability. Except for *Stenotrophomonas* sp. MKAL4, all strains accumulated a large

amount of chromium, lead, zinc, nickel and manganese, suggesting that strains could be used as cleaning agents for bioremediation. All isolates were resistant to lincomycin in the agar medium, whereas they were sensitive to this antibiotic in the liquid medium. This could be because the antibiotic must diffuse in a solid medium, while in a liquid medium, it is directly in contact with the bacterial strain (Mokale et al., 2011). Also, *Hymenobacter* sp. MKAL2 was resistant to novobiocin, bacitracin and tetracycline. Ciprofloxacin displaying the highest inhibitory activity was used to investigate its relative mechanism action against bacterial strains. Ciprofloxacin reduced considerably viable cell numbers over 24 h. The ciprofloxacin increased crystal violet uptake in strains resulting in a change in permeability and structure of the bacterial cell wall layer. Furthermore, ciprofloxacin inhibited biofilm formation significantly by strains, due probably to the inhibition of quorum sensing signalling pathways involved in biofilm formation.

Cellulose is the earth's most widely used plant polymer and material in industries. Its degradation into fermentable sugars, especially fructose, is beneficial in many applications. Fructose can be produced via two steps: enzymatic hydrolysis of cellulose to glucose followed by isomerization of glucose into fructose. Of no question, it is more cost-effective to convert cellulose into fructose via a one-step process. The present investigation has explored cellulase and glucose isomerase-producing bacteria from soil sources. *Paenathrobacter* sp. MKAL1, *Hymenobacter* sp. MKAL2, *Mycobacterium* sp. MKAL3, *Stenotrophomonas* sp. MKAL4, *Chryseobacterium* sp. MKAL5 and *Bacillus* sp. MKAL6 produced cellulase and glucose isomerase (GI). These strains are novel wild-type cellulase and GI producers and can be potential precursors acting synergistically in the one-step conversion of cellulose into fructose using wheat straw. The optimization strategy of these scaled maximum GI production during a short time using a software method, cocultures, and whole-cell immobilized forms with multiple exploitable characteristics

could reduce the time and cost of current bioconversion processes. Some bacterial strains displayed non-hemolytic nature, antagonistic activities, antibiotic susceptibility, and good adhesive and aggregating capacity, indicating they could be potentially probiotics in the aquaculture industry. Also, bacterial strains showed high tolerance to heavy metals, which could benefit metal phytoremediation. Therefore, analysis of characteristics of soil bacteria provides essential information on soil health, diversity of heavy metal-resistant bacteria and development of effective bioremediation measures. On the other hand, some classes of enzymes appear as characteristics of certain species, genera, or microbial families. Others are likely to contain two types of enzymes or more or none. In our study, bacterial strains exhibited various enzyme activities. The assistance provided is far from negligible and can only increase as the analytical data multiply.

These results provide evidence for the potential use of these bacterial strains in lignocellulosic biomass bioprocess industries. At this stage of knowledge, we suggest for the future:

(1) To purify these cellulases and glucose isomerases for hydrolysis and saccharification of wheat straw,

(2) The immobilization studies of purified glucose isomerases for hydrolysis and saccharification of wheat straw,

(3) The studies on the division of labour (relationship between substrate chemical complexity and bacterial enzymes produced by each partner) for a better understanding of the synergistic mechanism in coculture for enzyme enhancing in the wheat straw fermentation process,

(4) To explore end products from the wheat straw fermentation process using various analytical tools such as GC-MS, HPLC, FTIR etc.,

(5) an in-depth genetic study of virulence, antibiotic and heavy metal resistance genes for clarifying pathogenicity or non-pathogenicity of soil bacteria.

References

Abada EA, Elbaz RM, Sonbol H, korany SM (2021). Optimization of Cellulase Production from *Bacillus albus* (MN755587) and Its Involvement in Bioethanol Production. *Polish J Environ Stud*, 30, 2459-2466.

Ahmad T, Sharma A, Gupta G, Mansoor S, Jan S, Kaur B, Paray BA, Ahmad A (2020). Response surface optimization of cellulase production from *Aneurinibacillus aneurinilyticus* BKT-9: an isolate of urban Himalayan freshwater. *Saudi J Biol Sci*, 27, 2333-2343.

Anu, Kumar S, Kumar A, Kumar V, Singh B (2021). Optimization of cellulase production by *Bacillus subtilis* subsp. subtilis JJBS300 and biocatalytic potential in saccharification of alkaline pretreated rice straw. *Prep Biochem Biotechnol*, 51, 697-704.

Blair EM, Dickson KL, O'Malley MA (2021). Microbial communities and their enzymes facilitate degradation of recalcitrant polymers in anaerobic digestion. *Curr Opin Microbiol*, 64, 100-108.

Cortes-Tolalpa L, Salles JF, van Elsas JD (2017). Bacterial synergism in lignocellulose biomass degradation – complementary roles of degraders as influenced by complexity of the carbon source. *Front Microbiol*, 8, 1628.

Dai J, Dong A, Xiong G, Liu Y, Hossain MS, Liu S, Gao N, Li,S, Wang J, Qiu D (2020). Production of highly active extracellular amylase and cellulase from *Bacillus subtilis* ZIM3 and a recombinant strain with a potential application in tobacco fermentation. *Front Microbiol*, 11, 1539.

Deng L, Zhang T, Che D (2013) Effect of water washing on fuel properties, pyrolysis and combustion characteristics, and ash fusibility of biomass. *Fuel Process Technol*, 106, 712-720.

Deng YJ, Wang SY (2016). Synergistic growth in bacteria depends on substrate complexity. *J Microbiol*, 54, 23-30.

Deng YJ, Wang SY (2017). Complex carbohydrates reduce the frequency of antagonistic interactions among bacteria degrading cellulose and xylan. *FEMS Microbiol Lett*, 364.

Fatima B, Javed MM (2020). Production, purification and physicochemical characterization of D-xylose/glucose isomerase from *Escherichia coli* strain BL21. *3 Biotech*, 10, 39.

Finore I, Lama L, Di Donato P, Romano I, Tramice A, Leone L, Nicolaus B, Poli A (2019). *Parageobacillus thermantarcticus*, an antarctic cell factory: from crop residue valorization by green chemistry to astrobiology studies. *Diversity*, 11, 128.

Ghosh S, Chowdhury R, Bhattacharya P (2016). Mixed consortia in bioprocesses: role of microbial interactions. *Appl Microbiol Biotechnol*, 100, 4283-4295.

Goswami K, Deka BHP, Saikia R (2022). Purification and characterization of cellulase produced by *Novosphingobium* sp. Cm1 and its waste hydrolysis efficiency and bio-stoning potential. *J Appl Microbiol*, 132, 3618-3628.

Hussain AA, Abdel-Salam MS, Abo-Ghalia HH, Hegazy WK, Hafez SS (2017). Optimization and molecular identification of novel cellulose degrading bacteria isolated from Egyptian environment. *J Genet Eng Biotechnol*, 15, 77-85.

Jia X, Liu C, Song H, Ding M, Du J, Ma Q, Yuan Y (2016). Design, analysis and application of synthetic microbial consortia. *Synth Syst Biotechnol*, 1, 109-117.

Kazeem MO, Shah UKM, Baharuddin AS, Rahman NA (2016). Enhanced cellulase production by

a novel thermophilic *Bacillus licheniformis* 2D55: Characterization and application in lignocellulosic saccharification. *BioResources*, 11, 5404-5423.

Krishnaswamy VG, Sridharan R, Kumar PS, Fathima MJ (2022). Cellulase enzyme catalyst producing bacterial strains from vermico post and its application in low-density polyethylene degradation. *Chemosphere*, 288, 132552.

Li F, Xie Y, Gao X, Shan M, Sun C, Niu YD, Shan A (2020). Screening of Cellulose Degradation Bacteria from Min Pigs and Optimization of its Cellulase Production. *Electron J Biotechnol*, 48, 29-35.

Liu KX, Li HQ, Zhang J, Zhang ZG, Xu J (2016). The effect of non-structural components and lignin on hemicellulose extraction. *Bioresour Technol*, 214:755-760.

Lu Y, Wang Y, Xu G, Chu J, Zhuang Y, Zhang S (2010). Influence of high solid concentration on enzymatic hydrolysis and fermentation of steam-exploded corn stover biomass. *Appl Biochem Biotechnol*, 160, 360-369.

Mokale KAL, Ngono NRA, Kuiate JR, Koanga MML, Tchinda TA, Mouokeu RS, Biyiti L, Amvam ZPH (2011). Antibacterial and antioxidant properties of the methanolic extract of the stem bark of *Pteleopsis hylodendron* (Combretaceae). *Chemother Res Pract*, 2011, 218750.

Molina GCE, de la Rosa G, Gonzalez CJ, Sánchez Y, Castillo-Michel H, Valdez-Vazquez I, Balcazar E, Salmerón I (2018). Optimization of culture conditions for production of cellulase by *Stenotrophomonas maltophilia*. *BioResources*, 13, 8358-8372.

Morozova VV, Gusakov AV, Andrianov RM, Pravilnikov AG, Osipov DO, Sinitsyn AP (2010). Cellulases of *Penicillium verruculosum*. *Biotechnol J*, 5, 871-880.

Ning Z, Xue B, Wang H (2021). Evaluation of the adhesive potential of bacteria isolated from

meat-related sources. *Appl Sci*, 11, 10652.

Nkohla A, Okaiyeto K, Nwodo UU, Mabinya LV, Okoh AI (2017). Endoglucanase and xylanase production by *Chryseobacterium* species isolated from decaying biomass. *Polish J Environ Stud*, 26, 2651-2660.

Nwagu TN, Ugwuodo CJ, Onwosi CO, Inyima O, Uchendu OC, Akpuru C (2020). Evaluation of the probiotic attributes of Bacillus strains isolated from traditional fermented African locust bean seeds (Parkia biglobosa), "daddawa". *Ann Microbiol*, 70, 20.

Pramanik SK, Mahmud S, Paul GK, Jabin T, Naher K, Uddin MS, Zaman S, Saleh MA (2020). Fermentation optimization of cellulase production from sugarcane bagasse by *Bacillus pseudomycoides* and molecular modeling study of cellulase. *Curr Res Microb Sci*, 2, 100013.

Qiao J, Dong B, Li Y, Zhang B, Cao Y (2009). Cloning of a beta-1,3-1,4-glucanase gene from *Bacillus subtilis* MA139 and its functional expression in *Escherichia coli*. *Appl Biochem Biotechnol*, 152, 334-342.

Romero MAD, Yao T, Chen M-H, Oles RE, Lindemann SR (2021). Fine carbohydrate structure governs the structure and function of human gut microbiota independently of variation in glycosyl residue composition. *bioRxiv*, 2021.

Sharma HK, Xu C, Qin W (2021). Isolation of bacterial strain with xylanase and xylose/glucose isomerase (GI) activity and whole cell immobilization for improved enzyme production. *Waste Biomass Valor*, 12, 833-845.

Souzanchi S, Nazari L, Rao, Yuan Z, Tan Z, Xu C (2019). Catalytic isomerization of glucose to fructose using heterogeneous solid base catalysts in a continuous-flow tubular reactor: Catalyst screening study. *Catal Today*, 319, 76-83.

Sreena CP, Sebastian D (2018). Augmented cellulase production by *Bacillus subtilis* strain MUS1 using different statistical experimental designs. *J Genet Eng Biotechnol*, 16, 9-16.

Tan H, Miao R, Liu T, Yang L, Yang Y, Chen C, Lei J, Li Y, He J, Sun Q, Peng W, Gan B, Huang Z (2018). A bifunctional cellulase-xylanase of a new *Chryseobacterium* strain isolated from the dung of a straw-fed cattle. *Microb Biotechnol*, 11, 381-398.

Thi Nguyen HY, Tran GB (2018). Optimization of fermentation conditions and media for production of glucose isomerase from *Bacillus megaterium* using response surface methodology. *Scientifica (Cairo)*, 2018, 6842843.

Van Dyk JS, Sakka M, Sakka K, Pletschke BI (2009). The cellulolytic and hemi-cellulolytic system of *Bacillus licheniformis* SVD1 and the evidence for production of a large multi-enzyme complex. *Enzyme Microb Technol*, 45, 372-378.

Van Wyk N, Navarro D, Blaise M, Berrin JG, Henrissat B, Drancourt M, Kremer L (2017). Characterization of a mycobacterial cellulase and its impact on bioflm- and drug-induced cellulose production. *Glycobiology*, 27, 392-399.

Xu Z, Lu Z, Soteyome T, Ye Y, Huang T, Liu J, Harro JM, Kjellerup BV, Peters BM (2021). Polymicrobial interaction between *Lactobacillus* and *Saccharomyces cerevisiae*: coexistence relevant mechanisms. *Crit Rev Microbiol*, 47, 386-396.

Ye M, Sun L, Yang R, Wang Z, Qi KZ (2017). The optimization of fermentation conditions for producing cellulase of Bacillus amyloliquefaciens and its application to goose feed. *R Soc Open Sci*, 4, 171012.

Zhang J, Wang Y, Du X, Qu Y (2020). Selective removal of lignin to enhance the process of preparing fermentable sugars and platform chemicals from lignocellulosic biomass. *Bioresour Technol*, 303, 122846.

Appendix 1. Effect of carbon sources on cellulase production by strains MKAL1, MKAL2, MKAL3, MKAL4, MKAL5 and MKAL6

Strains	Concentrations (%)	Cellulase activity (U/mL)						
		CMC	Sucrose	Glucose	Fructose	Sorbitol	Mannitol	Xylose
MKAL1	0.5	0.00 ± 0.00	27.55 ± 6.79	0.00 ± 0.00	0.00 ± 0.00	0.00 ± 0.00	0.00 ± 0.00	4.08 ± 0.07
	1	3.66 ± 0.84	158.27 ± 10.48	7.43 ± 0.83	7.51 ± 0.98	3.55 ± 0.83	7.63 ± 0.64	17.19 ± 2.02
	1.5	13.22 ± 2.53	118.72 ± 11.60	10.64 ± 2.38	21.16 ± 8.08	5.15 ± 0.56	9.83 ± 1.03	25.56 ± 7.51
	2	4.71 ± 0.95	83.42 ± 15.83	4.05 ± 0.96	8.06 ± 0.84	33.34 ± 8.98	44.22 ± 7.13	8.70 ± 0.75
	2.5	2.57 ± 0.79	45.66 ± 12.99	2.81 ± 0.05	7.53 ± 0.93	27.33 ± 4.51	38.87 ± 6.78	6.22 ± 1.04
MKAL2	0.5	0.00 ± 0.00	15.87 ± 6.47	0.00 ± 0.00	0.00 ± 0.00	0.00 ± 0.00	1.12 ± 0.02	0.00 ± 0.00
	1	4.16 ± 1.07	40.79 ± 4.31	4.60 ± 1.05	1.22 ± 0.08	6.22 ± 1.31	8.07 ± 1.88	1.54 ± 0.07
	1.5	8.63 ± 0.43	63.10 ± 1.95	7.59 ± 1.97	2.07 ± 0.65	34.01 ± 1.01	17.38 ± 0.99	12.58 ± 1.13
	2	16.50 ± 1.36	78.87 ± 4.71	8.16 ± 1.82	13.11 ± 1.66	10.70 ± 1.66	40.20 ± 5.47	26.57 ± 3.47
	2.5	5.01 ± 0.71	53.33 ± 9.47	7.63 ± 1.22	10.67 ± 1.64	8.81 ± 0.61	35.55 ± 4.31	24.33 ± 3.01
MKAL3	0.5	0.00 ± 0.00	21.69 ± 6.77	0.00 ± 0.00	0.00 ± 0.00	0.00 ± 0.00	0.00 ± 0.00	0.00 ± 0.00
	1	9.66 ± 0.75	62.69 ± 4.94	0.00 ± 0.00	0.00 ± 0.00	9.10 ± 1.89	6.68 ± 0.96	0.00 ± 0.00
	1.5	0.00 ± 0.00	100.82 ± 8.93	15.40 ± 2.62	0.00 ± 0.00	31.52 ± 7.02	39.72 ± 6.66	9.33 ± 2.07
	2	0.00 ± 0.00	88.48 ± 6.08	1.98 ± 0.25	0.93 ± 0.08	44.01 ± 7.06	35.16 ± 5.05	11.81 ± 2.68
	2.5	0.00 ± 0.00	67.90 ± 9.21	0.00 ± 0.00	0.00 ± 0.00	40.59 ± 6.55	32.32 ± 3.91	8.84 ± 1.73
MKAL4	0.5	0.00 ± 0.00	24.44 ± 5.50	0.00 ± 0.00	0.00 ± 0.00	0.00 ± 0.00	5.59 ± 0.88	0.00 ± 0.00
	1	2.64 ± 0.14	92.59 ± 6.97	0.00 ± 0.00	0.00 ± 0.00	4.97 ± 0.76	15.80 ± 2.64	2.32 ± 0.60
	1.5	3.79 ± 0.37	109.08 ± 2.73	3.21 ± 0.71	3.81 ± 0.37	11.78 ± 1.03	22.25 ± 5.82	2.68 ± 0.22
	2	10.93 ± 0.83	190.30 ± 6.42	7.89 ± 0.95	39.44 ± 2.96	56.96 ± 4.75	27.25 ± 4.27	3.34 ± 1.08
	2.5	5.99 ± 0.90	175.53 ± 7.87	5.36 ± 0.88	33.31 ± 3.02	50.47 ± 5.23	24.44 ± 2.87	1.56 ± 0.66
MKAL5	0.5	0.00 ± 0.00	15.70 ± 4.41	0.00 ± 0.00	0.00 ± 0.00	0.00 ± 0.00	0.00 ± 0.00	0.00 ± 0.00
	1	5.67 ± 0.08	68.42 ± 9.27	1.89 ± 0.23	4.14 ± 1.27	0.00 ± 0.00	7.01 ± 1.50	7.44 ± 1.55
	1.5	11.51 ± 0.95	134.76 ± 9.11	3.62 ± 0.49	10.03 ± 1.06	0.00 ± 0.00	7.31 ± 0.44	6.66 ± 1.07
	2	3.13 ± 0.54	106.97 ± 10.05	7.60 ± 1.99	9.90 ± 1.15	0.00 ± 0.00	8.51 ± 1.19	1.27 ± 0.15
	2.5	1.08 ± 0.09	74.97 ± 8.44	4.83 ± 0.59	6.66 ± 1.02	0.00 ± 0.00	5.53 ± 0.87	0.00 ± 0.00
MKAL6	0.5	0.00 ± 0.00	7.87 ± 1.65	0.00 ± 0.00	0.00 ± 0.00	0.00 ± 0.00	9.38 ± 1.11	8.83 ± 1.04
	1	6.27 ± 0.79	14.58 ± 2.66	0.00 ± 0.00	0.00 ± 0.00	3.97 ± 0.44	20.30 ± 0.57	16.11 ± 2.87
	1.5	11.62 ± 1.68	186.54 ± 7.23	4.39 ± 0.93	3.15 ± 1.07	27.48 ± 0.58	44.99 ± 0.99	35.45 ± 6.98
	2	18.06 ± 1.30	153.51 ± 2.31	34.90 ± 5.65	23.33 ± 4.28	22.25 ± 0.70	33.60 ± 0.99	48.52 ± 3.89
	2.5	5.87 ± 0.80	110.68 ± 6.37	29.89 ± 5.03	20.07 ± 3.87	18.83 ± 2.05	29.64 ± 2.31	44.45 ± 4.15

CMC: carboxymethylcellulose; MKAL1: *Paenarthrobacter* sp. MKAL1; MKAL2: *Hymenobacter* sp. MKAL2; MKAL3: *Mycobacterium* sp. MKAL3; MKAL4: *Stenotrophomonas* sp. MKAL4; MKAL5: *Chryseobacterium* sp. MKAL5; MKAL6: *Bacillus* sp. MKAL6; Data are shown as mean values from triplicates with corresponding standard error bars.

Appendix 2. Effect of nitrogen sources on cellulase production by strains MKAL1, MKAL2, MKAL3, MKAL4, MKAL5 and MKAL6

Strains	Conc. (%)	Cellulase activity (U/mL)								
		Yeast extract	Malt extract	Casein hydrolysate	Peptone	Tryptone	Ammonium chloride	Ammonium nitrate	Ammonium sulfate	Urea
MKAL1	0.05	13.22 ± 0.53	2.27 ± 0.61	0.00 ± 0.00	0.00 ± 0.00	0.00 ± 0.00	0.00 ± 0.00	0.00 ± 0.00	0.00 ± 0.00	0.00 ± 0.00
	0.5	13.56 ± 0.80	7.23 ± 1.10	5.26 ± 0.58	6.55 ± 0.69	9.17 ± 0.67	4.93 ± 0.52	5.25 ± 0.57	8.38 ± 0.92	0.00 ± 0.00
	1	15.34 ± 1.42	11.80 ± 2.73	19.62 ± 2.55	19.23 ± 3.73	17.52 ± 2.81	12.65 ± 1.87	15.24 ± 1.79	18.48 ± 1.96	0.00 ± 0.00
	1.5	12.85 ± 0.64	8.78 ± 0.99	15.42 ± 1.73	13.56 ± 1.74	15.03 ± 1.44	7.88 ± 0.88	11.84 ± 1.59	10.20 ± 1.77	0.00 ± 0.00
	2	6.68 ± 0.88	4.52 ± 0.91	12.12 ± 1.44	9.06 ± 0.94	10.31 ± 1.78	0.46 ± 0.06	3.12 ± 0.80	4.00 ± 0.92	0.00 ± 0.00
MKAL2	0.05	16.50 ± 1.36	1.06 ± 0.62	6.99 ± 0.87	0.00 ± 0.00	0.00 ± 0.00	0.00 ± 0.00	0.00 ± 0.00	0.00 ± 0.00	0.00 ± 0.00
	0.5	20.50 ± 1.35	7.02 ± 0.71	8.92 ± 1.00	7.62 ± 0.80	8.42 ± 0.67	0.00 ± 0.00	8.11 ± 1.21	0.00 ± 0.00	0.00 ± 0.00
	1	13.03 ± 1.09	3.91 ± 0.87	10.03 ± 1.34	12.59 ± 1.93	11.85 ± 1.46	0.00 ± 0.00	0.00 ± 0.00	0.00 ± 0.00	0.00 ± 0.00
	1.5	12.26 ± 1.86	2.50 ± 0.77	18.88 ± 0.84	16.49 ± 0.95	16.33 ± 1.82	0.00 ± 0.00	0.00 ± 0.00	0.00 ± 0.00	0.00 ± 0.00
	2	11.65 ± 1.04	0.00 ± 0.00	13.06 ± 1.70	14.34 ± 1.99	12.36 ± 1.45	0.00 ± 0.00	0.00 ± 0.00	0.00 ± 0.00	0.00 ± 0.00
MKAL3	0.05	9.66 ± 0.75	2.39 ± 0.41	4.04 ± 0.47	4.32 ± 0.29	5.03 ± 0.30	6.58 ± 0.29	5.19 ± 0.72	0.00 ± 0.00	0.00 ± 0.00
	0.5	9.90 ± 0.96	2.43 ± 0.49	7.28 ± 0.53	7.00 ± 1.25	8.91 ± 0.50	8.94 ± 0.49	7.88 ± 0.80	5.45 ± 0.49	0.00 ± 0.00
	1	10.46 ± 0.46	2.24 ± 0.74	9.18 ± 0.63	7.33 ± 0.86	13.11 ± 0.38	12.32 ± 0.52	9.80 ± 0.42	8.32 ± 0.36	0.00 ± 0.00
	1.5	11.71 ± 0.59	0.90 ± 0.08	13.38 ± 1.13	9.74 ± 0.54	14.00 ± 0.91	7.75 ± 0.70	6.53 ± 0.89	13.93 ± 1.46	0.00 ± 0.00
	2	11.21 ± 1.59	0.00 ± 0.00	11.31 ± 0.52	8.89 ± 0.64	11.62 ± 0.71	2.73 ± 0.96	5.98 ± 0.63	10.37 ± 1.19	0.00 ± 0.00
MKAL4	0.05	10.93 ± 0.83	8.53 ± 0.44	14.66 ± 0.78	7.53 ± 0.51	10.98 ± 0.72	1.87 ± 0.50	1.48 ± 0.68	0.44 ± 0.09	0.00 ± 0.00
	0.5	11.63 ± 1.00	10.47 ± 1.45	15.27 ± 1.55	14.63 ± 1.58	13.00 ± 1.64	3.02 ± 0.27	2.81 ± 0.43	2.22 ± 0.38	0.00 ± 0.00
	1	12.70 ± 0.86	6.19 ± 1.01	17.84 ± 0.73	16.21 ± 0.65	15.83 ± 0.61	2.45 ± 0.75	0.89 ± 0.07	8.79 ± 1.34	0.00 ± 0.00
	1.5	16.58 ± 1.28	4.82 ± 0.93	21.80 ± 1.14	19.77 ± 0.68	19.08 ± 2.14	0.00 ± 0.00	0.00 ± 0.00	0.00 ± 0.00	0.00 ± 0.00
	2	14.08 ± 1.15	0.00 ± 0.00	19.75 ± 1.82	17.98 ± 1.49	18.14 ± 1.60	0.00 ± 0.00	0.00 ± 0.00	0.00 ± 0.00	0.00 ± 0.00
MKAL5	0.05	11.51 ± 0.95	3.60 ± 0.73	3.43 ± 0.60	3.65 ± 0.76	5.14 ± 0.71	1.04 ± 0.35	2.63 ± 0.40	2.77 ± 0.65	0.00 ± 0.00
	0.5	11.76 ± 0.96	6.52 ± 0.95	5.28 ± 0.58	4.49 ± 1.13	5.82 ±0.64	3.09 ± 0.83	4.66 ± 0.56	5.19 ± 0.88	4.66 ± 0.56
	1	12.29 ± 1.84	15.26 ± 1.47	17.75 ± 1.49	7.95 ± 0.96	11.89 ± 1.62	0.00 ± 0.00	0.00 ± 0.00	6.03 ± 0.59	0.00 ± 0.00
	1.5	7.36 ± 0.97	2.77 ± 0.63	14.04 ± 1.64	13.43 ± 1.68	13.40 ± 1.45	0.00 ± 0.00	0.00 ± 0.00	7.5 ± 0.80	0.00 ± 0.00
	2	6.57 ± 0.86	1.57 ± 0.40	12.29 ± 1.21	10.00 ± 1.31	11.61 ± 1.62	0.00 ± 0.00	0.00 ± 0.00	7.01 ± 0.64	0.00 ± 0.00
MKAL6	0.05	18.06 ± 1.30	9.79 ± 1.96	8.07 ± 0.97	8.69 ± 1.06	8.91 ± 1.68	5.23 ± 0.94	0.00 ± 0.00	0.00 ± 0.00	6.03 ± 0.62
	0.5	19.07± 2.54	10.54 ± 2.13	10.82 ± 1.63	16.56 ± 1.61	14.09 ± 1.92	8.60 ± 0.67	0.00 ± 0.00	8.31 ± 1.50	9.74 ± 1.89
	1	21.72 ± 2.49	12.60 ± 1.47	16.20 ± 2.50	17.12 ± 1.90	18.29 ± 1.84	0.00 ± 0.00	0.00 ± 0.00	7.86 ± 1.97	4.58 ± 0.80
	1.5	26.60 ± 3.36	5.17 ± 1.10	26.52 ± 2.12	26.20 ± 3.56	26.55 ± 2.12	0.00 ± 0.00	0.00 ± 0.00	0.00 ± 0.00	0.00 ± 0.00
	2	23.19 ± 3.70	4.71 ± 0.82	17.89 ± 2.50	17.62 ± 1.78	20.77 ± 2.99	0.00 ± 0.00	0.00 ± 0.00	0.00 ± 0.00	0.00 ± 0.00

Conc.: concentration; Only MKAL6 degraded CMC without a nitrogen source in the culture medium (3.60 ± 0.88 U/mL); MKAL1: *Paenarthrobacter* sp. MKAL1; MKAL2: *Hymenobacter* sp. MKAL2; MKAL3: *Mycobacterium* sp. MKAL3; MKAL4: *Stenotrophomonas* sp. MKAL4; MKAL5: *Chryseobacterium* sp. MKAL5; MKAL6: *Bacillus* sp. MKAL6; Data are shown as mean values from triplicates with corresponding standard error bars.

Appendix 3. Effect of salts on cellulase production by strains MKAL1, MKAL2, MKAL3, MKAL4, MKAL5 and MKAL6

Strains	Concentrations (mM)	Cellulase activity (U/mL)					
		KCl	NaCl	$CaCl_2$	$AlCl_3$	$MgCl_2$	$MnCl_2$
MKAL1	0.5	19.62 ± 2.55	2.62 ± 0.50	2.65 ± 0.60	3.42 ± 0.58	4.27 ± 0.89	0.00 ± 0.00
	1	19.90 ± 0.84	4.38 ± 0.72	2.71 ± 0.81	4.63 ± 0.62	4.50 ± 0.47	0.00 ± 0.00
	2.5	21.15 ± 3.29	3.60 ± 0.55	3.93 ± 0.68	3.61 ± 0.75	3.87 ± 0.81	0.00 ± 0.00
	4	12.47 ± 1.07	1.44 ± 0.22	1.12 ± 0.46	2.18 ± 0.23	2.22 ± 0.68	0.00 ± 0.00
	5	7.15 ± 0.29	0.70 ± 0.06	0.51 ± 0.03	1.89 ± 0.51	1.86 ± 0.65	0.00 ± 0.00
MKAL2	0.5	20.50 ± 1.35	11.82 ± 0.43	9.87 ± 0.17	9.12 ± 0.61	10.39 ± 1.06	0.90 ± 0.26
	1	20.83 ± 0.15	13.39 ± 2.01	12.25 ± 0.78	12.25 ± 2.53	10.36 ± 0.60	3.94 ± 1.00
	2.5	21.20 ± 2.35	7.03 ± 1.04	10.49 ± 1.43	21.21 ± 2.26	12.48 ± 1.22	0.49 ± 0.03
	4	16.50 ± 2.35	6.84 ± 0.86	9.56 ± 0.72	20.36 ± 1.57	11.13 ± 1.09	0.00 ± 0.00
	5	15.66 ± 1.89	5.67 ± 0.74	9.09 ± 0.54	19.19 ± 0.26	10.64 ± 1.05	0.00 ± 0.00
MKAL3	0.5	14.00 ± 0.91	1.22 ± 0.046	1.76 ± 0.14	0.018 ± 0.00	0.77 ± 0.08	0.00 ± 0.00
	1	15.55 ± 0.10	2.05 ± 0.85	2.06 ± 0.76	1.30 ± 0.07	1.77 ± 0.09	0.00 ± 0.00
	2.5	16.39 ± 1.41	0.36 ± 0.09	0.18 ± 0.08	0.22 ± 0.04	0.42 ± 0.09	0.00 ± 0.00
	4	15.09 ± 2.01	0.00 ± 0.00	0.00 ± 0.00	0.00 ± 0.00	0.00 ± 0.00	0.00 ± 0.00
	5	14.16 ± 0.41	0.00 ± 0.00	0.00 ± 0.00	0.00 ± 0.00	0.00 ± 0.00	0.00 ± 0.00
MKAL4	0.5	21.80 ± 1.14	8.78 ± 0.31	4.64 ± 1.71	7.64 ± 0.35	8.23 ± 0.59	0.29 ± 0.11
	1	21.84 ± 1.88	9.95 ± 0.45	10.00 ± 0.91	10.50 ± 0.88	9.23 ± 0.59	0.79 ± 0.19
	2.5	19.99 ± 1.87	11.00 ± 1.05	9.16 ± 1.55	8.77 ± 1.55	7.99 ± 0.45	0.00 ± 0.00
	4	14.38 ± 1.93	10.08 ± 2.09	7.78 ± 0.68	6.07 ± 1.38	4.14 ± 0.95	0.00 ± 0.00
	5	10.94 ± 1.65	8.63 ± 1.21	4.93 ± 0.56	5.47 ± 1.09	3.59 ± 0.40	0.00 ± 0.00
MKAL5	0.5	17.75 ± 1.49	0.67 ± 0.29	2.37 ± 0.33	0.83 ± 0.08	12.16 ± 0.31	0.00 ± 0.00
	1	18.06 ± 0.52	1.69 ± 0.41	2.46 ± 0.35	1.57 ± 0.46	13.17 ± 0.32	0.00 ± 0.00
	2.5	18.53 ± 1.09	0.96 ± 0.09	0.99 ± 0.09	0.41 ± 0.09	20.05 ± 2.29	0.78 ± 0.10
	4	14.16 ± 0.57	0.00 ± 0.00	0.00 ± 0.00	0.00 ± 0.00	16.01 ± 1.47	0.00 ± 0.00
	5	13.72 ± 1.99	0.00 ± 0.00	0.00 ± 0.00	0.00 ± 0.00	14.73 ± 0.59	0.00 ± 0.00
MKAL6	0.5	26.60 ± 3.36	9.79 ± 0.83	11.08 ± 0.96	9.68 ± 1.55	9.55 ± 0.36	0.00 ± 0.00
	1	26.84 ± 1.43	11.32 ± 0.54	13.06 ± 1.36	11.95 ± 0.47	12.17 ± 1.59	0.13 ± 0.06
	2.5	27.01 ± 2.29	7.71 ± 0.94	9.72 ± 0.86	9.28 ± 1.40	8.33 ± 0.46	0.11 ± 0.02
	4	25.99 ± 2.68	6.06 ± 1.02	8.36 ± 1.08	8.45 ± 1.03	6.76 ± 1.16	0.00 ± 0.00
	5	21.83 ± 1.76	5.55 ± 0.74	6.97 ± 0.68	6.15 ± 1.07	5.53 ± 0.64	0.00 ± 0.00

Controls were 4.16 ± 0.40, 10.92 ± 2.45, 0.09 ± 0.00, 7.94 ± 1.28, 1.38 ± 0.41, 7.14 ± 0.71 U/mL for MKAL1, MKAL2, MKAL3, MKAL4, MKAL5 and MKAL6, respectively; MKAL1: *Paenarthrobacter* sp. MKAL1; MKAL2: *Hymenobacter* sp. MKAL2; MKAL3: *Mycobacterium* sp. MKAL3; MKAL4: *Stenotrophomonas* sp. MKAL4; MKAL5: *Chryseobacterium* sp. MKAL5; MKAL6: *Bacillus* sp. MKAL6; Data are shown as mean values from triplicates with corresponding standard error bars.

Appendix 4. Effect of salts on cellulase production by strains MKAL1, MKAL2, MKAL3, MKAL4, MKAL5 and MKAL6

Strains	Concentrations (mM)	Cellulase activity (U/mL)					
		$CoCl_2$	$NiCl_2$	$ZnCl_2$	$CrCl_3$	$PbCl_2$	$BaCl_2$
MKAL1	0.5	2.05 ± 0.48	4.09 ± 0.39	4.43 ± 1.06	5.80 ± 1.38	5.14 ± 1.62	4.10 ± 0.79
	1	6.02 ± 0.79	4.10 ± 0.71	5.08 ± 1.45	5.98 ± 1.17	5.26 ± 0.70	4.16 ± 0.81
	2.5	4.25 ± 0.61	4.34 ± 0.87	4.83 ± 0.83	6.04 ± 0.98	4.37 ± 0.77	3.48 ± 0.70
	4	3.31 ± 0.34	4.07 ± 0.76	4.25 ± 0.25	5.49 ± 0.93	4.01 ± 0.22	2.87 ± 0.66
	5	2.84 ± 0.46	3.76 ± 0.94	3.56 ± 1.80	4.97 ± 0.39	3.58 ± 0.54	2.13 ± 0.15
MKAL2	0.5	14.76 ± 1.23	10.58 ± 1.19	3.30 ± 0.02	14.38 ± 2.73	12.28 ±2.37	8.11 ± 1.19
	1	15.43 ± 1.50	9.56 ± 0.95	3.66 ± 0.98	6.69 ± 1.14	5.64 ± 1.60	8.83 ± 1.09
	2.5	23.23 ± 1.90	12.30 ± 1.70	5.95 ± 0.90	4.17 ± 0.19	3.12 ± 0.89	0.82 ± 0.05
	4	16.23 ± 1.98	11.96 ± 1.22	5.09 ± 0.65	3.99 ± 0.60	1.06 ± 0.08	0.00 ± 0.00
	5	15.59 ± 1.52	10.67 ± 1.34	4.81 ± 0.56	3.12 ± 0.84	0.00 ± 0.00	0.00 ± 0.00
MKAL3	0.5	0.19 ± 0.03	0.00 ± 0.00	0.00 ± 0.00	0.53 ± 0.12	0.35 ± 0.05	0.43 ± 0.03
	1	1.18 ± 0.09	0.00 ± 0.00	0.00 ± 0.00	1.51 ± 0.82	1.81 ± 0.71	1.51 ± 0.68
	2.5	0.00 ± 0.00	1.76 ± 0.74	1.93 ± 0.33	0.00 ± 0.00	0.00 ± 0.00	0.00 ± 0.00
	4	0.00 ± 0.00	0.00 ± 0.00	0.00 ± 0.00	0.00 ± 0.00	0.00 ± 0.00	0.00 ± 0.00
	5	0.00 ± 0.00	0.00 ± 0.00	0.00 ± 0.00	0.00 ± 0.00	0.00 ± 0.00	0.00 ± 0.00
MKAL4	0.5	9.76 ± 1.31	9.49 ± 1.39	0.00 ± 0.00	0.11 ± 0.03	0.17 ± 0.06	0.00 ± 0.00
	1	24.38 ± 2.60	10.12 ± 1.27	0.00 ± 0.00	0.21 ± 0.08	0.43 ± 0.09	0.01 ± 0.00
	2.5	19.99 ± 1.87	10.52± 1.20	0.00 ± 0.00	0.00 ± 0.00	0.00 ± 0.00	0.00 ± 0.00
	4	14.38 ± 1.93	10.08 ± 2.09	0.00 ± 0.00	0.00 ± 0.00	0.00 ± 0.00	0.00 ± 0.00
	5	10.94 ± 1.65	8.63 ± 1.21	0.00 ± 0.00	0.00 ± 0.00	0.00 ± 0.00	0.00 ± 0.00
MKAL5	0.5	0.00 ± 0.00	0.03 ± 0.00	0.00 ± 0.00	0.00 ± 0.00	0.00 ± 0.00	0.00 ± 0.00
	1	0.00 ± 0.00	0.37 ± 0.04	0.00 ± 0.00	2.19 ± 0.49	0.00 ± 0.00	0.00 ± 0.00
	2.5	2.36 ± 0.29	0.00 ± 0.00	0.00 ± 0.00	0.00 ± 0.00	0.00 ± 0.00	0.00 ± 0.00
	4	0.00 ± 0.00	0.00 ± 0.00	0.00 ± 0.00	0.00 ± 0.00	0.00 ± 0.00	0.00 ± 0.00
	5	0.00 ± 0.00	0.00 ± 0.00	0.00 ± 0.00	0.00 ± 0.00	0.00 ± 0.00	0.00 ± 0.00
MKAL6	0.5	12.82 ± 0.86	9.49 ± 0.42	0.10 ± 0.03	2.13 ± 0.94	4.37 ± 1.32	3.61 ± 1.13
	1	28.71 ± 1.22	10.04 ± 0.94	0.69 ± 0.04	4.34 ± 1.13	5.88 ± 1.03	3.70 ± 0.89
	2.5	22.94 ± 1.42	11.45 ± 0.82	0.91 ± 0.12	6.27 ± 1.34	3.90 ± 0.43	1.76 ± 0.10
	4	18.81 ± 2.05	9.91 ± 1.41	0.54 ± 0.08	5.15 ± 0.73	1.01 ± 0.02	0.00 ± 0.00
	5	16.97 ± 2.15	7.77 ± 0.87	0.47 ± 0.06	3.39 ± 0.18	0.00 ± 0.00	0.00 ± 0.00

Controls were 4.16 ± 0.40, 10.92 ± 2.45, 0.09 ± 0.00, 7.94 ± 1.28, 1.38 ± 0.41, 7.14 ± 0.71 U/mL for MKAL1, MKAL2, MKAL3, MKAL4, MKAL5 and MKAL6, respectively; MKAL1: *Paenarthrobacter* sp. MKAL1; MKAL2: *Hymenobacter* sp. MKAL2; MKAL3: *Mycobacterium* sp. MKAL3; MKAL4: *Stenotrophomonas* sp. MKAL4; MKAL5: *Chryseobacterium* sp. MKAL5; MKAL6: *Bacillus* sp. MKAL6; Data are shown as mean values from triplicates with corresponding standard error bars.

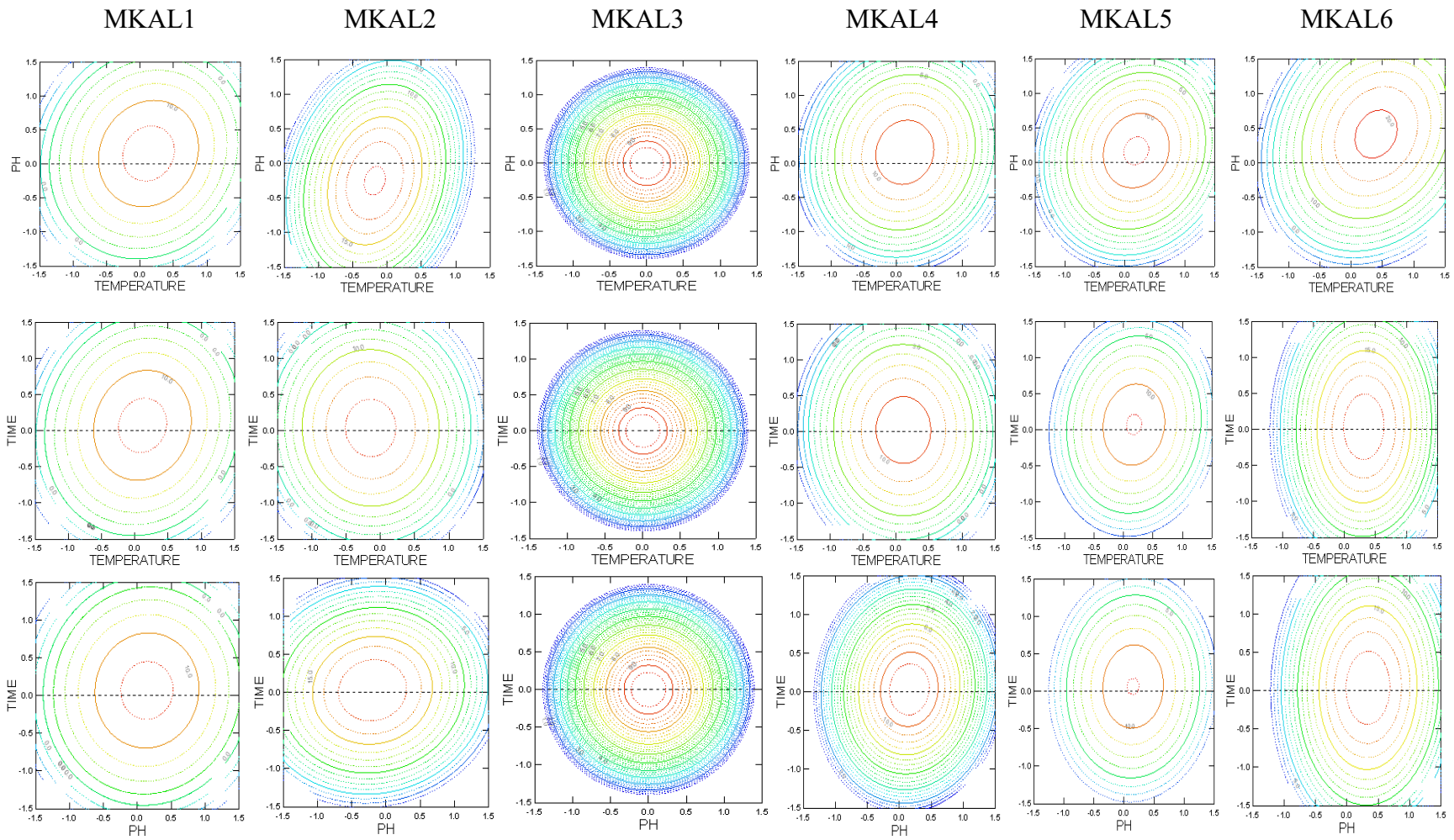

Appendix 5. The contour plots between the temperature, pH and fermentation time showing the interactive effects on cellulase activity in the CMC medium by MKAL1, MKAL2, MKAL3, MKAL4, MKAL5 and MKAL6. MKAL1: *Paenarthrobacter* sp. MKAL1; MKAL2: *Hymenobacter* sp. MKAL2; MKAL3: *Mycobacterium* sp. MKAL3; MKAL4: *Stenotrophomonas* sp. MKAL4; MKAL5: *Chryseobacterium* sp. MKAL5; MKAL6: *Bacillus* sp. MKAL6.

e

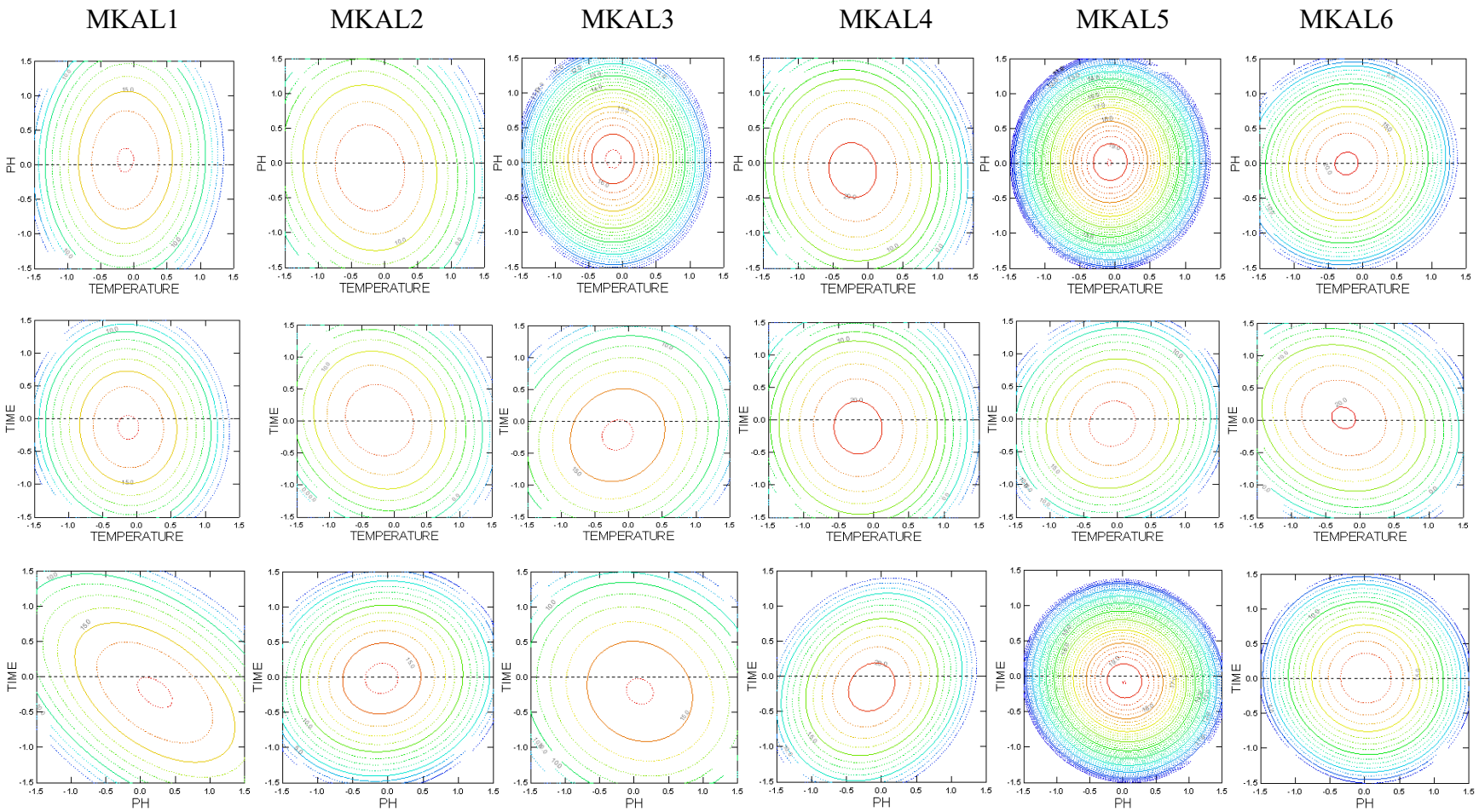

Appendix 6. The contour plots between the temperature, pH and fermentation time showing the interactive effects on the glucose isomerase activity in the wheat straw medium by MKAL1, MKAL2, MKAL3, MKAL4, MKAL5 and MKAL6. MKAL1: *Paenarthrobacter* sp. MKAL1; MKAL2: *Hymenobacter* sp. MKAL2; MKAL3: *Mycobacterium* sp. MKAL3; MKAL4: *Stenotrophomonas* sp. MKAL4; MKAL5: *Chryseobacterium* sp. MKAL5; MKAL6: *Bacillus* sp. MKAL6

Appendix 7. Effect of pH on glucose isomerase production in bacterial cocultures

Bacterial culture	Glucose isomerase activity (U/mL)					
	pH 5	pH 6	pH 7	pH 8	pH 9	pH 10
MKAL1	0.02 ± 0.00	8.14 ± 1.18	8.00 ± 0.58	9.85 ± 1.96	8.11 ± 2.36	7.76 ± 1.66
MKAL2	0.00 ± 0.00	8.42 ± 2.03	10.03 ± 2.57	5.05 ± 1.08	10.44 ± 2.09	5.83 ± 1.80
MKAL3	0.00 ± 0.00	9.96 ± 1.56	8.90 ± 2.91	4.06 ± 0.75	12.25 ± 3.02	4.91 ± 0.27
MKAL4	0. 00 ± 0.00	8.01 ± 1.50	7.82 ± 1.34	3.37 ± 0.53	7.31 ± 1.45	5.80 ± 1.21
Coculture A (1:4)	0.00 ± 0.00	1.10 ± 0.02	9.67 ± 2.59	19.62 ± 1.86	10.14 ± 2.91	3.55 ± 1.28
Coculture B (3:2)	0.00 ± 0.00	1.20 ± 0.04	7.32 ± 1.10	20.09 ± 2.10	11.77 ± 2.79	3.74 ± 1.80
Coculture C (1:4)	0.19 ± 0.04	0.71 ± 0.00	6.99 ± 0.16	18.11 ± 1.69	8.98 ± 1.88	5.81 ± 1.87
Coculture G (1:4)	0.12 ± 0.02	3.15 ± 0.25	7.60 ± 1.95	16.03 ± 1.89	7.89 ± 2.63	3.94 ± 0.44
Coculture J (3:2)	0.06 ± 0.00	3.41 ± 0.06	8.95 ± 1.41	15.17 ± 1.29	8.21 ± 2.91	4.40 ± 0.28

MKAL1: *Paenarthrobacter* sp. MKAL1; MKAL2: *Hymenobacter* sp. MKAL2; MKAL3: *Mycobacterium* sp. MKAL3; MKAL4: *Stenotrophomonas* sp. MKAL4; MKAL5: *Chryseobacterium* sp. MKAL5; MKAL6: *Bacillus* sp. MKAL6; Coculture A: MKAL1and MKAL2; Coculture B: MKAL1 and MKAL3; Coculture C: MKAL1 and MKAL4; Coculture G: MKAL2 and MKAL4; Coculture J: MKAL3 and MKAL4; Data are shown as mean values from triplicates with corresponding standard error bars.

Appendix 8. Effect of pH on cell growth in bacterial cocultures

Bacterial culture	Bacterial biomass (OD_{600})					
	pH 5	pH 6	pH 7	pH 8	pH 9	pH 10
MKAL1	0.12 ± 0.06	1.22 ± 0.08	2.22 ± 0.45	1.93 ± 0.22	2.17 ± 0.39	2.13 ± 0.32
MKAL2	0.20 ± 0.07	1.78 ± 0.09	1.54 ± 0.88	2.35 ± 0.24	1.50 ± 0.85	1.96 ± 0.29
MKAL3	0.15 ± 0.02	1.82 ± 0.18	1.87 ± 0.10	2.29 ± 0.18	1.74 ± 0.01	2.21 ± 0.39
MKAL4	0.14 ± 0.01	1.72 ± 0.20	1.46 ± 0.83	2.33 ± 0.15	1.44 ± 0.82	1.80 ± 0.13
Coculture A (1:4)	0.21 ± 0.06	1.25 ± 0.04	2.19 ± 0.52	3.05 ± 0.56	2.17 ± 0.35	2.01 ± 0.35
Coculture B (3:2)	0.34 ± 0.8	1.19 ± 0.11	2.24 ± 0.43	3.18 ± 0.58	2.27 ± 0.32	2.17 ± 0.39
Coculture C (1:4)	0.39 ± 0.09	0.98 ± 0.05	2.29 ± 0.34	3.12 ± 0.57	2.39 ± 0.33	2.39 ± 0.27
Coculture G (1:4)	0.11 ± 0.06	1.07 ± 0.06	2.22 ± 0.33	3.31 ± 0.68	2.20 ± 0.32	1.82 ± 0.12
Coculture J (3:2)	0.10 ± 0.04	1.18 ± 0.12	2.27 ± 0.38	3.44 ± 0.63	2.12 ± 0.43	1.85 ± 0.23

MKAL1: *Paenarthrobacter* sp. MKAL1; MKAL2: *Hymenobacter* sp. MKAL2; MKAL3: *Mycobacterium* sp. MKAL3; MKAL4: *Stenotrophomonas* sp. MKAL4; MKAL5: *Chryseobacterium* sp. MKAL5; MKAL6: *Bacillus* sp. MKAL6; Coculture A: MKAL1and MKAL2; Coculture B: MKAL1 and MKAL3; Coculture C: MKAL1 and MKAL4; Coculture G: MKAL2 and MKAL4; Coculture J: MKAL3 and MKAL4; Data are shown as mean values from triplicates with corresponding standard error bars.

(A)

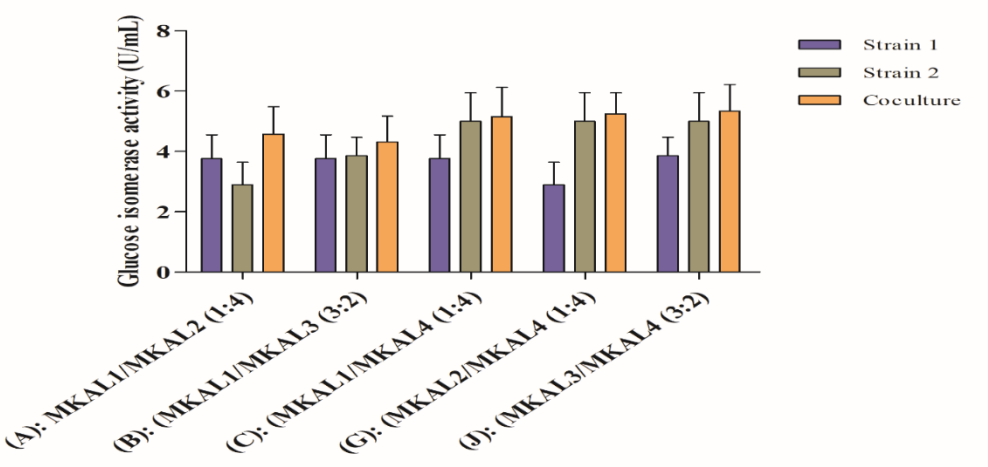

(B)

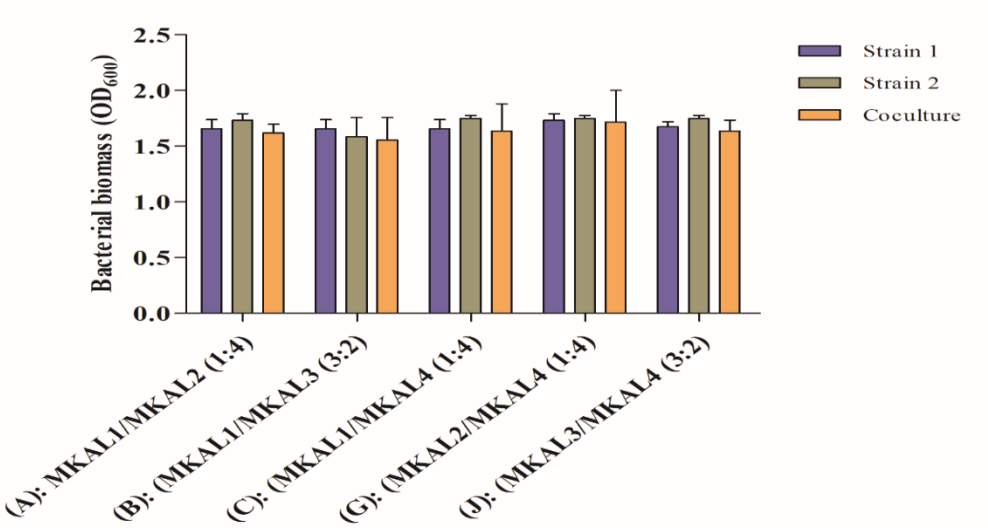

Appendix 9. Effect of xylose on glucose isomerase production (A) and cell growth (B) in bacterial cocultures. MKAL1: *Paenarthrobacter* sp. MKAL1; MKAL2: *Hymenobacter* sp. MKAL2; MKAL3: *Mycobacterium* sp. MKAL3; MKAL4: *Stenotrophomonas* sp. MKAL4; MKAL5: *Chryseobacterium* sp. MKAL5; MKAL6: *Bacillus* sp. MKAL6; Coculture A: MKAL1and MKAL2; Coculture B: MKAL1 and MKAL3; Coculture C: MKAL1 and MKAL4; Coculture G: MKAL2 and MKAL4; Coculture J: MKAL3 and MKAL4. Data are shown as mean values from triplicates with corresponding standard error bars.

Publication list

(1) **Mokale KAL**, Shrestha S, Jiang ZH, Xu CC, Sun F, Qin W (2022). High-fructose corn syrup production and its new applications for 5-hydroxymethylfurfural and value-added furan derivatives: Promises and challenges. *Journal of Bioresources and Bioproducts*, In press (Chapter 1).

(2) **Mokale KAL**, Chio C, Khatiwada JR, Shrestha S, Chen X, Li H, Zhua Y, Jiang ZH, Xu CC, Qin W (2022). Characterization of glucose isomerase-producing bacteria and optimization of fermentation conditions for producing glucose isomerase using biomass, *Green Chemical Engineering*, In press (Chapter 2).

(3) **Mokale KAL**, Chio C, Khatiwada JR, Shrestha S, Chen X, Han S, Li H, Jiang ZH, Xu CC, Qin W (2022). Characterization of Cellulose-Degrading Bacteria Isolated from Soil and the Optimization of Their Culture Conditions for Cellulase Production. *Applied Biochemistry and Biotechnology* (Chapter 3)

(4**) Mokale KAL**, Chio C, Khatiwada JR, Shrestha S, Chen X, Zhu Y, Ngono NRA, Agbor AG, Jiang ZH, Xu CC, Qin W (2022). Coculture and immobilization of cellulolytic bacteria for enhanced glucose isomerase production from wheat straw. *Biotechnology and Bioprocess Engineering* (Submitted) (Chapter 4)

(5) **Mokale KAL**, Chio C, Khatiwada JR, Shrestha S, Chen X, Zhu Y, Ngono NRA, Agbor AG, Jiang ZH, Xu CC, Qin W (2022). Soil Lignocellulolytic bacteria exhibit virulence factors, resistance to antibiotics and heavy metals, and biofilm-forming capabilities. *Annals of Microbiology* (Submitted) (Chapter 5)